Microbial dimethylsulfide (DMS) degradation in anoxic sediments

Stephania Tsola

Submitted in partial fulfilment of the requirements of the

Degree of Doctor of Philosophy

School of Biological and Behavioural Sciences

December 2022

I, Stephania Tsola, confirm that the research included within this thesis is my own work or that where it has been carried out in collaboration with, or supported by others, that this is duly acknowledged below and my contribution indicated. Previously published material is also acknowledged below.

I attest that I have exercised reasonable care to ensure that the work is original, and does not to the best of my knowledge break any UK law, infringe any third party's copyright or other Intellectual Property Right, or contain any confidential material.

I accept that the College has the right to use plagiarism detection software to check the electronic version of the thesis.

I confirm that this thesis has not been previously submitted for the award of a degree by this or any other university.

Signature:

Date: 20/12/2022

Details of collaborations and publications:

Chapter 3: This chapter was published in Environmental Microbiology under the same title with myself as the lead author.

Citation: Tsola, S.L., Zhu, Y., Ghurnee, O., Economou, C.K., Trimmer, M., and Eyice, Ö. (2021) Diversity of dimethylsulfide-degrading methanogens and sulfate-reducing bacteria in anoxic sediments along the Medway Estuary, UK. *Environ Microbiol* **23**: 4434–4449.

The preparation of the *mcrA* library was conducted by Dr C.K. Economou. 16S rRNA amplicon sequencing analysis was carried out with support from Dr Y. Zhu. Dr I.A. Sanders helped with sediment collection. Sulfate analysis was conducted by Dr S. Bennett at the Warwick Integrative Synthetic Biology Centre (WISB). I completed all other experimental and bioinformatic analyses.

Chapter 4: The gravel-dominated riverine incubations (Rivers Pant and Rib) were set up and monitored by two MSc students A.A. Prevodnik and L.F. Sinclair, under my supervision. Dr I.A. Sanders helped with all sediment collection. The preparation of the 16S rRNA and *mcrA* libraries was conducted by Dr C.K. Economou. I completed all other experimental and bioinformatic analyses.

Chapter 5: The Baltic Sea sediment sampling was conducted by Assoc. Prof. V. Brüchert, Dr I.A. Sanders and Dr Ö. Eyice. Experimental design for the microcosm incubations was carried out by Dr Y. Zhu and Dr Ö. Eyice. Dr Y. Zhu set up and monitored the incubation experiments and Dr C.K. Economou prepared the *mcrA* sequence library. Sulfate analysis was conducted by

Dr S. Bennett at the Warwick Integrative Synthetic Biology Centre (WISB). I completed all other experimental and bioinformatic analyses.

Chapter 6: All RNA work was performed by Dr C.K. Economou. The U.S. Department of Energy Joint Genome Institute completed the metagenomics and metatranscriptomics sequencing and initial bioinformatics analyses. I completed all other experimental and bioinformatic analyses.

This PhD research project was supervised by Dr Özge Eyice and Prof. Mark Trimmer and I was funded by the Queen Mary University of London PhD studentships.

Abstract

Dimethylsulfide (DMS) is the most abundant biogenic organosulfur compound emitted into the atmosphere. In anoxic sediments, DMS degradation leads to methane, a potent greenhouse gas. Alongside methanogens, sulfate-reducing bacteria (SRB) also degrade DMS, depending on sulfate availability. However, little is known about DMS degradation in anoxic sediments. This PhD aimed to explore the potential for DMS-dependent methane production and the diversity and metabolism of DMS-degrading microorganisms in anoxic sediments.

Sediment was sampled along the salinity gradient of the Medway Estuary to understand how sulfate concentrations affect DMS-dependent methanogenesis. Sediment was also collected from rivers, important contributors to the global methane budget. Furthermore, we studied DMS degradation in the Baltic Sea following a phytoplankton bloom, which releases dimethylsulfoniopropionate, a major DMS precursor. The sediment samples were incubated with DMS as the only carbon and energy source. The methanogen and SRB diversities were analysed using taxonomic (16S rRNA) and functional genes (*mcrA, dsrB*). Samples from the Baltic Sea incubations were also selected for metagenomics and metatranscriptomics analyses.

Results showed a 39%-92% methane yield from DMS in all sediment samples, indicating a high potential for DMS-dependent methanogenesis in anoxic sediments regardless of sulfate availability. *Methanomethylovorans*, *Methanococcoides* and *Methanolobus* were the most dominant DMS-degrading methanogens depending on sediment salinity, implying niche-partitioning likely driven by sulfate concentrations. In addition, DMS degradation initiated

sulfate recycling in all low-sulfate incubations, thus affecting the sulfur cycle. Lastly, metagenomics and metatranscriptomics analyses showed for the first time that DMS could be degraded via the activity of trimethylamine and methanol methyltransferases rather than previously characterised DMS methyltransferases.

This PhD project is the first cultivation-independent study of DMS-degrading microorganisms in anoxic sediments. It highlights the significance of anaerobic DMS degradation for global methane production and the carbon and sulfur cycles.

Acknowledgments

During a four-year PhD project, it is natural to be inspired and supported by many people, but none helped me overcome my PhD hurdles more than my supervisor Dr Özge Eyice. Thank you for guiding me when I was lost and overthinking as a PhD student. Most importantly, though, thank you for always giving me the freedom and independence to explore my scientific interests and capabilities. Your help with experimental design and scientific writing, as well as your sharing of experiences within academia and your overall approach to science, is something I will never forget.

Secondly, I must thank my co-supervisor, Prof. Mark Trimmer, for valuable discussions about experiments and for instructions on how to best present my data.

A massive thank you to Dr Chloe Economou, Dr Yizhu Zhu and Dr Ian Sanders for always offering encouragement, technical and fieldwork assistance and beneficial discussions on science.

I would also like to thank all past and present PhD and MSc students in the QMUL Fogg Building for their friendship and for always giving me a shoulder to cry on when experiments went wrong. I want to give a special shout-out to Pasca Francelle, Susie Hawthorne, Doro Kinkel, Wenbin Kang, Nayeli Castelan, Yuling Feng, Anja Prevodnik, Yueyue Si, and Lorena Sinclair.

This PhD would never have been completed without the help of my family and friends. Thank you to my fantastic parents and siblings for their mental support and love and for always believing in me despite not always fully understanding what I am doing. Thank you to Chris Renta, Sarah Lovett, Claire Paulus and Oli Davidson for countless wine and whine sessions and for supporting me even when I am bad at texting.

Lastly, thank you to Lizzie Loake for always sticking with me and showing me how to be happy.

Table of Contents

Abstract **4**

Acknowledgments **6**

Table of Contents **8**

List of Tables **11**

List of Figures **12**

Abbreviations and acronyms **15**

1 Introduction **18**

1.1 The Sulfur cycle **18**

1.2 Sulfate reduction and sulfate-reducing bacteria **19**

1.3 Key organosulfur compounds **21**

1.3.1 Dimethylsulfoniopropionate (DMSP) 21

1.3.2 Dimethylsulfide (DMS) 22

1.3.3 Methanethiol (MeSH) 23

1.3.4 Dimethylsulfoxide (DMSO) 24

1.4 DMS cycle in the environment **25**

1.4.1 Sources of DMS 25

1.4.2 Sinks of DMS 29

1.5 Methanogenesis **31**

1.5.1 Hydrogenotrophic methanogenesis 32

1.5.2 Acetoclastic methanogenesis 33

1.5.3 Methylotrophic methanogenesis 35

1.6 Diversity of anaerobic microorganisms degrading DMS **37**

1.6.1 DMS-degrading methanogens 37

1.6.2 DMS-degrading SRB 40

1.6.3 Interactions between DMS-degrading methanogens and SRB 42

1.7 Aims and objectives **43**

2 Materials and methods **45**

2.1 Incubation set-up **45**

2.2 Analytical measurements **47**

2.3 General molecular techniques **50**

2.3.1 DNA extraction 50

2.3.2 Polymerase Chain Reaction (PCR) 50

2.4 High-throughput sequencing **53**

2.4.1 Sample preparation 53

2.4.2 Amplicon sequencing analysis 54

2.5 Quantitative polymerase chain reaction (qPCR) **56**

2.6 Statistical analysis **59**

2.7 Metagenomics **60**

2.7.1 DNA sample preparation 60
2.7.2 Metagenomics analysis 60
2.7.3 Functional and taxonomic analysis 62
2.8 Metatranscriptomics 62
2.8.1 RNA sample preparation 62
2.8.2 Metatranscriptomics analysis 63
2.8.3 Functional and taxonomic analysis 64
2.8.4 Stop codon correction of sequences 65
2.9 Phylogenetic analysis of the mcrA gene 66
3 Diversity of dimethylsulfide-degrading methanogens and sulfate-reducing bacteria in anoxic sediments along the Medway Estuary, UK 68
3.1 Introduction 68
3.2 Site locations and sediment sampling 71
3.3 Results 72
3.3.1 DMS degradation leads to methane production along the sulfate gradient of the Medway Estuary 72
3.3.2 Taxonomic and functional diversities in the sediment incubations 76
3.4 Discussion 87
4 Identification of DMS-degrading microorganisms in anoxic riverbeds 97
4.1 Introduction 97
4.2 Site characteristics and sediment sampling 100
4.3 Results 102
4.3.1 Sediment characterisation and incubation monitoring 102
4.3.2 DMS-degrading methanogens in riverine sediments 105
4.3.3 SRB in riverine sediments 109
4.3.4 Total archaea and bacteria in riverine sediments 115
4.4 Discussion 124
5 Depth profile of microbial DMS degradation in Baltic Sea sediments 130
5.1 Introduction 130
5.2 Study area and sampling 133
5.3 Results 136
5.3.1 Depth profiles of DMS, methane, CO_2 and sulfate in the sediments 136
5.3.2 Depth profiles of methanogen diversity and abundance 142
5.3.3 Depth profiles of SRB diversity and abundance 147
5.3.4 Depth profile of total archaea and bacteria 153
5.3.5 Metagenomics analysis 159
5.4 Discussion 163
6 Metabolism of anaerobic DMS degradation 167
6.1 Introduction 167
6.2 Results 168
6.3 Discussion 176

7 Conclusions and future perspectives 180
References 185
Appendix 207

List of Tables

Table 1.1. Isolated methanogenic archaea able to degrade DMS 38
Table 2.1. Bunsen coefficient for each sampling location. 48
Table 2.2. Forward and reverse dsrB primer sequences. 52
Table 2.3. Forward and reverse dsrB qPCR primer sequences. 57
Table 3.1. Shannon (H) indices 77
Table 3.2. Spearman's rank correlation coefficients 79
Table 4.1. Grain size characterisation of the four rivers sampled. 102
Table 4.2. Shannon (H) indices for the methanogens in the riverine sediment samples 107
Table 4.3. Spearman's rank correlation coefficients (r_s) 108
Table 4.4. Shannon (H) indices for SRB in the riverine sediment samples. 110
Table 4.5. Spearman's rank correlation coefficients (r_s) 114
Table 4.6. Shannon (H) indices for archaea in the riverine sediment samples. 118
Table 4.7. Spearman's rank correlation coefficients (r_s) 120
Table 4.8. Shannon (H) indices for bacteria in the riverine sediment samples 121
Table 4.9. Spearman's rank correlation coefficients (r_s) 124
Table 5.1. Sulfate concentrations used in the microcosms per sampling station and depth 135
Table 5.2. Spearman's rank correlation coefficients (r_s) 145
Table 5.3. Spearman's rank correlation coefficients (r_s) 151
Table 5.4. Spearman's rank correlation coefficients (r_s) 156
Table 5.5. Spearman's rank correlation coefficients (r_s) 159
Table 5.6. Metagenome assembled genomes constructed from metagenome datasets from each sampling station at depth 19-22 cm. 161

List of Figures

Figure 1.1. Dissimilatory sulfate reduction 20
Figure 1.2. A simplified graph summarising the various sources and sinks of DMS in the atmosphere, the water column and sediments 25
Figure 1.3. Hydrogenotrophic methanogenesis pathway. 33
Figure 1.4. Acetoclastic methanogenesis pathway. 34
Figure 1.5. Methylotrophic methanogenesis pathway. 36
Figure 1.6. Methanogenesis pathway via DMS in Methanosarcina barkeri and M. acetivorans. 40
Figure 3.1. Sampling locations along the Medway Estuary. 71
Figure 3.2. A) Average DMS amounts degraded (primary axis) and average cumulative methane amounts produced (secondary axis) in the DMS-amended incubations. **B)** Total amounts of DMS degraded and methane produced at the end of the incubation in sediments incubated with DMS. **C)** Total amount of CO_2 produced at the end of the incubation. 74
Figure 3.3. Sulfate concentrations (mM) before and after the incubation experiment for the freshwater, brackish and marine samples 75
Figure 3.4. A) Genus-level taxonomy of the mcrA sequences in the original and DMS incubated freshwater, brackish and marine sediments from the Medway Estuary. **B)** Principal components analysis of the mcrA sequences (PC1 – 44%, PC2 – 27%). 78
Figure 3.5. A) Genus-level taxonomy of the archaeal 16S rRNA gene sequences in the original and DMS incubated freshwater, brackish and marine sediments from the Medway Estuary**. B)** Principal components analysis of the archaeal sequences (PC1 – 37%, PC2 – 30%). 80
Figure 3.6. Mean copy number/g sediment of the mcrA gene for methanogens before and after the DMS incubation 81
Figure 3.7. A) Family-level taxonomy of the dsrB sequences in the original and DMS incubated freshwater, brackish and marine sediments from the Medway Estuary **B)** Principal components analysis of the dsrB sequences (PC1 – 48%, PC2 – 40%) 83
Figure 3.8. Mean copy number/g sediment of the dsrB gene for SRB before and after the DMS incubation 84
Figure 3.9. A) Genus-level taxonomy of the bacterial 16S rRNA gene sequences in the original and DMS incubated freshwater, brackish and marine sediments from the Medway Estuary**. B)** Principal components analysis of the bacterial sequences (PC1 – 60%, PC2 – 15%) 86
Figure 3.10. Diagram showing the proposed role of Sulfurimonas in the freshwater sulfur cycle initiated by DMS degradation. 93
Figure 4.4.1. Map showing the river sampling sites 101
Figure 4.2. Average DMS degradation and methane production in river sediment incubations using DMS as the only energy and carbon source. 103
Figure 4.3. Total amounts of DMS degraded and, methane and CO_2 produced during the river sediment incubations 104
Figure 4.4. Relative abundance of all methanogenic archaea at genus level in the riverine sediment samples following the amplification of the mcrA gene 106
Figure 4.5. Principal Coordinate Analysis (PCoA) plots of the mcrA sequences based on Bray-Curtis dissimilarity metrics 108
Figure 4.6. Mean copy number of the mcrA gene per gram of sediment. 109
Figure 4.7. Relative abundance of all SRB at genus level in the riverine sediment samples following the amplification of the dsrB gene 111

Figure 4.8. Principal Coordinate Analysis (PCoA) plots of the dsrB sequences based on Bray-Curtis dissimilarity metrics. 112
Figure 4.9. Principal Coordinate Analysis (PCoA) plots of the dsrB sequences based on Bray-Curtis dissimilarity metrics 113
Figure 4.10. Mean copy number g^{-1} sediment of the dsrB gene for all SRB 115
Figure 4.11. Mean copy number g^{-1} sediment of the 16S rRNA gene for all bacteria and archaea 116
Figure 4.12. Relative abundance of the total archaeal diversity at genus level in the riverine sediment samples following the amplification of the 16S rRNA gene 118
Figure 4.13. Principal Coordinate Analysis (PCoA) plots of the archaeal sequences based on Bray-Curtis dissimilarity metrics 119
Figure 4.14. Relative abundance of the bacterial diversity at genus level in the riverine sediment samples following the amplification of the 16S rRNA gene 122
Figure 4.15. Principal Coordinate Analysis (PCoA) plots of the archaeal sequences based on Bray-Curtis dissimilarity metrics. 123
Figure 5.1. Concentrations of methane and sulfate per depth in the three sampling stations. cmbf: cm below seafloor. 132
Figure 5.2. Map of the Himmerfjärden Estuary and the Baltic Sea showing the three sampling sites H2, H3 and H5 134
Figure 5.3. Average DMS amounts degraded (primary axis) and average methane amounts produced (secondary axis) in the DMS amended incubations. 137
Figure 5.4. Average DMS degradation and methane and CO_2 production in the Baltic Sea sediment samples across all sampling sites (H2, H3 and H5) and depths. 138
Figure 5.5. Average sulfate concentrations in the microcosms upon starting the incubations and at their end in the Baltic Sea sediment samples across all sampling sites and depths. 141
Figure 5.6. Relative abundance of all methanogens at genus level following the amplification of the mcrA gene. 143
Figure 5.7. Principal coordinate analysis (PCoA) plot of the mcrA sequences based on Bray-Curtis dissimilarity metrics.. 144
Figure 5.8. Mean copy number g^{-1} sediment of the mcrA gene for all methanogens separated per sampling site and treatment 146
Figure 5.9. Relative abundance of all SRB at genus level following the amplification of the dsrB gene 148
Figure 5.10. Principal coordinate analysis (PCoA) plot of the dsrB sequences based on Bray-Curtis dissimilarity metrics 149
Figure 5.11. Principal coordinate analysis (PCoA) plot of the dsrB sequences based on Bray-Curtis dissimilarity metrics. 150
Figure 5.12. Mean copy number g^{-1} sediment of the dsrB gene for all SRB separated per sampling site and treatment 152
Figure 5.13. Relative abundance of all archaea at genus level following the amplification of the 16S rRNA gene 154
Figure 5.14. Principal coordinate analysis (PCoA) plot of the 16S rRNA archaeal sequences based on Bray-Curtis dissimilarity metrics. 155
Figure 5.15. Relative abundance of all bacteria at genus level following the amplification of the 16S rRNA gene. Some of the legend entries for bacteria with low relative abundance (<2%) have been removed for clarity. 157

Figure 5.16. Principal coordinate analysis (PCoA) plot of the 16S rRNA bacterial sequences based on Bray-Curtis dissimilarity metrics. 158
Figure 5.17. Maximum likelihood phylogenetic tree of cultured methanogens containing the mcrA gene. 162
Figure 6.1. Map showing the three methanogenesis pathways and their genes 168
Figure 6.2. Genes involved in methane production via the methylotrophic methanogenesis pathway 169
Figure 6.3. Presence and absence of the genes involved in methane production in the four Methanolobus MAGs constructed using the metagenomics datasets 170
Figure 6.4. Genes common in all three methanogenesis pathways 173
Figure 6.5. Genes involved in methane production via the acetoclastic and hydrogenotrophic methanogenesis pathways 174
Figure 6.6. Genes involved in sulfur cycling 175

Abbreviations and acronyms

‰ – Per mille
AMP – Adenosine monophosphate
ANOVA – Analysis of variance
APS – adenosine 5'-phosphosulfate
ASV – Amplicon sequence variants
ASW – Artificial seawater
ATP – adenosine triphosphate
bp – Base pairs
BSA – Bovine serum albumin
CCN – Cloud condensation nuclei
CLAW – Charlson-Lovelock-Andreae-Warren
cm – Centimetre
cmbsf – Centimetres below seafloor
CoB – Coenzyme B
CoM – Coenzyme M
Comp – Completeness
Con – Control
Cont – Contamination
CPM – Copies per million
DIC – Dissolved inorganic carbon
DMS – Dimethylsulfide
DMSO – Dimethylsulfoxide
DMSOP– Dimethylsulfoxonium propionate
DMSP – Dimethylsulfoniopropionate
DNA – Deoxyribonucleic acid
DOE JGI – U.S. Department of Energy Joint Genome Institute
EC – Enzyme commission
FID – Flame ionisation detector
FPD – Flame photometric detector
FPKM – Fragments per kilobase of transcript per million fragments mapped
g – Grams
Gb – Gigabyte
gDNA – Genomic deoxyribonucleic acid
h – Hour
H – Shannon diversity index
HPC – High performance computing
ID – Identification
kJ – Kilojoule
KO – KEGG orthology

K_s – Affinity constant
L – Litre
m – Metre
M – Molar
MAG – Metagenome-assembled genome
MeSH – Methanethiol
MIMAG – Minimum information about a metagenome-assembled genome
min – Minute
mL – Millilitre
mm – Millimetre
mM – Millimolar
mol – Mole
NCBI – National centre for biotechnology information
nM – Nanomolar
Ø – Diameter
^oC – Degrees Celsius
Ori – Original
OTU – Operational taxonomic unit
PCA – Principal component analysis
PCoA – Principal coordinate analysis
PCR – Polymerase chain reaction
PERMANOVA - Permutational multivariate analysis of variance
PPi – Inorganic pyrophosphate
ppm – Parts per million
QMUL – Queen Mary, University of London
qPCR – Quantitative polymerase chain reaction
RNA – Ribonucleic acid
rpm – Rates per minute
rRNA – Ribosomal ribonucleic acid
r_s – Spearman's rank correlation coefficient
sec – Second
SMTZ – Sulfate-methane transition zone
spp – Several species
SRB – Sulfate-reducing bacteria
Tg – Teragrams
TMA – Trimethylamine
tRNA – Transfer ribonucleic acid
w/v – Weight per volume
$\Delta G^{o\prime}$– Standard Gibbs free energy at pH=7
µL – Microlitre

μM – Micromolar
μmol – Micromole
Σ – Total

1 Introduction

1.1 The Sulfur cycle

Sulfur (S^0) is an abundant element in the biosphere and a fundamental component of all living organisms. It is most often found as an organosulfur compound or metal sulfide rather than in its elemental form. Sulfur is also present in various compounds including amino acids (e.g. cysteine, methionine and taurine), secondary metabolites such as plant-derived glucosinolates and cysteine sulfoxides, vitamins, lipids and polysaccharides (Hill *et al.*, 2022).

About 97 Tg of sulfur compounds are cycled each year from the bioshere back to the ocean through the sulfur cycle, which involves a variety of metabolic processes (sulfide oxidation and disproportionation, sulfate reduction; Qian *et al.*, 2019). These processes are very closely linked with the global carbon cycle.

Dissimilatory sulfate reduction, also known as sulfate respiration, plays a major role in the biogeochemical sulfur and carbon cycles (Crowe *et al.*, 2014). More than 50% of the organic carbon mineralisation in marine sediments is related to dissimilatory sulfate reduction (Qian *et al.*, 2019). Stable sulfur isotopes have shown dissimilatory sulfate reduction evolved nearly 3.5 billion years ago, suggesting it contributed to the primordial sulfur cycle (Wagner *et al.*, 1998).

Sulfide oxidation reverses the reduction of sulfate, converting hydrogen sulfide (an end product of sulfate reduction) and sulfide minerals to oxidised sulfur molecules (eg. sulfite and

thiosulfate). The oxidised sulfur molecules can then be used by microorganisms during sulfur disproportionation (Fike *et al.*, 2015).

1.2 Sulfate reduction and sulfate-reducing bacteria

During the dissimilatory sulfate reduction pathway, microorganisms use inorganic sulfate as their final electron acceptor and oxidise energy substrates resulting in the production of hydrogen sulfide (Qian *et al.*, 2019). This process can be carried out by both bacteria and archaea. However, most prokaryotes that can reduce sulfate are bacteria, therefore the term sulfate-reducing bacteria (SRB) is used here instead of sulfate-reducing prokaryotes.

SRB are present in a wide array of anoxic ecosystems including marine, estuarine and saltmarsh sediments, wetlands, cyanobacterial microbial mats, rice fields, even deep-sea hydrothermal vents (Muyzer and Stams, 2008; Barton and Fauque, 2009; Pester *et al.*, 2012). Organisms characterised as SRB are phylogenetically and metabolically diverse. They have successfully adapted to almost all ecosystems, coping with extreme physico-chemical conditions, including high temperatures and pressure (Barton and Fauque, 2009).

More than 220 SRB species across 60 genera have been described until now. These belong to five bacterial phyla: *Desulfotomaculum, Desulfosporomusa* and *Desulfosporosinus* (Firmicutes), *Deltaproteobacteria*, *Thermodesulfovibrio* (*Nitrospira*) and two phyla represented by *Thermodesulfobium narugense* and *Thermodesulfobacterium/Thermodesulfatator* (Itoh *et al.*, 1998, 1999; Castro *et al.*, 2000; Mori *et al.*, 2003; Muyzer and Stams, 2008). There are also two

groups within Archaea: the euryarchaeotal genus *Archaeoglobus* and the two crenarchaeotal genera *Thermocladium* and *Caldivirga* (Dahl and Truper, 2001; Barton and Fauque, 2009). Briefly, in the dissimilatory sulfate reduction pathway, sulfate (SO_4^{2-}) is first reduced to sulfite (SO_3^{2-}), which is then converted to sulfide (S^{2-}). The enzyme sulfur adenyltrasferase (Sat) catalyses the attachment of sulfate to ATP forming adenosine 5'-phosphosulfate (APS; Figure 1.1; Dahl *et al.*, 1990; Dahl and Trüper, 2001). APS is then reduced to sulfite by the adenylylsulfate reductase (AprAB; Dahl and Trüper, 2001), which is further reduced to sulfide either by a sulfite reductase or the dissimilatory sulfite reductase (Dsr; Dahl and Trüper, 2001).

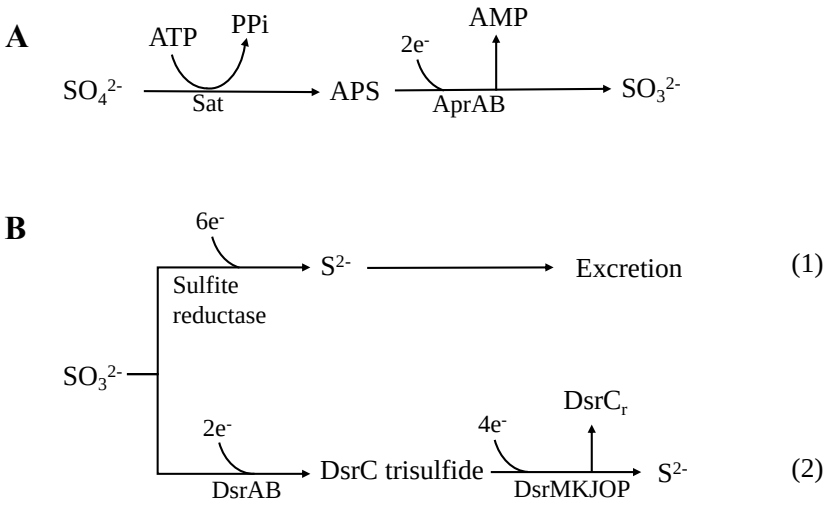

Figure 1.1. Dissimilatory sulfate reduction. **A)** Activation of sulfate (SO_4^{2-}) and production of sulfite (SO_3^{2-}). **B)** Proposed sulfite reduction pathways for the production of sulfide (S^{2-}). ATP: adenosine triphosphate; PPi: inorganic pyrophosphate; APS: adenosine 5'-phosphosulfate; AMP: adenosine monophosphate; Sat: sulfur adenyltrasferase; AprAB: adenylylsulfate reductase; Dsr; dissimilatory sulfite reductase; e^-: electrons.

1.3 Key organosulfur compounds

1.3.1 Dimethylsulfoniopropionate (DMSP)

Dimethylsulfoniopropionate (DMSP) is a common organosulfur compound, which is produced at petagram amounts every year in oceans and sediments (Ksionzek *et al.*, 2016; Zhang *et al.*, 2019). DMSP can be found in certain macroalgae and phytoplankton such as dinoflagellates and species like *Emiliana huxleyi*, *Polysiphonia fastigiata* or *Phaeocystis* (Challenger and Simpson, 1948; Liss *et al.*, 1994; Wolfe and Steinke, 1996). Some vascular plants, for example the cordgrass *Spartina alterniflora* commonly found in salt marshes, can also produce DMSP (Dacey *et al.*, 1987; Bacic *et al.*, 1998). Corals and their zooxanthellae, are other examples of DMSP-containing organisms, leading to high amounts of DMSP being released in the surrounding areas (Broadbent *et al.*, 2002; Broadbent and Jones, 2004).

The exact role of DMSP still remains unknown, however it is suggested that it is produced primarily for its anti-stress properties since it can act as an osmoprotectant, a grazing deterrent, an antioxidant, and a hydrostatic pressure protectant (Cosquer *et al.*, 1999; Sunda *et al.*, 2002; Strom *et al.*, 2003; Curson *et al.*, 2011; Zheng *et al.*, 2020). It can also act as a signalling molecule during chemoattraction (Seymour *et al.*, 2010). The degradation products of DMSP also serve as a major source of energy, carbon and sulfur for microorganisms (Kiene and Linn, 2000; Simó *et al.*, 2009). Overall, the importance of DMSP for the sulfur cycle is vast when considering Sievert *et al.* (2007) suggested that the DMSP amounts produced only by marine photoautotrophs accounts for 5×10^{13} moles of sulfur per year, yet its importance is further increased by its role as the main precursor of dimethylsulfide.

1.3.2 Dimethylsulfide (DMS)

Dimethylsulfide [$(CH_3)_2S$, DMS] is a volatile organosulfur compound and the most abundant form of biogenic sulfur in the atmosphere. Approximately 28 Tg of DMS are released from the oceans every year (Lana *et al.*, 2011). It is part of both the biogeochemical sulfur and carbon cycles and has been found to act as a signal for higher organisms such as seals and foraging seabirds (Talou *et al.*, 1990; Johnston *et al.*, 2008; Kalinová *et al.*, 2009). Cooking of certain vegetables, for example corn and cabbage, and seafood, produces DMS, explaining the smell these foods are associated with.

About 80% of the total DMS is found in the marine environment (Watts, 2000). The remaining 20% is produced either anthropogenically, such as the paper, brewery and agricultural industries, or naturally in soils, wetlands, salt marshes and estuaries (Keenan and Lindsay, 1968; Scarlata and Ebeler, 1999; Watts, 2000; Rappert and Müller, 2005; Catalan *et al.*, 2009; Crespo *et al.*, 2012).

DMS, when released to the atmosphere, acts as cloud condensation nuclei (CCN) due to its oxidation into sulfate aerosols (Shaw, 1983). CCN are particles that help create cloud droplets, leading to the alteration of cloud reflectivity (albedo; Twomey, 1977; Quinn and Bates, 2011). Charlson *et al.* (1987) proposed the CLAW hypothesis suggesting that an abundance of CCN produced by DMS increases cloud cover, changing the levels of radiation reaching the ground,

and cooling the environment. The changes in surface temperature and solar radiation can then in turn impact DMS production rates, thus creating a climatic feedback loop.

Nowadays the CLAW hypothesis is characterised as too simplistic, mainly because its core hypothesis, that DMS is the only contributor to the formation of CCN is not accurate (Kulmala, 2003; Boy *et al.*, 2005; Sipilä *et al.*, 2010). Studies have shown that CCN can also be derived from sea salt and organic compounds (polysaccharides, proteins, amino acids, and microorganisms) in sea spray, contradicting the CLAW hypothesis that assumed DMS was a significant source of CCN (Twohy and Anderson, 2008; Hawkins and Russell, 2010). Also, the lack of experimental evidence showing the DMS climate loop and the low sensitivity between DMS flux and CCN numbers suggest that the CLAW hypothesis may not be valid (Carslaw *et al.*, 2010; Quinn and Bates, 2011).

1.3.3 Methanethiol (MeSH)

Methanethiol (MeSH), also known as methylmercaptan, is an important organosulfur compound with an odour comparable to rotten cabbage. It is widely found in the environment due to it being a product of decaying biomass. It is used for the detection of natural gas leaks, which would otherwise be odourless (Schäfer and Eyice, 2019). MeSH is a product of DMS degradation and also DMSP demethylation (de Bont *et al.*, 1981; Reisch *et al.*, 2011).

Generally, MeSH is very reactive so the majority of it stays in the water column and takes part in the sulfur cycle. MeSH can be oxidised by aerobic bacteria such as *Hyphomicrobium* and *Thiobacillus* (Suylen *et al.*, 1987; Gould and Kanagawa, 1992; Eyice *et al.*, 2018). It can also be assimilated into sulfur-containing amino acids like methionine and cysteine (Kiene *et al.*, 1999). Another sink of MeSH in the environment is its microbial methylation to DMS (Carrión *et al.*, 2015). Lastly, MeSH in anoxic ecosystems can be degraded by methanogenic archaea and SRB leading to the production of methane, carbon dioxide (CO_2) and hydrogen sulfide (Zinder and Brock, 1978; Lomans *et al.*, 1999).

1.3.4 Dimethylsulfoxide (DMSO)

Dimethylsulfoxide (DMSO) is a nonvolatile compound found in surface waters and the atmosphere, and can be produced via anthropogenic activities such as paper production, and DMS photooxidation (Andreae, 1980; Brimblecombe and Shooter, 1986). DMSO can further arise from the degradation of bacterial or algal-produced dimethylsulfoxonium propionate (DMSOP; Thume *et al.*, 2018). DMSO can also be reduced back to DMS, creating a cycle between these compounds (more details in Section 1.4.2; Zinder and Brock, 1978). Overall, Hatton *et al.* (1996) showed DMSO was present in the oceans at levels similar to DMSP.

For years, DMSO has been used in medicine since it can penetrate membranes, act as an anti-inflammatory compound, can relieve pain locally and has weak bacteriostasis abilities (Capriotti and Capriotti, 2012).

1.4 DMS cycle in the environment

1.4.1 Sources of DMS

There are various sources of DMS in the environment. It can be produced as a breakdown product of DMSP or by the bacterial transformation of MeSH and DMSO (Figure 1.2; White, 1982; McEwan *et al.*, 1991; Yamamoto *et al.*, 1995; Jonkers *et al.*, 1996; Stefels *et al.*, 2007; Carrión *et al.*, 2017). DMS is also formed during the metabolism of amino acids that contain sulfur (methionine and cysteine), the methylation of sulfide and the degradation of methoxylated aromatic compounds (Figure 1.2; Kadota and Ishida, 1972; Zinder and Brock, 1978; Kiene and Capone, 1988; Bak *et al.*, 1992 Lomans *et al.*, 2001).

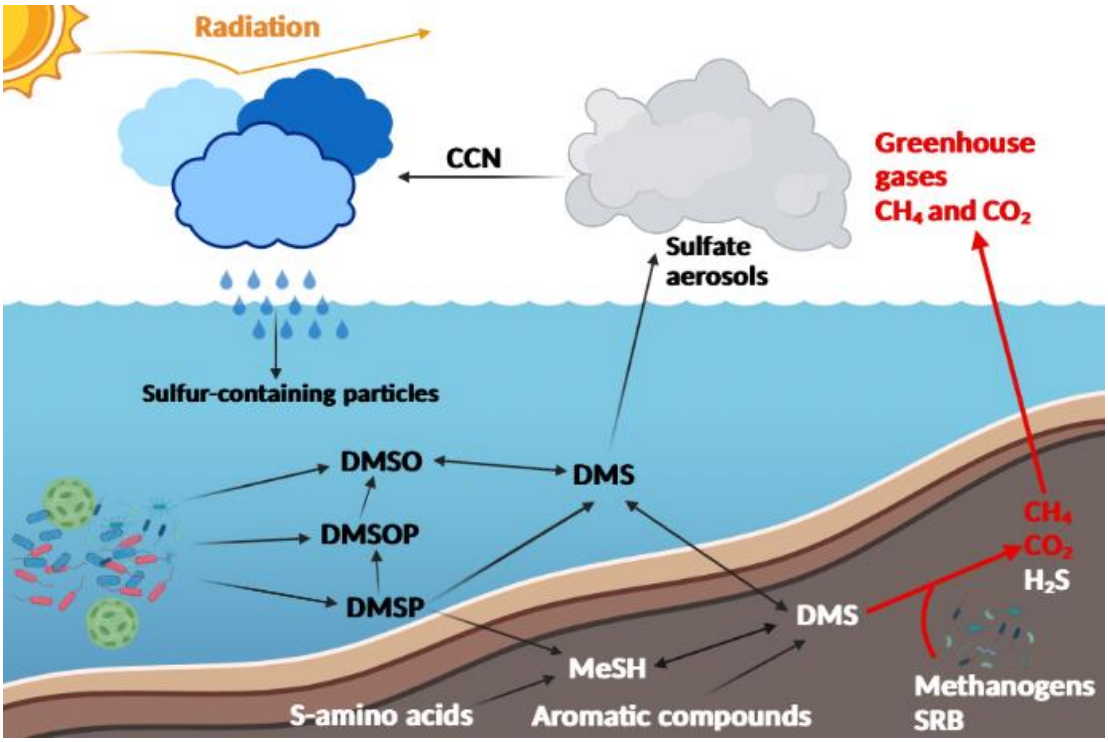

Figure 1.2. A simplified graph summarising the various sources and sinks of DMS in the atmosphere, the water column and sediments. Created with BioRender.com.

1.4.1.1 DMSP breakdown

In saline environments, DMS is, primarily, the breakdown product of DMSP, which is released from cells and dissolved in the environment after viral attacks, zooplankton grazing, oxidative stress, and/or senescence (Dacey and Wakeham, 1984; Matrai and Keller, 1993; Dacey *et al.*, 1994; Wolfe *et al.*, 1994; Wolfe and Steinke, 1996; Malin *et al.*, 1998). The majority of the released DMSP remains in the water column in dissolved form but some of it is degraded to DMS after it is cleaved with DMSP lyases found in microorganisms and some eukaryotes (Yoch, 2002; Johnston *et al.*, 2008; Alcolombri *et al.*, 2015).

There are currently four known superfamilies containing DMSP lyases, known as "Ddd+" (DMSP-dependent DMS releasing) enzymes (Todd *et al.*, 2007). Only one eukaryotic DMSP lyase family, Alma, has been identified thus far from algae and corals (Alcolombri *et al.*, 2015).

DMS production from DMSP is not seen as often in freshwater ecosystems but examples of this production pathway still exist. Ginzburg *et al.* (1998) were able to show that blooms from the freshwater dinoflagellate *Peridinium gatunense* caused DMS production in the freshwater lake Sea of Galilee (Israel). Furthermore, Yoch *et al.* (2001) showed that after addition of DMSP to river sediments, certain Gram-positive bacteria of the genus *Rhodococcus* could produce DMS.

1.4.1.2 MeSH methylation

MeSH can be methylated to DMS by some aerobic bacteria via the MeSH-dependent DMS production pathway (Mdd), which involves the gene *mddA* (Carrión *et al.*, 2015). MddA is a membrane-bound S-adenosyl-Met-dependent methyltransferase, which produces MeSH via S-methylation. A wide range of phylogenetically distinct bacteria contain the *mddA* gene. Isolation studies using soils (grassland, forest and agricultural) and sediments (lake, river and marine) showed strains of *Pseudomonas*, *Acinetobacter*, *Gemmobacter*, *Phyllobacterium*, *Rhizobium*, *Ensifer*, and *Sinorhizobium* convert MeSH to DMS (Carrión *et al.*, 2017).

1.4.1.3 DMSO reduction

DMSO can be reduced to DMS in animals (cats, cows), plants and various bacteria (e.g. *Escherichia coli*, *Salmonella paratyphi, Morganella morganii*; Ando *et al.*, 1957; Distefano and Borgstedt, 1964; Smale *et al.*, 1975; Tiews *et al.*, 1975). Zinder and Brock (1978) showed DMSO was reduced to DMS during anaerobic incubations of lake sediments and sewage sludge. Later studies showed DMSO is reduced to DMS via a DMSO respiration complex, DmsABC (McCrindle *et al.*, 2005).

In anaerobic sediments, DMSO reduction to DMS by SRB can be coupled to methane oxidation since SRB are known to form symbiotic consortia with methane oxidising bacteria in sulfate-rich environments (Jonkers *et al*., 1996; Orphan *et al.*, 2001). This coupling of DMSO reduction and methane oxidation could reduce the amount of methane observed following the degradation of

DMS to methane (see section 1.6). On the other hand, some research suggests DMSO could be inhibitory for methane oxidation (Saari and Martikainen 2003).

1.4.1.4 Sulfur-containing amino acid degradation

Methionine and cysteine are essential sulfur-containing protein amino acids, unlike homocysteine and taurine, which are also sulfur-containing amino acids but do not get incoorporated into proteins. Methionine normally serves as a precursor for cysteine and can be synthesised from carbohydrates, organic and inorganic nitrogen and sulfur sources in most plants, fungi and bacteria (Willke, 2014). Algal decomposition has been suggested as a major source of methionine in aquatic environments (Lu *et al.*, 2013).

Methionine and cysteine can both lead to the production of MeSH, which can be methylated to DMS. Zinder and Brock (1978) showed that methionine degradation produced MeSH in the anoxic sediments of Lake Mendota (Wisconsin, USA). Likewise, Kiene and Capone (1988) showed MeSH production after methionine and S-methyl cysteine addition in anoxic sediment collected from Flax Pond saltmarsh dominated by *Spartina alterniflora* (New York, USA). MeSH is produced by demethiolation (removal of the CH_3SH group) of the sulfur-containing amino acids, catalysed by methionine γ-lyase (Bentley and Chasteen, 2004). A similar enzyme S-alkylcysteine lyase catalyses the demethiolation of S-methylcysteine (Esaki and Soda, 1987; Bentley and Chasteen, 2004). The demethylation of S-methylcysteine can also be catalysed by the methionine γ-lyase (Kadota and Ishida, 1972). Once MeSH is produced it can be methylated to DMS.

1.4.1.5 Methoxylated aromatic compound demethylation

The methyl goups of methoxylated aromatic compounds (syringic acid, syringate and 3,4,5-trimethoxybenzoate) can give rise to DMS in both freshwater and marine environments (Finster *et al.*, 1990; Bak *et al.*, 1992; Kiene and Hines, 1995). Bak *et al.* (1992) isolated acetogenic *Pelobacter* bacteria (strains TMBS4 and SA2) able to use compounds such as syringate and 3,4,5-trimethoxybenzoate to form MeSH and DMS. Generally, growing on methoxylated aromatic compounds involves demethylation of the methoxy groups catalysed by a methyltransferase (Kiene and Hines, 1995). The methyl- group is then accepted either by sulfide to produce MeSH or MeSH to produce DMS (Lomans *et al.*, 2001)

1.4.2 Sinks of DMS

The multiple pathways mentioned above result in the production of large quantities of DMS but only about 10% of the produced DMS is released into the atmosphere (Schäfer *et al.*, 2010). Instead, the majority of DMS is used as a sulfur, carbon and energy source by microorganisms (Figure 1.2; Zeyer *et al.*, 1987; Smith and Kelly, 1988; Kiene and Bates, 1990; Fuse *et al.*, 2000).

DMS can be degraded in both oxic and anoxic environments including soils, plant rhizospheres, seawater, marine algae cultures, microbial mats and humans (Schäfer *et al.*, 2010). Below I have briefly documented on aerobic DMS degradation as a carbon and energy source but the main focus of this PhD is the anaerobic degradation of DMS, which I expand on in section 1.6.

DMS can be oxidised photochemically to DMSO as described by Brimblecombe and Shooter (1986). Furthermore, a biotic route to DMSO production via DMS degradation involves purple phototrophic bacteria such as *Rhodovulum sulfidophilum* growing on DMS by using it as an electron donor (Hanlon *et al.*, 1994). Overall, in phototrophic bacteria, DMS is oxidised to DMSO in order to provide an electron donor for the fixation of CO_2 (Zeyer *et al.*, 1987). Certain phototrophic green sulfur bacteria can also use DMS when growing on thiosulfate, hydrogen sulfide and other reduced sulfur compounds (Vogt *et al.*, 1997).

Zhang *et al.* (1991) were the first to document *Pseudomonas acidovorans* DMR-11 (now *Delftia acidovorans*) producing DMSO from DMS during heterotrophic DMS metabolism with no DMS carbon assimilation. This pathway was also shown in *Sagittula stellata* E-37 (Gonzalez *et al.*, 1997). Another bacterium known to oxidise DMS is *Acinetobacter* sp. strain 20B from which the enzyme catalysing DMS oxidation, dimethylsulfide oxygenase, was characterised (Horinouchi *et al.*, 1997, 1999). Another heterotrophic bacterium *Ruegeria pomeroyi* can also oxidise DMS to DMSO via a trimethylamine monooxygenase (Tmm; Lidbury *et al.*, 2016). Interestingly, Tmm is present in about 20% of bacteria in marine surface waters so DMSO could be an even bigger DMS sink than originally thought (Chen *et al.*, 2011).

DMS can also lead to the production of MeSH. During this pathway a dissimilatory dimethylsulfide monooxygenase (DmoAB) converts DMS to MeSH and formaldehyde (de Bont *et al.*, 1981). DmoAB was first purified and characterised from *Hyphomicrobium sulfonivorans*,

a bacterium isolated from garden soil, but has also been found in many other organisms, including *Hyphomicrobium* sp. S, *Hyphomicrobium* sp. EG, and *Thiobacillus thioparus* T5 (de Bont *et al.*, 1981; Suylen *et al.*, 1987; Visscher *et al.*, 1991; Borodina *et al.*, 2000; Boden *et al.*, 2011). The produced MeSH can then be further degraded to formaldahyde, hydrogen peroxide and hydrogen sulfide using the methanethiol oxidase (MTO) as shown by Eyice *et al.* (2018) in the DMS-degrading *Hyphomicrobium* sp. VS.

In anoxic environments DMS can be degraded by methylotrophic methanogens (methane production using one-carbon compounds) and SRB in salt marshes, estuaries and freshwater ecosystems as outlined in section 1.6 (Kiene *et al.*, 1986; Kiene and Capone, 1988; Lomans *et al.*, 1999; Lyimo *et al.*, 2009; Tsola *et al.*, 2021).

1.5 Methanogenesis

Methane is one of the most potent greenhouse gases in the atmosphere with ~28 times more global warming potential than CO_2 over a 100-year period (Saunois *et al.*, 2020). Methane also contributes to the Earth's radiative forcing via interacting with infrared radiation and being a precursor of tropospheric ozone, another important greenhouse gas (Fiore *et al.*, 2015; Monks *et al.*, 2015).

Methane production (methanogenesis) occurs in anoxic sediments as well as anaerobic digestors, landfills and the gut of many animals (Ciais *et al.*, 2013; Fiore *et al.*, 2015; Kallistova *et al.*, 2017). Anthropogenic activity and animals emit 500-600 Tg of methane per year, which is equal

to about 64% of the total methane emissions (Conrad, 2009; Kallistova *et al.*, 2017). The other 36% is emitted from natural sources such as wetlands, estuaries and rivers (Kallistova *et al.*, 2017).

Methanogenesis is carried out by methanogenic archaea, which are strict anaerobes. Despite their narrow metabolic specialization they are geographically and phylogenetically diverse. Methanogens can produce methane using H_2/CO_2, formate, acetate and methylated compounds such as methanol and DMS (Kallistova *et al.*, 2017).

There are three pathways of methanogenesis: hydrogenotrophic, acetoclastic, and methylotrophic. In all three pathways, the final step is catalysed by methyl-coenzyme M reductase (Mcr), making it the key enzyme of methanogenesis (Thauer, 2019).

1.5.1 Hydrogenotrophic methanogenesis

Hydrogenotrophic methanogenesis involves the reduction of CO_2 to methane using hydrogen as the electron donor (Figure 1.3). Formate and more rarely ethanol, carbon monoxide and secondary alcohols can also be used as electron donors (Liu and Whitman, 2008). This methanogenesis pathway is the most common among the described methanogens and occurs in six out of the eight methanogen orders: *Methanobacteriales, Methanococcales, Methanomicrobiales, Methanosarcinales, Methanopyrales*, and *Methanocellales* (Liu and Whitman, 2008; Sakai *et al.*, 2008; Thauer *et al.*, 2008).

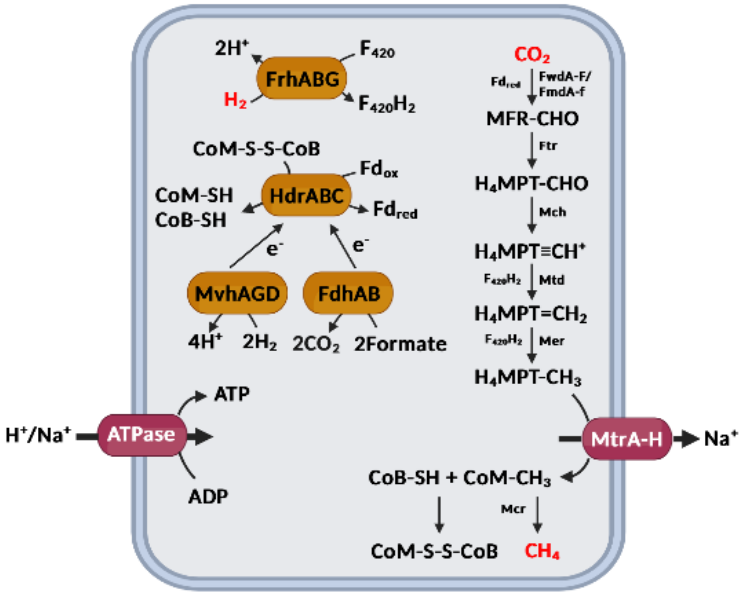

Figure 1.3. Hydrogenotrophic methanogenesis pathway. FwdA-F/FmdA-F: formylmethanofuran dehydrogenase, Ftr: formylmethanofurantetrahydromethanopterin formyltransferase, Mch: methenyltetrahydromethanopterin cyclohydrolase, Mtd: methylenetetrahydromethanopterin dehydrogenase, Mer: 5,10- methylenetetrahydromethanopterin reductase, MtrA-H: tetrahydromethanopterin S-methyltransferase, Mcr: methylcoenzyme M reductase, FrhABG: coenzyme F_{420}-reducing hydrogenase, HdrABC: soluble heterodisulfide reductase, MvhAGD: F_{420}-non-reducing hydrogenase, FdhAB: formate dehydrogenase, ATPase: ATP synthase, CoB: coenzyme B, CoM: coenzyme M, H_4MPT: tetrahydromethanopterin, MFR: methanofuran, Fd: ferredoxin, $F_{420}H_2$: reduced coenzyme F_{420}, MP: methanophenazine. This figure was adapted from Kurth *et al.*, 2020 under CC BY 4.0 and created with BioRender.com.

1.5.2 Acetoclastic methanogenesis

In acetoclastic methanogenesis, acetate is dismutated and the carboxyl-group is oxidised to CO_2 whereas the methyl-group is reduced to methane (Figure 1.4). Acetoclastic methanogenesis is

only performed by the genera *Methanosarcina* and *Methanothrix* (previously *Methanosaeta*) of the order *Methanosarcinales* (Liu and Whitman, 2008). Acetoclastic methanogenesis is considered the least diverse methanogenesis pathway (Liu and Whitman, 2008).

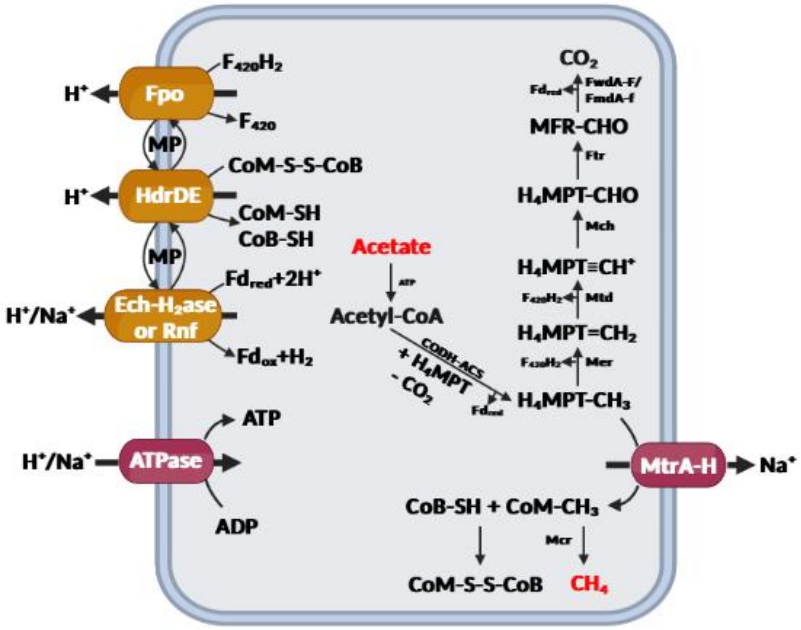

Figure 1.4. Acetoclastic methanogenesis pathway. FwdA-F/FmdA-F: formylmethanofuran dehydrogenase, Ftr: formylmethanofurantetrahydromethanopterin formyltransferase, Mch: methenyltetrahydromethanopterin cyclohydrolase, Mtd: methylenetetrahydromethanopterin dehydrogenase, Mer: 5,10- methylenetetrahydromethanopterin reductase, MtrA-H: tetrahydromethanopterin S-methyltransferase, Mcr methylcoenzyme M reductase, FpoA-O: $F_{420}H_2$ dehydrogenase, HdrDE: membrane-bound heterodisulfide reductase, Ech-H_2ase: energy-converting hydrogenase, Rnf: Na^+-translocating ferredoxin:NAD^+ oxidoreductase complex, ATPase: ATP synthase, CODH-ACS: Acetyl-CoA decarbonylase/synthase, CoB: coenzyme B, CoM: coenzyme M, H_4MPT: tetrahydromethanopterin, MFR: methanofuran, Fd: ferredoxin, $F_{420}H_2$: reduced coenzyme F_{420}, MP: methanophenazine. This figure was adapted from Kurth *et al.*, 2020 under CC BY 4.0 and created with BioRender.com.

1.5.3 Methylotrophic methanogenesis

Methylotrophic methanogenesis involves the metabolism of methylated compounds such as methanol, methylamines, DMS and MeSH to produce methane (Figure 1.5). This pathway is carried out by members of the orders *Methanosarcinales*, *Methanobacteriales* and *Methanomassiliicoccales* and can be classified in two groups based on the presence or absence of cytochromes. Methylotrophs with cytochromes gain the required electrons for the reduction of the methyl-groups via the oxidation of additional methyl-groups to CO_2. Methylotrophs lacking cytochromes require external hydrogen as their electron donor (Liu and Whitman, 2008; Thauer *et al.*, 2008; Vanwonterghem *et al.*, 2016).

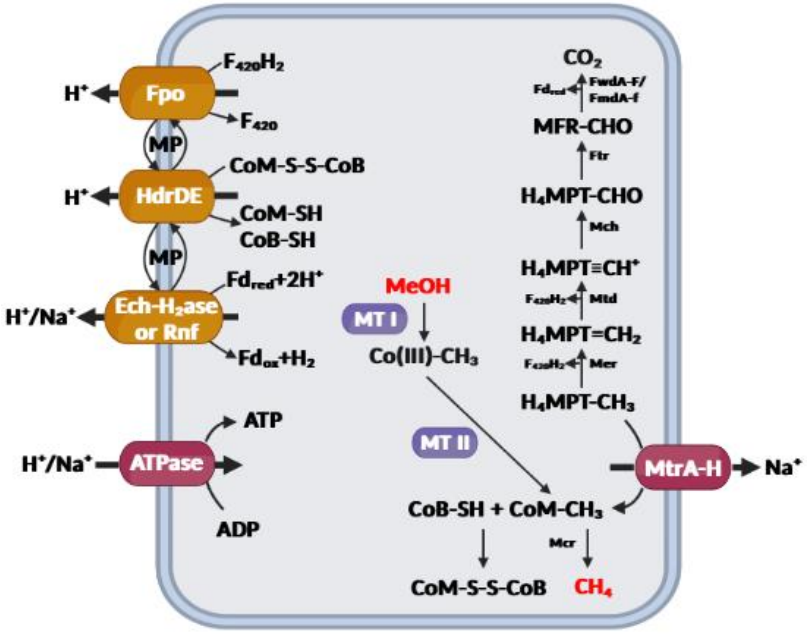

Figure 1.5. Methylotrophic methanogenesis pathway. FwdA-F/FmdA-F: formylmethanofuran dehydrogenase, Ftr: formylmethanofurantetrahydromethanopterin formyltransferase, Mch: methenyltetrahydromethanopterin cyclohydrolase, Mtd: methylenetetrahydromethanopterin dehydrogenase, Mer: 5,10- methylenetetrahydromethanopterin reductase, MtrA-H: tetrahydromethanopterin S-methyltransferase, Mcr: methylcoenzyme M reductase, FpoA-O: $F_{420}H_2$ dehydrogenase, HdrDE: membrane-bound heterodisulfide reductase, Ech-H_2ase: energy-converting hydrogenase, Rnf: Na^+-translocating ferredoxin:NAD^+ oxidoreductase complex, ATPase: ATP synthase, MTI and MTII: methyltransferase, CoB: coenzyme B, CoM: coenzyme M, H_4MPT: tetrahydromethanopterin, MFR: methanofuran, Fd: ferredoxin, $F_{420}H_2$: reduced coenzyme F_{420}, MP: methanophenazine. This figure was adapted from Kurth *et al.*, 2020 under CC BY 4.0 and created with BioRender.com.

1.6 Diversity of anaerobic microorganisms degrading DMS

1.6.1 DMS-degrading methanogens

Methanogenic archaea that degrade DMS in anoxic environments follow the methylotrophic methanogenesis pathway and have been isolated from estuaries, saline lakes and various other freshwater and marine ecosystems (Kiene *et al*., 1986; Liu *et al.*, 1990; Kadam *et al.,* 1994; Lomans *et al.*, 1999). The isolates were from various genera including *Methanolobus*, *Methanomethylovorans*, *Methanosarcina*, and *Methanosalsus* (Table 1.1).

Table 1.1. Isolated methanogenic archaea able to degrade DMS. The "Substrates" column contains all substrates besides DMS each isolate has been shown to utilise for their growth. Me: Methanol; Ma: Methylamines, MeSH: Methanethiol; Ac: acetate.

Methanogen	**Substrates**	**Reference**
Methanolobus taylorii	Me, Ma, MeSH	(Kiene *et al.*, 1986; Oremland *et al.*, 1989; Oremland and Boone, 1994)
Methanolobus bombayensis	Me, Ma, MeSH	(Kadam *et al.*, 1994)
Methanolobus oregonensis	Me, Ma, MeSH	(Liu *et al.*, 1990)
Methanosarcina siciliae	Me, Ma, MeSH, Ac	(Ni and Boone, 1991; Elberson and Sowers, 1997)
Methanosarcina acetivorans	Me, Ma, MeSH, Ac	(Sowers *et al.*, 1984)
Methanosarcina semesiae	Me, Ma, MeSH	(Lyimo *et al.*, 2000)
Methanohalophilus zhilinae	Me, Ma, MeSH, Ac	(Boone *et al.*, 1986; Mathrani *et al.*, 1988)
Methanomethylovorans hollandica	Me, Ma, MeSH	(Lomans *et al.*, 1999)

During DMS degradation by methanogens, 1 mol of DMS is degraded to 1.5 moles of methane and 0.5 moles of CO_2 (Equation 1; Finster *et al.*, 1992; Scholten *et al.*, 2003).

$$(CH_3)_2S + 1.5H_2O \rightarrow 1.5CH_4 + 0.5HCO_3^- + HS^- + 1.5H^+ \quad (1)$$

$\Delta G^{o\prime}$=-69.6 kJ/mol DMS

The pathway of DMS degradation to methane production follows Figure 1.5 but a closer view specific to DMS is provided in Figure 1.6. Overall, the metabolism of DMS-degradation is not well studied. The few studies on DMS metabolism that have been conducted thus far showed that in *Methanosarcina barkeri* and *M. acetivorans* methylthiol:coenzyme M methyltransferase (MtsAB), specifically polypeptide MtsA, tranfers the methyl group from DMS to a methanethiol corrinoid protein leading to the release of MeSH (Tallant and Krzycki, 1997; Tallant *et al.*, 2001; Fu and Metcalf, 2015). The same methyltransferase, MtsA, transfers the methyl group from the corrinoid protein to coenzyme M (CoM) forming methyl-CoM (Tallant *et al.*, 2001). Methyl-CoM is then reduced to methane in a reductive demethylation reaction catalysed by methyl-coenzyme M reductase (Mcr; Thauer, 2019).

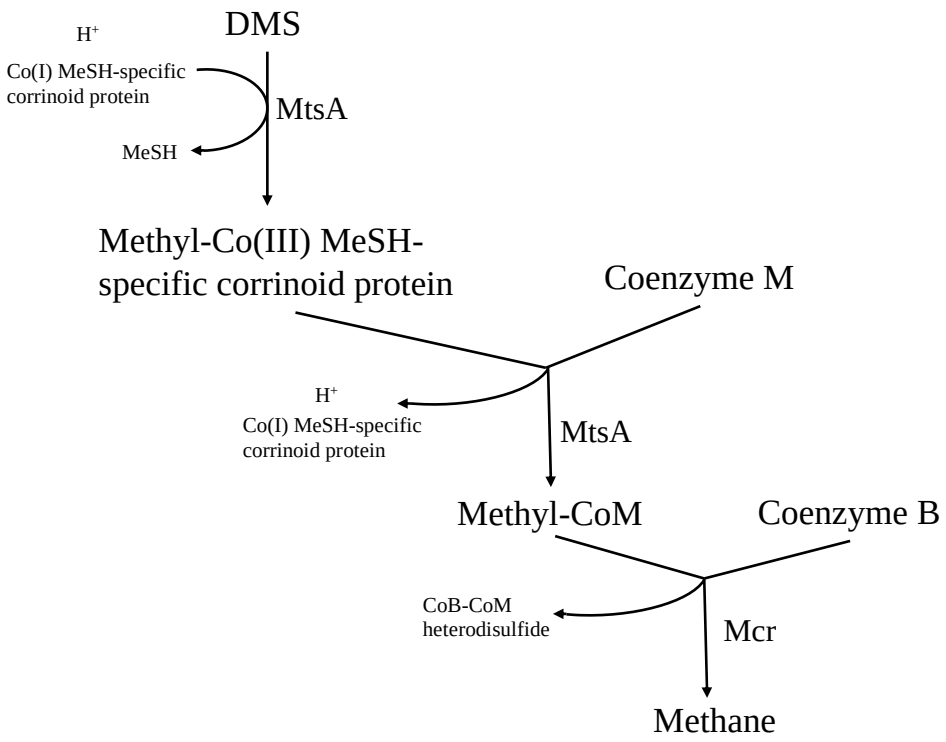

Figure 1.6. Methanogenesis pathway via DMS in *Methanosarcina barkeri* and *M. acetivorans*. MeSH: Methanethiol; MtsA: methylthiol:coenzyme M methyltransferase polypeptide A; CoB: Coenzyme B; CoM: Coenzyme M; Mcr: methyl-coenzyme M reductase.

1.6.2 DMS-degrading SRB

DMS is one of the numerous substrates SRB can grow on yet very few species that degrade DMS have been cultivated so far (Tanimoto and Bak, 1994; Lomans *et al.*, 2002; Lyimo *et al.*, 2009). Tanimoto and Bak (1994) isolated gram-positive *Desulfotomaculum* strains (TDS2 and SDN5) that can degrade DMS from thermophilic fermentor sludge. Another SRB, *Desulfosarcina* strain SD1 was isolated from mangrove sediments (Lyimo *et al.*, 2009).

During DMS degradaton by SRB, 1 mol of DMS is degraded to 2 moles of CO_2 (Equation 2; Tanimoto and Bak, 1994; Scholten *et al.*, 2003).

$$(CH_3)_2S + 1.5SO_4^{2-} \rightarrow 2HCO_3^- + 2.5HS^- + 1.5H^+ \quad (2)$$

$\Delta G^{o`}$=-94.5 kJ/mol DMS

Despite having identified some SRB able to degrade DMS, the genetic basis of this process remains unexplored. Most evidence for the degradation of DMS by SRB originates from inhibitor studies, a common practise when examining the role of individuals in mixed microbial communities. Molybdate (MoO_4^{2-}) and tungstate (WO_4^{2-}) are the most commonly used SRB inhibitors, since both are group VI anions which share many chemical similarities with sulfate (SO_4^{2-} ; Ishimoto *et al.*, 1954; Peck Jr., 1959; Banat and Nedwell, 1984).

The first SRB inhibition study to explore DMS degradation was by Oremland and Taylor (1978), where they used molybdate to inhibit sulfate-reduction to separate sulfidogenesis from methanogenesis in anoxic marine sediments. Lyimo *et al.* (2009) using a similar experiment where they selectively inhibited SRB and methanogens, showed that DMS degradation was dominated by SRB in anoxic mangrove sediments. A drawback of these inhibition studies is that molybdate and tungstate are known cofactors for numerous enzymes so these inhibitors could affect the activity of non-SRB microorganisms (Schwarz *et al.*, 2009; Seelmann *et al.*, 2020). The redox potential could also be affected since molybdate forms complexes with sulfides, lowering the concentration of available free sulfides (Lustwerk and Burdige, 1995). These

complexes could also intefere with the activity of microorganisms requiring sulfide as their sulfur source (Lomans *et al.*, 2002).

1.6.3 Interactions between DMS-degrading methanogens and SRB

SRB and methanogens potentially compete for DMS in saline environments where sulfate is available (Kiene *et al.*, 1986; Kiene, 1988). Generally, competition between microorganisms depends on the kinetic properties of the interacting microbial groups, for example their maximum growth rate and substrate affinity (Mattei *et al.*, 2015). In this case, it would also depend on the sulfate availability since SRB require it for their metabolic needs. Studies have shown that SRB have higher affinity for hydrogen and acetate thus outcompeting methanogens for these substrates, leading to methanogenesis becoming dominant only when sulfate has been depleted (Oremland and Taylor, 1978; King *et al.*, 1983; King, 1984). However, little research has been conducted on the affinity and growth rates of methanogens and SRB on DMS.

Many studies on DMS degradation that used SRB (tungstate or molybdate) and methanogen inhibitors (sodium 2-bromoethanesulfonate), showed that SRB outcompeted methanogens in anoxic marine sediments when DMS was in low concentrations (Zinder *et al.*, 1984; Kiene and Visscher, 1987; Kiene, 1988; Lie *et al.*, 1999; Lyimo *et al.*, 2002, 2009; Zhuang *et al.*, 2012). This was further supported by studies showing *Desulfosarcina* sp. strain SD1 having a DMS and MeSH affinity constant of <0.5 μM suggesting that in environments with low DMS concentrations, SRB were more likely to dominate DMS degradation over methanogens (Lyimo *et al.*, 2009).

The opposite has been shown when DMS was in high concentrations. *Desulfosarcina* sp. strain SD1 had a low growth rate on DMS (0.01 h^{-1}) compared to a previously isolated mangrove methanogen *Methanosarcina semesiae* (0.07 h^{-1}) which would explain why methanogens outcompete SRB when DMS concentrations are high (Lyimo *et al.*, 2000, 2009).

On the other hand, in freshwater environments where sulfate is a limiting factor, DMS was mainly converted to methane, suggesting methanogens were more active than SRB, which require sulfate (Lomans *et al.*, 1997; Lomans *et al.*, 1999; Lyimo *et al.*, 2009).

1.7 Aims and objectives

Methanogens and SRB can degrade DMS in anoxic sediments depending on sulfate availability, producing methane and CO_2, both important greenhouse gases. Despite their importance, only little is known about the diversity and metabolism of DMS-degrading microorganisms in anoxic environments.

The aim of this PhD project was to explore the potential for DMS-degradation and the diversity, metabolism and abundance of DMS-degrading microorganisms in anoxic sediments.

During this project, I had six main hypotheses:

i. DMS degradation is a widespread and important process for methane generation in anoxic sediments.
ii. Different anoxic sediments have different microbial communities that degrade DMS.
iii. Methanogens are the most prevalent DMS degraders in anoxic freshwater sediments.
iv. SRB and methanogens actively degrade DMS in saline environments.
v. Active DMS-degrading methanogens express methylthiol:coenzyme M methyltransferase (MtsAB).
vi. DMS-degrading SRB express the dissimilatory sulfate reduction genes *dsrAB*, *aprAB* and *sat*.

These hypotheses entail the exploration of the communities that anaerobically degrade DMS in selected ecosystems. To achieve this, the project was separated into specific objectives:

i. Identify DMS-degrading microorganisms in anoxic sediments along the sulfate gradient of an estuary.
ii. Identify DMS-degrading microorganisms in riverine sediments.
iii. Characterise the depth-profile of DMS-degrading microorganisms in Baltic Sea sediments following a phytoplankton bloom.
iv. Characterise the metabolic pathways of DMS degrading populations in anoxic sediments.

2 Materials and methods

2.1 Incubation set-up

All sediment samples were collected from various sites using corers and were transported to the Queen Mary University of London laboratories at 4 ^{o}C. The sediment was extracted from the corers using a sterile syringe plunger and the 3-10 cm sediment depth section (besides Chapter 5 where different sections were used – Table 5.1) was separated and homogenised for further analysis, namely DNA extraction and setting up incubations. The incubations (3-5 replicates) were set up in serum bottles (140 mL – Chapters 3 and 4; 50 mL – Chapter 5; Wheaton, USA) and contained 2.5-10 g of sediment and 20-40 ml of artificial seawater (ASW). The ASW consisted of 0.32 M NaCl, 10 mM $MgSO_4 \cdot 7H_2O$, 8.8 mM $NaNO_3$, 3.1 mM $CaCl_2 \cdot 2H_2O$, 10 mM $MgCl_2 \cdot 6H_2O$, 9 mM Trizma base, 0.21 mM $K_2HPO_4 \cdot 3H_2O$, trace elements, and vitamins (Wyman *et al.*, 1985; Wilson *et al.*, 1996).

Both vitamin and trace elements solutions were mixed using the protocol in DSMZ's media 141, with minor amendments to the trace elements solution to contain $FeC_6H_6O_7$ (5 g) instead of $N(CH_2CO_2H)_3$ and no $Na_2WO_4 \cdot 2\ H_2O$. Full-strength ASW was used for all marine sediment incubations, whereas the ASW was diluted to 50% and 1% with sterile distilled water for brackish and freshwater sediment incubations, respectively. The sulfate concentrations in the incubations were adjusted according to published data and *in situ* measurements for each sampling site.

Each sample was amended with DMS as the only energy and carbon source. At the beginning of the incubation experiments, all samples were amended with 2 μmol g^{-1} DMS. When this first DMS addition was depleted, another 2-4 μmol g^{-1} DMS were added. After the DMS was depleted, 4-8 μmol g^{-1} DMS were amended to the incubations and each subsequent DMS amendment. This incremental DMS addition was done to avoid DMS toxicity.

Two sets of controls were established in triplicate alongside the incubations with DMS. One set contained no DMS to monitor biological activity not directly attributed to DMS. The second set had DMS and thrice autoclaved sediment to monitor the sediment adsorption of DMS. All incubations were placed in the dark to avoid the photochemical destruction of DMS (Brimblecombe and Shooter, 1986).

At the end of the incubation period, 3 mL of slurry were removed with a gas-tight syringe and transferred to gas-tight vials (3 mL Exetainer, Labco, UK). After this, each serum bottle was opened, and the remaining slurry was transferred into a 50 mL centrifuge tube for centrifugation at 1,000 rpm for 6 min (ALC laboratory centrifuges PK131R, UK). The supernatant was decanted into a 15 mL centrifuge tube, and the sediment was kept intact in the 50 mL centrifuge tube. Both tubes were placed at -20 and -80 ^{o}C, respectively, until further analysis.

2.2 Analytical measurements

During the incubation experiments, a 500 µL gas-tight syringe (Hamilton, UK) was used to sample 100 µL of headspace gas from each serum bottle. DMS was measured using a gas chromatograph (Agilent Technologies, 6890A Series, USA) fitted with a flame photometric detector (FPD) and a J&W DB-1 column (30 m x 0.32 mm Ø; Agilent Technologies, USA). The oven temperature was set at 180 ºC, and zero grade N_2 (BOC, UK) was used as the carrier gas (26.7 mL min^{-1}). FPD run at 250 ºC with H_2 and air (BOC, UK) at a flow rate of 40 and 60 mL min^{-1}, respectively. DMS standards were prepared by diluting >99% DMS (Sigma-Aldrich, USA) in distilled water previously made anaerobic with N_2 (oxygen-free, BOC, UK). DMS concentrations were calculated from peak areas calibrated against these standards.

Methane and CO_2 were measured using a gas chromatograph (Agilent Technologies, USA, 6890N Series) fitted with a flame ionisation detector (FID), Porapak (Q 80/100) packed stainless steel column (1.83 m x 3.18 mm Ø; Supelco, USA), and hot-nickel catalyst which reduced CO_2 to methane (Agilent Technologies, USA; Sanders *et al.*, 2007). The oven temperature was set at 30 ºC, and zero grade N_2 (BOC, UK) was used as the carrier gas (14 mL min^{-1}). FID run at 300 ºC with H_2 and air (BOC, UK) at a flow rate of 40 and 430 mL min^{-1}, respectively. The methane and CO_2 concentrations were calculated from the gas chromatograph peak areas after calibrating them against certified gas mixture standards (100 ppm methane, 3700 ppm CO_2, 100 ppm N_2O, balance N_2; BOC, UK).

All methane concentrations were corrected for the headspace-water partitioning using Henry's law (based on Wiesenburg and Guinasso, 1979) to calculate the total methane in each microcosm. Methane gas solubility (Bunsen) coefficients were calculated for each sampling location (Table 2.1) due to changes in salinity, according to the equation:

$$\ln b = A_1 + A_2\,(100/T) + A_3\,\ln(T/100) + S\,[B_1 + B_2\,(T/100) + B_3\,((T/100)^2)]$$

where b is the Bunsen coefficient, A_i and B_i are constants, T is the temperature in degrees Kelvin, and S is the salinity in parts per thousand (Wiesenburg and Guinasso, 1979).

Table 2.1. Bunsen coefficient for each sampling location (Wiesenburg and Guinasso, 1979).

Site	Salinity (‰)	Bunsen coefficient
Freshwater	0.3	0.033
Brackish	6	0.032
Marine	32	0.027

The total production of CO_2 was the sum of the change of CO_2 in the headspace and the total dissolved inorganic carbon ($\Sigma DIC = CO_2 + HCO_3^- + CO_3^{2-}$) in the water phase. The CO_2 in the headspace was measured together with methane using a gas chromatograph. For the ΣDIC, after the termination of the experiments, 3 mL of supernatant from each incubation was collected with a syringe and transferred to 3 mL gas-tight vials (Exetainer, Labco, UK). The ΣDIC samples were fixed using 24 µL $ZnCl_2$ (50% w/v). Next, a 1 mL headspace was created in the 3 mL vials using a two-way system, where liquid was slowly removed while N_2 (oxygen-free, BOC, UK)

was introduced into the headspace. 100 µL 35% HCl were injected via the septa, the vials were shaken to acidify the samples fully, and CO_2 in the headspace was measured. The standard curve was created using an inorganic calibration series (0.1-8 mM) of Na_2CO_3 (Sigma-Aldrich, USA; Trimmer *et al.*, 2009; Shelley *et al.*, 2017).

Due to gas production, repeat addition of DMS and removal of headspace during the gas chromatography measurements, some pressure build-up was expected in the incubations. Despite this, a slight change in pressure was only observed in the incubation vials towards the end of the experiments. This could have resulted in an underestimation of the DMS, CO_2 and methane measurements at this point of the experiment but methane production had already reached stationary phase when the pressure change was observed.

For the sulfate measurements, porewater collected from the incubations was filtered using 0.2 µm syringe filters (PTFE hydrophilic; Fisher Scientific, USA). The filtered samples were analysed using an ICS-5000 Dual Gradient RFIC Ion Chromatograph (Thermo Fisher Scientific, USA) equipped with a Dionex IonPac AS11-HC-4 µm column (2x250 mm) and a Dionex IonPac AG11-HC-4 µm guard column (2x50 mm). For anion analysis, a gradient of 1.5-22 mM KOH (Dionex EGC 500 KOH, with CR-ATC column) was used as eluent.

2.3 General molecular techniques

2.3.1 DNA extraction

DNA was extracted from 0.25 g sediment using the DNeasy Powersoil kit (Qiagen, NL) following the manufacturer's instructions. 3 µL of each sample were mixed with 1 µL 6x DNA loading dye (Thermo Scientific, USA) and 2 µL ultra-pure water and viewed on a 0.8% agarose gel to determine if the DNA extractions were successful. DNA was quantified using the Qubit dsDNA BR Assay Kit and the Qubit 2.0 Fluorometer (Invitrogen, CA, USA).

2.3.2 Polymerase Chain Reaction (PCR)

2.3.2.1 General bacterial and archaeal gene

The V4 region of the bacterial and archaeal 16S rRNA genes was amplified using the universal primer set 515F (Parada) and 806R (Apprill) (515F: 5'-GTGCCAGCMGCCGCGGTAA-3', 806R: 5'-GACTACHVGGGTWTCTAAT-3'; Apprill *et al.*, 2015; Parada *et al.*, 2016). All PCRs were carried out using the iCycler thermal cycler (Bio-Rad, USA).

Each 16S rRNA PCR reaction contained 1 µL of DNA template, 0.5 µL of each primer (10 µM), 12.5 µL of OneTaq Quick-Load 2x Master Mix with standard buffer (NEB, USA), and 10.5 µL ultra-pure water. The PCR cycle started with an initial denaturation step at 94 ^{o}C for 30 sec. The amplification continued with 32 cycles of denaturation at 94 ^{o}C (30 sec), annealing at 55 ^{o}C (30 sec) and extension at 68 ^{o}C (30 sec). The PCR finished with a final extension step at 68 ^{o}C for 5 min. 5 µL of each sample were viewed after loading on a 1% agarose gel to determine if the PCR was successful.

All PCR products were cleaned using JetSeq Clean beads (1.4x; Meridian Bioscience, USA) following the manufacturer's instructions to remove free primers and primer dimers. The magnetic plate used during the PCR clean-up was DynaMag-96 Side Skirted (Invitrogen, USA), and the plate seals were Thermo Scientific's (USA) adhesive PCR film.

2.3.2.2 Methanogen marker gene

The archaeal-specific *mcrA* gene, which encodes the α-subunit of the methylcoenzyme M reductase, was used as the methanogen molecular marker. *mcrA* was amplified with a two-step PCR using the mcrIRD primer set (forward: 5'-TWYGACCARATMTGGYT-3', reverse: 5'-ACRTTCATBGCRTARTT-3'; Lever and Teske, 2015). All reactions were carried out using the iCycler thermal cycler (Bio-Rad, USA).

The initial PCR reaction contained 1 µL of DNA template, 1 µL of each primer (10 µM), 25 µL 2x MyTaq HS Red Mix (Meridian Bioscience, USA), and 22 µL ultra-pure water. The PCR consisted of a hot-start followed by 95 ^{o}C for 5 min and 39 cycles of 95 ^{o}C for 1 min, 51 ^{o}C for 1 min, 72 ^{o}C for 1 min. The final extension step was at 72 ^{o}C for 5 min. 5 µL of each sample were viewed on a 1% agarose gel to determine if the PCR was successful, and the PCR product was cleaned using JetSeq Clean beads (1.4x; Meridian Bioscience, USA).

2.3.2.3 SRB marker gene

The *dsrB* gene, used as the SRB molecular marker, encodes for the β-subunit of the dissimilatory sulfite reductase. *dsrB* was amplified using the primer mix DSR1728f (a-e) and rDSR4r (a-d) (Table 2.2; Vigneron *et al.*, 2018). All reactions were carried out using the iCycler thermal cycler (Bio-Rad, USA). The amplification consisted of a two-step PCR.

Table 2.2. Forward and reverse *dsrB* primer sequences (Vigneron *et al.*, 2018).

Forward Primers	Sequences (5'-3')	Reverse Primers	Sequences (5'-3')
DSR1728f-a	CAYACCCAGGGNTGG	rDSR4r-a	GTGTAACAGTTWCCRCA
DSR1728f-b	CAYACBCAAGGNTGG	rDSR4r-b	GTGTAGCAGTTDCCRCA
DSR1728f-c	CATACDCAGGGHTGG	rDSR4r-c	GTATAGCARTTGCCGCA
DSR1728f-d	CACACDCAGGGNTGG	rDSR4r-d	GTGAAGCAGTTGCCGCA
DSR1728f-e	CATACHCAGGGNTAY	-	-

The initial PCR reaction contained 1 µL of DNA template, 0.5 µL of each primer (five forward and four reverse primers; 25 µM), 12.5 µL 2x MyTaq Red Mix (Meridian Bioscience, USA), and 7 µL ultra-pure water. The cycle conditions consisted of 95 ^{o}C for 5 min, 25 cycles of 95 ^{o}C for 15 sec, 55 ^{o}C for 30 sec, 72 ^{o}C for 30 sec, and a final extension step at 72 ^{o}C for 7 min. 5 µL of each sample were viewed on a 1% agarose gel to determine if the PCR was successful, and the products were cleaned using JetSeq Clean beads (1.4x; Meridian Bioscience, USA).

2.4 High-throughput sequencing

2.4.1 Sample preparation

For the sequencing library preparation, a second *mcrA* and *dsrB* PCR was carried out to attach overhang adapters to the cleaned-up PCR products.

The *mcrA* reaction contained 2 µL of the clean PCR product, 0.5 µL of each primer containing the overhang adapters (10 µM), 12.5 µL 2x MyTaq HS Red Mix (Meridian Bioscience, USA), and 9.5 µL ultra-pure water. The reaction conditions included a hot-start followed by 95 ^{o}C for 3 min, 15 cycles of 95 ^{o}C for 20 sec, 55 ^{o}C for 15 sec, 72 ^{o}C for 15 sec and a final extension step at 72 ^{o}C for 5 min.

The *dsrB* reaction contained 2 µL of the clean *dsrB* PCR product, 0.1 µL of each primer containing the overhang adapters (25 µM), 12.5 µL 2x MyTaq Red Mix (Meridian Bioscience, USA), and 9.6 µL ultra-pure water. The reaction conditions were 95 ^{o}C for 5 min, 15 cycles of 95 ^{o}C for 15 sec, 60 ^{o}C for 30 sec, 72 ^{o}C for 30 sec and a final extension step at 72 ^{o}C for 7 min.

5 µL of each sample were viewed on a 1% agarose gel to determine the success of the PCR, and all products were cleaned using JetSeq Clean beads (1.4x; Meridian Bioscience, USA) following the manufacturer's instructions.

The PCR products from all three genes were further amplified for the addition of dual indices and Illumina sequencing adapters. Each reaction contained 2 µL of the clean PCR products, 1 µL of each primer (5 µM), 12.5 µL 2x Q5 Hot-start Ready mix (NEB, USA), and 8.5 µL ultra-pure water. The PCR program used was 98 ^{o}C for 3 min, 8 cycles of 98 ^{o}C for 20 sec, 55 ^{o}C for 15 sec, 72 ^{o}C for 15 sec and a final extension step at 72 ^{o}C for 5 min. 5 µL of each sample were viewed on a 1% agarose gel to determine if the PCR was successful. Following this, all samples were normalized using the SequalPrep Normalization Plate (96-well) kit (Invitrogen, USA), following the manufacturer's instructions, and sequenced using MiSeq Next Generation sequencing.

2.4.2 Amplicon sequencing analysis

The analysis of all amplicon sequencing data was performed using QIIME2 2019.1 (analysis in Chapter 3) and QIIME2 2021.11 (analysis presented in Chapters 4 and 5) on Queen Mary's Apocrita HPC facility, supported by QMUL Research-IT (King *et al.*, 2017; Bolyen *et al.*, 2019).

The FASTA files generated during sequencing were demultiplexed and imported into one QIIME artifact using the *qiime tools import* command with the –type 'SampleData[PairedEndSequencesWithQuality]' flag enabled. The artifact was then inserted into the DADA2 pipeline, implemented by the *qiime dada2* command in QIIME2 (Callahan *et al*., 2016). The DADA2 pipeline was used to trim the primer sequences, remove low-quality data, merge forward and reverse reads, and remove chimeras. Lastly, DADA2 assigned the data into Amplicon Sequence Variants (ASVs), which represent sequence variants down to the level of

single-nucleotide differences over the sequenced gene region (Callahan *et al.*, 2016). To analyse the sequences at the genus level, either ASVs were used (Chapters 4 and 5) or the ASVs were clustered into Operational Taxonomic Units (OTUs) using 99% (16S rRNA gene) and 85% (*mcrA* and *dsrB* genes) similarity thresholds (Chapter 3).

Taxonomy was assigned to the OTUs and ASVs using pre-trained Naive Bayes classifiers, trained using the feature-classifier command in QIIME2 (Bokulich *et al.*, 2018). The classifiers were trained using gene-specific databases. More specifically, the database used for the 16S rRNA samples was Greengenes 13.8 99% (DeSantis *et al.*, 2006) for the data presented in Chapter 3. For the data in Chapters 4 and 5, a custom-made SILVA database (Quast *et al.*, 2013) was constructed using RESCRIPt (Robeson *et al.*, 2021). Custom databases were used for the *mcrA* and *dsrB* samples, either created by Wilkins *et al.* (2015; *mcrA* gene; Chapter 3) and Pelikan *et al.* (2016; *dsrB* gene; Chapter 3) or prepared by me. My custom *mcrA* and *dsrB* databases were prepared using FunGenes (Fish *et al.*, 2013), Python 3.10.8 and the RESCRIPt (Robeson *et al.*, 2021) package in QIIME2 2021.11 (Bolyen *et al.*, 2019).

2.5 Quantitative polymerase chain reaction (qPCR)

Quantitative PCR (qPCR) of the *mcrA* and *dsrB* genes was carried out to quantify their copy number in the sediment samples using a CFX384 Touch Real-Time PCR Detection System (Bio-Rad Laboratories, USA).

mcrA qPCR was performed using the primers mlas-mod-F and mcrA-rev-R (forward: 5'-GGYGGTGTMGGDTTCACMCARTA-3', reverse: 5'-CGTTCATBGCGTAGTTVGGRTAGT-3'; Steinberg and Regan, 2009; Angel *et al.*, 2012). Each reaction contained 0.5 µL gDNA (normalised to the sample with the lowest concentration: 2 ng/µL – Chapter 3, 3 ng/µL – Chapter 4, and 4 ng/µL – Chapter 5), 0.1 µL of each primer (10 µM), 2.5 µL SensiFAST SYBR (No-ROX; Meridian Bioscience, USA), and 1.8 µL ultra-pure water. The *mcrA* cycling conditions were 95 ^{o}C for 3 min, followed by 40 cycles of 95 ^{o}C for 15 sec, 65 ^{o}C for 30 sec, and 72 ^{o}C for 20 sec.

dsrB was amplified using the primer mix dsrB_F1a-h and 4RSI1a-f (Table 2.3; Lever *et al.*, 2013). Each reaction contained 0.5 µL gDNA (normalised at 2 ng/µL – Chapter 3, 3 ng/µL – Chapter 4, and 4 ng/µL – Chapter 5), 0.5 µL BSA (10 mg/mL), 0.25 µL of each primer mix (mix contained 2 µM of each primer), 2.5 µL SsoAdvanced Universal SYBR Green Supermix (Bio-Rad Laboratories, USA), and 1 µL ultra-pure water. The cycling conditions for the *dsrB* gene were 98 ^{o}C for 2 min, followed by 45 cycles of 95 ^{o}C for 30 sec, 56 ^{o}C for 30 sec, and 72 ^{o}C for 20 sec, and a final step of 72 ^{o}C for 5 min.

Table 2.3. Forward and reverse *dsrB* qPCR primer sequences (Lever *et al.*, 2013).

Forward Primer	Sequences (5'-3')	Reverse Primer	Sequences (5'-3')
F1a	CACACCCAGGGCTGG	4RSI1a	CAGTTACCGCAGTACAT
F1b	CATACTCAGGGCTGG	4RSI1b	CAGTTACCGCAGAACAT
F1c	CATACCCAGGGCTGG	4RSI1c	CAGTTGCCGCAGTACAT
F1d	CACACTCAAGGTTGG	4RSI1d	CAGTTTCCGCAGTACAT
F1e	CACACACAGGGATGG	4RSI1e	CAGTTGCCGCAGAACAT
F1f	CACACGCAGGGATGG	4RSI1f	CAGTTTCCACAGAACAT
F1g	CACACGCAGGGGTGG	-	-
F1h	CATACGCAAGGTTGG	-	-

In Chapter 4, the 16S rRNA gene was used as a proxy of microbial biomass and was amplified using the universal primer set 515F (Parada) and 806R (Apprill) (515F: 5'-GTGCCAGCMGCCGCGGTAA-3', 806R: 5'-GACTACHVGGGTWTCTAAT-3'; Apprill *et al.*, 2015; Parada *et al.*, 2016). Each qPCR reaction contained 0.5 µL gDNA (normalised at 3 ng/µL), 0.1 µL of each primer (10 µM), 2.5 µL SensiFAST SYBR (No-ROX; Meridian Bioscience, USA), and 1.8 µL ultra-pure water. The cycling conditions for the 16S rRNA gene were 95 ^{o}C for 3 min, followed by 30 cycles of 95 ^{o}C for 10 sec, 55 ^{o}C for 15 sec, and 72 ^{o}C for 20 sec, and a final step of 72 ^{o}C for 5 min.

Standard curves were produced for the *mcrA* and *dsrB* genes using a serial 10-fold dilution of clones containing each gene. For the clone production, the genes were ligated into a pJET 1.2 vector using the CloneJET PCR Cloning kit (Thermo Fisher Scientific, USA) following the

manufacturer's instructions and then cloned into 5-alpha competent *Escherichia coli* cells (NEB, USA) via chemical transformation. The transformation reaction was spread on Luria-Bertani (LB) agar plates containing 100 µg/mL ampicillin (100 mg/mL) and incubated overnight at 37 °C. After incubation, colonies were randomly picked and their plasmid DNA was extracted using the Monarch plasmid miniprep kit (NEB, USA) following the manufacturer's instructions and sequenced using Eurofins Genomics' TubeSeq Service to confirm the cloning was successful. Plasmid DNA containing the correct gene inserts was used for the qPCR standard curve.

During 16S rRNA qPCR in Chapter 4, the standard curve consisted of a 16S rRNA gene amplified from pure *E. coli* DNA using the qPCR primers and the PCR conditions mentioned in Section 2.3.2.1. Following the amplification, the product was purified using the Monarch PCR and DNA clean-up kit (NEB, USA) as per the manufacturers instructions.

All qPCR reactions were set up in triplicate using a Mosquito HV (SPT Labtech, UK). After the final extension, a melt curve analysis was performed to detect non-specific DNA products by increasing the temperature from 65 °C to 95 °C in 0.5 °C increments.

The efficiency of all reactions was between 90% and 110%, and the R^2 value for the standard curves was >99%. All data were analysed using the CFXMaestro software for CFX Real-Time PCR Instruments (Bio-Rad Laboratories, USA). CFXMaestro automatically calculated the efficiency and R^2 values of the standard curve and generated a file containing all C_q values. Using this file, the gene copies g^{-1} sediment for all samples were calculated after

taking into consideration the gDNA normalisation performed for qPCR and the amount of sediment used during DNA extractions.

2.6 Statistical analysis

All amplicon sequencing results from Chapters 4 and 5 were transformed from QIIME 2 2021.11 artifacts (Bolyen *et al.*, 2019) to R (4.2.1) format (RStudio 2022.07.1; R Core Team, 2020) using R package qiime2R (Bisanz, 2018). Then, R package file2meco (Liu *et al.*, 2022) was used to import the data into the R package microeco (Liu *et al.*, 2021), which was used for all statistical analyses presented in Chapters 4 and 5. PAST (4.2) was used for all analyses in Chapter 3 (Hammer *et al.*, 2001).

The Shannon index (H) was calculated using PAST (Chapter 3; Hammer *et al.*, 2001) and microeco (Chapters 4 and 5; Liu *et al.*, 2021). The same package and software were also used for conducting permutation tests of multivariate homogeneity of group dispersions (999 permutations), including ANOVA and pairwise PERMANOVA (9999 permutations). The principal coordinate analyses (PCoA) with Bray-Curtis dissimilarity using the microbial abundance from Chapters 4 and 5 were plotted using microeco (Liu *et al.*, 2021), whereas principal component analyses (PCA) with the Chapter 3 data were conducted using PAST (Hammer *et al.*, 2001). Spearman's correlation analyses (r_s) between the first three PCA/PCoA coordinates and specific experimental variables, such as consumed DMS, produced methane and CO_2, and sulfate concentrations, were conducted using PAST (4.2; Hammer *et al.*, 2001).

All data in Chapters 4 and 5 were visualised using R (4.2.1) on RStudio (2022.07.1; R Core Team, 2020) and R package ggplot2 (Wickham, 2016). Data visualisation in Chapter 3 was conducted using Microsoft Excel (16.67).

2.7 Metagenomics

2.7.1 DNA sample preparation

Metagenomics analysis was conducted by the U.S. Department of Energy (DOE) Joint Genome Institute (JGI). All DNA samples were prepared according to the DOE JGI guidelines and quality criteria. Nanodrop One (Thermo Scientific, USA) was used for absorbance measurements. The $A_{260/280}$ ratio of the samples was between 1.6 and 2.0, whereas the $A_{260/230}$ ratio was between 1.8 and 2.2. Qubit 2.0 Fluorometer (Invitrogen, USA) was used to quantify the DNA and the samples had a concentration range of 23-87 ng/µL and a volume above 25 µL.

2.7.2 Metagenomics analysis

DOE JGI performed the metagenomics analysis following a well-established JGI-created workflow, which included steps on assembly, feature prediction, annotation and binning of metagenomic datasets (Clum *et al.*, 2021). The workflow was implemented following a 2x150 bp sequencing step on the Illumina NovaSeq 6000 platform. The data were then processed to remove contamination, adapter sequences and low-quality reads. After filtering, the reads were assembled with metaSPAdes (3.13.0; Nurk *et al.*, 2017) and mapped back to contigs using BBMap (38.44; Bushnell, 2014). The assembled contigs were then used for feature prediction. The workflow predicted noncoding RNA genes (tRNAs: tRNAscan-SE

2.0.6; Chan and Lowe, 2019, other noncoding RNA: cmsearch from the INFERNAL 1.1.3 package using the Rfam 13.0 database; Nawrocki and Eddy, 2013; Kalvari *et al.*, 2018), clustered regularly interspaced short palindromic repeats (CRISPR; JGI modified version of CRT-CLI 1.2; Bland *et al.*, 2007) and protein-coding genes (CDSs; Prodigal 2.6.3 and GeneMarkS-2 1.07; Hyatt *et al.*, 2010; Lomsadze *et al.*, 2018).

Functional annotation consisted of associating CDSs with KEGG orthology (KO) terms and Enzyme Commission (EC) numbers (lastal 1066 - LAST package; Kiełbasa *et al.*, 2011), clusters of orthologous genes (COGs; Galperin *et al.*, 2015) assignments, SMART (01_06_2016; Letunic and Bork, 2018) domains, SUPERFAMILY (1.75; Gough *et al.*, 2001) assignments, CATH-FunFam (4.2.0; Sillitoe *et al.*, 2019) annotations and Pfam (30; Finn *et al.*, 2016), and TIGRFAM (15.0; Haft *et al.*, 2013) annotations using HMMER 3.1b2 (Mistry *et al.*, 2013). Taxonomic annotation of the CDSs was completed using the best LAST hits during the KO term assignment during functional annotation.

MetaBAT (2.12.1; Kang *et al.*, 2015) generated genome bins using the assembled contigs. The genome bins were then analysed for contamination removal. Genome completion and contamination estimates were determined using CheckM (1.0.12; Parks *et al.*, 2015). Using the contaminations estimates alongside rRNA and tRNA information from the annotation steps, the genome bins were assigned high quality (HQ) or medium quality (MQ) values per the Minimum Information about a Metagenome-Assembled Genome (MIMAG) standards (Bowers *et al.*, 2017). For each bin, two methods were used to determine their phylogenetic lineage, an internal Integrated Microbial Genome (IMG; Chen *et al.*, 2021) program and GTDB-tk (0.2.2; Chaumeil *et al.*, 2020).

2.7.3 Functional and taxonomic analysis

The MetaCyc and KEGG databases were used to find the most appropriate pathways and genes associated with methanogenesis and the sulfur cycle and a list of 108 genes was compiled (Caspi *et al.*, 2014; Kanehisa *et al.*, 2022). Using this list of genes, the gene abundance profiles were found in the metagenomics datasets. The output contained information on gene count, and any gene with a count >0 was recorded as present in the data.

The gene counts were normalised using the CPM (copies per million) normalisation method (Robinson and Oshlack, 2010), which was calculated using the below equation:

$$\mathrm{CPM} = \mathrm{Scale\_Factor}\ \frac{\mathrm{GeneCount}}{\mathrm{TotalGeneCount}}$$

where Scale_Factor = 10^6. Once the data were normalised, the CPM values were log-transformed. R (4.2.1) on RStudio (2022.07.1) and ggplot2 were used to make a heatmap showing the $\log_{10}$(CPM) values for each gene (Wickham, 2016; R Core Team, 2020).

JGI also created metagenome-assembled genomes (MAGs) from the Baltic Sea samples. After filtering out the MAGs relevant to DMS degradation (methanogens and SRB), the presence or absence of the genes previously identified were recorded.

2.8 Metatranscriptomics

2.8.1 RNA sample preparation

DOE JGI conducted the metatranscriptomics analysis. All samples were treated with RNase-free DNase, and degradation was measured using a Tapestation 2200 (Agilent Technologies,

USA). Absorbance was measured using a Nanodrop One (Thermo Scientific, USA), and the $A_{260/280}$ ratio was greater than 1.8 in all samples. The Qubit 2.0 Fluorometer (Invitrogen, CA, USA) was used to quantify the total RNA in the samples and the concentration ranged between 17 ng/µL and 88 ng/µL. The sample volume was above 25 µL.

2.8.2 Metatranscriptomics analysis

DOE JGI performed the metatranscriptomics analysis following a well-established JGI-created workflow. The workflow was implemented following a 2x152 bp sequencing step on the Illumina NovaSeq S4 platform. The data were processed to remove contamination, adapter sequences and low-quality reads using BBDuk (38.87; Bushnell, 2014).

After filtering, the reads were assembled with MEGAHIT (1.2.9; Li *et al.*, 2015), and the final assembly and coverage information were generated using BBMap (38.86; Bushnell, 2014). The assembled contigs were then used for structural annotation. The workflow predicted noncoding RNA genes (tRNAs: tRNAscan-SE 2.0.7; Chan and Lowe, 2019, other noncoding RNA: cmsearch from the INFERNAL 1.1.3 package using the Rfam 13.0 database; Nawrocki and Eddy, 2013; Kalvari *et al.*, 2018), clustered regularly interspaced short palindromic repeats (CRISPR; JGI modified version of CRT-CLI 1.2; Bland *et al.*, 2007) and protein-coding genes (CDSs; Prodigal 2.6.3 and GeneMark.hmm-2 (1.05; Hyatt *et al.*, 2010; Lomsadze *et al.*, 2018).

Functional annotation consisted of associating CDSs with KO terms and Enzyme Commission (EC) numbers (lastal 1066 - LAST package; Kiełbasa *et al.*, 2011), COG (2003;

Galperin *et al.*, 2015) assignments, SMART (01_06_2016; Letunic and Bork, 2018) domains, SUPERFAMILY (1.75; (Gough *et al.*, 2001) assignments, CATH-FunFam (4.2.0; Sillitoe *et al.*, 2019) annotations, Pfam (30; Finn *et al.*, 2016), and TIGRFAM (15.0; Haft *et al.*, 2013) annotations using HMMER 3.1b2 (Mistry *et al.*, 2013). Taxonomic annotation of the CDSs was completed using the best LAST hits during the KO term assignment during functional annotation.

2.8.3 Functional and taxonomic analysis

Upon receipt of the data from DOE JGI, all files that contained gene mapping information were downloaded. These included a file containing a specific JGI ID number and information on copy number and gene size (bp), but no gene name or other gene identifiers, such as KO number and EC number, were provided. All information regarding gene identification was in a separate file containing the JGI ID number and gene name and identifier (KO number in most cases). This file was also downloaded.

The above two files were then merged according to the JGI ID number using the code:

join < (sort A.txt) < (sort B.txt) > joined.txt

Once the two files were joined, the correct information for each gene was extracted, using the Linux *grep* command. Next, using a custom python script any unnecessary data were removed from the individual files so that only information regarding the gene name (JGI ID, gene name and gene identifier), copy number and gene size (bp) were included. All data was collected into a new file which was then transformed accordingly for input into R Studio (2022.07.1; R 4.2.1; R Core Team, 2020). Similarly to the metagenomics data, all copy

number data were normalised and log-transformed and ggplot2 was used to visualise the data in heatmap format (Wickham, 2016).

The normalisation used for the metatranscriptomics copy numbers is called FPKM (fragments per kilobase of transcript per million fragments mapped) and was calculated using the below equation (Zhao *et al.*, 2021):

$$\text{FPKM} = \frac{ReadCount \times 10^3 \times 10^6}{TotalReads \times GeneSize(bp)}$$

2.8.4 Stop codon correction of sequences

The genes encoding methyltransferases for key methylated compounds trimethylamine, dimethylamine and monomethylamine naturally contain an in-frame amber codon (UAG; James *et al.*, 2001; Hao *et al.*, 2002; Krzycki, 2005; Mahapatra *et al.*, 2006). These studies showed that this in-frame amber codon does not act as a stop codon during the synthesis of these methyltransferases. However computer programs cannot differentiate between this naturally-occurring non-terminating codon and a normal stop codon.

To correct this error, the DOE JGI metatranscriptomics files were filtered to only contain the gene IDs and sequences associated with methyltransferases using *grep* and the tool *seqtk* with the command *subseq*. The total sequence number was reduced by manually removing any amino acid sequences not ending in the amber stop codon. Then, the JGI online tool Chromosome Viewer was accessed, which lets one view all genes in each scaffold. When Chromosome Viewer presented two fragments associated with the same gene, their

sequences and copy number data were merged. All gene sizes (amino acid length) were cross-checked with published data to further support the assumption that the two fragments were from an erroneously fragmented single gene. All genes found to contain the amber stop codon identified as tri-, di- and mono-methylamine encoding sequences similar to previously published data (James *et al.*, 2001; Hao *et al.*, 2002; Krzycki, 2005; Mahapatra *et al.*, 2020).

2.9 Phylogenetic analysis of the mcrA gene

The PhyloFunDB pipeline, with minor amendments in the final steps, was used for the phylogenetic tree construction (Costa *et al.*, 2022). This pipeline involved using a Snakemake file (Snakefile; Mölder *et al.*, 2021) to query NCBI for the *mcrA* gene and extract the gene region using NCBI Entrez API (Sayers, 2010; Agarwala *et al.*, 2016; Costa *et al.*, 2022). After the automatic removal of duplicated and unverified samples and extraction of all relevant accession numbers and sequences, the files were inputted into Mothur (Schloss *et al.*, 2009), which trimmed the sequences to a user-defined minimum size (350 bp). Then FrameBot (Wang *et al.*, 2013) filtered, and frameshift corrected all the sequences based on a curated protein database that Costa *et al.* (2022) prepared. The remaining sequences were aligned using MAFFT (Nakamura *et al.*, 2018) and re-entered into Mothur (Schloss *et al.*, 2009) for further filtering and chimera removal. Next, the sequences were clustered into OTUs using a distance matrix calculated by Mothur (Schloss *et al.*, 2009). Specifically, the OTU clustering cut-off for the *mcrA* gene was 0.16 based on Yang *et al.* (2014), 0.35 was chosen as the distance matrix cut-off, and 350 base pair sequences were set as the minimum size (Costa *et al.*, 2022). OTUs were chosen for the phylogenetic tree, instead of ASVs, to decrease sequence complexity during phylogenetic tree visualisation. *mcrA* sequences from uncultured methanogens were manually removed, and three *mcrA* sequences from

Methanolobus oregonensis, *Methanolobus taylorii* and *Methanolobus tindarius*, which were not originally downloaded from the NCBI database, were added (Agarwala *et al.*, 2016). All nucleic acid sequences were then translated into amino acid sequences using Prodigal (Hyatt *et al.*, 2010) and realigned using MAFFT (Nakamura *et al.*, 2018). The final amino acid sequence file was input into IQ-TREE (1.6.12; Nguyen *et al.*, 2015) to create the phylogenetic tree. ModelFinder was used to find the best-fit model for my data, mtZOA+F+G4 (Kalyaanamoorthy *et al.*, 2017), and branch confidence levels were determined by ultrafast bootstrap statistical analysis (1000 replicates; Hoang *et al.*, 2018). Visualisation and annotation of the tree were accomplished using iTOL (v.5; Letunic and Bork, 2021), and *Methanopyrales* was used as the out-group.

All steps outlined above were completed using QMUL's Apocrita HPC facility, supported by QMUL Research-IT (King *et al.*, 2017).

3 Diversity of dimethylsulfide-degrading methanogens and sulfate-reducing bacteria in anoxic sediments along the Medway Estuary, UK

3.1 Introduction

Methane (CH_4) is a potent greenhouse gas with ~28 times the global warming potential of carbon dioxide (CO_2) over 100 years (Myhre *et al.*, 2013). Total global methane emissions are estimated to range between 550-594 Tg per year (Saunois *et al.*, 2020), around 60% of which is produced by methanogenic archaea (Conrad, 2020). Research efforts have mostly focused on the acetoclastic (acetate) and hydrogenotrophic (CO_2 and hydrogen) methanogenesis pathways, although it has been acknowledged that methylotrophic methanogenesis is the dominant methanogenic pathway in saline ecosystems e.g. marine and estuarine sediments (Lazar *et al.*, 2011; Zhuang *et al.*, 2016).

Dimethylsulfide (DMS) is an abundant methylated sulfur compound with an annual atmospheric flux of 24.5±5.3 Tg and with significant roles in both the global carbon and sulfur cycles as well as in atmospheric chemistry (Charlson *et al.*, 1987; Watts, 2000). Early studies reported that the degradation of DMS and its metabolic intermediate MeSH in anoxic sediments was coupled to both methane production and sulfate reduction, suggesting these compounds to be competitive substrates for methanogens and sulfate-reducing bacteria (SRB) in sulfate-containing sediments (Kiene *et al.*, 1986; Kiene and Capone, 1988; Chapter 1). Still, we know little about the pathways of DMS biotransformation in anoxic environments.

Pioneering research was also undertaken to isolate DMS-degrading methanogens of the genera *Methanomethylovorans*, *Methanolobus*, *Methanosarcina* and *Methanohalophilus* from freshwater and saline sediments (Mathrani *et al.*, 1988; Liu *et al.*, 1990; Ni and Boone, 1991; Finster *et al.*, 1992; Kadam *et al.*, 1994; Oremland and Boone, 1994; Lomans *et al.*, 1999). In addition to methanogens, DMS-degrading SRB of the genera *Desulfotomaculum* (Tanimoto and Bak, 1994) and *Desulfosarcina* (Lyimo *et al.*, 2009) were also obtained from a thermophilic fermenter and mangrove sediment, respectively. However, it is not known if these isolated species represent the actual diversity of the DMS-degrading microbial populations in anoxic sediments.

A few studies also tested for competition between methanogens and SRB for DMS, and showed that SRB outcompeted methanogens in sulfate-rich anoxic saltmarsh and mangrove sediments, where DMS concentrations were low e.g. 1-10 μM (Kiene, 1988; Lyimo *et al.*, 2009). This was potentially due to SRB exhibiting high affinities for DMS, as is the case for *Desulfosarcina* strain SD1 (K_s <0.5 μM; Lyimo *et al.*, 2009). However, this strain grows extremely slowly on DMS (0.01 h^{-1}) compared to DMS-degrading methanogen *Methanosarcina semesiae* (0.07 h^{-1}), which implies that slow-growing DMS-degrading SRB may be outcompeted by DMS-degrading methanogens at high DMS concentrations (Lyimo *et al.*, 2009). The outcome of this competition has significant consequences for the global methane and carbon cycles as it directly affects how much of the DMS carbon is converted into methane and CO_2. Yet, the effect of sulfate on the diversity of microbial populations underlying DMS degradation in anoxic sediments remain largely unexplored.

Estuarine sediments are ideal ecosystems to study anaerobic DMS degradation and how sulfate availability affects the fate of its carbon (i.e. produced as methane or CO_2). They sustain high methane production (Middelburg *et al.*, 2002; Borges and Abril, 2011) and contain comparable DMS concentrations (>50 nM) to marine surface waters (Sciare *et al.*, 2002; Hu *et al.*, 2005; Lana *et al.*, 2011). Furthermore, tidal estuaries have a natural salinity (and sulfate as the major ion) gradient along the full extent of the estuary, where river water with low sulfate concentrations (0.01-0.2 mM) mixes with marine water, where sulfate concentration is usually high at ~28 mM (Canfield *et al.*, 2005; Dürr *et al.*, 2011). We, therefore, incubated freshwater, brackish and marine sediments collected from along the Medway Estuary (UK; Figure 3.1) under anoxia with DMS as the only carbon and energy source using near *in situ* sulfate concentrations. This study represents the first in-depth analysis of the diversity and abundance of DMS-degrading microorganisms in anoxic sediments and provides new insights into DMS degradation in estuarine sediments with contrasting sulfate content.

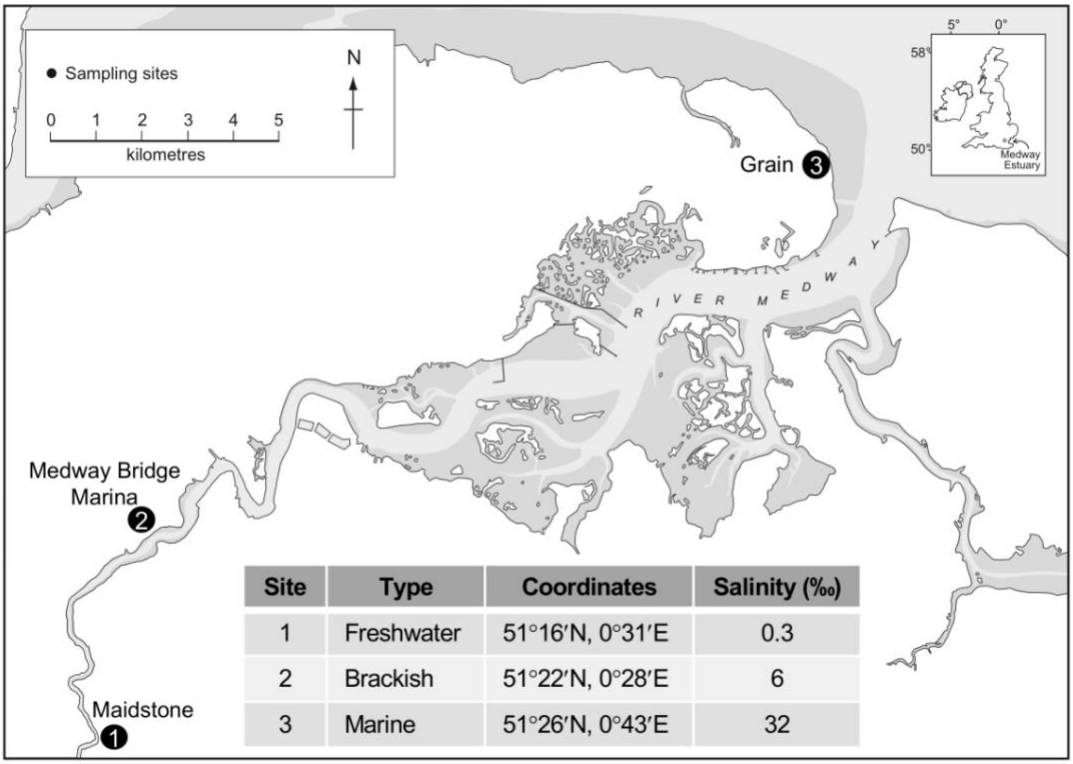

Site	Type	Coordinates	Salinity (‰)
1	Freshwater	51°16′N, 0°31′E	0.3
2	Brackish	51°22′N, 0°28′E	6
3	Marine	51°26′N, 0°43′E	32

Figure 3.1. Sampling locations along the Medway Estuary. 1) Maidstone - freshwater sampling site. 2) Medway Bridge Marina - brackish site. 3) Grain - marine site. Sampling was conducted on 28/11/2018 at low tide. The atmospheric temperature was 12.5 ºC.

3.2 Site locations and sediment sampling

The Medway Estuary is a macrotidal estuary located in Kent, South East England. Sediment was sampled using Perspex corer tubes (3.5 cm in diameter) at low tide from three locations along the natural salinity gradient of the estuary, namely Maidstone (freshwater site, salinity 0.3‰), Medway Bridge Marine (brackish site, salinity 6‰) and Grain (marine site, salinity 32‰) in November 2018 (Figure 3.1).

Five replicated incubations were established per location using 5 g of sediment and 40 mL of ASW (Wyman *et al.*, 1985; Wilson *et al.*, 1996). Full strength ASW was used for marine sediment incubations, while it was diluted to 50% and 1% with sterile distilled water for

brackish and freshwater sediment incubations, respectively. The sulfate concentrations in the incubation bottles were adjusted according to *in situ* salinities of each location (0.1 mM, 14 mM and 29 mM for freshwater, brackish and marine sediments, respectively) and were amended with DMS as the carbon and energy source. Additionally, two sets of control incubations were set up: without DMS to monitor endogenous methane production and with twice-autoclaved sediment samples as abiotic controls to monitor the sediment adsorption of DMS. The incubation bottles were kept at ~21 ^{o}C in the dark to avoid the photochemical destruction of DMS (Brimblecombe and Shooter, 1986).

3.3 Results

3.3.1 DMS degradation leads to methane production along the sulfate gradient of the Medway Estuary

DMS was consumed and methane produced concurrently in sediments incubated with DMS, while no transient methanethiol was observed. The DMS-amended incubations produced between 29 and 40 μmol methane g^{-1} wet sediment, whilst all the negative control incubations, which lacked DMS, produced significantly lower amounts of methane (0.15-0.35 μmol methane g^{-1} wet sediment; $p<0.001$). Another set of negative control incubations was prepared using autoclaved sediment samples and amended with DMS to quantify DMS adsorption and whether methane would be produced. These controls showed no methane production, but ~4 μmol of DMS was removed in all samples due to sediment complexation (Kiene *et al.*, 1986). Incubations were terminated when the methanogens entered the stationary phase at 37, 22, and 62 days in the freshwater, brackish, and marine sediment incubations, respectively (Figure 3.2.A).

The freshwater sediment incubations consumed a total of 56±0.1 μmol DMS g^{-1} wet sediment and produced 34±0.8 μmol methane g^{-1} wet sediment by the end of their 37-day incubation (Figure 3.2.B). Assuming that 1 mole of DMS yields 1.5 moles of methane (Equation 1; Chapter 1; Finster *et al.*, 1992), then the average amount of methane produced corresponds to ~41% of the theoretical methane yield (84 μmol g^{-1}). As CO_2 is an end product of both methanogenic and sulfidogenic DMS-degradation pathways (Equations 1 and 2; Chapter 1), CO_2 concentrations were measured at the end of the incubation period. The total amount of CO_2 in the freshwater incubations was 4.8±0.6 μmol g^{-1} wet sediment (Figure 3.2.C), which was significantly lower than the stoichiometric value for the methanogenic DMS degradation (28 μmol; $p<0.001$).

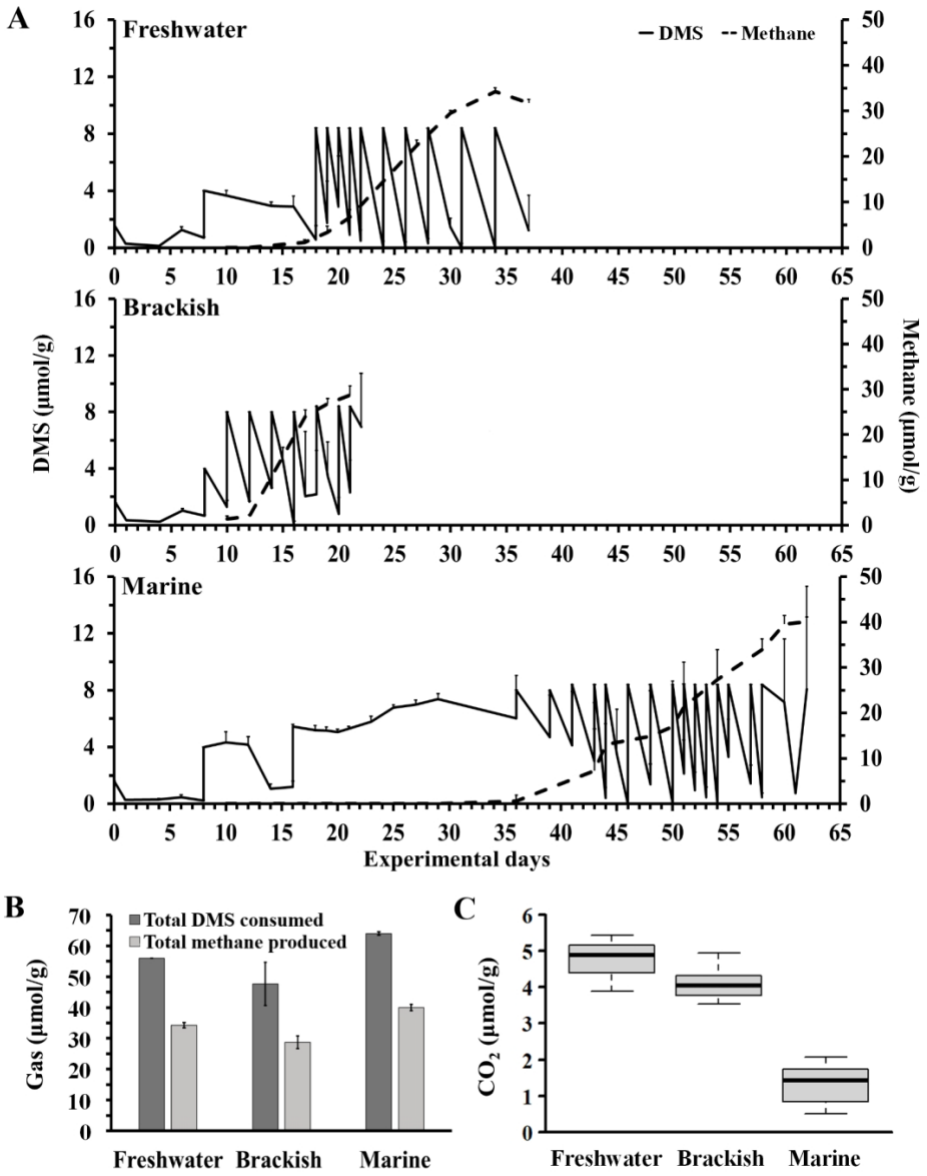

Figure 3.2. A) Average DMS amounts degraded (primary axis) and average cumulative methane amounts produced (secondary axis) in the DMS-amended incubations. Top – freshwater, Middle – brackish, Bottom – marine sediments. **B)** Total amounts of DMS degraded and methane produced at the end of the incubation in sediments incubated with DMS. **C)** Total amount of CO_2 produced at the end of the incubation. Error bars represent standard error above and below the average of five replicates.

The brackish sediment incubations, despite being amended with sulfate, required the shortest incubation time (22 days) to reach stationary phase in comparison to the freshwater and marine sediment incubations. A total of 49±7 μmol DMS g^{-1} wet sediment was degraded, while 29±2 μmol methane g^{-1} wet sediment was produced, which is equivalent to ~39% of the theoretical methane production (73.5±10.5 μmol g^{-1}; Figure 3.2.B). The total amount of CO_2 was similar to the freshwater incubations at 4.1±0.5 μmol g^{-1} wet sediment (Figure 3.2.C), which was greatly lower than the theoretical value for the methanogenic route (24.5 μmol g^{-1}). Sulfate reduction was also observed in the brackish incubations, where ~60% of the sulfate amended to the incubations (114 μmol g^{-1} wet sediment) was consumed, decreasing the sulfate concentration to 45 μmol g^{-1} wet sediment (Figure 3.3).

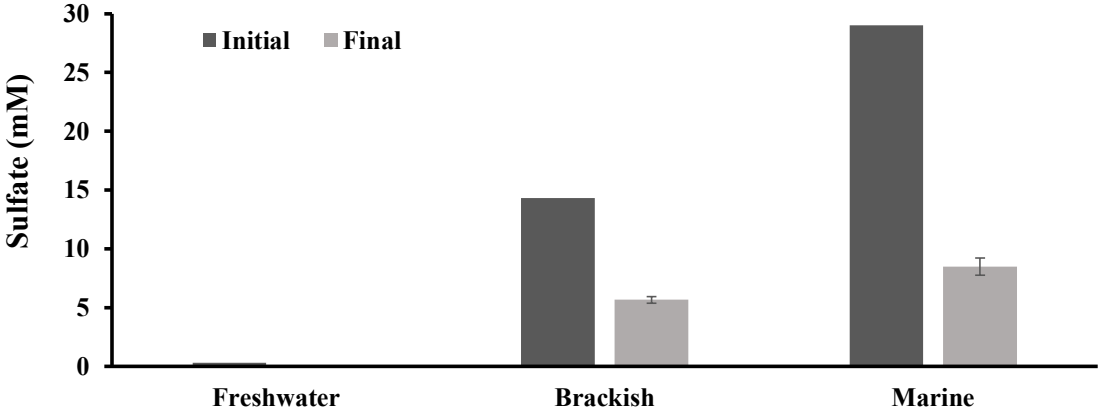

Figure 3.3. Sulfate concentrations (mM) before and after the incubation experiment for the freshwater, brackish and marine samples. The initial concentration is the sulfate added to the artificial seawater used in the microcosm experiment. The final concentration was measured after the incubations were terminated. Error bars represent standard error above and below the average of five replicates.

DMS degradation, methane production and sulfate reduction were also detected in the marine sediment incubations, however, a prolonged lag phase for methane production was observed in these samples (35 days). After the lag phase, a total of 64±0.6 μmol DMS g^{-1} wet sediment was consumed and 40±1.1 μmol methane g^{-1} wet sediment was produced within 27 days (Figure 3.2.B). This amount of methane corresponds to ~42% of the theoretical methane yield (96 μmol g^{-1}). The total amount of CO_2 was 3±0.6 μmol g^{-1} wet sediment when the marine incubations were terminated, which was significantly lower than the 32 μmol g^{-1} theoretical yield assuming the methanogenic route ($p<0.001$; Figure 3.2.C). Sulfate added to the incubations (230 μmol g^{-1} wet sediment) was also consumed in the marine sediments, however, as in the brackish sediments, it was not totally depleted and only reduced to 70 μmol g^{-1} wet sediment at the end of the incubation. This indicates sulfate availability was not the limiting factor for the SRB to degrade DMS in the brackish and marine sediments (Figure 3.3).

3.3.2 Taxonomic and functional diversities in the sediment incubations

A total of $1.9x10^6$, $6.4x10^5$, and $4.8x10^5$ quality-filtered, chimera-free sequences were obtained for the 16S rRNA, *mcrA*, and *dsrB* genes, respectively. A total of 15,111 distinct bacterial and archaeal operational taxonomic units (OTUs) were assigned at 99% identity, whilst 523 and 1,702 OTUs were assigned for *mcrA* and *dsrB* genes at 85% identity.

3.3.2.1 Methanogen diversity

The *mcrA* gene sequences and the Shannon diversity indices (Table 3.1) showed that each sediment type had a distinct methanogen diversity before and after being incubated with DMS ($p<0.001$).

Table 3.1. Shannon (H) indices for methanogens, SRB, archaea, and bacteria in the sediment samples. Significant changes in the Shannon diversity index (H) were observed between original and DMS-amended samples in each site for the microbial communities ($p<0.05$) besides the brackish and marine bacterial communities and the freshwater archaeal and bacterial communities ($p>0.05$). Significant changes were also found between the original sediment samples ($p<0.001$ besides the bacterial community where $p<0.05$) and DMS-amended samples ($p<0.001$). F: freshwater DMS samples, FO: freshwater original samples. B: brackish DMS samples, BO: brackish original samples. M: marine original samples, MO: marine original samples.

Shannon, H	Freshwater			Brackish			Marine		
	Ori	Con	DMS	Ori	Con	DMS	Ori	Con	DMS
Methanogens	1.9 ± 0.06	1.7 ± 0.10	1.1 ± 0.10	1.9 ± 0.05	1.8 ± 0.05	1.0 ± 0.27	2.4 ± 0.07	2.5 ± 0.04	0.1 ± 0.06
SRB	1.2 ± 0.06	1.2 ± 0.01	1.1 ± 0.11	0.8 ± 0.17	1.1 ± 0.05	1.6 ± 0.46	1.7 ± 0.04	1.1 ± 0.23	1.3 ± 0.02
Archaea	2.3 ± 0.12	2.0 ± 0.09	1.4 ± 0.17	2.7 ± 0.03	2.3 ± 0.14	0.6 ± 0.11	1.3 ± 1.07	1.2 ± 0.69	0.2 ± 0.05
Bacteria	4.5 ± 0.08	4.4 ± 0.12	4.4 ± 0.05	4.3 ± 0.07	3.6 ± 0.24	3.4 ± 0.25	4.2 ± 0.09	3.8 ± 0.30	3.6 ± 0.34

There was a statistically significant difference between the original sediments and the DMS-amended sediments (pairwise PERMANOVA; $p=0.0001$), while the control incubations with no additional DMS were not significantly different to the original sediments (Figure 3.4.A; pairwise PERMANOVA, $p>0.05$). This was also supported by the PCA of the *mcrA* sequences (Figure 3.4.B), which showed a clear separation of the DMS-amended sediments from the original sediments and the controls.

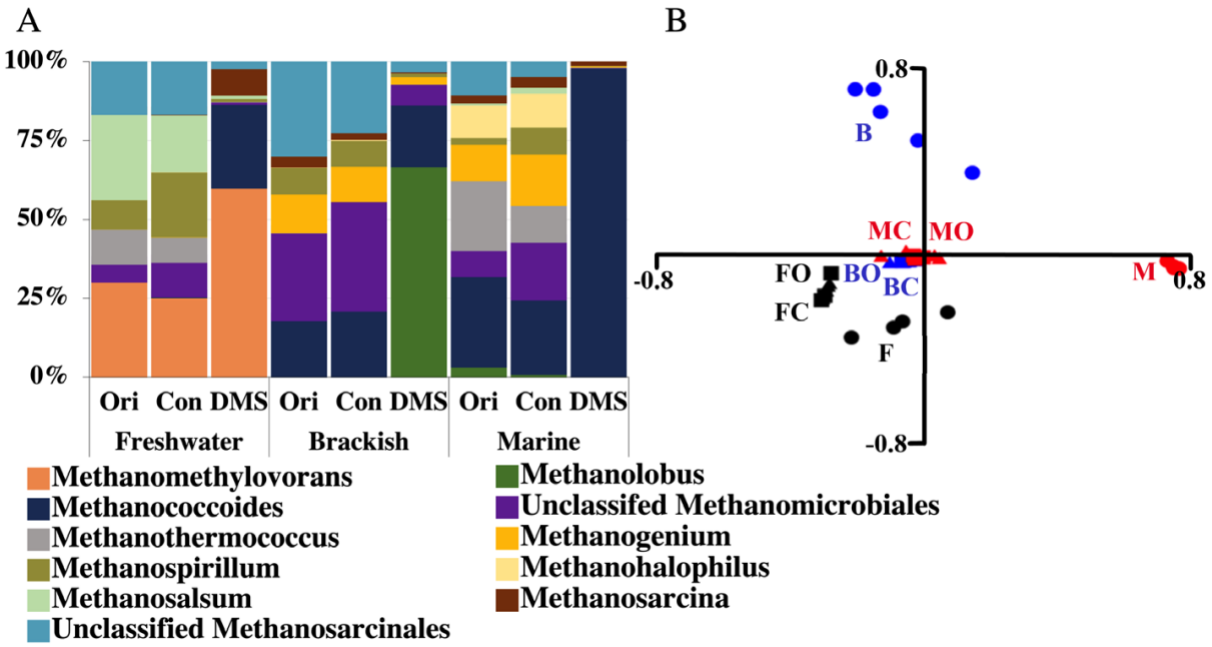

Figure 3.4. A) Genus-level taxonomy of the *mcrA* sequences in the original and DMS incubated freshwater, brackish and marine sediments from the Medway Estuary. Percentages show the average relative abundances of the taxa calculated using five replicates. Ori: Original sediment samples. Con: Control incubations with no added DMS. DMS: Sediment samples incubated with DMS. **B)** Principal components analysis of the *mcrA* sequences (PC1 – 44%, PC2 – 27%). F: freshwater sediment DMS incubations (black, dot), FO: freshwater original sediment (black, square), FC: freshwater sediment control incubation (black, square), B: brackish sediment DMS incubations (blue, dot), BO: brackish original sediment (blue, square), BC: brackish sediment control incubation (blue, square), M: marine sediment DMS incubations (red, dot), MO: marine original sediment (red, square) and MC: marine sediment control incubation (red, square). Note that OTUs with relative abundances <2% were not shown in the Figure.

Correlation analysis (Table 3.2) revealed that the DMS consumption (p=0.007), methane production (p=0.005), the initial sulfate concentrations (p=0.03) and the concentrations of the total sulfate consumed in the incubations (p=0.02) affected the methanogen diversity in the samples.

Table 3.2. Spearman's rank correlation coefficients between the first two principal components from the genus-level sequencing analysis of the *mcrA* (methanogens), *dsrB* (SRB) and 16S rRNA (archaea and bacteria) genes and the total DMS consumed (µmol), methane yield (µmol), initial sulfate concentrations (mM) and total sulfate consumed after DMS incubation (mM). Statistically significant values are in bold. ***: p<0.001; **: p<0.01; *: p<0.05.

	Methanogens		**SRB**		**Archaea**		**Bacteria**	
Variable	**PC1**	**PC2**	**PC1**	**PC2**	**PC1**	**PC2**	**PC1**	**PC2**
DMS consumed (µmol)	**0.49****	-0.11	-0.01	-0.26	0.13	**-0.70*****	**0.39***	0.02
Methane yield (µmol)	**0.38***	-0.13	-0.17	-0.20	0.18	**-0.53*****	**0.47****	-0.04
Initial sulfate (mM)	**0.68*****	**0.67*****	0.13	-0.13	**-0.49****	-0.20	**0.41***	**0.90*****
Consumed sulfate (mM)	**0.53*****	0.32	-0.05	**-0.32***	-0.10	**-0.37***	**0.72*****	**0.45****

In both the original and DMS-amended freshwater sediments, the most dominant family was *Methanosarcinaceae*. Within this, the genera *Methanomethylovorans* (27%±4%) and *Methanosalsum* (23%±1%), which were shown to degrade DMS previously were the most abundant in the original samples (Liu *et al.*, 1990; Lomans *et al.*, 1999; Figure 3.4.A).

After incubating with DMS, *Methanomethylovorans* dominated the freshwater sediment at 66%±8% of the methanogen community (p=0.04), whereas *Methanosalsum* relative abundance decreased to 1%±2% (p<0.001; Figure 3.4.A). *Methanococcoides* relative abundance also increased in the freshwater DMS incubations, where they comprised

29%±7% of the sequences (p=0.008; Figure 3.4.A) despite being undetectable in the original samples. These results are consistent with the archaeal 16S rRNA sequencing data, which showed that the methanogens in the DMS-amended samples were predominantly affiliated with *Methanomethylovorans* (52%±18%; Figure 3.5).

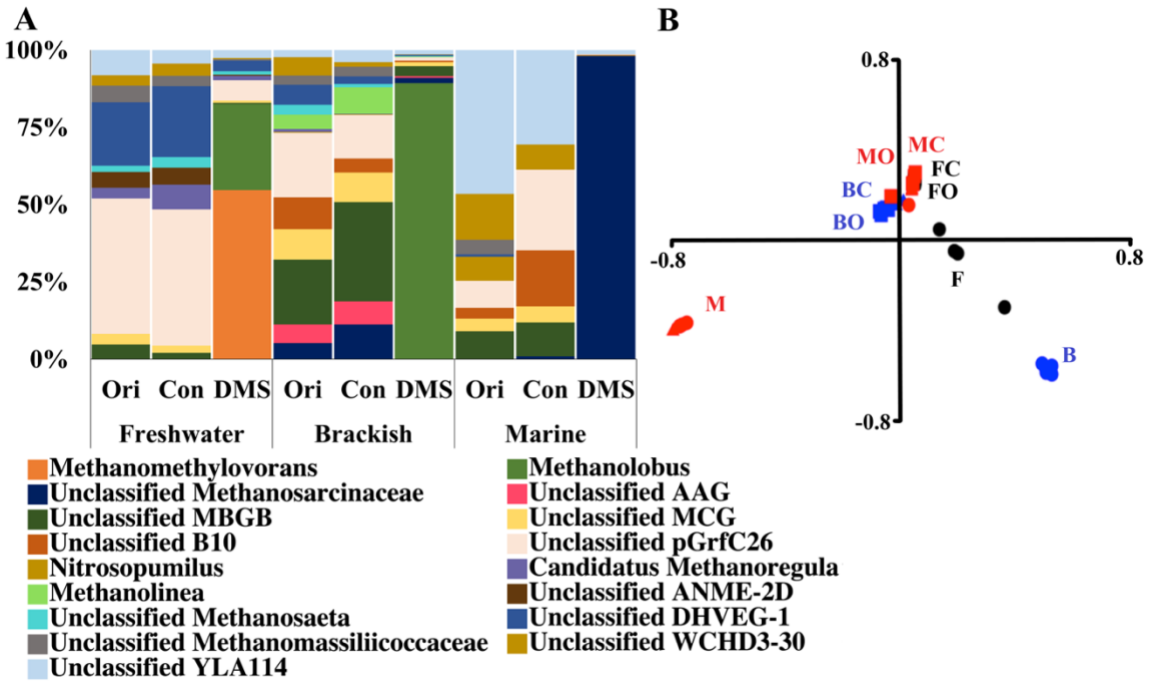

Figure 3.5. A) Genus-level taxonomy of the archaeal 16S rRNA gene sequences in the original and DMS incubated freshwater, brackish and marine sediments from the Medway Estuary**.** Percentages show the average relative abundances of the taxa calculated using five replicates. Ori: Original sediment samples. Con: Control incubations with no added DMS. DMS: Sediment samples from DMS incubations. **B)** Principal components analysis of the archaeal sequences (PC1 – 37%, PC2 – 30%). F: freshwater DMS samples (black, dot), FO: freshwater original samples (black, square), FC: freshwater sediment control incubation (black, square), B: brackish DMS samples (blue, dot), BO: brackish original samples (blue, square), BC: brackish sediment control incubation (blue, square), M: marine original samples (red, dot), MO: marine original samples (red, square) and MC: marine sediment control incubation (red, square).

Quantification of the *mcrA* gene showed that the methanogen abundance increased ~47-fold from $1.4x10^6 \pm 3.9x10^5$ copies g^{-1} to $6.6x10^7 \pm 1.5x10^7$ copies g^{-1} in the freshwater sediments, showing growth of methanogens in DMS-amended samples (Figure 3.6).

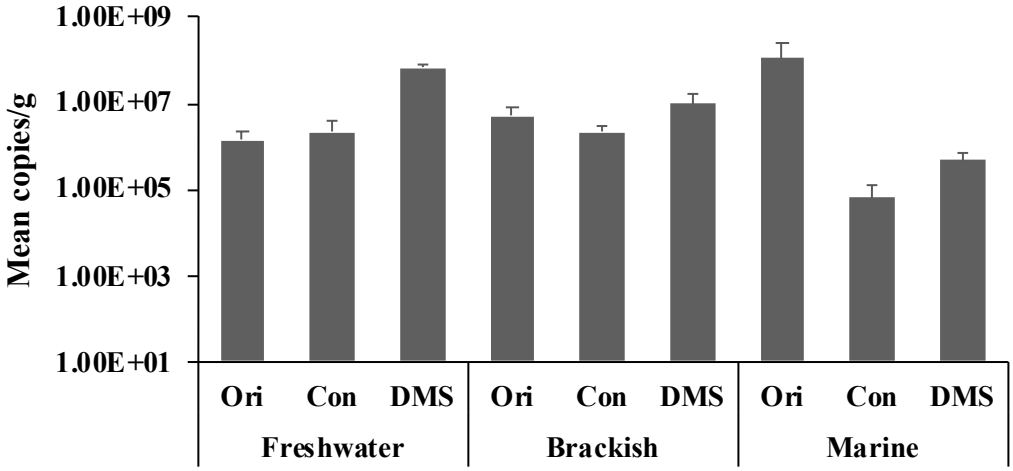

Figure 3.6. Mean copy number/g sediment of the *mcrA* gene for methanogens before and after the DMS incubation. Ori: Original sediment samples. Con: Incubation controls without DMS. DMS: Sediment samples collected from DMS incubations at the end of the incubation period (37, 22 and 62 days for freshwater, brackish and marine incubations). Error bars represent standard error above and below the average of five replicates.

In the original brackish sediment samples, unclassified *Methanosarcinales* (26%±3%) and unclassified *Methanomicrobiales* (25%±1%) were the most abundant taxa (Figure 3.4.A). Their relative abundances decreased to 2%±1% and 7%±2% ($p<0.001$), respectively, when the sediment was incubated with DMS, whilst *Methanolobus* became the most prevalent genus with a dramatic increase to 73%±11% from 3% ($p<0.001$). This was also supported by the archaeal 16S rRNA sequencing data, which demonstrated the dominance of *Methanolobus* (87%±2%) in the DMS-amended incubations (Figure 3.5). Moreover, the

abundance of methanogens increased from $4.9x10^6 \pm 8.5x10^5$ copies g^{-1} to $1.3x10^7 \pm 1.8x10^6$ copies g^{-1} in the DMS-amended brackish sediments (Figure 3.6).

Methanococcoides (*Methanosarcinaceae* family) was the most abundant methanogenic genus in the original marine sediment samples at 23%±5% of the sequences, followed by *Methanothermococcus* (from the *Methanococcaceae* family) at 18%±5% (Figure 3.4.A). After incubations with DMS, *Methanococcoides* remained the most abundant genus with a sharp increase in the relative abundance to 98%±1% ($p<0.001$; Figure 3.4.A), suggesting this genus to be the only detectable DMS-degrading methanogenic taxon in the marine sediment. 16S rRNA sequencing data showed 97%±2% of the sequences in the DMS-amended marine sediment were closely related to unclassified *Methanosarcinaea* (Figure 3.5), which are likely from the *Methanococcoides* in the samples as was determined by *mcrA* sequencing. The original marine sediment had $6.1x10^5 \pm 1.9x10^5$ copies g^{-1} methanogen abundance, which increased to $1.8x10^7 \pm 3.9x10^6$ copies g^{-1} after growth on DMS (Figure 3.6).

3.3.2.2 SRB diversity

Analyses of the *dsrB* sequences (Figure 3.7.A) and Shannon diversity indices (Table 3.1) showed each original sediment sample had a significantly different SRB diversity ($p<0.001$). Pairwise PERMANOVA tests with the brackish sediment samples showed a statistically significant difference in SRB diversity between the original sediment, DMS-amended incubations and control incubations (Figure 3.7.A; $p=0.0001$). The PCA of the *dsrB* sequences explained 89% of the total variability between the samples from the different sites (Figure 3.7.B). The second principal component of the *dsrB* analysis correlated significantly with the total concentrations of sulfate consumed by the end of the incubations ($p<0.001$;

Table 3.2). This indicates the role that sulfate concentration plays on the SRB diversity while the effect on the DMS degradation was not significant.

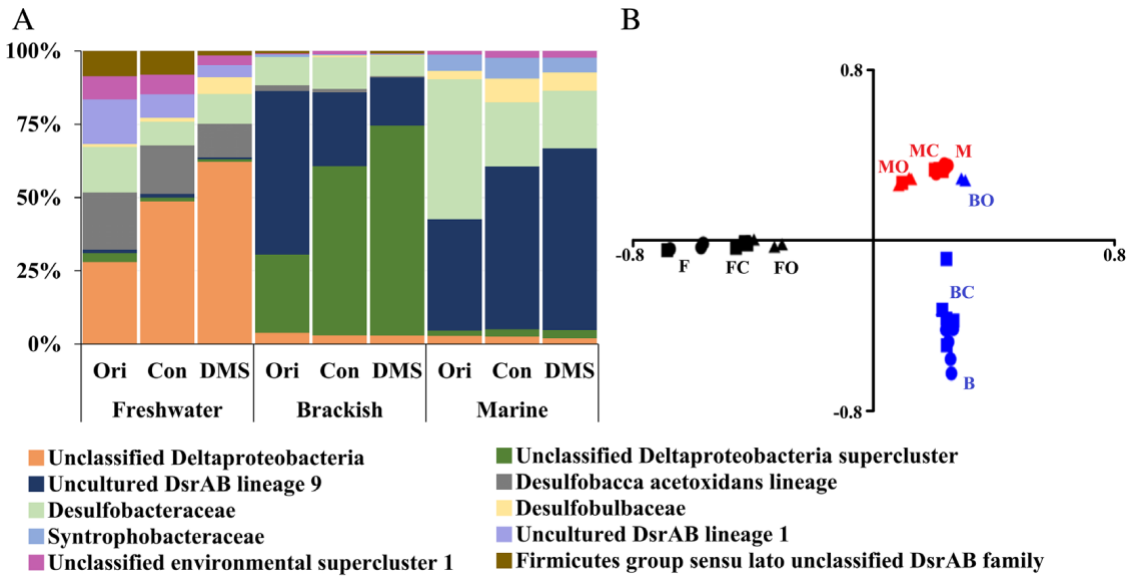

Figure 3.7. A) Family-level taxonomy of the *dsrB* sequences in the original and DMS incubated freshwater, brackish and marine sediments from the Medway Estuary**.** Percentages show the average relative abundances of the taxa calculated using five replicates. Ori: Original sediment samples. Con: Control incubations with no added DMS. DMS: Sediment samples incubated with DMS. **B)** Principal components analysis of the *dsrB* sequences (PC1 – 48%, PC2 – 40%). F: freshwater sediment DMS incubations (black, dot), FO: freshwater original sediment (black, square), FC: freshwater sediment control incubation (black, square), B: brackish sediment DMS incubations (blue, dot), BO: brackish original sediment (blue, square), BC: brackish sediment control incubation (blue, square), M: marine sediment DMS incubations (red, dot), MO: marine original sediment (red, square) and MC: marine sediment control incubation (red, square). Note that OTUs with relative abundances <2% were not shown in the Figure.

A remarkable increase in the relative abundance of unclassified *Deltaproteobacteria* from 29%±6% to 63%±16% was observed in the freshwater sediments incubated with DMS (p=0.02), making it the most abundant recognised SRB taxon in these samples (Figure 3.7.A). The addition of DMS resulted in a dramatic ~50-fold increase in the *dsrB* abundance to $3.7x10^7 \pm 3.3x10^6$ copies g^{-1} from $3.4x10^2 \pm 1.4x10^2$ copies g^{-1} (p=0.04; Figure 3.8).

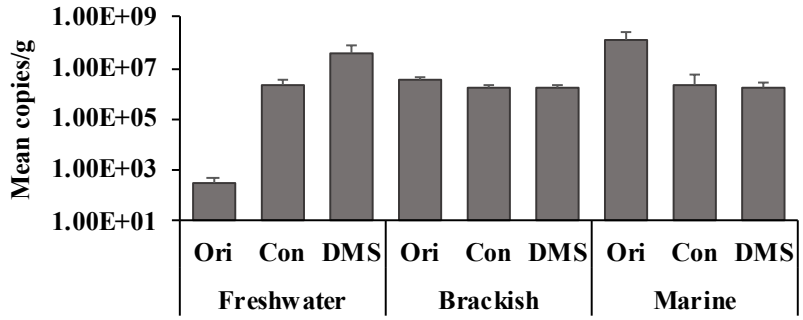

Figure 3.8. Mean copy number/g sediment of the *dsrB* gene for SRB before and after the DMS incubation. Ori: Original sediment samples. Con: Incubation controls without DMS. DMS: Sediment samples collected from DMS incubations at the end of the incubation period (37, 22 and 62 days for freshwater, brackish and marine incubations). Error bars represent standard error above and below the average of five replicates.

The *dsrB* sequences from the original brackish sediments were mainly composed of unclassified *Deltaproteobacteria* supercluster (27%±6%) and uncultured DsrAB lineage 9 (56%±24%) whilst unclassified *Deltaproteobacteria* supercluster dominated the DMS-amended sediments (71%±7%; Figure 3.7.A). Concurrently, the relative abundance of uncultured DsrAB lineage 9 reduced to 16%±5%. Despite the change in the composition of SRB, there was not a marked difference in the average *dsrB* abundances between the original and DMS-amended brackish samples ($3.3x10^6 \pm 2.7x10^5$ and $1.6x10^6 \pm 1.6x10^5$, respectively; Figure 3.8).

In the original marine sediment, the majority of the *dsrB* sequences were affiliated with *Desulfobacteraceae* and uncultured dsrAB lineage 9, which represented 48%±5% and 38%±5% of the SRB community, respectively (Figure 3.7.A). After DMS addition, *Desulfobacteraceae* accounted for 20%±4% ($p<0.001$), whilst uncultured dsrAB lineage 9 had a sharp increase to 62%±3% and became the most dominant SRB in the samples ($p<0.001$). A significant decline was observed in the *dsrB* abundance, which reduced from $1.3x10^8 \pm 3.8x10^7$ copies g^{-1} to $2.1x10^6 \pm 2.5x10^5$ copies g^{-1} after DMS amendment (Figure 3.8).

The freshwater, brackish and marine sediment control incubations with no DMS had increased relative abundances of unclassified *Deltaproteobacteria* (49%±18%), unclassified *Deltaproteobacteria* supercluster (58%±12%) and uncultured *dsrAB* lineage 9 (56%±12%), respectively (Figure 3.7.A). These taxa likely utilised organic carbon in the sediments and sulfate provided in the growth medium.

3.3.2.3 Total bacterial diversity

The 16S rRNA sequence analysis and the Shannon diversity indices (Table 3.1) showed that in the brackish and marine sediments, incubated with DMS, bacterial diversity changed significantly ($p=0.0013$ and $p=0.02$, respectively, Figure 3.9.A), however the freshwater samples exhibited no statistically significant change; although unclassified *Methylophilales* increased from 1% to 5% in the freshwater DMS incubations. Pairwise PERMANOVA tests revealed significant differences between the original sediments, control incubations and DMS-amended incubations ($p=0.0001$) except for the brackish control and DMS-amended incubations (Figure 3.9.B). The first PCA component significantly correlated with the amount of DMS consumed ($p=0.002$), the methane yield ($p=0.001$), and both the initial

sulfate concentrations and total concentrations of sulfate consumed in the incubations ($p<0.001$; Figure 3.9.B; Table 3.2), indicating an effect of both sulfate and DMS on the bacterial community structure in the sediments.

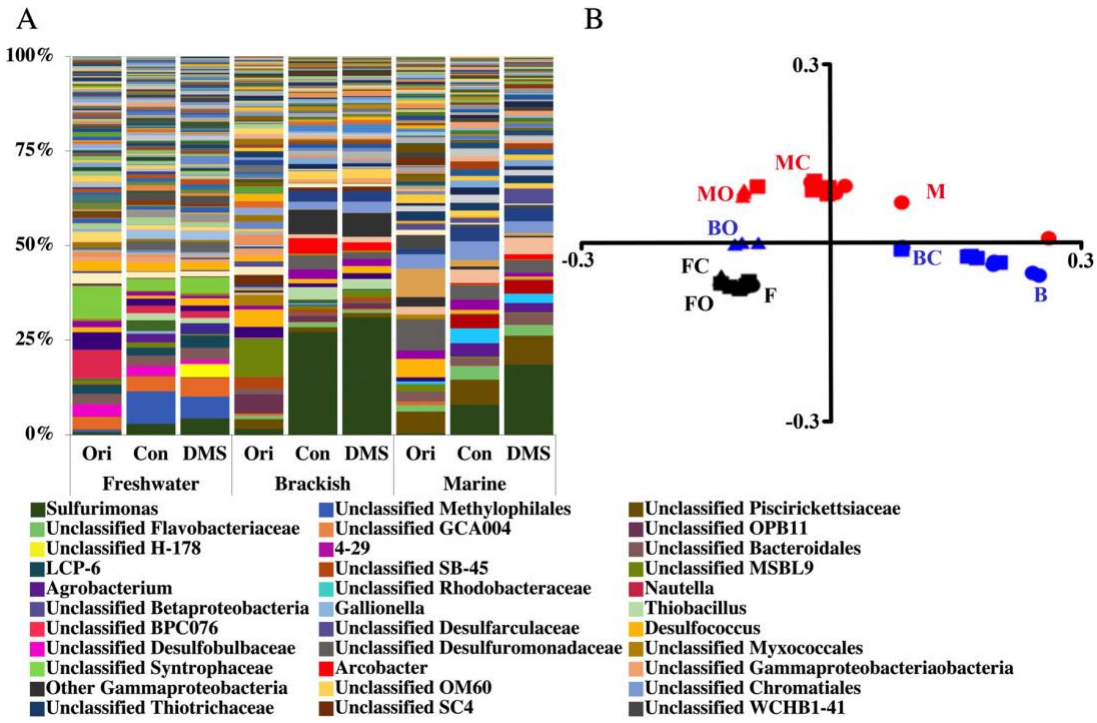

Figure 3.9. A) Genus-level taxonomy of the bacterial 16S rRNA gene sequences in the original and DMS incubated freshwater, brackish and marine sediments from the Medway Estuary**.** Percentages show the average relative abundances of the taxa calculated using five replicates. Ori: Original sediment samples. Con: Control incubations with no added DMS. DMS: Sediment samples incubated with DMS. **B)** Principal components analysis of the bacterial sequences (PC1 – 60%, PC2 – 15%). F: freshwater sediment DMS incubations (black, dot), FO: freshwater original sediment (black, square), FC: freshwater sediment control incubation (black, square), B: brackish sediment DMS incubations (blue, dot), BO: brackish original sediment (blue, square), BC: brackish sediment control incubation (blue, square), M: marine sediment DMS incubations (red, dot), MO: marine original sediment (red, square) and MC: marine sediment control incubation (red, square).

The most striking result of the 16S rRNA sequence analysis was the significant increase in the relative abundance of the chemoautotrophic, sulfur-oxidising bacterial genus *Sulfurimonas* in all sediment samples after incubation with DMS ($p<0.001$ for freshwater and brackish, $p=0.04$ for marine sediments). *Sulfurimonas* comprised a higher relative abundance in the DMS-amended, sulfate-containing brackish and marine sediments at 30%±7% and 18%±12, respectively, compared to the DMS-amended freshwater sediment (4.0%±0.1%; Figure 3.9A). It should be noted that the relative abundance of *Sulfurimonas* also increased in the control incubations but to a smaller extent than in the DMS-amended incubations (3%±0.1%, 26%±5% and 8%±3%, for freshwater, brackish and marine incubations, respectively). Furthermore, the relative abundance of sequences closely related to *Methylophilales* and *Piscirickettsiaceae* increased significantly to 5%±2% and 7%±2%, in freshwater and marine DMS incubations, respectively. These taxa have methylotrophic members that can degrade DMS, however their relative abundances increased also in freshwater and marine control incubations (8%±1% and 6%±2%, respectively; (de Zwart *et al.*, 1994; Eyice *et al.*, 2015). This either suggests that *Methylophilales* and *Piscirickettsiaceae* were not directly involved in DMS degradation in our sediments or that they carried out different functions in the control and DMS-amended incubations.

3.4 Discussion

The formation of methane to stoichiometrically relevant concentrations in freshwater, brackish and marine sediment samples after DMS amendment strongly suggests that the production of methane was a direct result of DMS degradation as has been shown previously (Zinder and Brock, 1978; Kiene *et al.*, 1986; Kiene, 1988; van der Maarel and Hansen, 1997; Lomans *et al.*, 2001). No MeSH was observed in incubations, indicating that MeSH, produced as a by-product of DMS degradation in the samples, was also degraded by the

microbial communities. Between 39%-42% of the theoretical methane yield was observed in sediments incubated with DMS, despite their contrasting sulfate content, thus indicating that sulfate availability has little or no effect on the methane conversion efficiencies along the Medway Estuary sediments. The methane yields of our DMS-amended samples are comparable to those observed by Kiene *et al.* (1986), who obtained 52%-63% yield in various anoxic sediments including from saltmarshes, freshwater, hypersaline and alkaline lakes. The difference between the methane yields is potentially due to the different characteristics of the sediments used in these studies. For instance, Kiene *et al.* (1986) obtained the highest methane yield from a saltmarsh, where high DMS production was shown to occur (Kiene, 1988). Other studies that used lake and saltmarsh sediments found approximately 28% methane conversion efficiency (Zinder and Brock, 1978; Kiene, 1988), which was likely a result of short incubation times (<2 days), prohibiting the DMS-degrading methanogens from reaching the exponential phase of growth.

A delay in methanogenesis was observed in our incubations (14, 12 and 35 days in freshwater, brackish and marine sediments, respectively), which might be due to multiple reasons. Firstly, methylotrophic methanogens in the sediments we studied were a small fraction of the total microbial diversity and might preferentially be mineralising methylamines *in situ*, abundant methylated compounds in marine sediments (Sun *et al.*, 2019). Hence, the DMS-degrading methanogens likely required time to acclimate to the laboratory conditions and become more abundant to produce detectable levels of methane in the incubations. Secondly, DMS concentrations are lower in natural estuarine sediments than those used in our experiments, therefore, in the brackish and marine sediments, SRB might be the active DMS-degraders due to their higher DMS affinity (Lyimo *et al.*, 2009). Interestingly, the brackish sediment we studied had a shorter lag phase for measurable

methanogenesis to begin than the freshwater and marine sediments, although the sulfate concentration in the brackish sediment was sufficient for high rates of sulfate reduction. Furthermore, there was remaining sulfate in both the brackish and marine sediments at the end of the incubation period, implying that the sulfate reduction likely depended on the availability of DMS and the initiation of methanogenesis was not directly related to sulfate concentration (Nedwell and Abram, 1979; Trimmer *et al.*, 1997). The effect of sulfate concentration on methanogenesis was studied in the Yarqon Estuary, where incubations with acetate and lactate under a sulfate gradient from 1 to 10mM (Sela-adler *et al.*, 2017) showed that the sulfate concentration did not affect the rates of methanogenesis or sulfate reduction. Overall, our study confirms the high methane production potential via DMS degradation in estuarine sediments, thus indicating DMS to be potentially an important methanogenic substrate in ecosystems even with high sulfate concentrations and emphasising the requirement to better understand the environmental control over the metabolism of DMS-degrading methanogens.

Using cultivation-independent methods, we detected the dominance of distinct methylotrophic methanogens in different parts of the sediments from the Medway Estuary. The genera *Methanomethylovorans*, *Methanolobus* and *Methanococcoides* dominated in the DMS-incubated freshwater, brackish and marine sediments, respectively. The clear grouping of putative DMS-degrading methanogens that correlated with the sulfate concentration in the incubations, strongly suggests sulfate-driven niche partitioning of DMS-degrading methanogens along the salinity gradient of the Medway Estuary sediments. Although several studies have focused on niche partitioning among methanogenic archaea in estuaries and shales (Carbonero *et al.*, 2014; Webster *et al.*, 2015; Youngblut *et al.*, 2015; Borton *et al.*, 2018), only a few have assessed the effect of sulfate on this process. Oakley *et al.* (2012)

studied the niche occupancy of methanogen genus *Methanosaeta* and sulfate-reducing genus *Desulfobulbus* in Colne Estuary (UK) sediments and found particular genotypes from both taxa at distinct points along the salinity gradient, which is consistent with niche partitioning. In another study on the Colne Estuary, Webster *et al.* (2015) reported that *Methanosaeta* dominated the brackish sediment, whilst *Methanococcoides*, *Methanolobus* and *Methanosarcina* dominated the marine sediment, suggesting that salinity may be a significant factor controlling the diversity and distribution of methanogens. Furthermore, Youngblut *et al.* (2015) tested the diversity among 56 *Methanosarcina mazei* isolates from the salinity gradient along the Columbia River Estuary and demonstrated that *M. mazei* strains had clade-level differences when they were grown on methylamine, indicating niche partitioning by substrate utilisation. A similar mechanism could have affected the distribution of DMS-degrading methanogens, particularly *Methanococcoides* spp., which were detected in all our samples at different relative abundances.

Methanomethylovorans, which were found in the freshwater DMS incubations, are known methylotrophic methanogens with *M. hollandica* being the first DMS-degrading methanogen isolated from a freshwater sediment (Lomans *et al.*, 1999). Now, it is well known that *Methanomethylovorans* spp. are typical freshwater methylotrophic isolates (Lomans *et al.*, 1999; Jiang *et al.*, 2005; Cha *et al.*, 2013). Hence, the high abundance of *Methanomethylovorans* in low-salinity sediments such as our freshwater sediment was not surprising. We also demonstrated that *Methanolobus* and *Methanococcoides* dominated the DMS-amended brackish and marine incubations, respectively, suggesting that these genera degraded DMS in these sediment samples. *Methanolobus* and *Methanococcoides* are prevalent methylotrophic methanogens in saline environments, like brackish lakes, tidal flats, and estuaries (Munson *et al.*, 1997; Purdy *et al.*, 2002; Wilms *et al.*, 2006; Watanabe *et al.*,

2009). Furthermore, species of the genus *Methanolobus*, which were isolated from estuarine and sea sediments, were shown to degrade DMS (Kadam *et al.*, 1994; Oremland and Boone, 1994). Likewise, *Methanococcoides* are obligate methylotrophic methanogens that can degrade methylated compounds such as methylamines, betaine, choline and methanol (L'Haridon *et al.*, 2014; Jameson *et al.*, 2019). None of the members of this genus have been shown to degrade DMS previously, yet our data suggest that known or novel *Methanococcoides* species use DMS as the carbon source in the Medway Estuary sediments.

In contrast to previous studies, we observed the growth of *Methanococcoides* also in DMS-amended freshwater and brackish sediments, using *mcrA* sequencing. This may be due to the members of this genus being transported from the marine site to the brackish and freshwater sites by tides where they then proliferated when the conditions became optimum for their growth. It is worth noting that archaeal 16S rRNA sequencing did not detect *Methanococcoides* in the freshwater DMS incubations but found sequences affiliated with *Methanolobus*, which is likely because of a higher number of representative sequences from *Methanolobus* in the 16S rRNA database. Overall, our findings show that *Methanococcoides* were the only detectable methanogens in the marine sediment incubations.

Incubating with DMS led to significant variation in the SRB composition and the total SRB abundance in all three sediments, despite the growth medium of the freshwater sediments having a low concentration of sulfate. Currently, there are around 240 pure cultures of sulfate-reducing microorganisms available, which greatly limits our ability to taxonomically define the SRB in our samples. *Deltaproteobacteria* were the most abundant SRB in the freshwater and brackish DMS incubations, whereas uncultured dsrAB lineage 9 dominated the marine DMS incubations. An increase in the relative abundances of *Deltaproteobacteria*

and uncultured dsrAB lineage 9 was also observed in the control incubations with no DMS, however this increase was greater in the DMS-amended incubations. It is likely that the SRB in the control incubations used available carbon in the sediments, while, in the DMS-amended incubations, they were involved in the cycling of DMS or its degradation products. The significant correlation between the sulfate concentration and SRB diversity indicates the effect of sulfate on the SRB community composition along the estuarine sediments, which is consistent with previous studies (Kondo *et al.*, 2007; Oakley *et al.*, 2010).

It is interesting that we detected a 50-fold increase in SRB abundance and a change in the relative abundances of distinct SRB in the freshwater sediments incubated with DMS, which were provided with low concentrations of sulfate representing estuarine conditions. These results suggest that SRB played a role in the cycling of DMS in these freshwater sediments. The notable changes in the SRB abundance in these incubations were likely due to a cryptic sulfur cycle, where sulfide, produced as an end product of DMS degradation, was rapidly recycled mainly to sulfate as previously observed in freshwater wetlands, lakes, and rivers (Jorgensen, 1990; Blodau *et al.*, 2007; Heitmann *et al.*, 2007; Berg *et al.*, 2019). We speculate that here, in the freshwater sediments, hydrogen sulfide was reoxidised biotically by microbial action and abiotically with Fe(III) to elemental sulfur, polysulfide and thiosulfate, which was disproportionated to sulfide and sulfate (Pester *et al.*, 2012). The occurrence of biotic cryptic sulfur cycling is also in line with the remarkable increase in the relative abundance of *Sulfurimonas* in the freshwater sediment samples after incubating with DMS. We suggest *Sulfurimonas*, a chemoautotrophic sulfur-oxidising taxon, ubiquitous to sediments, oxidised hydrogen sulfide produced via DMS degradation to thiosulfate and sulfate or completely to sulfate (Figure 3.10; Grote *et al.*, 2008; Lahme *et al.*, 2020). *Sulfurimonas* can utilise nitrate as the electron acceptor via autotrophic denitrification, which

was previously demonstrated to occur in anoxic ecosystems, where sulfide and nitrate profiles overlap such as in the Baltic Sea, Mariager Fjord (Denmark) and the Black Sea (Brettar and Rheinheimer, 1991; Brettar *et al.*, 2006; Jensen *et al.*, 2008; Zhang *et al.*, 2009; Fuchsman *et al.*, 2012). However, the freshwater growth medium in our incubations contained only 88 μM nitrate, which was likely consumed rapidly according to a previous study on Medway Estuary sediments (Shen *et al.*, 2019). Hence, the *Sulfurimonas* species in our incubations perhaps used iron oxides as the electron acceptor as it was found in high concentrations in the Medway Estaury sediments (Spencer, 2002). Alternatively, they might have used manganese oxides, which was previously proven in a *Sulfurimonas* isolate from the Black Sea water column (Henkel *et al.*, 2019). Since methane production took place in the DMS-amended freshwater samples but did not reach the theoretical conversion rates, it is likely that cryptic sulfur cycling led to simultaneous degradation of DMS via methanogenesis and sulfate-reduction, which produced hydrogen sulfide as an end product, contributing to the sulfur cycle in the freshwater sediment incubations.

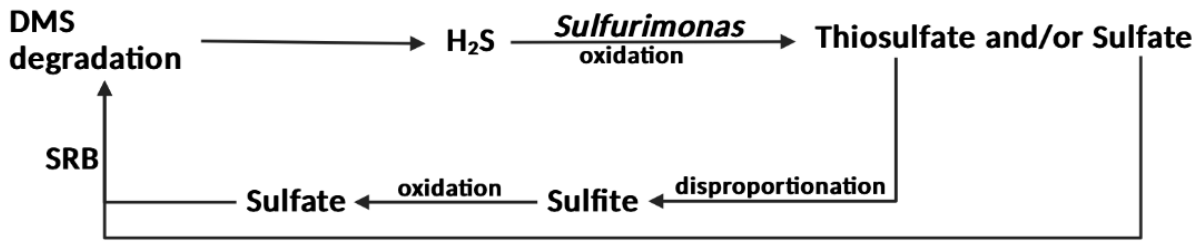

Figure 3.10. Diagram showing the proposed role of *Sulfurimonas* in the freshwater sulfur cycle initiated by DMS degradation.

The high relative abundance of *Sulfurimonas* in DMS-amended brackish and marine sediments derived from the 16S rRNA amplicon data suggests that DMS contributed to the cryptic sulfur cycling also in these incubations, as *Sulfurimonas* were previously linked to cryptic sulfur cycling in marine sediments and waters (Yao and Millero, 1996; Holmkvist *et al.*, 2011; Callbeck *et al.*, 2018). Although the control incubations exhibited an increased relative abundance of *Sulfurimonas*, the increases observed in the DMS-amended sediments were greater. It is possible that, in the control incubations, the *Sulfurimonas* species utilised hydrogen sulfide produced by SRB and the degradation of sulfur-containing amino acids, and assimilated the internal carbon and CO_2 in the sediments (Han and Perner, 2015).

DMS degradation by both methanogens and SRB gives rise to CO_2, the most important greenhouse gas. Interestingly, we observed lower CO_2 concentrations in our DMS-amended sediments than expected stoichiometrically. This discrepancy may be attributed to the substantial increase in the relative abundance of *Sulfurimonas*, which could fix CO_2 while oxidising the hydrogen sulfide produced through DMS degradation or thiosulfate produced via cryptic sulfur cycling (Sievert *et al.*, 2008). We calculated the HS^- production based on the stoichiometry of DMS-dependent methanogenesis (Equation 1; Chapter 1) and the methane concentrations in the incubations, which estimated the HS^- concentrations to be ~23 μmol g^{-1} wet sediment, ~19.5 μmol g^{-1} wet sediment and ~26.5 μmol g^{-1} wet sediment in freshwater, brackish and marine incubations, respectively. Sulfur-oxidising bacteria, such as *Sulfurimonas*, couple hydrogen sulfide or thiosulfate oxidation to CO_2 reduction with a stoichiometry of 1:0.5 or 1:2 to produce elemental sulfur or sulfate, respectively (Klatt and Polerecky, 2015). Therefore, it is plausible to assume that the missing CO_2 in our incubations (~ 23 μmol g^{-1} wet sediment, ~20.5 μmol g^{-1} wet sediment and ~29 μmol g^{-1} wet sediment in

freshwater, brackish and marine incubations, respectively) was used to oxidise hydrogen sulfide or thiosulfate, and produce elemental sulfur and sulfate.

It could also be argued that low CO_2 concentrations in our incubations were due to the activity of hydrogenotrophic methanogens, which use hydrogen and CO_2 to produce methane, however this is unlikely as our DMS-amended sediments were dominated by obligate methylotrophic methanogens and we did not detect hydrogenotrophic methanogens in these samples by *mcrA* sequencing. Alternatively, in the DMS-amended sediments, methylotrophic methanogens might have assimilated CO_2 into biomass or used it as a carbon source for mixotrophic growth as was recently shown for *Methanococcoides methylutens* in marine sediments (Yin *et al.*, 2019a).

In conclusion, our study addresses a major knowledge gap in the diversity of microbial populations underpinning anaerobic DMS degradation in anoxic sediments, which has so far only been characterised by cultivation-dependent methods. Here, we demonstrated that DMS degradation is a potentially important pathway to produce methane along the sulfate gradient of anoxic estuarine sediments and this process is carried out by recognised but distinct methylotrophic methanogens in different parts of the estuary, suggesting niche partitioning of DMS-degrading methanogens driven by sulfate concentration. In our incubations, we used DMS concentrations higher than the *in situ* concentrations and perhaps reflecting this, we observed a prolonged lag phase in methane production and higher methane yields than natural sediments produce. However, given the total global area of estuaries, we argue that the DMS-dependent methane production in estuarine sediments may be a globally significant process. Moreover, this process is likely important in other sulfate-rich ecosystems such as in saltmarsh and marine sediments, where DMS concentrations can be orders of magnitude

higher than in estuarine sediments. In addition to the methane production, DMS affects the sulfur cycle in sediments either due to its use as a growth substrate by SRB or via a cryptic sulfur cycle. Our study highlights the importance of further work to reassess the microbial diversity and pathways of methylotrophic methanogenesis in marine and marine-influenced sediments in order to better understand the methane and carbon cycles in the environment.

4 Identification of DMS-degrading microorganisms in anoxic riverbeds

4.1 Introduction

In the past, inland waters, such as lakes, rivers and streams, were often ignored when attempting to produce global carbon models. This was primarily a result of the small area they cover and the lack of research regarding carbon cycling (Cole *et al.*, 2007). In recent years, this view has changed (Aufdenkampe *et al.*, 2011). Inland waters are now considered sites where most carbon is rapidly metabolised and released into the atmosphere and to a lesser extent reaches the oceans (Battin *et al.*, 2009). Furthermore, Bastviken *et al.* (2011) showed that freshwater systems are often oversaturated in methane and CO_2 and produce 26.8 Tg methane per year releasing an equivalent of about 5% of the total methane emissions into the atmosphere (Stanley *et al.*, 2016). 5% may seem small, but these ecosystems account for less than 3% of the Earth's surface, suggesting they are methane hotspots (Shiklomanov, 1993; Stephens *et al.*, 2020). Some anoxic riverine sediments can even produce as much methane per unit area as peat bogs; for example, up to 1.4 µmol CH_4 L^{-1} were measured in River Frome (UK) sediments (Sanders *et al.*, 2007).

Rivers receive most of their carbon from the surrounding terrestrial systems (Cole and Caraco, 2001; Zeug and Winemiller, 2008). Various studies have predicted that climate change can lead to catchment and runoff changes in rivers and streams, which means that the amount of water entering the waterbodies can be affected, thus changing how much carbon rivers receive from the surrounding area (Hannaford, 2015; Donnelly *et al.*, 2017; Nolan *et al.*, 2017). Depending on geographical location, an increase in runoff in the winter and autumn months due to more precipitation and ice melt, and a decrease in the warmer months

due to extended dry periods will most likely occur (Donnelly *et al.*, 2017; Nolan *et al.*, 2017). Changes to inland water runoff will significantly affect sediment storage and increase nutrient loading (Whitehead *et al.*, 2009; Burt *et al.*, 2016). These changes can, in turn, potentially increase methanogenesis in riverine ecosystems. Furthermore, studies demonstrated that a 2 ^{o}C rise in temperature may increase river methane emissions by 8% (Shelley *et al.*, 2015). Overall, rivers are significant ecosystems for the global carbon cycle and are becoming increasingly important for methane production under changing climate.

Grain size is directly responsible for sediment permeability, organic and inorganic matter content and sediment oxygen concentrations, all of which affect sediment biogeochemistry and metabolic activities (Lohse *et al.*, 1995; Janssen *et al.*, 2005; Kamann *et al.*, 2007; Glud, 2008). Both sand and gravel riverbeds are considered permeable, yet permeability increases as the sediment becomes coarser, making gravel more permeable than sand (Wentworth, 1922; Lewis *et al.*, 2006; Pace *et al.*, 2021). When permeability is high ($> 10^{-12}$ m^2), nutrients, oxygen and organic matter can be transported more effectively from the water column to the sediment or within the sediment (Savant *et al.*, 1987; Thibodeaux and Boyle, 1987; Huettel and Gust, 1992). This creates anoxic zones in less permeable sandy riverbeds, where methane production has been observed (Jones and Mulholland, 1998; Trimmer *et al.*, 2009; Shen *et al.*, 2019). However, the pathways of methane production in river sediments are not well understood.

DMS is a methylated sulfur compound with an atmospheric flux of about 24.5 Tg per year and takes part in both the sulfur and carbon biogeochemical cycles (Charlson *et al.*, 1987; Watts, 2000). Most DMS is produced in the upper ocean layers, but studies have shown it can also be produced in freshwater lake and river sediments (Lomans *et al.*, 1997; Yoch *et al.*,

2001) via various pathways such as the degradation of methoxylated aromatic compounds, DMSP breakdown, MeSH methylation and DMSO reduction (Zinder and Brock, 1978; Finster *et al.*, 1990; Ginzburg *et al.*, 1998; Yoch *et al.*, 2001; Carrión *et al.*, 2015; Chapter 1).

Despite DMS originating from various sources in freshwater environments, the DMS concentrations found in freshwater systems are not well documented. In the past, DMS amounts in freshwater ecosystems were considered to be lower than in marine waters because of studies such as those by Nriagu and Holdway (1989) showing that the Great Lakes (North America) had average DMS concentrations of 5-27 ng/L. However, in the late 70s, the highest recorded concentration of DMS in a natural freshwater system was from a temperate lake, with a DMS concentration of 70 µg/L (Bechard and Rayburn, 1979). In the late 80s, Franzmann *et al.* (1987), when studying a meromictic lake in Antarctica, measured up to 98 µg/L DMS concentration. These values were ~1000 times higher than the previously measured mean concentrations in ocean waters (91 ng/L), thus challenging the view that DMS concentrations were low in freshwater ecosystems (Franzmann *et al.*, 1987).

DMS degradation has been associated with methanogenesis by methanogens and sulfate-reduction by sulfate-reducing bacteria (SRB; Kiene *et al.*, 1986; Kiene and Capone, 1988). Methanogenesis is thought to be the primary DMS degradation pathway in freshwater ecosystems, where sulfate concentration is low. DMS-degrading methanogens are of the genera *Methanomethylovorans*, *Methanolobus*, *Methanosarcina* and *Methanohalophilus,* yet only *Methanomethylovorans* is routinely associated with freshwater ecosystems (Mathrani *et al.*, 1988; Liu *et al.*, 1990; Ni and Boone, 1991; Finster *et al.*, 1992; Kadam *et al.*, 1994; Oremland and Boone, 1994; Lomans *et al.*, 1999; Tsola *et al.*, 2021). On the other hand, studies have suggested the existence of a cryptic sulfur cycle in freshwater wetlands, lakes

and rivers, which could indicate an activity of DMS-degrading SRB even in low sulfate environments (Jorgensen, 1990; Blodau *et al.*, 2007; Heitmann *et al.*, 2007; Berg *et al.*, 2019; Tsola *et al.*, 2021).

This study, therefore, aimed to quantify the anaerobic DMS degradation potential of river sediments as methane sources and to characterise the DMS-degrading microbial populations in river ecosystems with contrasting sediment grain size.

My hypotheses are:

1) DMS degradation leads to a rapid production of methane owing to active methanogens in river sediments.
2) Sediment grain size affects the potential for DMS-dependent methane production with lower methanogenesis rates in gravel-dominated riverbeds.
3) *Methanomethylovorans,* the methanogens most often associated with freshwater DMS degradation, are the dominant methanogens that degrade DMS in river sediments.
4) SRB may be involved in DMS degradation due to cryptic sulfur cycling.

4.2 Site characteristics and sediment sampling

Sediment samples were collected from four rivers (Pant, Rib, Medway and Nadder) in the UK in February 2019 and March 2021 (Figure 4.1). The rivers sampled can be separated into two categories depending on their sediment grain size. Rivers Pant and Rib had permeable gravel-dominated riverbeds, whereas Medway and Nadder had less permeable sand-dominated riverbeds.

Figure 4.4.1. Map showing the river sampling sites. Sediment sampling from Rivers Rib and Pant was conducted on 21/02/2019, from River Medway on 15/03/2021 and from River Nadder on 22/03/2021.

From each site, ~1 L of sediment from the top 5 cm layer was collected into Ziploc bags and was used to characterise the sediment grain size. The grain size was determined using sieves (2 mm and 0.0625 mm), and each size fraction was weighed separately to assess the distribution of the different grain sizes in each river. The Wentworth scale was used to determine whether the rivers had gravel or sand-dominated riverbeds, where gravel is all material coarser than 2 mm and sand is all material between 2 mm and 0.0625 mm (Wentworth, 1922).

Sediment was also collected from each river to set up incubations using Perspex corer tubes (3.5 cm in diameter, three per location). Five replicate incubations were set up per sampling site in 140 mL serum bottles, using 5 g of sediment and 40 mL of ASW (Wyman *et al.*, 1985;

Wilson *et al.*, 1996). The ASW was diluted to 1% with sterile distilled water to make it suitable for freshwater incubations with an *in situ* salinity of 0.1 mM.

4.3 Results

4.3.1 Sediment characterisation and incubation monitoring

Sediment grain size characterisation showed Rivers Pant and Rib had permeable gravel-dominated riverbeds, whereas Rivers Medway and Nadder had less permeable sand-dominated riverbeds (Table 4.1).

Table 4.1. Grain size characterisation of the four rivers sampled. Rivers Pant and Rib had gravel-dominated riverbeds. Rivers Medway and Nadder had sand-dominated riverbeds.

River	Gravel (%)	Sand (%)
Pant	**66.7**	33.3
Rib	**59.8**	40.2
Medway	14.0	**86.0**
Nadder	9.9	**90.1**

Despite the differences in sediment grain size, methane production was observed in all incubations with DMS amendment (Figure 4.2). A lag phase (> 9 days) appeared in all samples prior to methanogenesis, which could suggest SRB activity in these sediments or the methanogens adjusting to laboratory conditions and the additions of DMS. Furthermore, in two of the Rivers (Medway and Nadder) DMS production was observed in the first few days of the incubations (day 7 and 13, respectively). This is likely a result of the microorganisms using up endogenous DMS production substrates such as DMSP, DMSO, amino acids or aromatic compounds. No other DMS production spikes were observed throughout the incubation experiment.

The sand-dominated rivers (Medway and Nadder) exhibited the longest incubation period until methane production stopped (108 and 134 days, respectively), compared to the gravel-dominated Rivers Pant and Rib (54 days; Figure 4.2). However, total methane generation was highest in the sand-dominated sediments from Rivers Medway and Nadder, producing 193±1 and 167±2 µmol methane g^{-1} wet sediment, respectively (Figure 4.3). The highest DMS degradation was also observed in these river sediments, with 155±2 µmol DMS g^{-1} sediment and 121±2 µmol DMS g^{-1}. DMS degradation and methane production corresponded to 83% and 92% of the theoretical methane yields (232 µmol g^{-1} and 181 µmol g^{-1}), respectively, assuming 1 mol DMS is degraded to 1.5 moles CH_4 (Equation 1; Chapter 1).

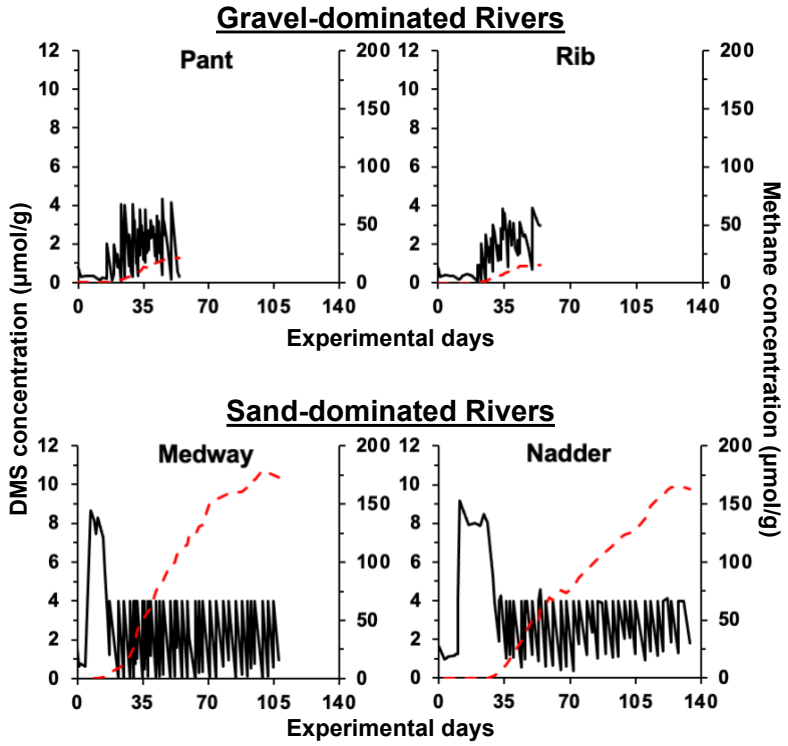

Figure 4.2. Average DMS degradation and methane production in river sediment incubations using DMS as the only energy and carbon source. Rivers Pant and Rib had gravel-dominated riverbeds, whereas Rivers Medway and Nadder had sand-dominated riverbeds. Error bars were omitted to make the graph legible.

DMS degradation and methane production were considerably lower in Rivers Pant and Rib compared to Rivers Medway and Nadder with 37±1 and 22±1 µmol g^{-1} wet sediment DMS degradation, and 22±1 and 15±0.5 µmol g^{-1} wet sediment methane production. These corresponded to 40% of the theoretical methane yield (54 µmol g^{-1}) in River Pant and 48% in River Rib (32 µmol g^{-1}) (Figure 4.3).

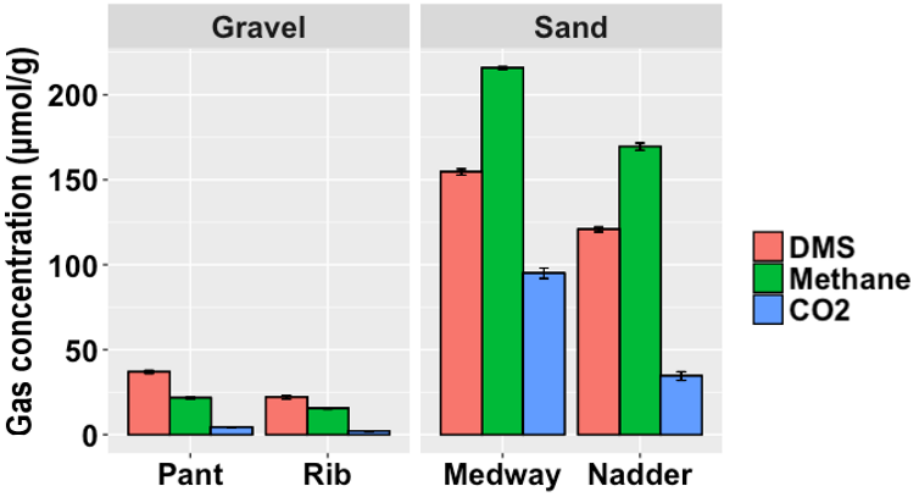

Figure 4.3. Total amounts of DMS degraded and, methane and CO_2 produced during the river sediment incubations. Error bars represent standard error above and below the average of five replicates.

CO_2 production was also measured at the end of the DMS incubations and was highest in the sand-dominated rivers (Medway and Nadder; Figure 4.3). The highest CO_2 production occurred in the River Medway incubations with 95±3 µmol CO_2 g^{-1} wet sediment, which is higher than the theoretical CO_2 yield (77 µmol g^{-1}), assuming that during methanogenesis 1 mol of DMS leads to the production of 0.5 moles of CO_2 (Equation 1; Chapter 1). The Medway controls, where no DMS was added, only exhibited 2.9 µmol CO_2 g^{-1} production, thus eliminating the possibility that the CO_2 production in the DMS-incubated samples

originated from *in situ* organic material. The discrepancy in CO_2 production suggests SRB activity in these incubations, which can occur in freshwater ecosystems due to cryptic sulfur cycling (Blodau *et al.*, 2007; Berg *et al.*, 2019). During SRB degradation of DMS, 1 mol of DMS is converted to 2 moles of CO_2 (Equation 2; Chapter 1). CO_2 concentrations in River Nadder sediment only accounted for 57% of the theoretical CO_2 yield (60 µmol CO_2 g^{-1}) despite having the second highest CO_2 production (34±3 µmol CO_2 g^{-1}), whereas the controls only had 2 µmol CO_2 g^{-1}. Rivers Pant and Rib had lower CO_2 production at 4.28±0.3 µmol CO_2 g^{-1} and 2.04±0.2 µmol CO_2 g^{-1}, respectively. These values corresponded to 12% of the theoretical CO_2 yield for River Pant (36 µmol CO_2 g^{-1}) and 9% for River Rib (22 µmol CO_2 g^{-1}). The controls for Rivers Pant and Rib produced less CO_2 than the incubations, 0.7 µmol CO_2 g^{-1} and 0.6 µmol CO_2 g^{-1}, respectively.

4.3.2 DMS-degrading methanogens in riverine sediments

To explore the methanogenic archaea responsible for DMS-dependent methane generation in riverine sediments, the *mcrA* gene, a common functional gene amongst methanogens, was sequenced. A total of $1.4x10^6$, quality-filtered, chimaera-free *mcrA* sequences were obtained and assigned to 5,240 ASVs (amplicon sequence variants).

There was a statistically significant change in the methanogen communities following the addition of DMS (PERMANOVA, $p<0.001$), yet no significant differences were observed between the rivers (PERMANOVA, $p>0.05$). This suggests that DMS-degrading methanogen diversity was not affected by sampling site and grain size.

In the original sediment samples, the dominating methanogen was an uncultured *Methanosarcinales*, which had a relative abundance of 41%-86% (Figure 4.4). Similarly, uncultured *Methanosarcinales* dominated in the incubation controls (32%-56%). *Methanomethylovorans* (family *Methanosarcinaceae*) became dominant in all river sediments incubated with DMS (Figure 4.4). Domination of a single genus is further supported by the alpha diversity, where the Shannon diversity significantly reduced after the addition of DMS in all incubations (Table 4.2; $p<0.05$).

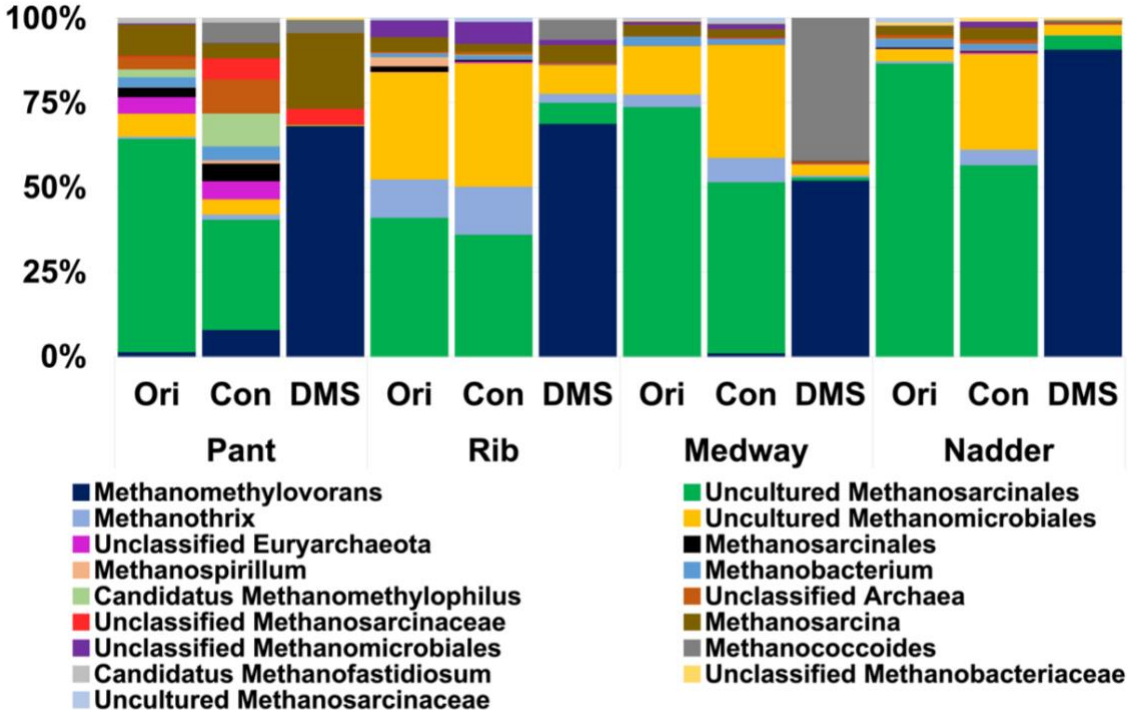

Figure 4.4. Relative abundance of all methanogenic archaea at genus level in the riverine sediment samples following the amplification of the *mcrA* gene. Ori: Original sediment samples before the incubations; Con: Controls during the incubation experiment; DMS: DMS-amended sediment.

Table 4.2. Shannon (H) indices for the methanogens in the riverine sediment samples. Significant changes in the indices were observed between original and DMS-amended samples from all sampling sites ($p<0.05$).

Shannon, H	Original	DMS
Pant	2.1 ± 0.3	0.5 ± 0.1
Rib	2.0 ± 0.1	1.0 ± 0.1
Medway	1.3 ± 0.2	0.3 ± 0.1
Nadder	1.3 ± 0.2	0.3 ± 0.1

Methanomethylovorans increased in the gravel-dominated River Pant from 2%±1% to 69%±7% and in River Rib from 0.04%±0% to 69%±5%. *Methanosarcina* (family *Methanosarcinaceae*) also increased in River Pant from 9%±3% to 22%±5%. In the sand-dominated rivers, Medway and Nadder, *Methanomethylovorans* dominated at 53%±14% and 91%±4%, respectively, after increasing from its original 0.4%±0.1% in River Medway and 0.01%±0% in River Nadder. In River Medway, *Methanococcoides* (family *Methanosarcinaceae*) also increased after DMS addition from 0.1%±0% to 42%±15% (Figure 4.4). *Methanococcoides* also increased in Rivers Pant (0.2%±0% to 4%±1%) and Rib (0.01%±0% to 6%±3%).

The change in methanogenic archaea following the DMS incubations can also be observed in the PCoA graph, where the methanogens exhibited two different clusters based on DMS addition (Figure 4.5). Spearman's r_s correlation analysis of the PCoA coordinates showed a significant positive correlation between PCo1, which accounted for 67.8% of the data, and DMS degradation, and methane and CO_2 production ($r_s= 0.9$, $p<0.001$), suggesting these parameters are the main reason for the changes in the methanogen communities (Table 4.3).

PCo2 correlated positively with grain size (r_s= 0.4, $p<0.05$), however no significant change was observed in the methanogen communities due to grain size (Table 4.3).

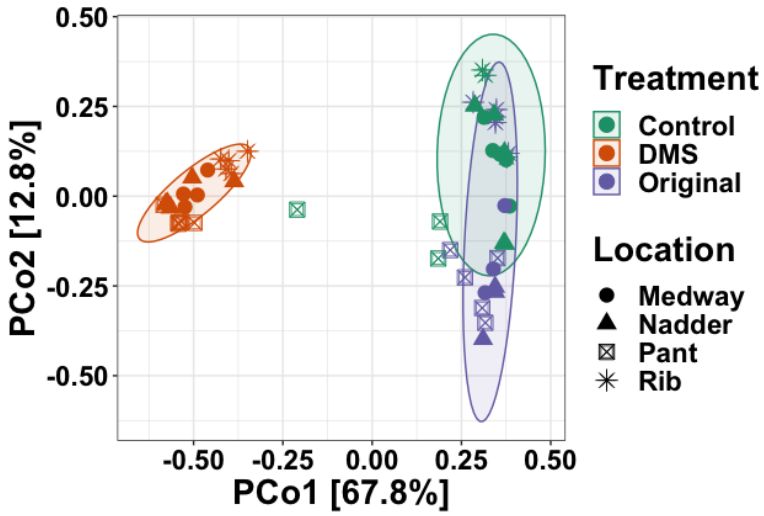

Figure 4.5. Principal Coordinate Analysis (PCoA) plots of the *mcrA* sequences based on Bray-Curtis dissimilarity metrics. Ellipses indicate 95% confidence intervals according to treatment data. Colour indicates treatment. Shapes indicate sampling site.

Table 4.3. Spearman's rank correlation coefficients (r_s) between total DMS consumed, total methane and CO_2 produced and grain size and the first two PCoA coordinates from the *mcrA* (methanogens) sequence analysis. The PCoA was based on Bray-Curtis dissimilarity metrics. Statistically significant values are in bold. ***: $p<0.001$; **: $p<0.01$; *: $p<0.05$.

Spearman's rank correlation (r_s)	PCo1	PCo2
DMS consumed (µmol)	**0.87*** **	0.03
Methane produced (µmol)	**0.87*** **	0.02
CO_2 produced (µmol)	**0.86*** **	0.02
Grain size (mm)	-0.08	**0.43***

Quantification of the *mcrA* gene abundances further supported that DMS degradation led to methanogenesis. After the addition of DMS, the methanogens increased in abundance compared to the original sediments (Figure 4.6). River Medway had the highest abundance of *in situ* methanogens, which exhibited the most significant increase from $2.3x10^{7}\pm0.6x10^{7}$ copies g^{-1} wet sediment to $9.1x10^{8}\pm1.8x10^{8}$ copies g^{-1} following the addition of DMS (Figure 4.6). The other three rivers exhibited similar original methanogen abundances despite the differences in riverbed grain size, yet, like River Medway, all increased following the addition of DMS (Figure 4.6).

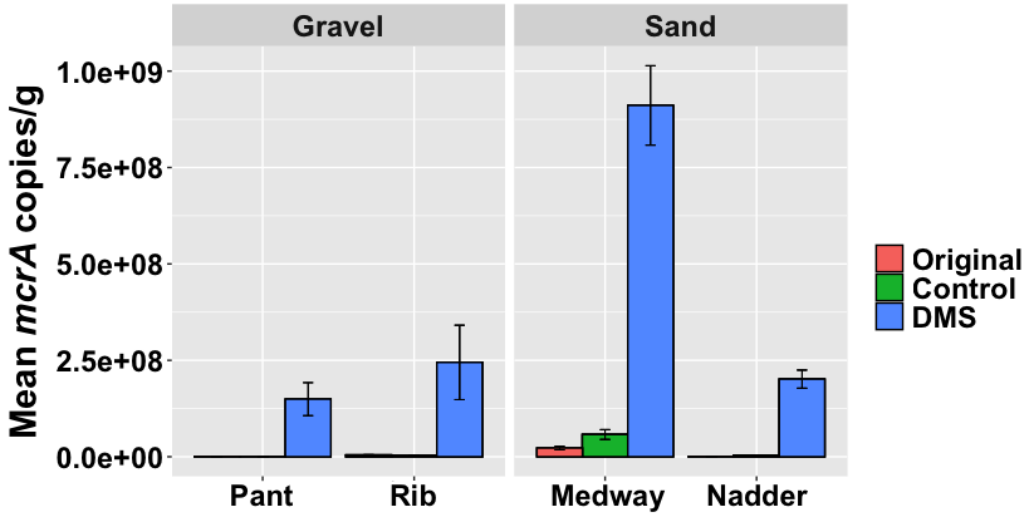

Figure 4.6. Mean copy number of the *mcrA* gene per gram of sediment. Original: Original sediment samples before the incubations; Control: Controls during the incubation experiment; DMS: Sediment samples from the DMS incubations. Error bars represent standard error above and below the average of five replicates.

4.3.3 SRB in riverine sediments

Freshwater sediments have low sulfate concentrations, yet SRB activity can occur in these ecosystems because of cryptic sulfur cycling (Jorgensen, 1990; Blodau *et al.*, 2007; Heitmann

et al., 2007; Berg *et al.*, 2019). Therefore, the *dsrB* gene was amplified and sequenced to analyse SRB abundance in riverine sediments following the addition of DMS. $5.9x10^5$ quality-filtered, chimaera-free *dsrB* sequences were obtained and assigned to 2,744 ASVs.

There were significant community changes in the original and DMS-incubated sediment samples (PERMANOVA; $p<0.05$). Despite these community changes, no changes were observed in SRB alpha-diversity, where similar species variety was observed between the original and DMS-incubated samples (Table 4.4).

Table 4.4. Shannon (H) indices for SRB in the riverine sediment samples. No significant changes were observed amongst the SRB diversities.

Shannon, H	Original	DMS
Pant	5.0 ± 0.0	5.6 ± 0.1
Rib	5.6 ± 0.1	5.1 ± 0.2
Medway	5.5 ± 0.2	5.1 ± 0.1
Nadder	5.2 ± 0.1	5.2 ± 0.1

In the original and control sediments, unclassified *Proteobacteria* dominated all sampling sites (36%-46%), followed by unclassified Bacteria (20%-34%; Figure 4.7). The most significant difference between the sediment samples was in the relative abundance of *Desulfobacca.* A higher relative abundance of *Desulfobacca* was observed in the original sediments from sand-dominated Medway (4%±2%) and Nadder (4%±2%), compared to the gravel-dominated Pant (undetected) and Rib (2%±0.5%; Figure 4.7). Following the addition of DMS, the relative abundance of *Desulfobacca* increased to 7%±1% in River Medway but remained the same in River Nadder (4%±2%). In River Pant, *Desulfobacca* increased to 1%±0.6%, whereas in River Rib it decreased to 1%±1% (Figure 4.7).

Furthermore, unclassified *Proteobacteria* and unclassified Bacteria remained the dominant taxa among the SRB populations at 33%-40% and 18%-30%, respectively. *Desulfobulbus* also increased in all sites after DMS addition, reaching 7% in Rivers Pant (±1.8%), Rib (±1.4%) and Medway (±0.5%), and 4%±1% in River Nadder (Figure 4.7). *Desulfosarcina*, a genus with a known DMS degrading strain (SD1), also increased in relative abundance in Rivers Pant (7%±0.4% from 1%±0.3%), Rib (4%±1.3% from 1%±0.4%) and Nadder (5%±2% from 2%±1%; Figure 4.7). In River Medway, *Desulfosarcina* reduced after the addition of DMS to 3%±0.3% from 7%±0.9% originally (Figure 4.7).

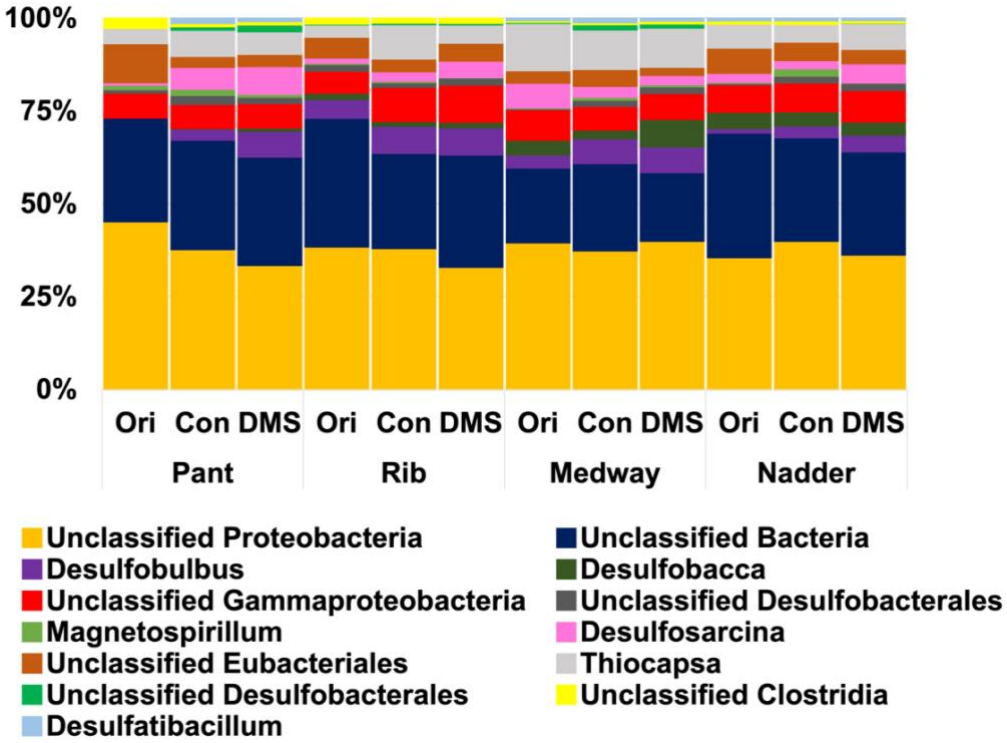

Figure 4.7. Relative abundance of all SRB at genus level in the riverine sediment samples following the amplification of the *dsrB* gene. Ori: Original sediment samples before the incubations; Con: Controls during the incubation experiment; DMS: DMS-amended sediments.

The PCoA analysis revealed distinct clusters showing SRB communities differed in each sampling site (PERMANOVA, $p<0.001$; Figure 4.8). On the other hand, no grouping was present when clustering the SRB according to DMS addition, despite the statistical analysis showing significant changes in the SRB diversity between the original and DMS-incubated samples (PERMANOVA, $p<0.05$; Figure 4.9). This is likely a result of the SRB riverine communities being so different from each other before and after the addition of DMS that the communities remained separate, thus expanding and overlapping the treatment specific PCoA ellipses.

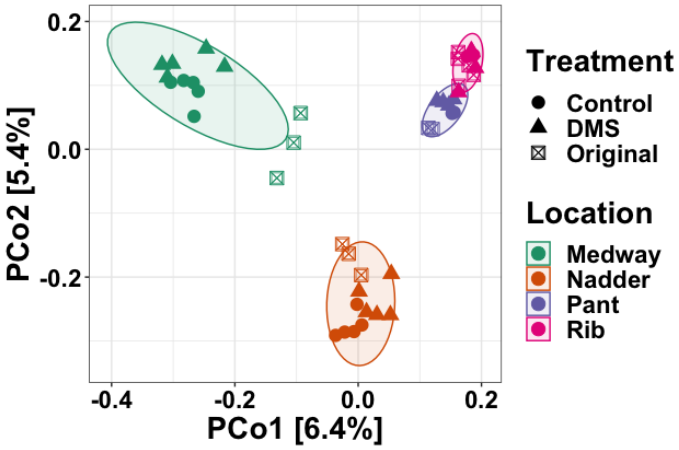

Figure 4.8. Principal Coordinate Analysis (PCoA) plots of the *dsrB* sequences based on Bray-Curtis dissimilarity metrics. Ellipses indicate 95% confidence intervals according to location data. Colour indicates sampling site. Shapes indicate treatment.

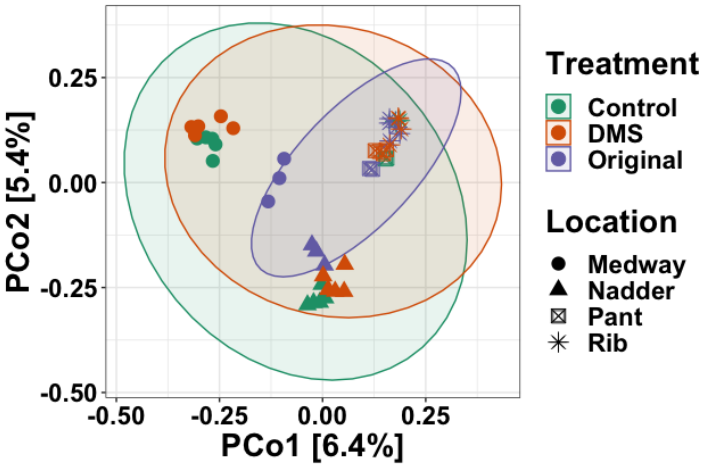

Figure 4.9. Principal Coordinate Analysis (PCoA) plots of the *dsrB* sequences based on Bray-Curtis dissimilarity metrics. Ellipses indicate 95% confidence intervals according to treatment data. Colour indicates treatment. Shapes indicate sampling site.

Spearman's r_s suggested that PCo1, which explained only 6.4% of the SRB variabilities, correlated with DMS degradation, and methane and CO_2 production ($p<0.05$), as well as grain size ($p<0.001$; Table 4.5). This suggests that SRB communities were affected by the addition of DMS in the incubations but that grain size also affected, to a lesser extent, the community composition, potentially by creating favourable conditions for different SRB at each sampling site. Despite these significant correlations, the PCoA only explained approximately 11.8% of the SRB variability suggesting these plots do not adequately describe the SRB communities. There was no statistically significant correlation between the parameters and PCo2 (5.4%; Table 4.5).

Table 4.5. Spearman's rank correlation coefficients (r_s) between total DMS consumed, total methane and CO_2 produced and grain size and the first two PCoA coordinates from the *dsrB* (SRB) sequence analysis. The PCoA was based on Bray-Curtis dissimilarity metrics. Statistically significant values are in bold. ***: p<0.001; **: p<0.01; *: p<0.05.

Spearman's rank correlation (r_s)	**PCo1**	**PCo2**
DMS consumed (µmol)	**-0.45***	-0.02
Methane produced (µmol)	**-0.45***	-0.02
CO_2 produced (µmol)	**-0.47***	-0.01
Grain size (mm)	**0.87*****	-0.24

Quantification of the *dsrB* gene showed that the sand-dominated River Medway had the highest SRB abundance among all original sediments with $1.6x10^6 \pm 0.5x10^6$ copies g^{-1}, which increased to $2.9x10^6 \pm 0.8x10^6$ copies g^{-1} following DMS addition (Figure 4.10). In the River Nadder, the SRB abundance increased from $3.9x10^5 \pm 1.3x10^5$ copies g^{-1} to $2.2x10^6 \pm 0.4x10^6$ copies g^{-1} following the DMS amendment (Figure 4.10). In gravel-dominated River Pant, SRB abundance increased from $7x10^4 \pm 0.6x10^4$ copies g^{-1} to $3.9x10^5 \pm 2x10^5$ copies g^{-1}, whilst it did not significantly change in River Rib ($9x10^4 \pm 2x10^4$ copies g^{-1} to $8.4x10^4 \pm 4.4x10^4$ copies g^{-1}; Figure 4.10).

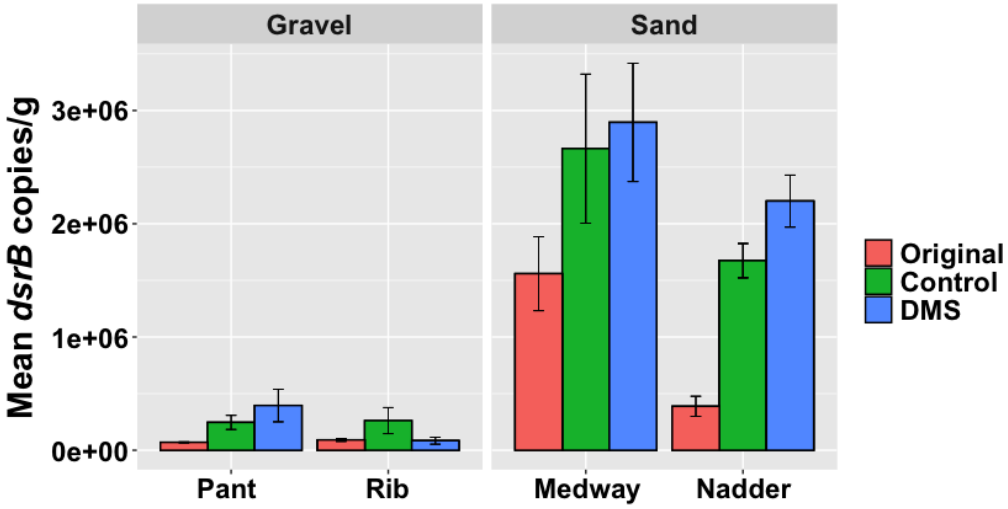

Figure 4.10. Mean copy number g^{-1} sediment of the *dsrB* gene for all SRB. Original: Original sediment samples before the incubations; Control: Controls during the incubation experiment; DMS: Sediment samples from the DMS incubations. Error bars represent standard error above and below the average of five replicates.

4.3.4 Total archaea and bacteria in riverine sediments

16S rRNA sequencing was carried out to determine the total diversity and relative abundance of bacteria and archaea in the riverine sediments. $2x10^6$ quality-filtered, chimera-free sequences were recovered and assigned to 26,701 ASVs. The data were then separated into the archaeal and bacterial populations (see sections 4.3.4.1 and 4.3.4.2).

Quantification of the 16S rRNA gene for all bacteria and archaea was conducted as a proxy of total riverine biomass in the original, control and DMS-incubated sediments. Results showed that in the original sediments the gravel-dominated Rivers Pant and Rib had a lower biomass ($4.8x10^5 \pm 2.8x10^5$ and $2.8x10^7 \pm 1.1x10^7$ copies g^{-1}, respectively) compared to the sand-dominated Rivers Medway ($1.8x10^8 \pm 0.2x10^8$ copies g^{-1}) and Nadder ($1.2x10^8 \pm 0.3x10^8$ copies g^{-1}; Figure 4.11).

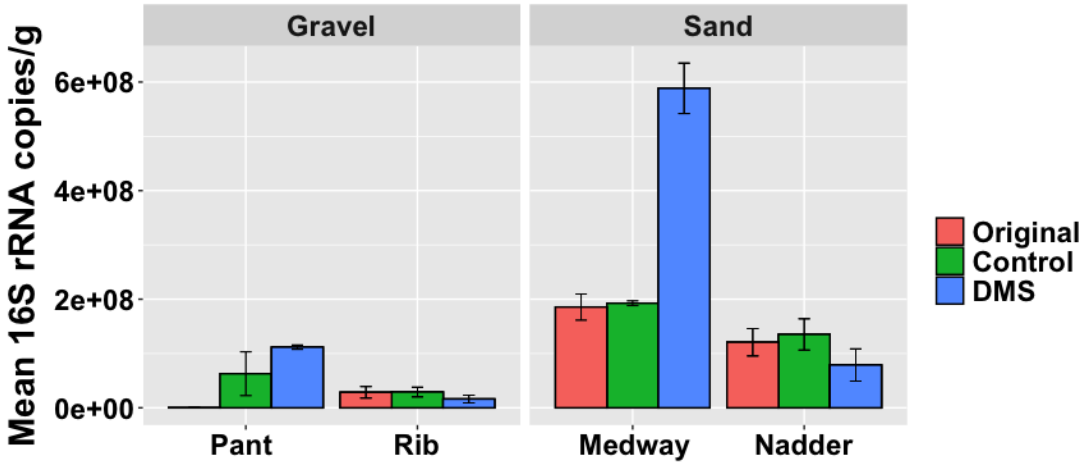

Figure 4.11. Mean copy number g^{-1} sediment of the 16S rRNA gene for all bacteria and archaea. The results can be used as a proxy for microbial biomass in the sediments. Original: Original sediment samples before the incubations; Control: Controls during the incubation experiment; DMS: Sediment samples from the DMS incubations. Error bars represent standard error above and below the average of five replicates.

Following the incubation experiment, bacterial and archaeal abundance increased in the DMS incubated sediments from Rivers Medway ($5.9x10^8 \pm 0.5x10^8$ copies g^{-1}) and Pant ($1.1x10^8 \pm 0.04x10^8$ copies g^{-1}). A decrease in abundance was observed in the DMS-incubated River Nadder ($7.9x10^7 \pm 3x10^7$ copies g^{-1}), whereas the decrease observed in River Rib ($1.6x10^7 \pm 0.7x10^7$ copies g^{-1}) was not statistically significant (Figure 4.11). The abundance measured in the incubation controls showed no significant changes compared to the original abundances, besides in River Pant where abundance increased to $6.3x10^7 \pm 4.9x10^7$ copies g^{-1} (Figure 4.11).

4.3.4.1 Archaeal diversity and relative abundance

The total archaeal communities changed significantly following the addition of DMS (PERMANOVA, $p<0.01$), yet no significant changes were observed between the sampling sites (PERMANOVA, $p>0.05$).

Unclassified *Bathyarchaeia* dominated in the original Rib, Medway and Nadder sediments (33%-44%), whereas *Nitrosarchaeum* dominated in the River Pant sediment with 41%±9%. Unclassified *Woesearchaeales* were found in high relative abundance in River Pant (18%±0.4%) and Nadder (27%±0.9%) while in low abundance in River Rib (3%±0.1%) and Medway (0.3%±0%; Figure 4.12). *Candidatus Nitrocosmicus* had a high relative abundance in River Medway (19%±13%) and low abundance in Rivers Pant (5%±2%) and Nadder (7%±7%), yet they were not present in River Rib. Unclassified *Nitrososphaeraceae* also appeared in high relative abundance in Rivers Pant (21%±3%), Medway (15%±5%) and Nadder (11%±1%) but in low abundance in River Rib (2%±1%). Interestingly, in the original sediments, River Rib had a higher archaeal diversity than all other rivers ($p<0.05$, Table 4.6).

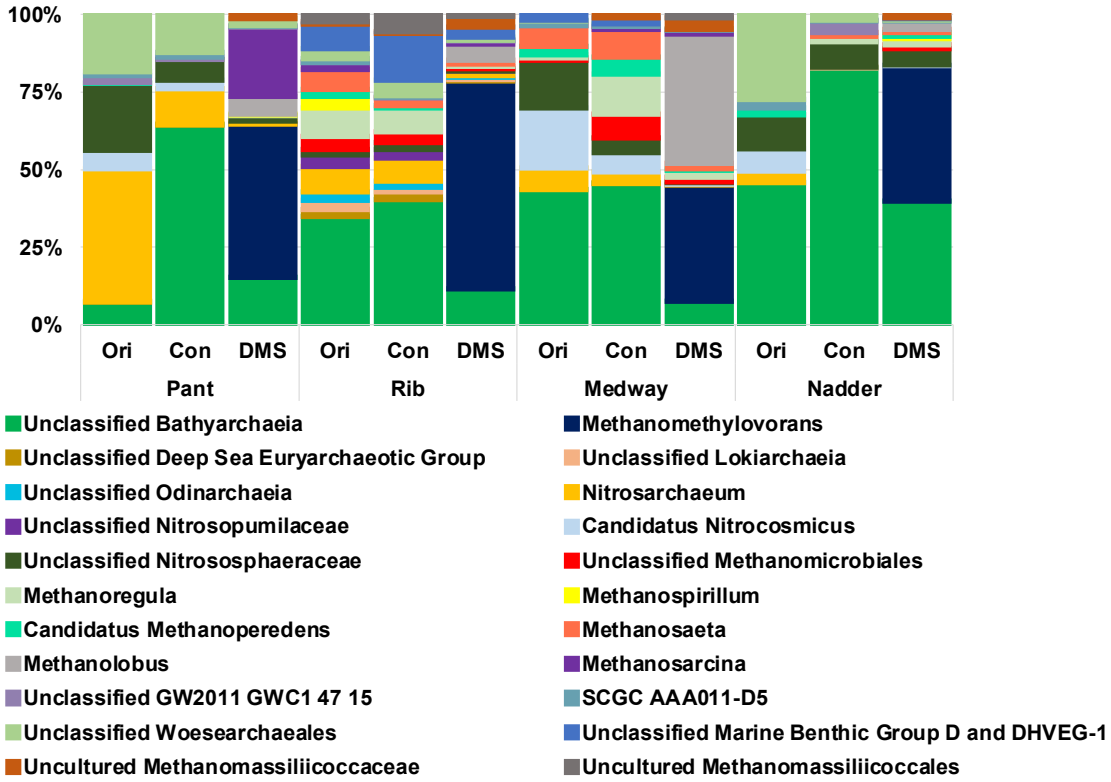

Figure 4.12. Relative abundance of the total archaeal diversity at genus level in the riverine sediment samples following the amplification of the 16S rRNA gene. Ori: Original sediment samples before the incubations; Con: Controls during the incubation experiment; DMS: DMS-amended sediment.

Table 4.6. Shannon (H) indices for archaea in the riverine sediment samples. All changes between original and DMS-incubated samples were significant ($p<0.05$) besides in the River Medway samples.

Shannon, H	Original	DMS
Pant	2.1 ± 0.3	2.8 ± 0.1
Rib	3.5 ± 0.1	2.8 ± 0.1
Medway	2.0 ± 0.5	2.8 ± 0.1
Nadder	1.8 ± 0.2	2.8 ± 0.1

Following the addition of DMS, unclassified *Bathyarchaeia* relative abundance decreased in all sediments besides River Pant, where it increased to 15%±1%. Furthermore, the dominant archaea in Rivers Pant, Rib and Nadder were *Methanomethylovorans*, which increased from undetected levels in the original sediments to 43%-66% (Figure 4.12). PCoA explained 27.5% of the variability in the archaeal communities and two clusters formed according to the treatment (Figure 4.13).

These results are consistent with the results obtained via the amplification of the *mcrA* gene (Figure 4.4). In River Medway, *Methanomethylovorans* increased from undetected to 37%±14%, yet they did not dominate the incubations (Figure 4.12). The dominant archaea following the addition of DMS in River Medway were *Methanolobus* (41%±15%; Figure 4.12). Interestingly, *Methanolobus* was not present in the *mcrA* sequencing results. This is perhaps due to differences that occur when comparing a taxonomic (16S rRNA) and a functional gene (*mcrA*).

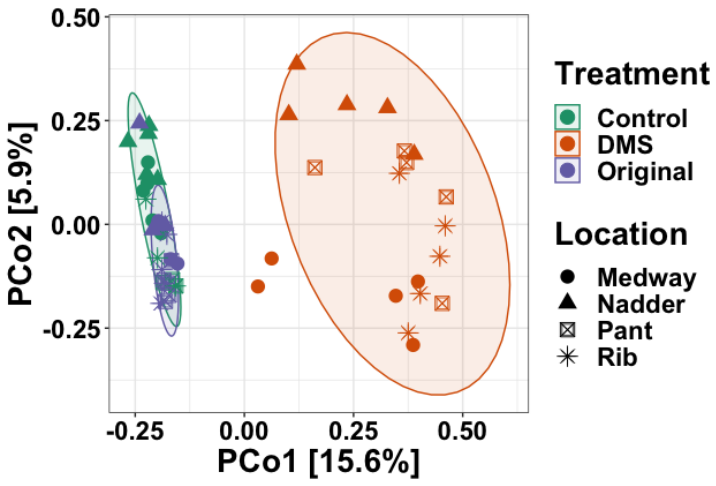

Figure 4.13. Principal Coordinate Analysis (PCoA) plots of the archaeal sequences based on Bray-Curtis dissimilarity metrics. Ellipses indicate 95% confidence intervals according to treatment data. Colour indicates treatment. Shapes indicate sampling site.

Spearman's correlation on the PCoA axes scores showed PCo1 correlated highly with DMS degradation and methane and CO_2 production suggesting these parameters affected the archaeal communities ($p<0.01$; Table 4.7). PCo2 did not correlate with any of the investigated parameters.

Table 4.7. Spearman's rank correlation coefficients (r_s) between total DMS consumed, total methane and CO_2 produced and grain size and the first two PCoA coordinates from the total archaeal sequence analysis. The PCoA was based on Bray-Curtis dissimilarity metrics. Statistically significant values are in bold. ***: $p<0.001$; **: $p<0.01$; *: $p<0.05$.

Spearman's rank correlation (r_s)	**PCo1**	**PCo2**
DMS consumed (µmol)	**-0.72*** **	-0.01
Methane produced (µmol)	**-0.71*** **	-0.02
CO_2 produced (µmol)	**-0.70*** **	-0.02
Grain size (mm)	0.04	0.19

4.3.4.2 Bacteria diversity and relative abundance

The bacterial communities were statistically different between sampling sites and between the original and DMS-incubated sediments, suggesting that there were dissimilarities between bacterial communities (PERMANOVA; $p<0.01$). On the other hand, bacterial alpha diversity only changed in the gravel-dominated sediments following the addition of DMS ($p<0.01$), suggesting that the variety of bacterial species only changed in Rivers Pant and Rib. In the original sediments, alpha diversity was very high (Shannon index >5) and remained high after DMS addition (Table 4.8).

Table 4.8. Shannon (H) indices for bacteria in the riverine sediment samples. All changes between original and DMS-incubated samples for the gravel-dominated riverbeds were significant ($p<0.01$). No significant changes were observed in the sand-dominated riverbeds.

Shannon, H	Original	DMS
Pant	5.8 ± 0.1	5.1 ± 0.1
Rib	5.6 ± 0.1	5.1 ± 0.1
Medway	4.6 ± 0.6	5.2 ± 0.1
Nadder	5.3 ± 0.0	5.2 ± 0.1

Most of the taxa in the bacterial communities had a relative abundance below 5%. The only taxon with a relative abundance above 5% was unclassified *Gastranaerophilales*, which increased to 14%±3% in the DMS incubated sediments from River Pant (originally undetected) and to 11%±4% in River Rib (originally 0.01%±0.01%), whereas it remained undetected in Rivers Medway and Nadder. In River Rib, unclassified *Hydrogenophilaceae* and *Ferritrophicum* (family *Ferritrophicaceae*) increased from undetected and 0.1%±0.06% to 7%±1% and 5%±1%, respectively, after incubation with DMS, whereas the same taxa remained <1% in Rivers Pant, Medway and Nadder (Figure 4.14). In the Medway, unclassified *Bacteroidetes-vadinHA17* dominated the original and DMS-incubated sediments at 5%±1.2. The dominant taxa in the DMS-incubated sediments from Nadder were *Sporobacter* (10%±3%) and unclassified *Thermodesulfovibrionia* (5%±0.5%; Figure 4.14).

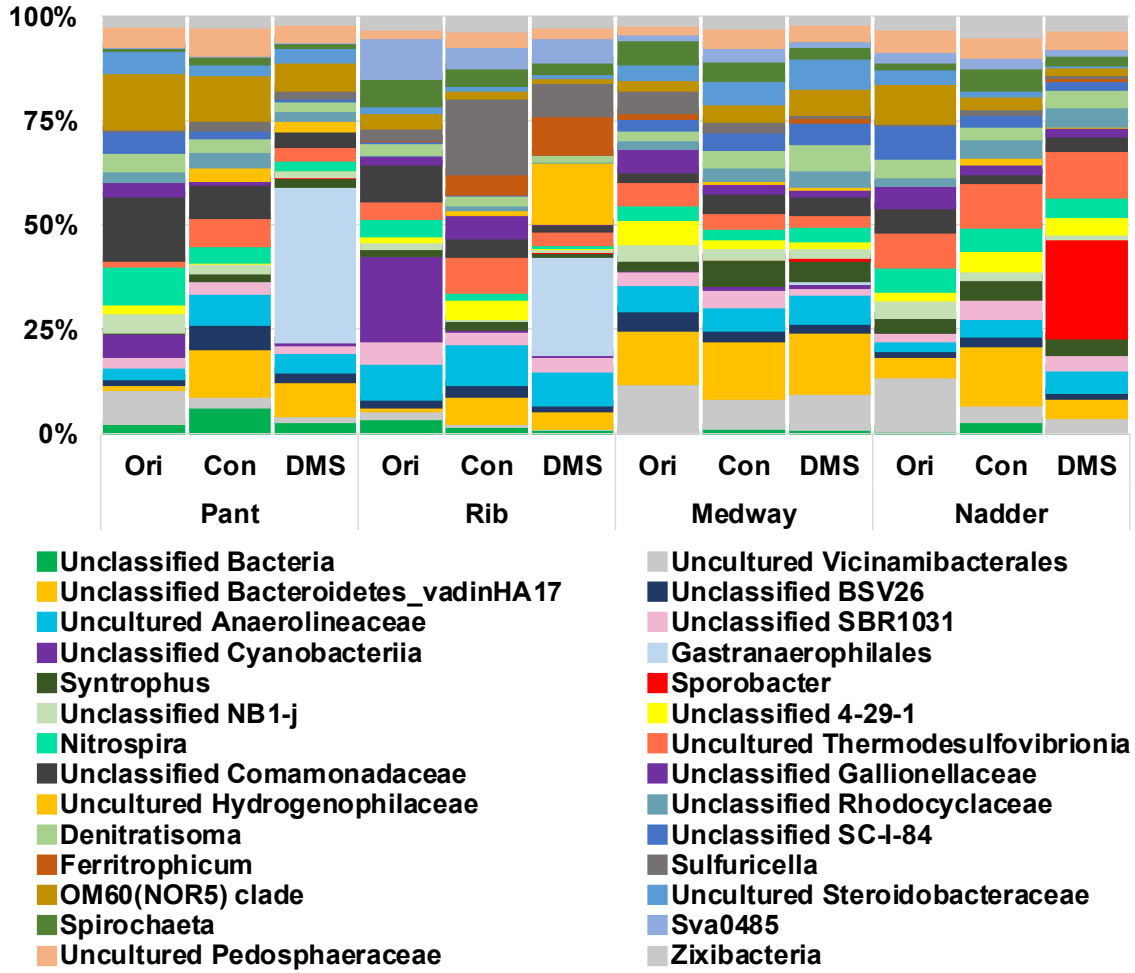

Figure 4.14. Relative abundance of the bacterial diversity at genus level in the riverine sediment samples following the amplification of the 16S rRNA gene. Ori: Original sediment samples before the incubations; Con: Controls during the incubation experiment; DMS: DMS-amended sediment.

The PCoA graph only explained 9.4% of the total variability in the bacterial communities although clustering was still observed between treatments (Figure 4.15).

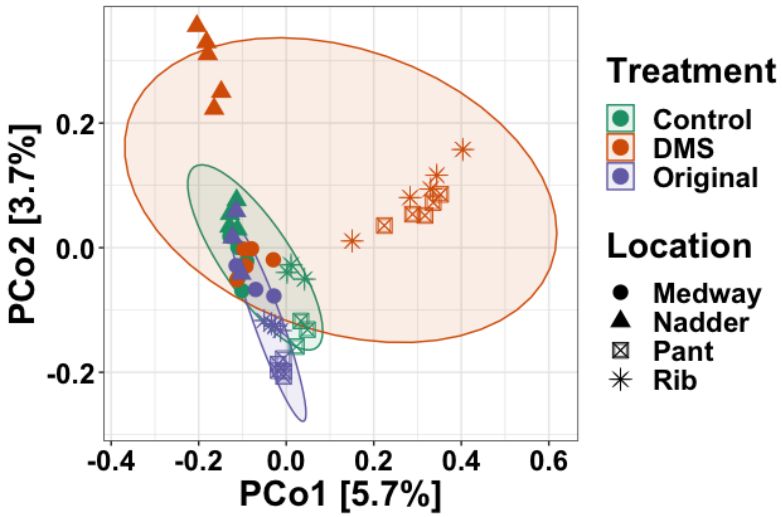

Figure 4.15. Principal Coordinate Analysis (PCoA) plots of the archaeal sequences based on Bray-Curtis dissimilarity metrics. Ellipses indicate 95% confidence intervals according to treatment data. Colour indicates treatment. Shapes indicate sampling site.

Spearman's correlation analysis on the PCoA coordinates showed that PCo1, which explained the bacterial data the most, correlated highly with grain size ($p<0.01$), suggesting the bacterial communities were different depending on riverbed type (Table 4.9). PCo2, on the other hand, correlated highly with DMS degradation and methane and CO_2 production, further showing that the addition of DMS affected the bacterial communities ($p<0.01$; Table 4.9).

Table 4.9. Spearman's rank correlation coefficients (r_s) between total DMS consumed, total methane and CO_2 produced and grain size and the first two PCoA coordinates from the total bacterial sequence analysis. The PCoA was based on Bray-Curtis dissimilarity metrics. Statistically significant values are in bold. ***: p<0.001; **: p<0.01; *: p<0.05.

Spearman's rank correlation (r_s)	PCo1	PCo2
DMS consumed (µmol)	-0.16	**0.68*** **
Methane produced (µmol)	-0.16	**0.68*** **
CO_2 produced (µmol)	-0.16	**0.67*** **
Grain size (mm)	**0.77*** **	-0.38

4.4 Discussion

Anaerobic DMS degradation and related methanogenesis in rivers are largely unexplored. In this chapter, I demonstrated that riverine sediments with sand-dominated riverbeds had a significant potential for DMS-dependent methane production, whereas gravel-dominated riverbeds had DMS-degradation potential to a lesser extent. The incubations contained DMS as the only carbon and energy source, so DMS should be the sole source of methanogenesis in these incubations. This is further supported by the proliferation of methylotrophic methanogens in all sediments following the addition of DMS. Also, no significant increases in hydrogenotrophic or acetoclastic methanogens were recorded.

There was a considerable difference in methanogenesis between rivers of different grain sizes. The gravel-dominated rivers Pant and Rib exhibited a 40%-48% theoretical methane yield, similar to my previous incubations from the Medway Estuary (39%-42%, Chapter 3; Tsola *et al.*, 2021). These theoretical methane yields are comparable to previous research by Kiene *et al.* (1986), who recorded 52%-63% yields in anoxic sediments from various ecosystems, including freshwater lakes. However, these methane yields were higher than

those observed by Zinder and Brock (1978), who, using sediment from Lake Mendota (USA), found approximately 28% DMS to methane conversion efficiency. This difference in yield is most likely a result of the very short incubation times (<2 days) in these experiments, which means that the methanogen communities could not reach their maximum potential (Zinder and Brock, 1978).

The sand-dominated Rivers Medway and Nadder had a theoretical methane yield of 83%-92% and, to the best of my knowledge, this is the highest recorded methane yield from DMS degradation. The difference between the gravel- and sand-dominated river methane yields is probably a result of different sediment characteristics (i.e. grain size) and the difference in biomass in the original sediments, as observed via 16S rRNA qPCR. Studies have shown that river nutrient levels are primarily affected by tributaries, seasonality, river flow and meteorological events (Hagy *et al.*, 2004; Sigleo and Frick, 2007; Murphy *et al.*, 2011; Tong *et al.*, 2015). A higher nutrient loading in combination with the permeability exhibited by sand-dominated riverbeds would mean more nutrients and organic material entering the sand-dominated sediments (Janssen *et al.*, 2005). These nutrients and organic material would remain in the sediments during incubation for microorganisms to use for their growth, thus affecting the methane yield between the gravel- and sand-dominated riverbeds. These nutrient loading differences can also lead to a lower methanogen carrying capacity in the gravel-dominated rivers also exhibited by the lower biomass in the original sediments, hence reaching the stationary phase of growth faster since fewer nutrients and organic material would be available. Furthermore, changes in methanogenesis between gravel- and sand-dominated riverbeds can also occur due to the difference in advection effect between grain sizes (Janssen *et al.*, 2005). A lower advective oxygen supply is probably present in the sand-dominated riverbeds compared to the gravel-dominated rivers since sand is smaller than

gravel, thus affecting methanogenesis (Wentworth, 1922). The potential existence of oxygen in the gravel-dominated riverbeds is further proven since aerobic taxa, such as unclassified *Comamonadaceae* and uncultured *Vicinamibacterales*, were present in the original gravel-dominated samples. However, the presence of oxygen does not mean methanogenesis is not naturally carried out in these rivers because anaerobic metabolism has been shown to occur in both sand and gravel-dominated riverbeds due to anoxic microsites in the sediments (Lansdown *et al.*, 2014, 2016; Shen *et al.*, 2019).

DMS degradation in River Medway incubations (83% theoretical methane yield) was also higher than the freshwater incubations of the Medway Estuary (41% theoretical methane yield) presented in Chapter 3. The same site was used during both sampling trips, so this vast difference in methane yield from DMS-degradation may not be expected; however, the previous sampling was carried out in November 2018, whereas the sampling for these incubations was in March 2021. Meteorological events such as rain can cause disturbance to the river's natural flow, which means intrusion of nutrients and organic material in the sediment does not occur in the same way. Reports from the UK Environmental Agency and the Met Office (2018; 2021; UK Government Web Archive) showed 7 mm of rainfall in the southeast of the UK in March 2021 but 18 mm of rainfall in November 2018. The higher rainfall and subsequent increase in river flow could increase aeration and decrease nutrient concentrations in the deeper sediment layers, potentially affecting methanogen communities (Tong *et al.*, 2015).

Methanomethylovorans dominated all sediments after DMS addition, regardless of riverbed grain size. *Methanomethylovorans* are known methylotrophic methanogens, which have been shown to degrade DMS in freshwater ecosystems (Lomans *et al.*, 1999; Jiang *et al.*, 2005;

Cha *et al.*, 2013; Tsola *et al.*, 2021). *Methanosarcina* also increased in Rivers Pant and Rib following the addition of DMS. Members of the genus *Methanosarcina* are universal and are known to utilise most methanogenesis substrates, including DMS (Sowers *et al.*, 1984; Ni and Boone, 1991; Elberson and Sowers, 1997; Lyimo *et al.*, 2000).

Methanococcoides, another methylotrophic methanogen genus, increased in Rivers Pant, Rib and Medway, following the addition of DMS. *Methanococcoides* are typically associated with saline environments like saltmarshes, brackish lakes and tidal flats (Munson *et al.*, 1997; Wilms *et al.*, 2006; Watanabe *et al.*, 2009). Previous studies have characterised *Methanococcoides* as obligate methylotrophic methanogens that can degrade methylamines, betaine, choline and methanol but no member of the *Methanococcoides* genus has been shown to degrade DMS before, besides in Chapter 3 where *Methanococcoides* dominated in the marine incubations and increased in both the brackish and freshwater Medway sampling sites following the addition of DMS (L'Haridon *et al.*, 2014; Jameson *et al.*, 2019; Tsola *et al.*, 2021; Liang *et al.*, 2022). The increase of *Methanococcoides* in these riverine incubations and Chapter 3 suggest this genus could have DMS degrading capabilities. On the other hand, Yin *et al.* (2019) showed that in marine sediments *Methanococcoides methylutens* was able to assimilate CO_2 into biomass or grow mixotrophically using CO_2 as its carbon source. In the study for this chapter, CO_2 was produced in all sediments after DMS addition and, besides in River Medway, production never achieved the theoretically expected values. This, alongside the fact that no member of the *Methanococcoides* genus has been found able to degrade DMS, could suggest this alternative growth pathway is occurring in the riverine sediments.

Methanolobus, another DMS-degrading methanogen associated with saline sediments, increased in all samples following the addition of DMS, according to the 16S rRNA data.

Wen *et al.* (2017) showed that *Methanolobus* were present in lake sediments. Furthermore, Narrowe *et al.* (2019) found *Methanolobus* in a low-salinity environment when investigating freshwater wetland sediment from Old Woman Creek (Ohio, USA). A plausible way *Methanolobus* and *Methanococcoides* were introduced to the riverine sediments studied here is via runoff from the surrounding terrestrial soils since both these taxa have been found in these types of soils before (Wen *et al.*, 2017). In the River Medway, the existence of both *Methanolobus* and *Methanococcoides* could also be a result of tidal mixing since this river forms the freshwater part of the macrotidal Medway Estuary. Specifically, these taxa could have been transported from the marine and brackish sides of the estuary, where they are usually found (Chapter 3; Tsola *et al.*, 2021).

CO_2 was produced in all sediments after DMS addition, especially in the sand-dominated River Medway, where yield reached 123% of the theoretically expected methanogenesis-derived CO_2, suggesting the possible involvement of SRB in DMS degradation. No changes to SRB diversity were identified following the incubations, yet SRB abundance significantly increased in the DMS incubated sediments, besides in River Rib. Also, *Desulfosarcina*, a known DMS degrading SRB, increased in relative abundance in Rivers Pant, Rib and Nadder (Lyimo *et al.*, 2009). SRB activity in these sediments is surprising when considering the low concentrations of sulfate typically found in freshwater ecosystems. Regardless of low sulfate concentrations, a strain of *Desulfobulbus propionicus* was isolated from freshwater sediment near Hannover, suggesting these SRB survive in freshwater ecosystems (Widdel and Pfennig, 1982). Similarly, *Desulfobulbus* and *Desulfobacca* were identified in freshwater Lake Tahu (China) recently, and *Desulfobacca* were also found in Lake Constance (Germany; Wörner and Pester, 2019; Chen *et al.*, 2022). Neither taxon has been identified as a DMS-degrader, yet both are characterised as generalist SRB and increased following the addition of DMS

suggesting they might be novel DMS-degrading SRB (Oude Elferink *et al.*, 1999; Brenner *et al.*, 2005).

On the other hand, if *Desulfobulbus* were not degrading DMS, they could be utilising propionate (Widdel and Pfennig, 1982). Propionate is one of the main intermediates produced during anaerobic degradation, so it is probably naturally occurring in these river sediments. Propionate oxidation by *Desulfobulbus* leads to the production of acetate and CO_2 (Widdel and Pfennig, 1982). The produced acetate can then be oxidised by *Desulfobacca*, as shown in the type species *D. acetoxidans*, thus leading to its increase in these riverine sediments (Oude Elferink *et al.*, 1999).

In conclusion, this was the first study investigating anaerobic DMS-degradation in rivers with contrasting sediment characteristics. Results showed that DMS is an important source of methane in riverine sediments, with sand-dominated riverbeds exhibiting a high DMS to methane conversion efficiency; however gravel-dominated sediments had comparatively a lower efficiency. *Methanomethylovorans* were the dominant DMS-degrading methanogens in all sampling sites. SRB activity was also present in these sediments, but no differences were observed between riverbed types. Despite this, certain SRB taxa (*Desulfobulbus* and *Desulfobacca*) increased following the addition of DMS suggesting the possible existence of novel DMS-degrading SRB in these freshwater ecosystems.

5 Depth profile of microbial DMS degradation in Baltic Sea sediments

5.1 Introduction

Dimethylsulfide (DMS) is a highly abundant volatile organosulfur compound with a global production of over 300 million tonnes each year (Curson *et al.*, 2011). The main precursor to DMS in the environment is dimethylsulfoniopropionate (DMSP), an osmolyte produced in significant quantities (~10^9 tonnes annually) by marine algae, phytoplankton, corals and plants such as *Spartina* and sugar cane (Yoch, 2002; Jackson and Stuckey, 2007; Sievert *et al.*, 2007; van Alstyne and Puglisi, 2007; Raina *et al.*, 2013; Alcolombri *et al.*, 2015). Recent studies showed that bacteria are also important DMSP producers in both oxic and anoxic coastal and marine sediments, suggesting these ecosystems are highly productive environments for bacterial DMSP and, consequently, DMS production (Curson *et al.*, 2017; Sun *et al.*, 2020; Zheng *et al.*, 2020). Other key sources of DMS in sediments include the degradation of sulfur-containing amino acids and methoxylated aromatic compounds, the reduction of dimethyl sulfoxide and the methylation of hydrogen sulfide and methanethiol (Zinder and Brock, 1978; Kiene and Hines, 1995; Carrión *et al.*, 2015).

In anoxic sediments, DMS can be degraded to potent greenhouse gases methane and carbon dioxide by methanogens from the genera *Methanomethylovorans*, *Methanolobus*, *Methanosarcina* and *Methanohalophilus*, which further highlights the environmental significance of DMS (Kiene *et al.*, 1986; Ni and Boone, 1991; Kadam *et al.*, 1994; Lomans *et al.*, 1999; Lomans *et al.*, 1999; Lyimo *et al.*, 2000). When there is available sulfate, sulfate-reducing bacteria (SRB) of the genera *Desulfotomaculum* and *Desulfosarcina* can also use DMS as a carbon source (Tanimoto and Bak, 1994; Lyimo *et al.*, 2009). Early studies

suggested that SRB outcompete methanogens for DMS in sulfate-containing anoxic sediments owing to their thermodynamic advantage (Lyimo *et al.*, 2009; Zhuang *et al.*, 2012). In contrast, in Chapter 3, I demonstrated that DMS-dependent methane yield was not affected by sulfate availability in estuarine sediments, although the diversity of DMS-degrading methanogens was affected (Tsola *et al.*, 2021).

In this chapter, I investigated the DMS degradation potential and the depth profile of DMS-degrading microorganisms in the sediments of the Baltic Sea, which is one of the largest brackish water bodies in the world. It is subjected to regular phytoplankton blooms that can be seen via satellite releasing DMSP in the water column (Hjerne *et al.*, 2019). For instance, phytoplankton blooms in the southwestern Baltic Sea can release an average of 18.5 nM of DMSP (Yanan Zhao *et al.*, 2021). These regular phytoplankton blooms alongside the Baltic Sea's brackish nature, where moderate salinity concentrations (<7‰; Lehmann *et al.*, 2022) are recorded, make the Baltic Sea a model ecosystem for studying microbial DMS-degradation.

Baltic Sea sediment samples were collected from seven depths (0-1 cm, 1-2 cm, 2-5 cm, 9-12 cm, 19-22 cm, 39-43 cm, and 60-65 cm) below the seafloor across three stations following a phytoplankton bloom in April 2018. Previous research showed the concentrations of methane and sulfate in the sampling sites and depths (Figure 5.1; Thang *et al.*, 2013).

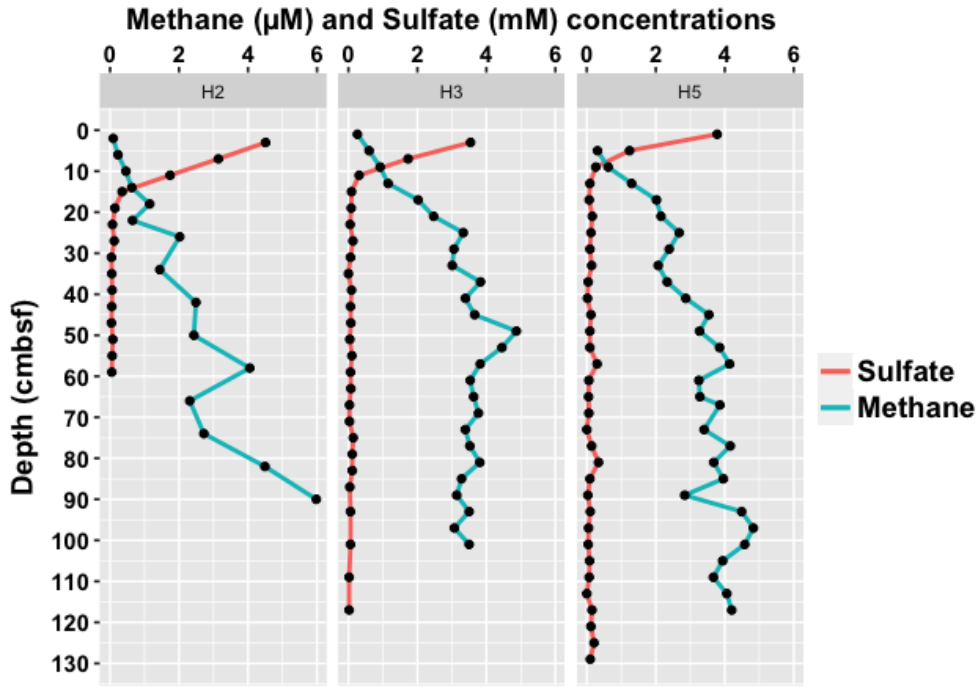

Figure 5.1. Concentrations of methane and sulfate per depth in the three sampling stations. cmbf: cm below seafloor. The figure was adapted from Thang *et al.*, 2013.

In this Chapter, I aimed to identify the diversity and abundance of DMS-degrading microorganisms in Baltic Sea sediments and to investigate how those populations could be affected by the sulfate concentration across the sediment depth. Through metagenomics and amplicon sequencing at 19-22 cm depth, I also aimed to understand the diversity of DMS-degrading microorganisms just below the sulfate-methane transition zone (SMTZ), where only methanogenesis is expected to be observed. This study gives the first insight into the depth-profile of anaerobic DMS-degrading microorganisms across a naturally occurring sulfate concentration gradient.

I had the following hypotheses:

1) DMS will lead to methane production, with higher amounts in the depths below the SMTZ, where there is no detectable sulfate.
2) The natural sulfate gradient will affect the diversity of DMS-degrading microorganisms with different SRB and methanogen taxa appearing at different depths.
3) Due to the brackish nature of the Baltic Sea, halophilic DMS-degrading methanogens will be dominant close to the seafloor.

5.2 Study area and sampling

Our study area (Himmerfjärden Estuary, Sweden; Figure 5.2) has a stable salinity (5-7‰) and receives discharge from an upstream sewage treatment plant leading to its eutrophication (Savage *et al.*, 2004). Due to the high level of eutrophication and regular phytoplankton blooms, hypoxic or anoxic conditions are observed in the bottom waters and sediments. Overall, three sampling sites were visited, H2 (N58°50'55, E17°47'42), H3 (N58°56'04, E17°43'81) and H5 (N59°02'21, E17°43'59). All three stations are part of a suite of long-term monitoring stations studying eutrophication in the Himmerfjärden Estuary (http://www2.ecology.su.se/dbHFJ/index.htm).

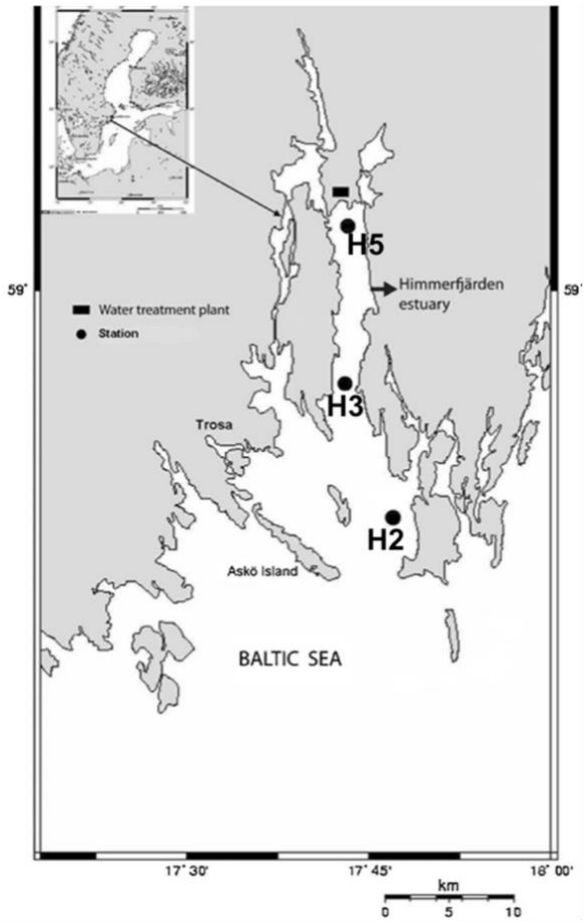

Figure 5.2. Map of the Himmerfjärden Estuary and the Baltic Sea showing the three sampling sites H2, H3 and H5. Askö Island is where the Marine Research Centre of Stockholm University is based. Inset map shows the whole Baltic Sea. The figure was adapted from Thang *et al.*, 2013. Copyright © 2012, Coastal and Estuarine Research Federation.

Each sampling site was visited using the research vessel R/V Limanda and sediment was collected using a multicorer (40 cm) and a gravity corer (140 cm). Once back at the Marine Research Centre of Stockholm University on the Askö Island, the sediment cores were partitioned into seven depths according to the sulfate measurements (Thang *et al.*, 2013). All sediment was placed into bags, sealed and kept at 4 ^{o}C until transfer to the UK. Upon arrival to the laboratory in the UK the next day, the sealed sediment bags were placed in an

anaerobic glove box (Belle Technology, UK) to prevent sediment exposure to oxygen and microcosms were set up immediately.

Three replicated incubations were established for each sampling location and depth using 2.5 g of sediment and 20 mL of artificial seawater and DMS as the only carbon and energy source (Wyman *et al.*, 1985; Wilson *et al.*, 1996). The sulfate concentration of the incubations was adjusted according to the *in situ* sulfate concentrations of sediment pore water from each depth, which ranged between 0 and 4.5 mM (Table 5.1). Two sets of replicated controls were also established. One set of controls contained no DMS, and the other set was established to check the adsorption of DMS by the sediment using thrice autoclaved sediment. The microcosms were incubated at 8 ºC, which was the sediment temperature at the time of sampling. All microcosms were kept in the dark to avoid the photochemical destruction of DMS (Brimblecombe and Shooter, 1986).

Table 5.1. Sulfate concentrations used in the microcosms per sampling station and depth.

	Sulfate concentration (mM)						
Depth	**0-1 cm**	**1-2 cm**	**2-5 cm**	**9-12 cm**	**19-22 cm**	**39-43 cm**	**60-65 cm**
Station H2	4.5	4.5	3	1	0.05	0.05	0
Station H3	4.5	4.5	3	1	0.05	0.05	0
Station H5	4.5	4.5	3	1	0.05	0.05	0

5.3 Results

5.3.1 Depth profiles of DMS, methane, CO_2 and sulfate in the sediments

Seven sediment layers collected from three sampling stations at the Baltic Sea were incubated with DMS as the only carbon and energy source, and with varying sulfate concentrations reflecting the *in situ* concentrations in the sediments. We terminated the incubations between day 82 and 128 when cumulative methane concentrations became stable. We observed a lag phase in all incubations before methane production was detected, although DMS degradation began within the first couple of days, suggesting SRB started to consume DMS before the methanogens (Figure 5.3).

DMS degradation and accompanying methane and CO_2 productions were observed in all sediment incubations except for the 60-65 cm (bottom) sediment layer from station H2, where no methane was produced despite DMS degradation (Figure 5.4). In some of the samples, DMS production was observed during the incubation experiment. This is likely a result of the microorganisms using up endogenous DMS production substrates such as DMSP. At a later Baltic Sea sampling expedition (June-July 2022), DMSP were carried out *in situ* and high amounts of DMSP were observed in these sediments, which could lead to DMS production in the incubations.

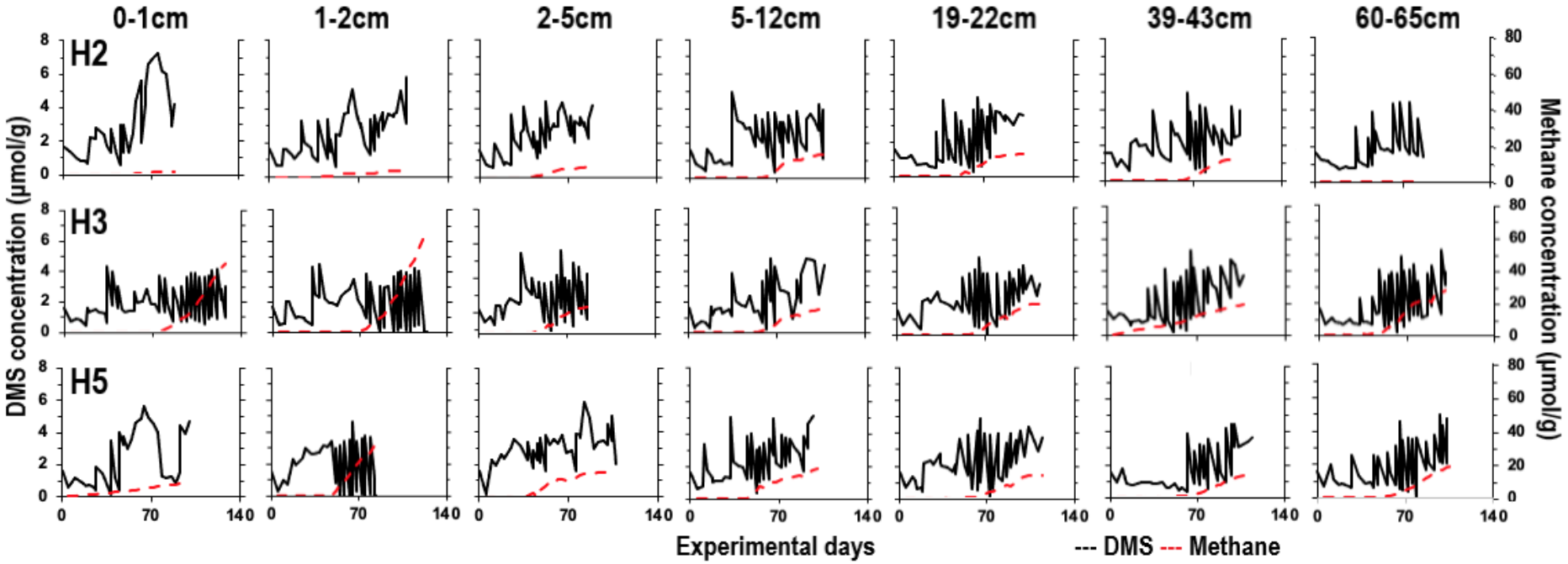

Figure 5.3. Average DMS amounts degraded (primary axis) and average methane amounts produced (secondary axis) in the DMS amended incubations. Top: Station H2; Middle: Station H3; Bottom: Station H5. Each row corresponds to the sampling depth indicated above each graph from station H2. Error bars were omitted to make the graph legible.

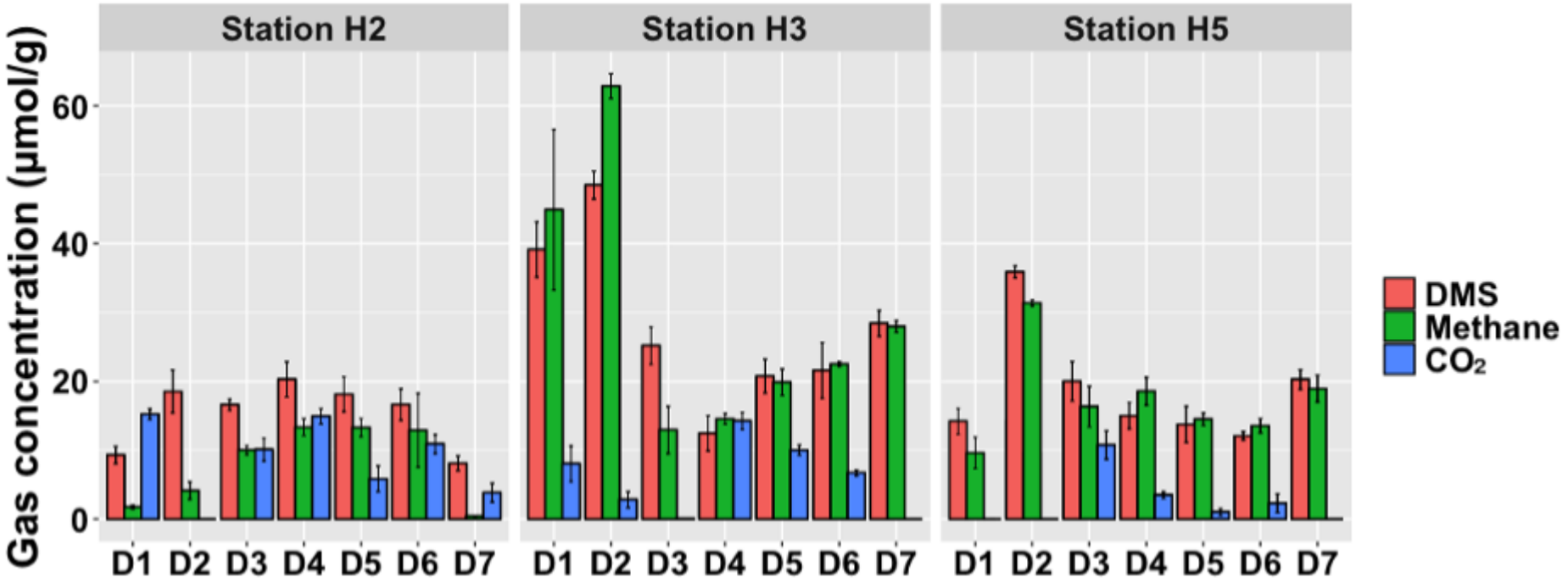

Figure 5.4. Average DMS degradation and methane and CO_2 production in the Baltic Sea sediment samples across all sampling sites (H2, H3 and H5) and depths. D1: 0-1 cm; D2: 1-2 cm; D3: 2-5 cm; D4: 9-12 cm; D5: 19-22 cm; D6: 39-43 cm; D7: 60-65 cm. Error bars represent standard error above and below the average of three replicates.

The greatest DMS consumption and methane production were recorded in the top two sediment layers (0-1 cm and 1-2 cm) from station H3, although those samples were provided with the highest concentration of sulfate (40 μmol g^{-1}; Figure 5.4). The DMS consumption was 39.1±4 and 48.5±2 μmol g^{-1} wet sediment, whilst the methane production was 44.9±11.6 and 62.9±1.8 μmol methane g^{-1} wet sediment, which corresponds to 77% and 86% of the theoretical methane yield assuming 1 mol of DMS yields 1.5 moles of methane (Equation 1, Chapter 1). The highest methane production (31.4±0.4 μmol g^{-1}) across the H5 sediment samples was found within the 1-2 cm depth. However, this is significantly lower than the H3 top sediment layer, where the highest methane production was observed, although similar amounts of DMS were consumed in both H3 and H5 incubations (39.1±4 and 35.9±0.9 μmol g^{-1}, respectively).

The highest theoretical methane yield (82%) among the H5 incubations was observed in the 9-12 cm layer, despite these samples having a relatively low DMS consumption (15±1.9 μmol DMS g^{-1}) and methane production (18.5±2 μmol methane g^{-1}; Figure 5.4). DMS degradation and methane production were generally low across H2 sediment incubations. Among the H2 incubations, the highest DMS consumption (20.3±2.6 μmol g^{-1}) occurred at depth 9-12cm whilst the maximum methane production occurred at depths 9-12 cm (13.3±1.2 μmol g^{-1}), 19-22 cm (13.3±1.3 μmol g^{-1}) and 39-43 cm (13.2±5.3 μmol g^{-1}). Depth 39-43 cm had the highest theoretical methane yield (53%) after degrading 16.6±2.3 μmol g^{-1} of DMS and producing 21.7±5.3 μmol methane g^{-1} (Figure 5.4).

In addition to methane, I also measured CO_2 in the incubations as it is one of the metabolic end products of anaerobic DMS degradation via both methanogenesis and sulfate reduction. The maximum CO_2 concentration (15.2±0.8 μmol CO_2 g^{-1} wet sediment) was measured in the top sediment from H2, where little methane production was measured (Figure 5.4). In the incubations where maximum methane production was observed (0-1 cm and 1-2 cm) at H3, the total amount of CO_2 was 8±2.5 μmol CO_2 g^{-1} and 2.8±1.1 μmol CO_2 g^{-1}, respectively, which were significantly lower than the theoretical CO_2 yields assuming only methanogenesis (19.5±2 μmol CO_2 g^{-1} and 24.2±1 μmol CO_2 g^{-1}, respectively) or sulfate reduction (58.8±8 μmol CO_2 g^{-1} and 72.6±4 μmol CO_2 g^{-1}, respectively) took place (Figure 5.4). Similarly, no CO_2 was found in the incubations from H5 top sediment (1-2 cm), where maximum methanogenesis was observed.

Sulfate reduction occurred in the top sediments (0-1 cm, 1-2 cm, 2-5 cm) from all sampling stations. In station H2, ~80% of the amended sulfate was used, bringing the sulfate concentration to 8±0.4 μmol g^{-1} wet sediment (Figure 5.5), suggesting that DMS degradation via the sulfate reduction route occurred. In the incubations from stations H3 and H5, where maximum methane production was observed, ~95% of the sulfate amended was consumed, decreasing the sulfate concentration to 2±0.2 μmol g^{-1} wet sediment (Figure 5.5). The sediment incubations from 9 cm and below were amended with 8 μmol g^{-1}, 0.4 μmol g^{-1} or no sulfate; however, they had increased sulfate concentrations ranging between 4±0.3 and 17±4.4 μmol g^{-1} wet sediment at the end of the incubation experiments, implying that sulfate production occurred in these samples via other mechanisms (Figure 5.5).

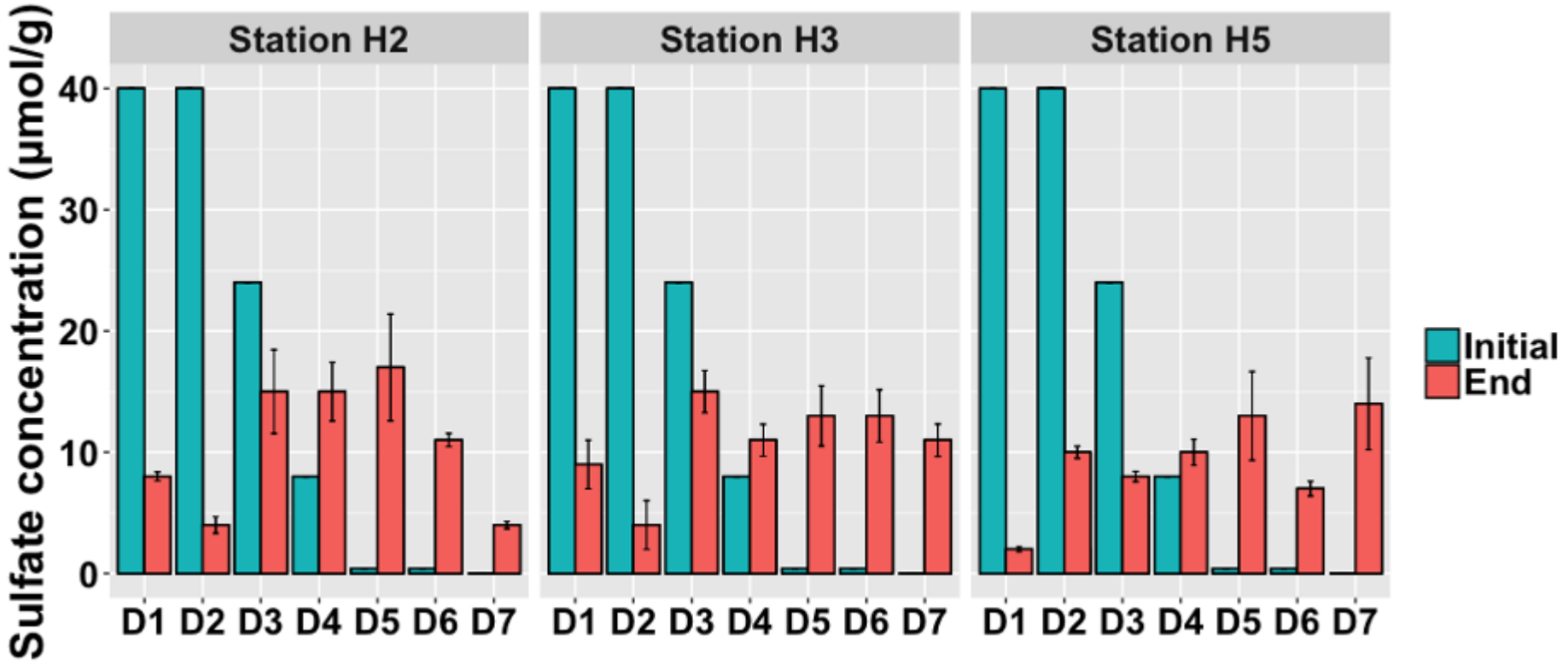

Figure 5.5. Average sulfate concentrations in the microcosms upon starting the incubations and at their end in the Baltic Sea sediment samples across all sampling sites and depths. D1: 0-1 cm; D2: 1-2 cm; D3: 2-5 cm; D4: 9-12 cm; D5: 19-22 cm; D6: 39-43 cm; D7: 60-65 cm. Error bars represent standard error above and below the average of three replicates.

5.3.2 Depth profiles of methanogen diversity and abundance

To characterise the methanogen diversity, the gene encoding for methyl-coenzyme M reductase subunit A (*mcrA*), a common functional gene for all known methanogens was sequenced. A total of $2.4x10^6$, quality-filtered, chimera-free *mcrA* sequences were obtained and assigned to 5,719 ASVs.

Results showed that all original samples had strong dominance of *Methanolobus* (47%-80%) from the *Methanosarcinaceae* family in the top four sediment layers down to SMTZ at 19 cm (Figure 5.6). Below this depth, the methanogen diversity becomes more varied with *Methanoculleus* (*Methanomicrobiaceae*; 37%-75%), unclassified Archaea (1%-36%) and *Candidatus Methanomethylophilus* (*Methanosarcinaceae*; 3%-42%) in addition to *Methanolobus* (3%-37%), highlighting a shift in methanogens below the SMTZ in Baltic Sea sediments.

All DMS-incubated samples, except for the H2 top and bottom layers, where little or no methane production was observed, were strongly dominated by *Methanolobus* (61%-99%) regardless of the sulfate concentration in the incubations (Figure 5.6). In the top layer (0-1 cm) sediment incubations from H2 and H5 stations, where the lowest amount of methane was produced, the relative abundance of *Methanolobus* exhibited no significant change compared to the original sediments. Instead, at this depth, unclassified *Methanomicrobia* had a sharp increase to 24%±3% and 22%±5%, respectively, although this class was not detected in the original samples.

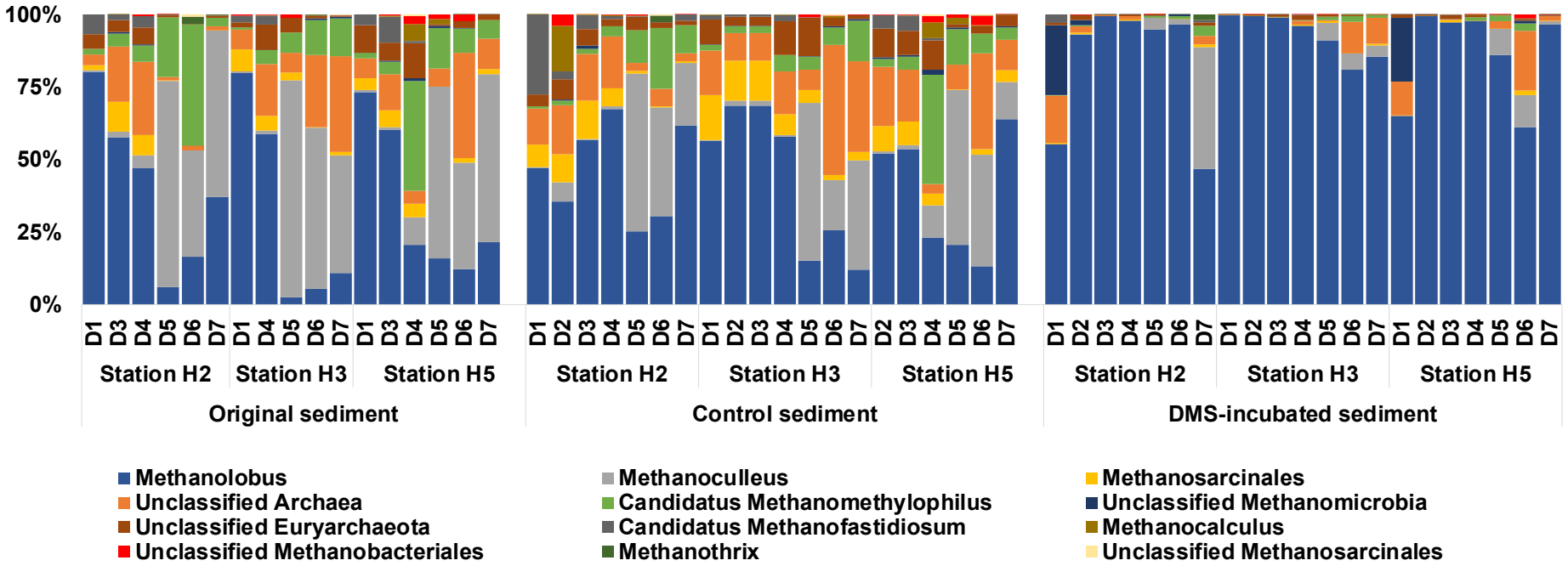

Figure 5.6. Relative abundance of all methanogens at genus level following the amplification of the *mcrA* gene. D1: 0-1 cm; D2: 1-2 cm; D3: 2-5 cm; D4: 9-12 cm; D5: 19-22 cm; D6: 39-43 cm; D7: 60-65 cm. Original: sediment samples before the addition of DMS; Control: Controls during the incubation experiment; DMS: DMS-incubated sediments.

Overall, there was a statistically significant difference between the original and DMS-amended sediments (PERMANOVA; $p<0.01$), unlike in the control incubations where no significant difference compared to the original sediments was observed (PERMANOVA, $p>0.05$). This demonstrates that the shift in the methanogen diversity in DMS-amended samples was due to the addition of DMS as the only carbon source.

To assess the factors influencing the methanogen community composition in the original and DMS-amended sediments, we conducted a principal coordinate analysis (PCoA), which separated the original and DMS-amended sediment samples (Figure 5.7).

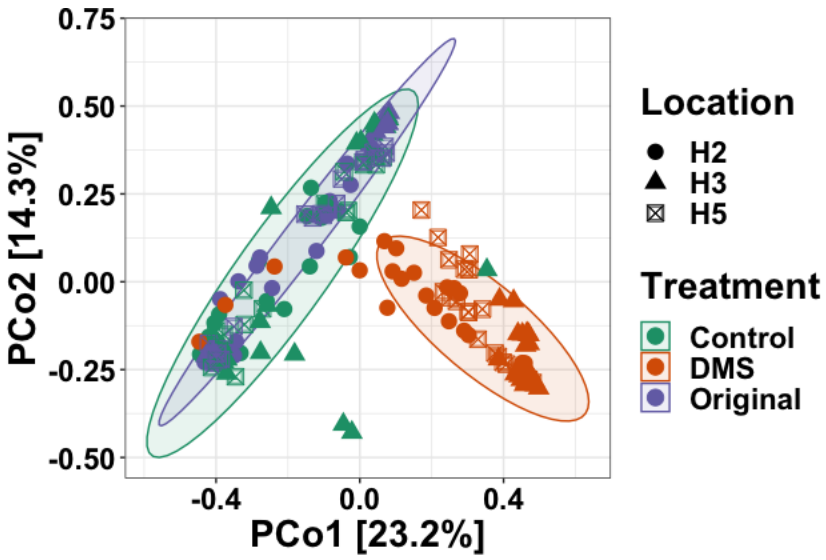

Figure 5.7. Principal coordinate analysis (PCoA) plot of the *mcrA* sequences based on Bray-Curtis dissimilarity metrics. Ellipses indicate 95% confidence intervals according to treatment data. Colour indicates treatment. Shapes indicate sampling site. Original: sediment samples before the addition of DMS; DMS: DMS-incubated sediments.

DMS being the cause of the methanogen shift is further supported by Spearman's correlation analysis. PCo1, which explains the methanogen data the most (23.2%), correlated positively with DMS degradation, methane and CO_2 productions (Table 5.2, $p<0.001$). PCo1 also correlated but to a lesser extent with depth and sulfate (Table 5.2; $p<0.05$). PCo2 (14.3%), however, significantly correlated with depth and sulfate (Table 5.2; $p<0.001$), suggesting these variables also affect the methanogen populations, yet to a lesser extent.

Table 5.2. Spearman's rank correlation coefficients (r_s) between total DMS consumed, total methane and CO_2 produced, depth, initial and end point sulfate and the first two PCoA coordinates from the *mcrA* (methanogens) sequence analysis. The PCoA was based on Bray-Curtis dissimilarity metrics. Statistically significant values are in bold. ***: $p<0.001$; **: $p<0.01$; *: $p<0.05$.

Spearman's rank correlation (r_s)	**PCo1**	**PCo2**
DMS consumed (µmol)	**0.85*** **	-0.17
Methane produced (µmol)	**0.84*** **	0.13
CO_2 produced (µmol)	**0.54*** **	-0.03
Initial sulfate (µmol)	**0.23***	**-0.56*** **
End sulfate (µmol)	**0.19***	**-0.42*** **
Depth (cm)	**-0.20***	**0.55*** **

The abundance of methanogens increased significantly in DMS incubations where methane production was observed compared to the original sediment samples (Figure 5.8, $p<0.05$). The highest *mcrA* gene numbers, $1.2x10^7 \pm 0.3x10^7$, $2.5x10^7 \pm 0.6x10^7$ and $3.1x10^7 \pm 0.3x10^7$ copies g^{-1} wet sediment, were found in incubations with maximum methane production (39-43 cm, 0-1 cm and 1-2 cm from H2, H3 and H5, respectively).

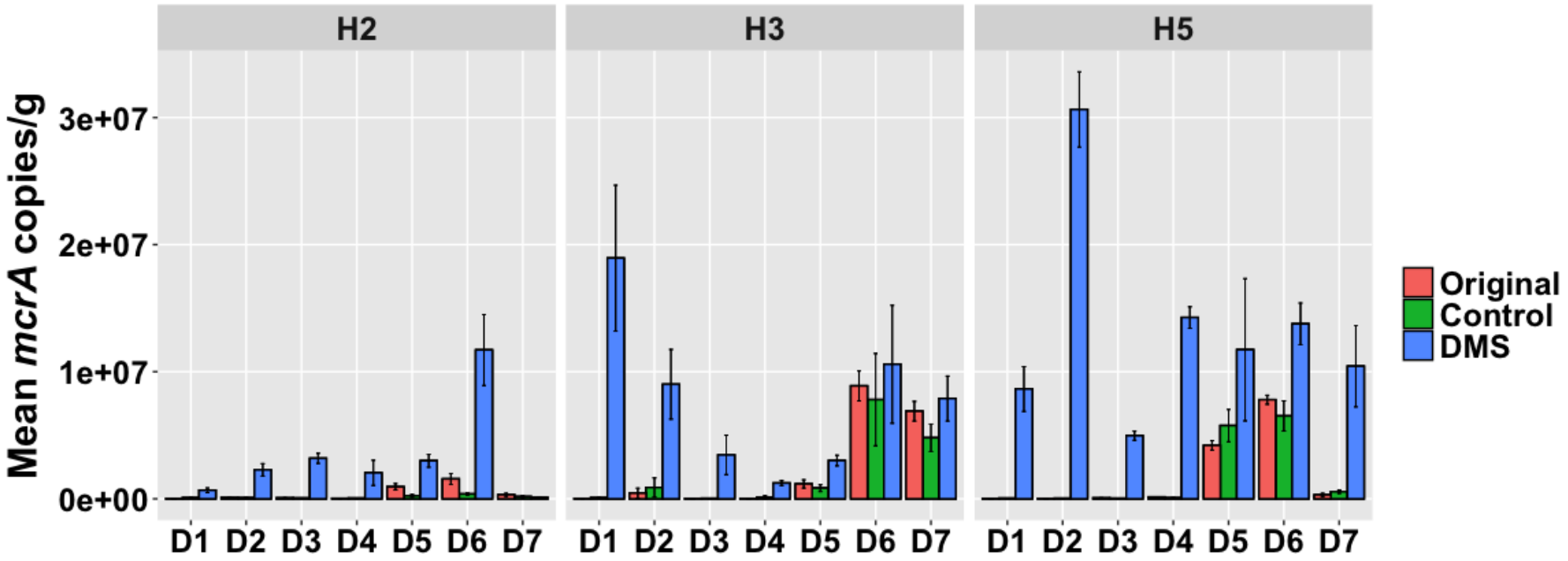

Figure 5.8. Mean copy number g^{-1} sediment of the *mcrA* gene for all methanogens separated per sampling site and treatment. Original: Original sediment samples before the incubations; Control: Controls during the incubation experiment; DMS: Sediment samples from the DMS incubations. Error bars represent standard error above and below the average of three replicates.

5.3.3 Depth profiles of SRB diversity and abundance

I analysed the SRB diversity via sequencing of the *dsrB* gene and obtained $1.1x10^6$ quality-filtered, chimera-free sequences, which were assigned to 2,221 ASVs.

DMS addition did not significantly change the SRB diversity (PERMANOVA, $p>0.05$); however, SRB relative abundance varied across depth. Overall, *Desulfosarcina*, unclassified *Proteobacteria*, unclassified Bacteria and *Desulfobulbus* dominated in both original and DMS-amended sediments from the three stations (Figure 5.9). The top depths (0-1 cm, 1-2 cm and 2-5 cm) of all original station sediments contained *Desulfosarcina* and unclassified *Proteobacteria* with relative abundances between 19%-47% and 24%-34%, respectively, and their abundances remained nearly the same in the DMS-amended incubations from the same depths (13%-45% and 27%-43%, respectively). In the original sediments below SMTZ, the relative abundance of *Desulfosarcina* significantly reduced to 0.5%-12% ($p<0.05$) while unclassified *Proteobacteria* and unclassified Bacteria significantly increased (29%-72%; $p<0.05$ and 6%-39%; $p<0.01$, respectively). Similarly, in the DMS incubated samples, at 19-22 cm depth and below, *Desulfosarcina* significantly reduced to 1%-13% ($p<0.05$), yet unclassified *Proteobacteria* and unclassified Bacteria relative abundance significantly increased to 54%-59% ($p<0.05$) and 8%-41% ($p<0.01$), respectively (Figure 5.9).

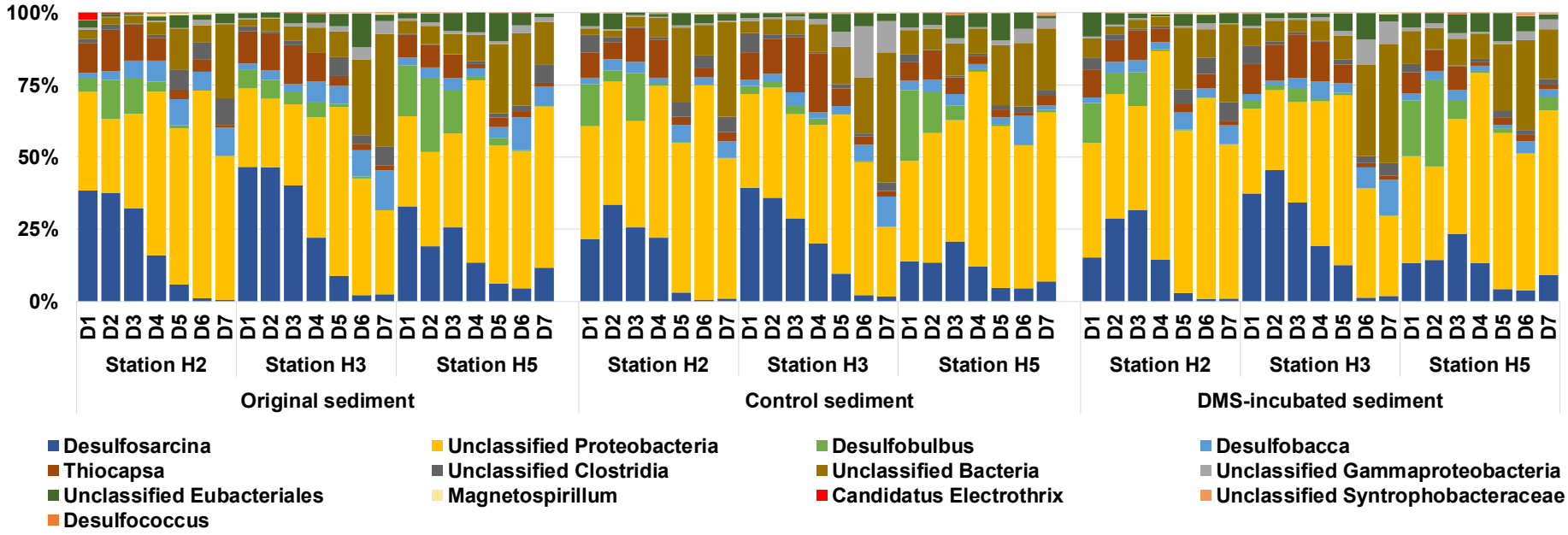

Figure 5.9. Relative abundance of all SRB at genus level following the amplification of the *dsrB* gene. D1: 0-1 cm; D2: 1-2 cm; D3: 2-5 cm; D4: 9-12 cm; D5: 19-22 cm; D6: 39-43 cm; D7: 60-65 cm. Original: sediment samples before the addition of DMS; Control: Controls during the incubation experiment; DMS: DMS-incubated sediments.

The lack of changes in SRB relative abundance before and after the addition of DMS is further presented in the PCoA graph, which shows no clustering according to treatment (Figure 5.10).

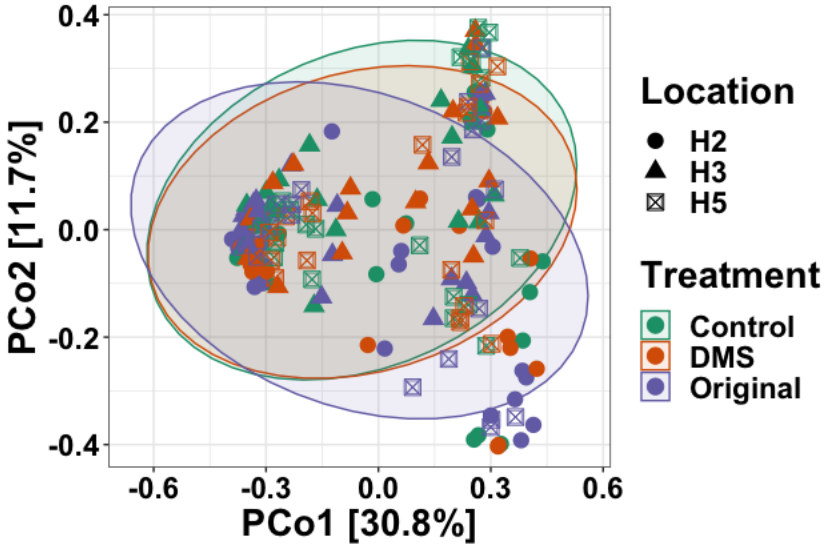

Figure 5.10. Principal coordinate analysis (PCoA) plot of the *dsrB* sequences based on Bray-Curtis dissimilarity metrics. Ellipses indicate 95% confidence intervals according to treatment data. Colour indicates treatment. Shapes indicate sampling site.

When the SRB relative abundance data were clustered according to depth, a clear separation was observed (Figure 5.11). The data from depths between 0-5 cm formed a group together, whereas depths below 19 cm formed a separate cluster. Depth 9-12 cm, on the other hand, spread across the PCo1 axis (Figure 5.11). The 9-12 cm depth corresponds to the SMTZ depth, where sulfate reduction and methane production co-exist, suggesting this depth acts as an intermediate site connecting the other depths.

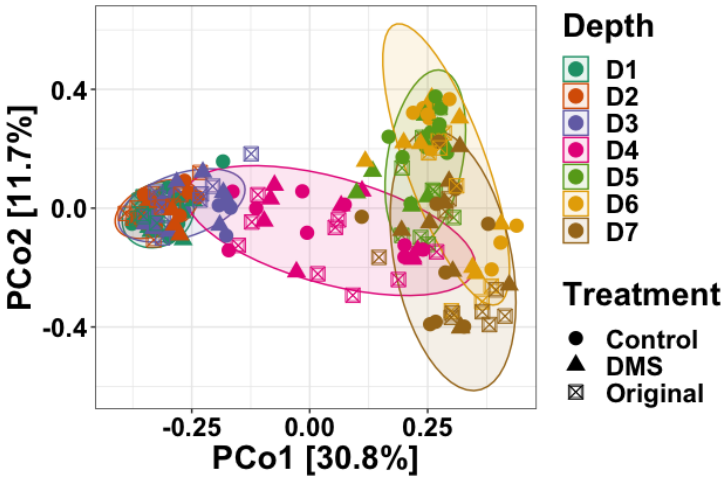

Figure 5.11. Principal coordinate analysis (PCoA) plot of the *dsrB* sequences based on Bray-Curtis dissimilarity metrics. Ellipses indicate 95% confidence intervals according to location data. Colour indicates depth. Shapes indicate treatment.

PCo1(30.8%), which is the main coordinate explaining the SRB data, correlated highly with depth and sulfate ($p<0.001$). Both PCo1 and PCo2 correlated at a lower extent with methane concentrations ($p<0.01$ and $p<0.05$, respectively), suggesting SRB populations are potentially affected by methane production (Table 5.3).

Table 5.3. Spearman's rank correlation coefficients (r_s) between the first two PCoA coordinates from the *dsrB* (SRB) sequence analysis and total DMS consumed, total methane and CO_2 produced, depth and initial and end point sulfate. The PCoA was based on Bray-Curtis dissimilarity metrics. Statistically significant values are in bold. ***: p<0.001; **: p<0.01; *: p<0.05.

Spearman's rank correlation (r_s)	**PCo1**	**PCo2**
DMS consumed (µmol)	-0.07	0.15
Methane produced (µmol)	**0.28****	**0.21***
CO_2 produced (µmol)	-0.04	0.08
Initial sulfate (µmol)	**-0.91*****	-0.04
End sulfate (µmol)	**-0.60*****	0.14
Depth (cm)	**0.91*****	0.04

The abundance of SRB increased significantly in the DMS incubations containing sediment close to the Baltic Sea floor (0-1 cm, 1-2 cm) compared to the original sediment samples (p<0.05; Figure 5.12). The *dsrB* copy numbers were the highest ($0.3x10^7$-$3.1x10^7$ copies g^{-1} wet sediment) within the DMS incubations with sediments down to the SMTZ (19-22 cm). SRB abundance decreased in sediments below 19-22 cm depth, where no statistically significant changes were observed between DMS-incubated and original sediments (Figure 5.12).

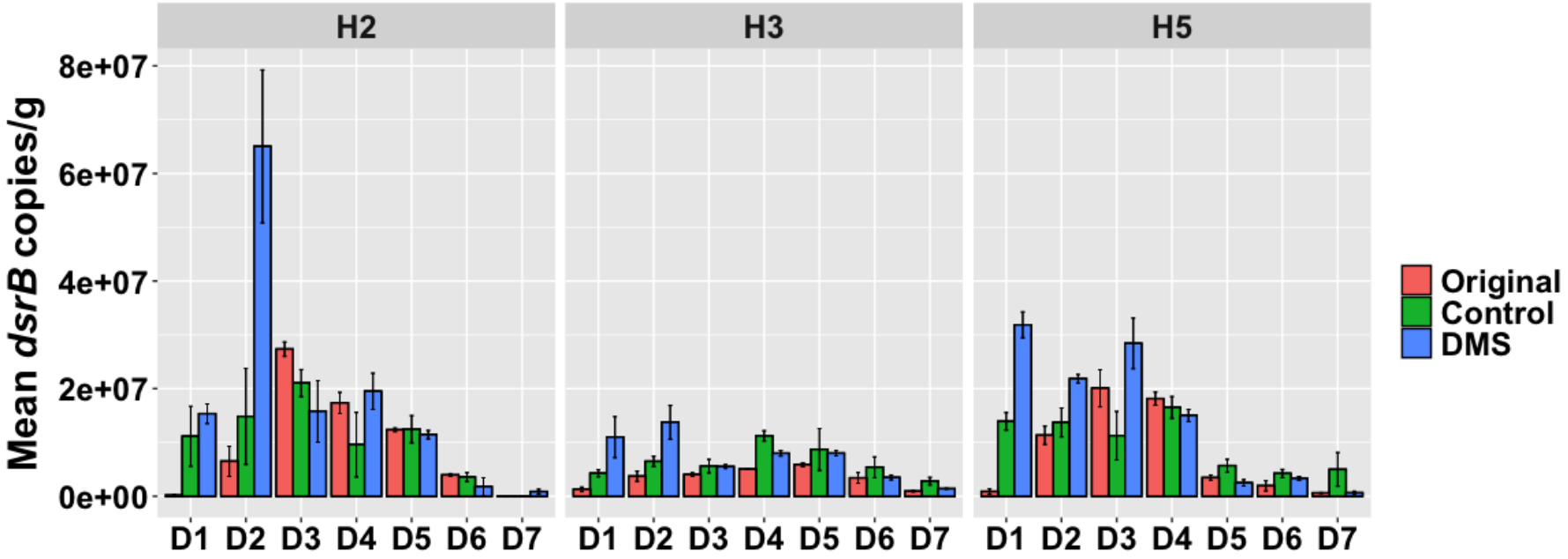

Figure 5.12. Mean copy number g^{-1} sediment of the *dsrB* gene for all SRB separated per sampling site and treatment. Original: Original sediment samples before the incubations; Control: Controls during the incubation experiment; DMS: Sediment samples from the DMS incubations. Error bars represent standard error above and below the average of three replicates.

5.3.4 Depth profile of total archaea and bacteria

The 16S rRNA gene was used to elucidate the total diversity and relative abundance of bacteria and archaea in the Baltic Sea sediment samples. A total of $4.5x10^6$ quality-filtered, chimera-free sequences were recovered, which were assigned to 70,720 ASVs. These were then separated into archaea and bacteria to understand how these populations potentially changed with DMS addition.

5.3.4.1 Archaea diversity and relative abundance

The addition of DMS led to significant changes in the diversity of archaea (PERMANOVA; $p<0.01$). Before the addition of DMS, *Candidatus Nitrosopumilus* (family *Nitrosopumilaceae*), a common ammonia oxidising archaeon, was the dominant genus in all sediments (39%-99%) besides station H5 depth 60-65 cm where *Ca. Nitrosopumilus* relative abundance was 14%±5% and an unclassified member of the *Woesearchaeales* order dominated (16%±0.3%; Figure 5.13). The dominance of *Ca. Nitrosopumilus* in most sediment samples continued after the addition of DMS, yet their relative abundance reduced due to the increase of *Methanolobus*, the methylotrophic methanogen genus which dominated the methanogen populations as determined by the *mcrA* sequencing. In the DMS-incubated samples, *Ca. Nitrosopumilus* dominated in station H2 (41%-77%) and nearly all sediments from station H3 (28%-64%) besides depth 60-65 cm were *Methanolobus* dominated at 40%±8% (Figure 5.13). At station H5, after the addition of DMS, *Ca. Nitrosopumilus* dominated depths 0-1 cm (67%±14%), 2-5 cm (43%±3%), 19-22 cm (24%±3%) and 39-43 cm (38%±3%), whereas *Methanolobus* dominated at depths 1-2 cm (50%±16%), 9-12 cm (30%±1%) and 60-65 cm (51%±7%).

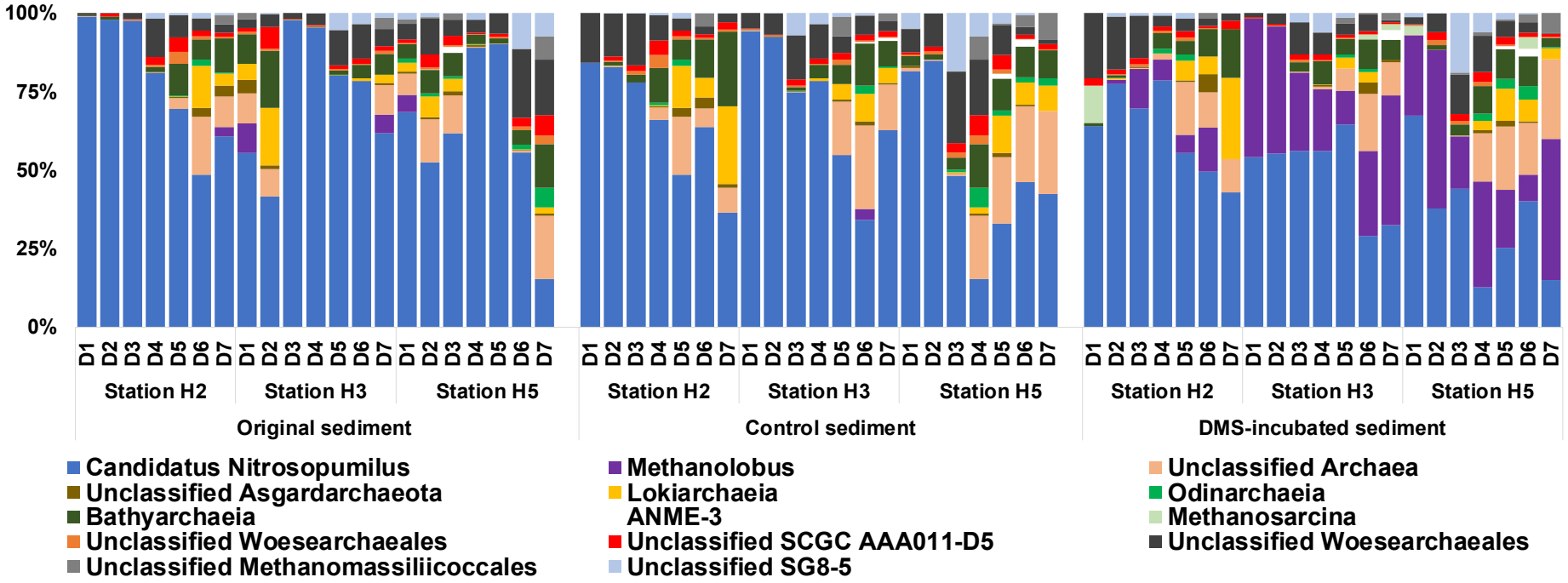

Figure 5.13. Relative abundance of all archaea at genus level following the amplification of the 16S rRNA gene. D1: 0-1 cm; D2: 1-2 cm; D3: 2-5 cm; D4: 9-12 cm; D5: 19-22 cm; D6: 39-43 cm; D7: 60-65 cm. Original: sediment samples before the addition of DMS; Control: Controls during the incubation experiment; DMS: Sediment samples incubated with DMS.

The changes in archaeal relative abundance following the addition of DMS are further supported by the PCoA graph, where two separate clusters are formed depending on the treatment (Figure 5.14).

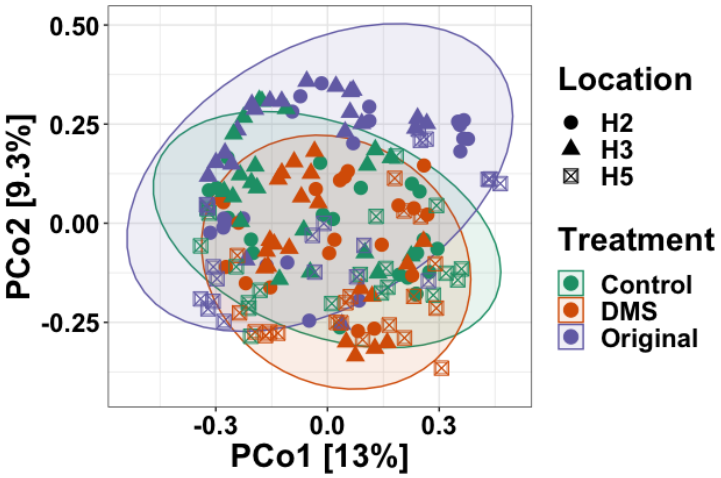

Figure 5.14. Principal coordinate analysis (PCoA) plot of the 16S rRNA archaeal sequences based on Bray-Curtis dissimilarity metrics. Ellipses indicate 95% confidence intervals according to treatment data. Colour indicates treatment. Shapes indicate sampling site.

Spearman's correlation analysis on the PCoA coordinates suggested that the changes in archaeal community structure are most likely a result of DMS since PCo2 correlated highly with DMS degradation, methane and CO_2 production (Table 5.4; $p<0.001$). On the other hand, the PCo1 axis correlated highly with depth and sulfate concentrations ($p<0.001$), indicating that the original archaeal populations could be affected by these parameters (Table 5.4; Figure 5.14). Regardless, the PCoA only explained about 22.3% of the total archaeal variability between the samples, indicating that the variables used in Spearman's correlation only affect a small proportion of the archaeal community structure.

Table 5.4. Spearman's rank correlation coefficients (r_s) between the first two PCoA coordinates from the 16S rRNA archaeal sequence analysis and total DMS consumed, total methane and CO_2 produced, depth and initial and end point sulfate. The PCoA was based on Bray-Curtis dissimilarity metrics. Statistically significant values are in bold. ***: p<0.001; **: p<0.01; *: p<0.05.

Spearman's rank correlation (r_s)	PCo1	PCo2
DMS consumed (µmol)	-0.15	**0.63*** **
Methane produced (µmol)	**0.20***	**0.59*** **
CO_2 produced (µmol)	-0.05	**0.47*** **
Initial sulfate (µmol)	**-0.79*** **	-0.10
End sulfate (µmol)	**-0.66*** **	0.001
Depth (cm)	**0.79*** **	0.10

5.3.4.2 Bacteria diversity and relative abundance

In the original sediments, unclassified *Cyanobacteria* dominated all sampling sites but with varying relative abundances (6%-20%). Other taxa such as unclassified *MBNT15*, unclassified *SG8-4* and unclassified *Thermodesulfovibrionia* increased below 22 cm of depth (Figure 5.15).

The addition of DMS led to significant changes in the communities of bacteria (PERMANOVA; p<0.01), and *Sulfurimonas* was the genus with the highest increase in relative abundance (p<0.001). *Sulfurimonas* dominated in the majority of DMS-amended sediments (12%-56%) besides depth 2-5 cm at stations H2 and H3, where unclassified *Desulfobulbaceae* dominated (6%-11%) and depth 9-12 cm at station H2, where unclassified *Methylophagaceae* was the dominant taxon (11%±2%; Figure 5.15).

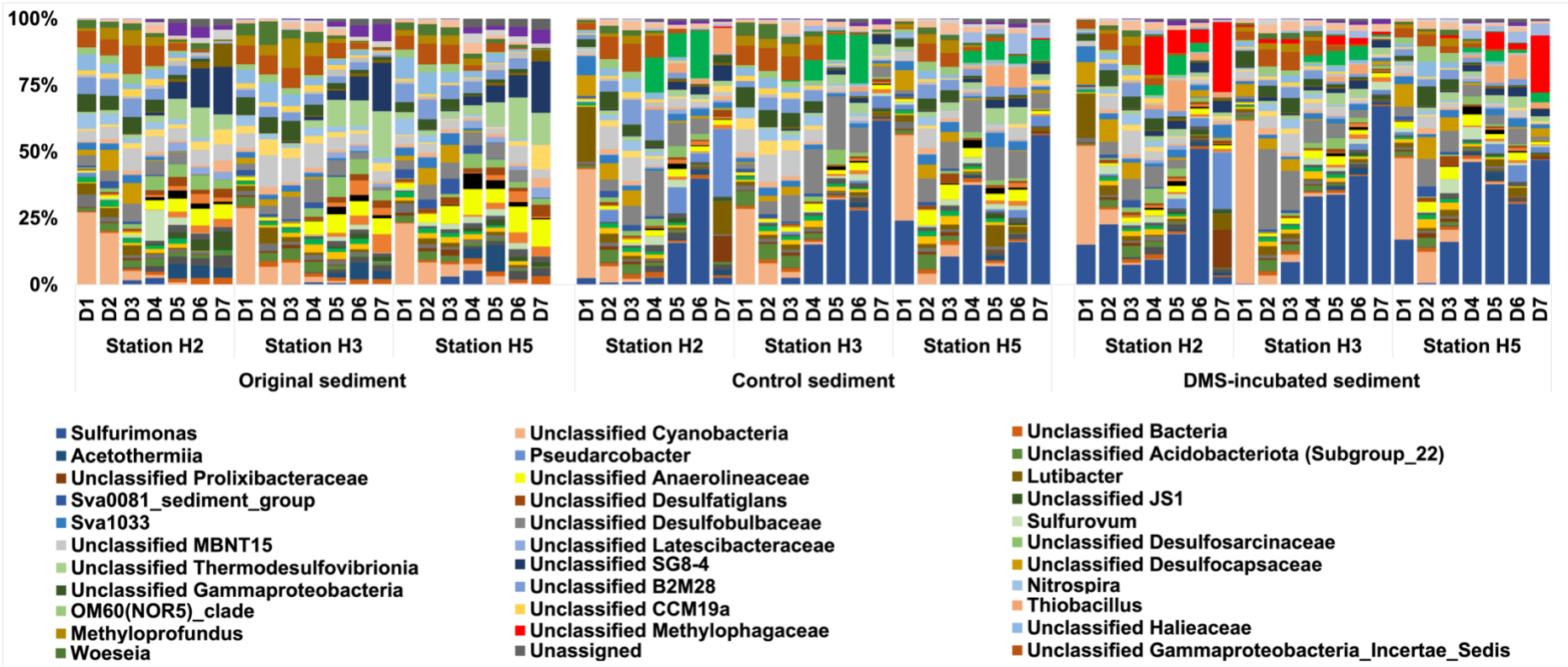

Figure 5.15. Relative abundance of all bacteria at genus level following the amplification of the 16S rRNA gene. Some of the legend entries for bacteria with low relative abundance (<2%) have been removed for clarity. D1: 0-1 cm; D2: 1-2 cm; D3: 2-5 cm; D4: 9-12 cm; D5: 19-22 cm; D6: 39-43 cm; D7: 60-65 cm. Original: sediment samples before the addition of DMS; Control: Controls during the incubation experiment; DMS: Sediment samples incubated with DMS.

The PCoA analysis only explained 11.2% of the bacterial community variations, yet two clusters were formed depending on treatment (Figure 5.16).

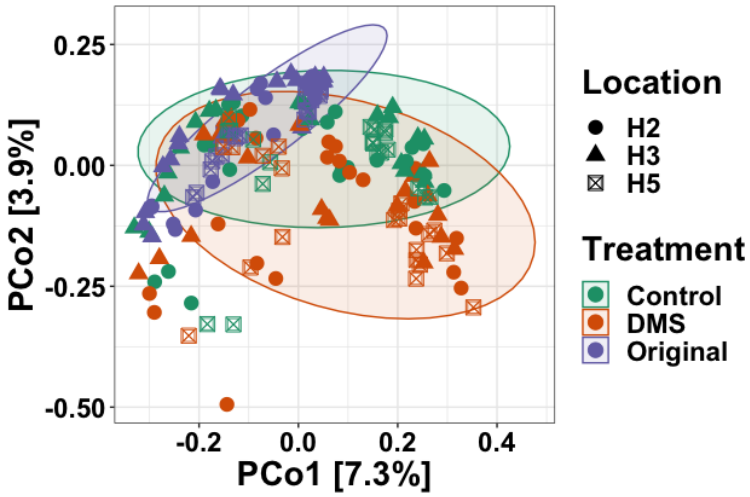

Figure 5.16. Principal coordinate analysis (PCoA) plot of the 16S rRNA bacterial sequences based on Bray-Curtis dissimilarity metrics. Ellipses indicate 95% confidence intervals according to treatment data. Colour indicates treatment. Shapes indicate sampling site.

Spearman's correlation does not conclusively show what might have affected the bacterial communities since PCo1 correlated with all of the environmental parameters tested (DMS degradation, methane and CO_2 production, depth and sulfate) and PCo2 with all parameters besides methane production ($p<0.001$; Table 5.5).

Table 5.5. Spearman's rank correlation coefficients (r_s) between the first two PCoA coordinates from the 16S rRNA bacterial sequence analysis and total DMS consumed, total methane and CO_2 produced, depth and initial and end point sulfate. The PCoA was based on Bray-Curtis dissimilarity metrics. Statistically significant values are in bold. ***: $p<0.001$; **: $p<0.01$; *: $p<0.05$.

Spearman's rank correlation (r_s)	PCo1	PCo2
DMS consumed (µmol)	**0.35*** **	**-0.43*** **
Methane produced (µmol)	**0.55*** **	-0.12
CO_2 produced (µmol)	**0.32*** **	**-0.38*** **
Initial sulfate (µmol)	**-0.75*** **	**-0.53*** **
End sulfate (µmol)	**-0.31*** **	**-0.52*** **
Depth (cm)	**0.76*** **	**0.56*** **

5.3.5 Metagenomics analysis

Metagenomics sequencing of the DMS-incubated sediments from 19-22 cm depth from the three stations was conducted to gain further insight into the methanogen populations degrading DMS to methane. At this depth, only methane production is expected. In total, 224 Gb of sequencing data were obtained, corresponding to 93 Gb from station H2, 64 Gb from H3 and 67 Gb from H5.

Methanolobus were found to be the dominant DMS-degrading methanogens in the Baltic Sea sediment incubations, which had relative abundances of 69%-87% amongst all archaea. This supports the findings of the *mcrA* sequence analysis.

A total of 44 metagenome-assembled genomes (MAGs) were constructed from the metagenomics datasets, four of which were MAGs affiliated with *Methanolobus* and were the only methanogen MAGs (Table 5.6). All MAGs were classified as medium quality according to the minimum information about a metagenome-assembled genome (MIMAG), developed by the Genomic Standards Consortium, primarily due to not containing all three rRNA genes (23S, 16S and 5S; Bowers *et al.*, 2017). A phylogenetic tree of the *mcrA* gene was also constructed (Figure 5.17), which includes the most abundant *mcrA* genes within the metagenomics datasets and the only *mcrA* gene found in the MAGs (H2D5-*Methanolobus*; Figure 5.17). Phylogenetic tree analysis suggests that novel *Methanolobus* species are present in these sediments.

Table 5.6. Metagenome assembled genomes constructed from metagenome datasets from each sampling station at depth 19-22 cm. Quality is based on the MIMAG (Bowers *et al.*, 2017). Comp: Completeness; Cont: Contamination. Methanogen MAGs are in bold.

Site	Kingdom	Organism	Comp	Cont	Bases	Genes	Quality
Station H2	Bacteria	*Sideroxydans (Nitromonadales)*	99.37%	0.03%	2,570,235	2,553	Medium
	Bacteria	*Sulfuricella (Nitrosomonadales)*	98.66%	1.18%	3,054,443	3,112	Medium
	Bacteria	*Sulfurimonas (Campylobacterales)*	98.36%	2.12%	2,640,566	2,642	Medium
	Bacteria	*Sulfurivermis (Thiohalomonadales)*	97.89%	0.94%	3,721,594	3,717	Medium
	Bacteria	*Thiobacillus (Burkholderiales)*	97.37%	4.37%	3,104,052	3,228	Medium
	Bacteria	*SLDE01 (Thiohalomonadales)*	91.02%	2.11%	2,870,290	2,863	Medium
	Bacteria	*SPDF01 (Gemmatimonadales)*	84.84%	7.24%	2,284,254	2,441	Medium
	Bacteria	*Mor1 (Acidobacteriota)*	84.22%	4.70%	3,172,399	3,142	Medium
	Bacteria	*UBA2270 (Desulfobulbales)*	83.70%	0%	2,242,279	2,255	Medium
	Bacteria	*M0040 (Desulfuromonadales)*	78.40%	1.45%	2,612,526	2,764	Medium
	Bacteria	*UBA9959 (Elusimicrobiales)*	66.07%	1.71%	2,008,712	2,008	Medium
	Bacteria	*UBA2258*	64.75%	0.20%	2,201,006	2,164	Medium
	Bacteria	*GWC2-71-9 (Gemmatimonadales)*	62.74%	4.50%	1,941,363	2,018	Medium
	Bacteria	*Lutibacter (Flavobacteriales)*	61.48%	2.74%	1,850,908	1,961	Medium
	Bacteria	*Pontiella (Kiritimatiellales)*	58.46%	0.54%	2,736,742	2,701	Medium
	Bacteria	*CG2-30-66-27 (MBNT15)*	52.66%	0.84%	982,015	1,132	Medium
	Bacteria	*Ignavibacteriaceae (Ignavibacteriales)*	52.42%	2.33%	1,514,737	1,573	Medium
	Bacteria	*SMWR01 (UBA9160)*	50.42%	6.45%	2,672,116	2,872	Medium
	Archaea	***Methanolobus (Methanosarcinales)***	**92.81%**	**1.96%**	**2,489,475**	**2,669**	**Medium**
	Archaea	*UBA7939 (Methanosarcinales)*	87.58%	0.65%	2,224,045	2,673	Medium
Station H3	Bacteria	*Thiobacillus (Burkholderiales)*	100%	0.48%	3,269,799	3,337	Medium
	Bacteria	*Sulfuricella (Nitrosomonadales)*	99.29%	0.98%	2,882,075	2,947	Medium
	Bacteria	*Gemmatimonadetes*	93.20%	4.95%	3,005,382	2,914	Medium
	Bacteria	*UBA9214 (Thiohalobacterales)*	77.45%	1.90%	2,684,927	2,952	Medium
	Bacteria	*Methylophagaceae (Nitrosococcales)*	72.41%	0.00%	2,112,498	2,215	Medium
	Bacteria	*UBA8639 (Nitrospirales)*	58.53%	4.02%	1,749,825	1,957	Medium
	Bacteria	*Ignavibacterium (Ignavibacteriales)*	57.37%	7.94%	1,714,699	1,870	Medium
	Bacteria	*CG2-30-66-27 (MBNT15)*	55.57%	0.84%	1,184,603	1,340	Medium
	Bacteria	*SPDF01 (Gemmatimonadales)*	53.44%	7.14%	1,471,751	1,636	Medium
	Bacteria	*BM004 (Desulfobulbales)*	53.06%	1.81%	1,085,505	1,216	Medium
	Archaea	*UBA10834 (Thermoplasmata)*	83.37%	1.20%	1,375,321	1,451	Medium
	Archaea	***Methanolobus (Methanosarcinales)***	**66.74%**	**1.31%**	**1,070,939**	**1,261**	**Medium**
Station H5	Bacteria	*Methylophagaceae (Nitrosococcales)*	99.18%	0.88%	2,928,202	2,798	Medium
	Bacteria	*Sulfuricella (Nitrosomonadales)*	95.50%	2.84%	3,050,167	3,151	Medium
	Bacteria	*M0040 (Desulfuromonadales)*	89.22%	0.65%	3,047,111	3,157	Medium
	Bacteria	*Sulfurimonas (Campylobacterales)*	79.44%	3.88%	1,756,086	1,894	Medium
	Bacteria	*UBA6164 (Gracilibacteria)*	76.99%	2.36%	1,161,215	2,152	Medium
	Bacteria	*UBA9214 (Thiohalobacterales)*	76.14%	7.30%	2,418,493	2,607	Medium
	Bacteria	*BM004 (Desulfobulbales)*	70.72%	1.52%	1,624,494	1,775	Medium
	Bacteria	*Lutibacter (Flavobacteriales)*	65.18%	3.28%	1,960,362	2,061	Medium
	Bacteria	*UBA2258*	62.76%	1.65%	1,130,384	1,198	Medium
	Archaea	***Methanolobus (Methanosarcinales)***	**88.89%**	**1.31%**	**2,579,227**	**2,760**	**Medium**
	Archaea	***Methanolobus (Methanosarcinales)***	**62.58%**	**0%**	**1,291,140**	**1,362**	**Medium**
	Archaea	*SMTZ1-45 (Thorarchaeales)*	54.35%	0.47%	677,230	810	Medium

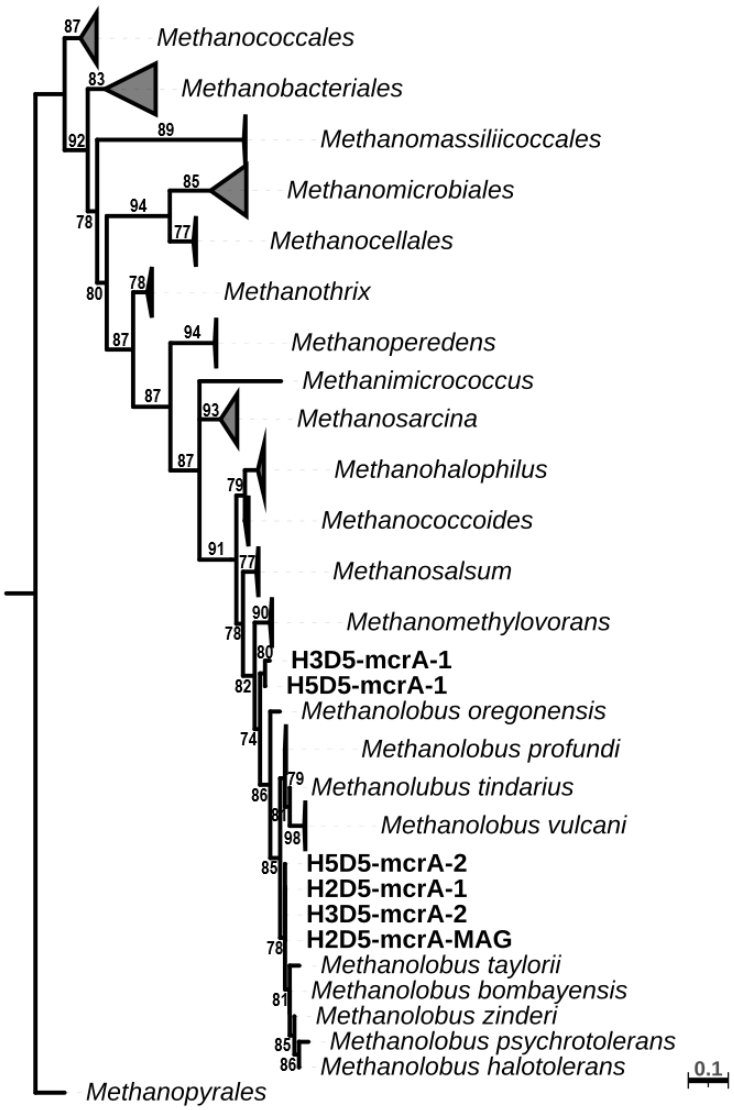

Figure 5.17. Maximum likelihood phylogenetic tree of cultured methanogens containing the *mcrA* gene. Bold labels correspond to the most abundant *mcrA* genes from my MAGs (station-mcrA-MAG) and metagenomics datasets (station-mcrA). The tree was constructed using IQTree (1.6.12) on QMUL's Apocrita HPC facility, supported by QMUL Research-IT (Nguyen *et al.*, 2015; King *et al.*, 2017). ModelFinder was used to find the best-fit model for the data (mtZOA+F+G4; Kalyaanamoorthy *et al.*, 2017). The values near each branch signifies the confidence level (in percentages) as determined by ultrafast bootstrap statistical analysis (1000 replicates; Hoang *et al.*, 2018). The tree is drawn to scale, with branch lengths accounting for substitutions per site. Visualisation and annotation were accomplished using iTOL (v.5; Letunic and Bork, 2021). *Methanopyrales* was used as the out-group.

Three of the MAGs constructed from the metagenome data were potentially SRB, two corresponding to *BM004* (order *Desulfobulbales*) and one corresponding to *UBA2270* (order *Desulfobulbales*) (Table 5.6). None of these could be taxonomically identified further, so their sulfate reduction abilities cannot be confirmed, yet all are within the order *Desulfobulbales*, which is primarily associated with dissimilatory sulfate reduction. Furthermore, two of the MAGs (H2D5-*UBA2270* and H5D5-*BM004*) contained all genes associated with dissimilatory sulfate reduction (*sat, aprAB,* and *dsrAB*). Two *Sulfurimonas* MAGs were also constructed (Table 5.6). *Sulfurimonas* are known to play an important role in sulfur cycling via sulfide oxidation (Grote *et al.*, 2008; Lahme *et al.*, 2020).

5.4 Discussion

Despite the environmental importance of DMS, particularly as a methane precursor in anoxic sediments, limited information concerning the microbial diversity of anaerobic DMS degradation is available. Here, we conducted the first study on the diversity of anaerobic DMS degradation using permanently anoxic/hypoxic sediments from the Baltic Sea, where high DMSP and methane concentrations are observed.

Our approach, combining sediment incubations with amplicon sequencing and metagenomics, has shown that DMS degradation potentially proceeds via methanogenesis and sulfate reduction across the sediment depths of the Himmerfjärden Estuary in the Baltic Sea. Higher methane yields following the DMS amendment were observed in two stations (H3 and H5), likely because they receive high organic carbon and nutrient load from the discharge of an upstream sewage treatment plant.

Amplicon sequencing and metagenomics analysis showed that *Methanolobus* were the dominant methanogens assimilating DMS and producing methane in our sediment incubations. This methanogen genus was also dominant in the original sediment samples down to SMTZ, but *Methanoculleus* and *Candidatus Methanomethylophilus* were in high relative abundance below this zone. This shows that *Methanolobus* carry out methylotrophic methanogenesis in Baltic Sea sediments, where sulfate is present, and they were enriched in the sediment incubations as a result of DMS amendment, implying that they potentially degrade DMS when it is available in the Baltic Sea sediments. *Methanolobus* are known DMS degraders. Several *Methanolobus* species capable of DMS degradation have been isolated from various environments, such as an oil well and marine and estuarine sediments (Ni and Boone, 1991; Kadam *et al.*, 1994). We also recently showed *Methanolobus* as the dominant DMS-degrading methanogen genus in brackish sediments from the Medway Estuary, UK (Tsola *et al.*, 2021; Chapter 3). Furthermore, a psychrotolerant *Methanolobus* strain that can use methanol and trimethylamine as its growth substrate has been isolated from saline lake sediment in Siberia, indicating that this genus has members capable of growth at low temperatures such as the ones in the Baltic Sea sediments (Chen *et al.*, 2018).

In the original and DMS-incubated Baltic Sea sediment samples, there is a shift in the SRB communities, with *Desulfosarcina* dominating the depths closer to the seafloor (0-5 cm) and unclassified *Proteobacteria* and Bacteria dominating at lower depths. However, DMS had no visible effect on SRB diversity in the sediment incubations. *Cyanobacteria*, known DMSP producers, were dominant in the first few layers of the Baltic Sea bed, which could lead to DMS production. A marine species of *Desulfosarcina* has previously been shown to degrade DMS (Lyimo *et al.*, 2009). This evidence suggests that *Desulfosarcina* could be actively degrading DMS in the Baltic Sea. This would also explain the increase in the abundance of

SRB in sediments close to the Baltic Sea floor. At these depths, DMS degradation was also observed, however, methane production was not high enough to justify the amounts of DMS degraded, further suggesting SRB activity. Furthermore, the top sediment depth (0-1 cm) at station H2, where little methane production was measured, exhibited high amounts of CO_2 production, a by-product of SRB activity.

In the sediments below 9-12 cm, higher sulfate amounts were recorded than initially added to the microcosms suggesting a sulfate production pathway is taking place in these sediments. This is most likely a result of DMS degradation similar to the hidden sulfur cycle observed in Chapter 3 (Figure 3.10). Hydrogen sulfide, the end product of DMS degradation, could be rapidly recycled to sulfate, as shown previously in wetlands, lakes and rivers (Jorgensen, 1990; Blodau *et al.*, 2007; Heitmann *et al.*, 2007; Berg *et al.*, 2019). Stoichiometrically, 17-37 µmol/g hydrogen sulfide should be produced from methanogenesis (1 DMS: 1 hydrogen sulfide; Equation 1; Chapter 1) and sulfate reduction (1 DMS: 2.5 hydrogen sulfide; Equation 2; Chapter 1) below 9-12 cm depth. If all hydrogen sulfide was then recycled to sulfate via oxidation (stoichiometrically 1:1), the incubations upon termination should contain 17-37 µmol/g sulfate (Klatt and Polerecky, 2015). This theoretical sulfate production is higher than the experimentally measured sulfate where 20%-66% less sulfate was observed (Appendix Table 1). Despite less sulfate than expected, concentrations were still higher than initially amended suggesting sulfate production. This sulfur cycling hypothesis below 9-12 cm is further supported by the increase in *Sulfurimonas* relative abundance in most sediments below 9 cm and the discrepancy in CO_2 concentrations at these lower depths. *Sulfurimonas* likely used CO_2 as a carbon source (Sievert *et al.*, 2008; Han and Perner, 2015). Indeed some *Sulfurimonas* species have been found in anoxic ecosystems such as the Black Sea, the Baltic Sea and Mariager Fjord in Denmark (Brettar and Rheinheimer, 1991; Brettar *et al.*, 2006;

Jensen *et al.*, 2008; Zhang *et al.*, 2009; Fuchsman *et al.*, 2012). Furthermore, *S. gotlandica*, a species isolated from the central Baltic Sea, can grow on nitrite and nitrate (Grote *et al.*, 2012; Labrenz *et al.*, 2013). It is likely that *Ca. Nitrosopumilus*, the dominant genus in the top sediments, provided the electron acceptor for *Sulfurimonas* to oxidise the hydrogen sulfide produced by DMS degradation in these sediments.

High CO_2 and low methane concentrations might also suggest anaerobic methane oxidation (AOM) occurring in the sediments. During AOM, consortia of SRB, most likely members of the *Desulfosarcina/Desulfococcus* clade, and anaerobic methane oxidisers utilise the produced methane leading to the production of CO_2, as has previously been shown in marine sediments (Orphan *et al.*, 2001; Nauhaus *et al.*, 2002; Milucka *et al.*, 2012). However, no known methane oxidisers were found in the sequence data from the DMS-incubated sediments, suggesting methane oxidation was not carried out.

In conclusion, this was the first study on the depth profile of DMS degradation as well as the underlying microbial community in sediments where a sulfate gradient exists. *Methanolobus*, a known DMS-degrading methanogen, was the dominant microorganism that utilised DMS in these sediments regardless of the sulfate concentrations. This genus was also present in the original Baltic Sea sediments, where high amounts of DMSP, a major DMS precursor, were observed, suggesting *Methanolobus* likely degrade DMS in the Baltic Sea. Furthermore, high relative abundance of SRB taxa with potential DMS degrading capabilities suggests SRB could already be adapted to DMS degradation in these sediments.

6 Metabolism of anaerobic DMS degradation

6.1 Introduction

Previous research on anaerobic DMS degradation has mostly focused on process measurements regarding sulfate reduction and methane production whilst the metabolic pathways of anaerobic DMS degradation have received less attention. Only a few studies have been conducted on either *Methanosarcina barkeri* or *Methanosarcina acetivorans*, which suggested that methylsulfide-specific methyltransferases encoded by the *mts* genes are required for anaerobic catabolism of DMS (Tallant and Krzycki, 1997; Tallant *et al.*, 2001; Fu and Metcalf, 2015). It was demonstrated that acetate-grown *M. barkeri* could degrade DMS via the activity of dimethylsulfide:coenzyme M methyltransferase composed of two subunits (MtsA and MtsB). MtsA was shown to catalyse both the methylation of a corrinoid subunit, MtsB, and the demethylation of the methyl-bound MtsB with DMS and CoM (Tallant *et al.*, 2001). Later, Fu and Metcalf (2015) showed that MtsD and MtsF are specific enzymes for DMS and MT metabolism in *M. acetivorans* C2A, respectively. Nevertheless, the metabolic pathways of anaerobic DMS degradation in the environment are undocumented.

In this chapter, Baltic Sea sediments from 19-22 cm depth at all three sampling sites (H2, H3 and H5; Chapter 5), were selected for metagenomics and metatranscriptomics analysis. This depth is the lowest point of the sulfate-methane transition zone (SMTZ), where sulfate concentrations become undetectable and only methanogenesis exists, thus being ideal for investigating DMS degradation by methanogens (Maltby *et al.*, 2018). Through metagenomics and metatranscriptomics, the aim was to provide the first insight into the genetic and metabolic potential of DMS-degrading methanogens and assess their activity in anoxic sediments.

6.2 Results

I screened for 108 genes, comprising 78 genes involved in methane production (Figure 6.1) and 30 genes in the sulfur cycle within the metagenomics and metatranscriptomics datasets (Appendix Tables 2-6). Due to complications during sequencing, metatranscriptomics analysis from station H2 was not achieved, so only data from stations H3 and H5 will be presented. However, metagenomics analysis from all three stations was successful.

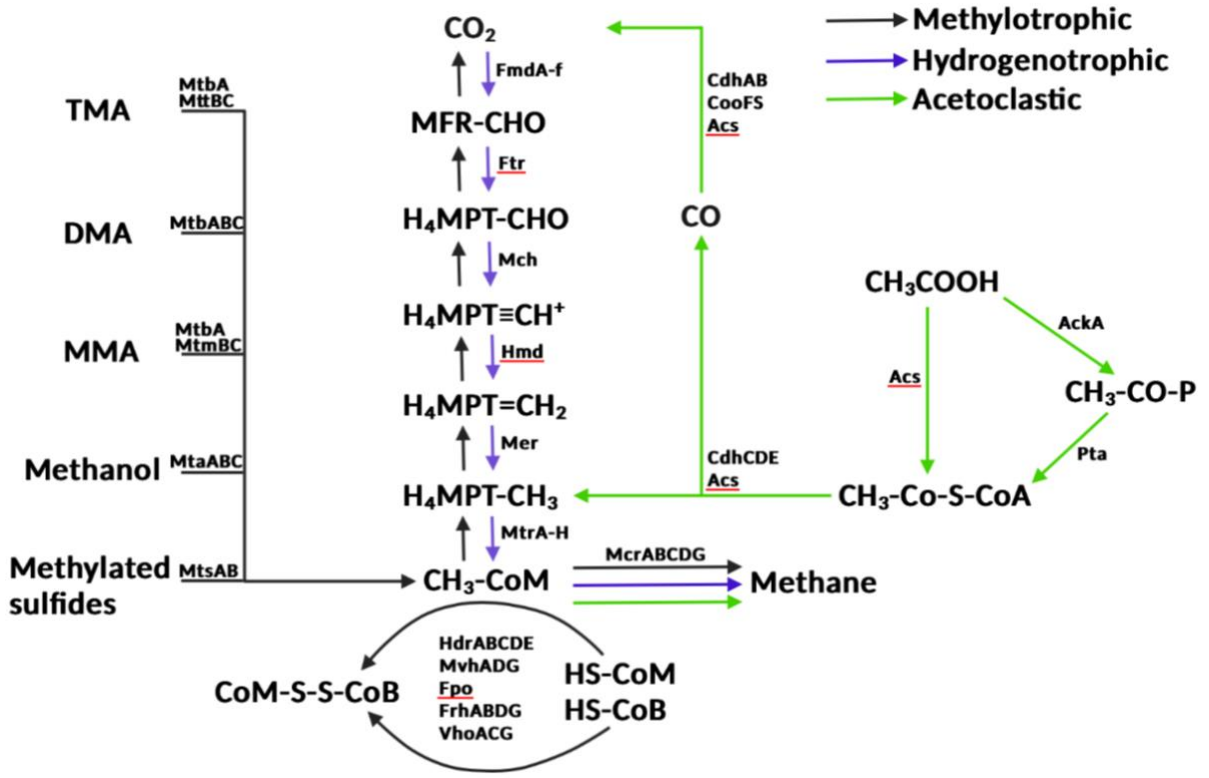

Figure 6.1. Map showing the three methanogenesis pathways and their genes

Notably, the relative expression of the *mts* genes encoding for MeSH- and DMS-methyltransferases originally found in *Methanosarcina barkeri* and *M. acetivorans* (*mtsA*, *mtsB, mtsD, mtsF and mtsH*; Chapter 1) was <0.3% or undetectable in the metatranscriptomics datasets (Figure 6.2.B). These genes mostly associated with *Methanosarcina* spp. (primarily *M. lacustris*) with sequence similarity around 84%-98%. One

out of the 13 *mtsD* sequences also associated with *Methanococcoides* (similarity 82%) and another five associated with *Methanomethylovorans* (similarity 85%-92%). The *mts* genes were absent in the metagenome from the H2 sample and had very low abundance (<0.03%) in the samples from H3 and H5 (Figure 6.2.A). These genes were also not found in the four *Methanolobus* MAGs that were constructed from the metagenomics datasets (Figure 6.3.A; Chapter 5).

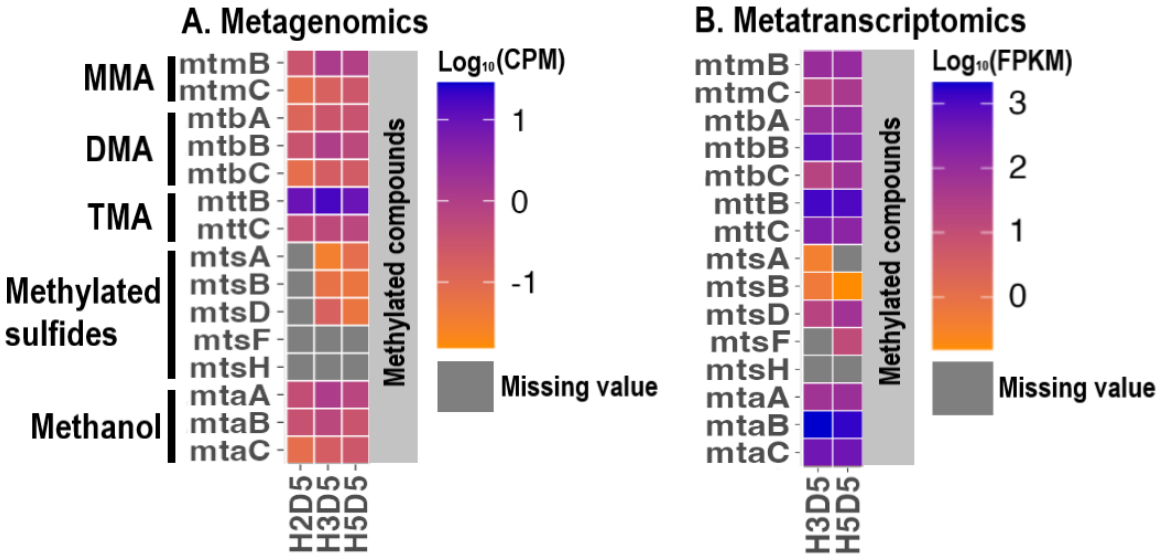

Figure 6.2. Genes involved in methane production via the methylotrophic methanogenesis pathway. **A.** Metagenomics normalised gene copy numbers. **B.** Metatranscriptomics normalised gene copy numbers. CPM: Copies per million; FPKM: Fragments per kilobase of gene per million reads. MMA: monomethylamine; DMA: dimethylamine; TMA: trimethylamine; Methylated sulfides: DMS, MeSH and methylthiopropanoate.

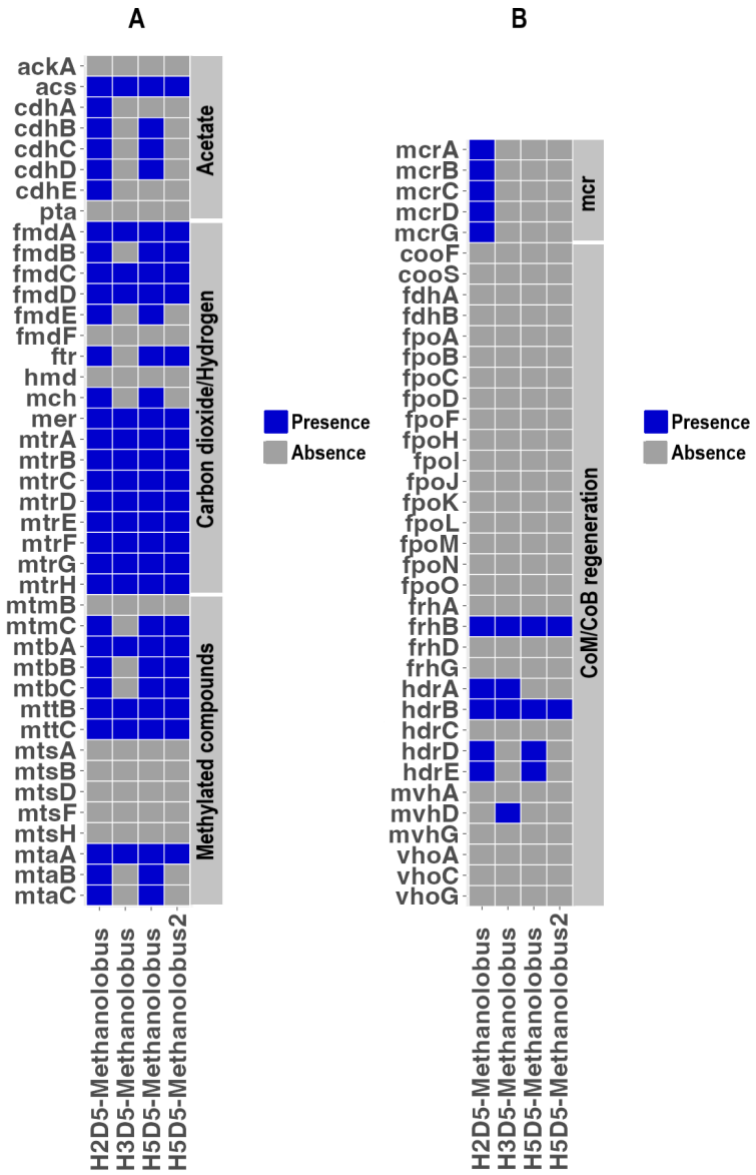

Figure 6.3. Presence and absence of the genes involved in methane production in the four Methanolobus MAGs constructed using the metagenomics datasets. **A.** Genes involved in the three methanogenesis pathways. **B.** Methanogenesis genes common in all pathways. Acetate: Acetoclastic methanogenesis; Carbon dioxide/Hydrogen: Hydrogenotrophic methanogenesis; Methylated compounds: Methylotrophic methanogenesis. CoM: Coenzyme M; CoB: Coenzyme B. H2D5-Methanolobus: MAG from station H2, Comp: 93%, Cont: 2%; H3D5-Methanolobus: MAG from station H3, Comp: 67%, Cont: 1%; H5D5- Methanolobus: MAG from station H5, Comp: 89%, Cont: 1%; H5D5- Methanolobus2: second MAG from station H5, Comp: 63%, Cont: 0%. Comp: Completeness; Cont: Contamination.

The trimethylamine- (*mttB*) and methanol-specific (*mtaB*) methyltransferases were found in significant numbers with a relative expression of 5.4% and 9%, respectively, despite the *mts* genes being lowly expressed. Overall, the relative expression of the whole gene clusters encoding dimethylamine-, and especially trimethylamine- and methanol-specific methyltransferases (*mtbAB*, *mttBC* and *mtaABC*, respectively) was higher than that of the *mts* genes. Specifically, in the H3 metatranscriptomics data, *mtbABC* had an average relative abundance of 1.4%, *mttBC* 3.6% and *mtaABC* 4.2% (Figure 6.2.B). In station H5, the average relative abundance of *mtbABC* was 0.7%, *mttBC* 2.9% and *mtaABC* 3.5% (Figure 6.2.B). All of these highly expressed genes were primarily from *Methanolobus* spp. with 76%-94% similarity to known species. These genes were also present in the metagenomics datasets, where *mtbABC* had a relative abundance of 0.3%-0.4%, *mttBC* of 2%-4% and *mtaABC* 0.2%-0.6% (Figure 6.2.A). Following the metagenomics analysis, *mttB* was found in significantly higher relative abundance (6%; $p<0.001$) than all other genes (Figure 6.2.A).

The entire gene clusters of *mtaABC*, *mtbABC* and *mttBC* were also present in the two most complete *Methanolobus* MAGs (H2D5-*Methanolobus* and H5D5-*Methanolobus*; Figure 6.3.A). The genes encoding for monomethylamine corrinoid protein gene (*mtmC*) and methylamine corrinoid protein Co-methyltransferase (*mtmB*) were expressed in lower amounts compared to the other methanol and methylamine methyltransferases in the metatranscriptomes (0.15% and 0.51%, respectively), despite having a metagenomics relative abundance (0.3% and 0.9%, respectively) similar to *mtbABC* and *mtaABC* (Figure 6.2). *mtmB* was not present in the *Methanolobus* MAGs, whereas *mtmC* was present in all MAGs besides *Methanolobus* from station H3 (H3D5-*Methanolobus*; Figure 6.3.A).

In addition to the genes specific to methylotrophic methanogenesis, I searched for genes encoding key enzymes common to all methanogenic pathways (Appendix Table 5). I found that all the genes in the *mcrABCDG* operon, which encodes methyl-CoM reductase catalysing the final step in methane formation, had a relative expression >1% in both metatranscriptomics datasets (Figure 6.4.B). In line with *mcrA* sequence analysis, the genes found with high copy numbers within the metagenomics and metatranscriptomics sequences were assigned to *Methanolobus* spp. These genes were also present in the most complete *Methanolobus* MAG (H2D5-*Methanolobus*; Figure 6.3.B). I further showed that the transcripts of several other genes in central methanogenic pathways (e.g. *mtrA-H*, *hdrABCD*, *mvdADG*, *frhB*; Appendix Table 5) were found in high levels; however, *fpo* and *vho* gene transcripts catalysing coenzyme B/coenzyme M regeneration were not found (Figure 6.4.B). These genes were also absent in the metagenomics datasets (Figure 6.4.A).

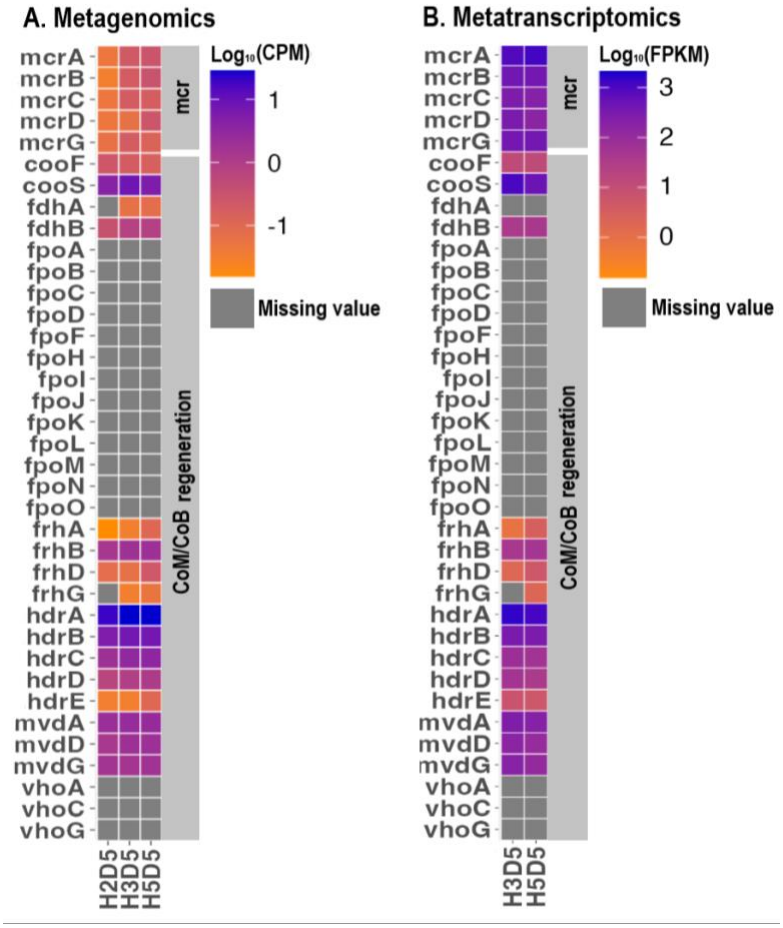

Figure 6.4. Genes common in all three methanogenesis pathways. A. Metagenomics normalised gene copy numbers. B. Metatranscriptomics normalised gene copy numbers. CPM: Copies per million; FPKM: Fragments per kilobase of gene per million reads; CoM: Coenzyme M; CoB: Coenzyme B.

Most of the genes involved in acetoclastic methanogenesis (*ack*, *acs*, *coo*, *cdh*, *pta*; Appendix Table 2) and hydrogenotrophic methanogenesis (*fmd*, *ftr*, *mch*, *mer*; Appendix Table 3) had a relative expression between 0.1%-5% but *hmd* was undetected in the metagenomics datasets (Figure 6.5). It should, however, be kept in mind that the genes involved in hydrogenotrophic methanogenesis (CO_2 fixation) are also utilised during methylotrophic methanogenesis in reverse reactions (CO_2 production; Lyu *et al.*, 2018) and during anaerobic methane oxidation (Qian *et al.*, 2022).

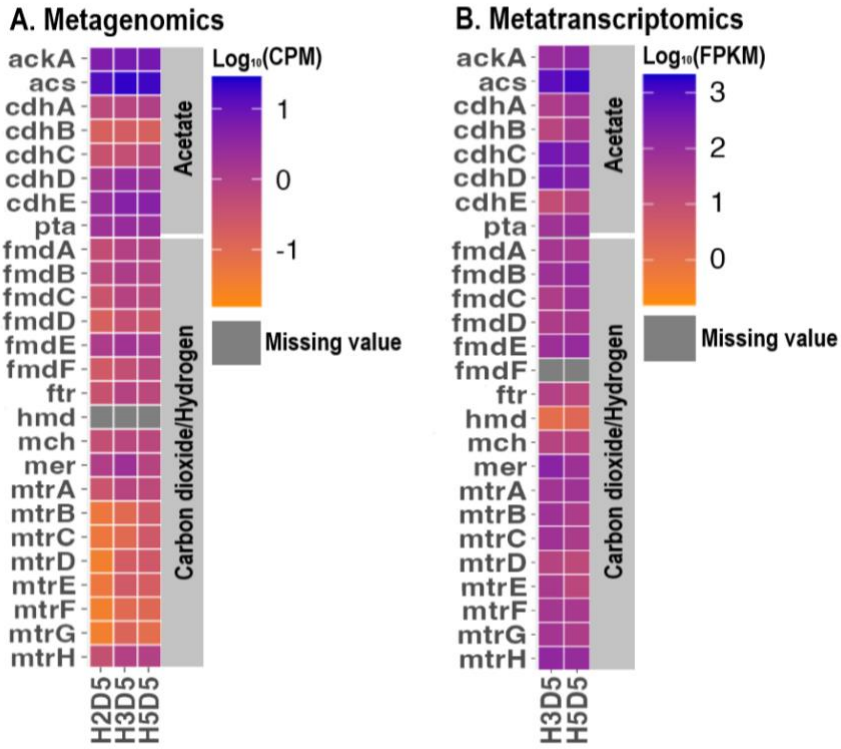

Figure 6.5. Genes involved in methane production via the acetoclastic and hydrogenotrophic methanogenesis pathways. **A.** Metagenomics normalised gene copy numbers. **B.** Metatranscriptomics normalised gene copy numbers. CPM: Copies per million; FPKM: Fragments per kilobase of gene per million reads; Acetate: Acetoclastic methanogenesis; Carbon dioxide/Hydrogen: Hydrogenotrophic methanogenesis.

Since SRB can also degrade DMS using sulfate as the electron acceptor, I explored the pathways of sulfur transformation (Figure 6.6). Specifically, I investigated the pathways for dissimilatory sulfate reduction and oxidation, assimilatory sulfate reduction, sulfur disproportionation, sulfur reduction, sulfur oxidation and the SOX systems (Appendix Table 6). Among these, the most highly expressed genes in the metatranscriptomics datasets were *dsrAB* (5.8%), *aprAB* (6.3%) and *sat* (3.5%), responsible for dissimilatory sulfate reduction, and *sqr* (3.6%) involved in sulfide oxidation (Figure 6.6.B). The genes involved in SOX

systems had a lower expression compared to the other sulfur transformation genes, at 0.2%-0.9% (Figure 6.5.B). *soeABC* were not present in the metatranscriptomics and metagenomics datasets, whereas *sdo* and *psrC* were present in low relative abundance (0.01% and 0.002%, respectively) only in the metagenomics data (Figure 6.6).

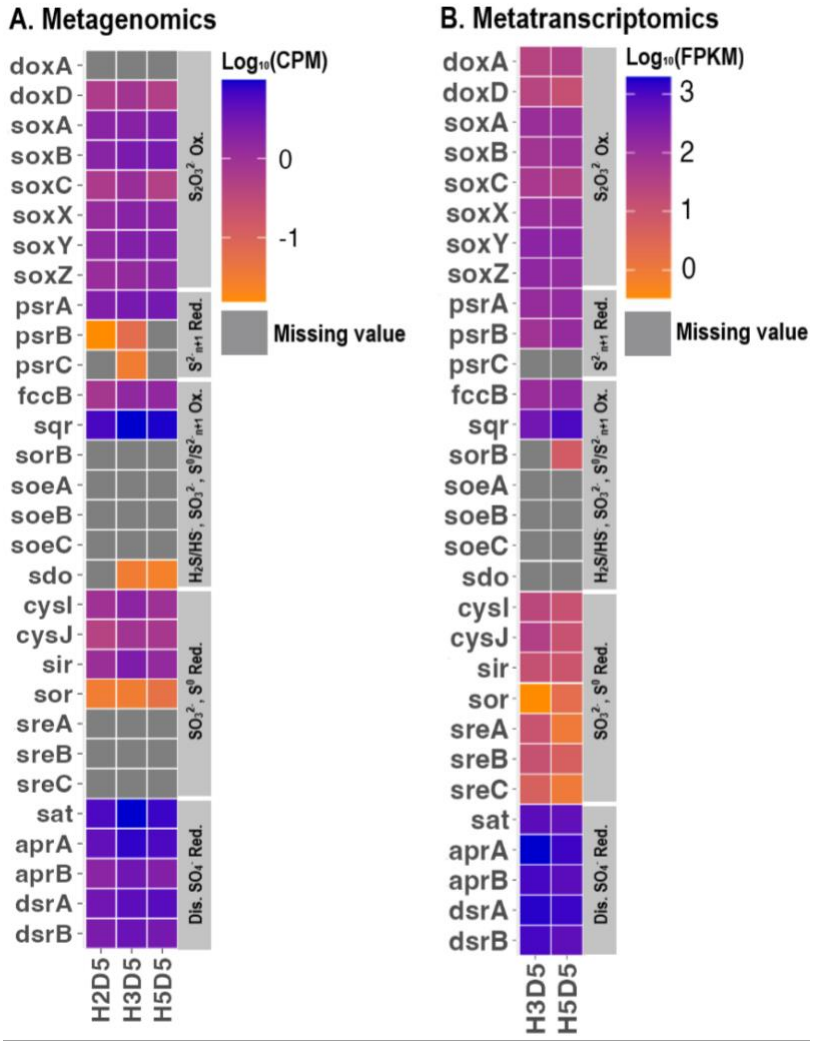

Figure 6.6. Genes involved in sulfur cycling. **A.** Metagenomics normalised gene copy numbers. **B.** Metatranscriptomics normalised gene copy numbers. CPM: Copies per million; FPKM: Fragments per kilobase of gene per million reads; $S_2O_3^{2-}$ Ox: Thiosulfate oxidation; S^{2-}_{n+1} Red: Polysulfide reduction; H_2S/HS^-, SO_3^{2-}, S^0/S^{2-}_{n+1} Ox: Hydrogen sulfide/bisulfide, sulfite and sulfur/polysulfide oxidation; SO_3^{2-}, S^0 Red: Sulfite and sulfur reduction; Dis. SO_4^{2-} Red: Dissimilatory sulfate reduction.

6.3 Discussion

DMS is an important organosulfur compound taking part in both the biogeochemical sulfur and carbon cycles. It is also a methane precursor in anoxic sediments through its degradation by anaerobic microorganisms. However, there is limited information on the metabolism of anaerobic DMS degradation. Here, I explored the metabolic pathways of DMS-degradation in anoxic sediments from the Baltic Sea.

An important result of this study was the lack or very low detection of methylsulfide-specific methyltransferases (methylthiol:CoM methyltransferase - *mts* genes) in the metagenomics and metatranscriptomics datasets (Tallant and Krzycki, 1997; Tallant *et al.*, 2001; Fu and Metcalf, 2015). However, the transcriptional profiles of genes encoding for TMA- and methanol-methyltransferases (*mttB* and *mtaB*) showed much higher levels of gene expression than the *mts* genes in the DMS-amended sediments.

Metagenomics and metatranscriptomics data analysis showed that the highly expressed methyltransferases (*mttB* and *mtaB*) were affiliated most closely with *Methanolobus*. *Methanolobus* species, for example *M. taylorii* and *M. bombayensis*, have been shown to degrade both methanol and methylamines in the past (Kadam *et al.*, 1994; Oremland and Boone, 1994). *mttB* was also present in the four *Methanolobus* MAGs constructed from the metagenomics data, whereas *mtaB* was only present in two of the *Methanolobus* MAGs (H2D5-*Methanolobus* and H5D5-*Methanolobus*), but this might be due to the incomplete construction of the other two genomes (H3D5-*Methanolobus* and H5D5-*Methanolobus*2). This suggests that these *Methanolobus* use methyltransferases typically associated with TMA and methanol for the degradation of DMS, suggesting these genes are not always substrate specific.

Contrary to our findings, Tallant *et al.* (2001) found that the methylamine-specific methylcobalamin:CoM methyltransferase, MtbA, did not catalyse the methylation of cobalamin with DMS in *Methanosarcina barkeri*, but DMS did not inhibit *mtbA*, either. Furthermore, it was shown that cell suspensions of TMA-grown cells of *Methanolobus taylori* did not metabolise DMS (Oremland *et al.*, 1989). Regardless, our results suggest differential expression of *mtaA* and *mtbA* according to the growth substrate, which is in line with previous research suggesting multiple homologs of genes can be differentially expressed, allowing for the switch between different growth substrates (Kremer *et al.*, 1994). For instance, methanol and acetate-grown *Methanosarcina thermofila* contain multiple homologs of the methanol:CoM methyltransferase system genes (Ding *et al.*, 2002). Galagan *et al.* (2002) showed *Methanosarcina acetivorans* had multiple methyltransferase homologs as well, yet none resembled the *M. barkeri* methylsulfide methyltransferase genes despite being able to grow on methylsulfides (Paul and Krzycki, 1996). Bose *et al.* (2008), continuing the work on *M. acetivorans*, showed that *mtaA* and *mtbA* genes can be expressed during growth on substrates such as acetate beside TMA and methanol. Indeed, our findings indicate that homologs of TMA and methanol methyltransferases could be participating in DMS metabolism.

The three gene clusters associated with dissimilatory sulfate reduction, including indirect sulfite oxidation, *dsrAB*, *aprAB* and *sat*, were all highly expressed in the metatranscriptomics data (Dahl and Truper, 2001; Anantharaman *et al.*, 2018). This is not surprising considering there is SRB activity in these sulfate-rich Baltic Sea sediments (Chapter 5).

According to taxonomic profiling, the most abundant SRB in the metatranscriptomics datasets were *Desulfopila* in stations H3 and H5 and *Desulfotalea* only in H5. *Desulfopila* is

an SRB genus with two validly published halophilic species, *D. aestuarii* and *D. inferna* (Suzuki *et al.*, 2007; Gittel *et al.*, 2010). Both species have a wide range of organic electron donors, such as fumarate, lactate and pyruvate, yet neither was tested for DMS-degradation (Suzuki *et al.*, 2007; Gittel *et al.*, 2010). *Desulfotalea* is also an SRB genus with psychrophilic species such as *D. psychrophile* and *D. arctica*, both isolated from sediments off the coast of Svalbard, suggesting they can survive in the Baltic Sea sediments and thrive in these low-temperature incubations (8 ºC; Chapter 5; Knoblauch *et al.*, 1999). Similarly to *Desulfopila*, *Desulfotalea* can use various electron acceptors such as lactate and hydrogen, yet DMS was not tested as a growth substrate (Knoblauch *et al.*, 1999). Overall, the metatranscriptomics datasets suggest both genera are present and active in the Baltic Sea sediments. It is, therefore, surprising that they were undetected by *dsrB* or 16S rRNA amplicon sequencing, as shown in Chapter 5. This suggests that the primers used in this study do not amplify the full array of SRB abundance or that the taxonomic databases need to be updated. Both should be addressed in future research. Regardless, *Desulfopila* and *Desulfotalea* could be using DMS as their electron donor during sulfate reduction. Alternatively, both genera might be degrading common *in situ* substrates often found in saline sediments, such as lactate, butyrate and hydrogen (Sørensen *et al.*, 1981; Christensen, 1984; Parkes *et al.*, 1989).

Metatranscriptomics also showed that Station H5 contained a high copy number of *dsrB* genes from *Desulfosarcina*, *aprB* genes from *Desulfococcus* and *sat* genes from *Desulfogranum*. From these three genera, only *Desulfosarcina* have previously been associated with DMS degradation (Lyimo *et al.*, 2009). *Desulfosarcina* and *Desulfococcus* were also found in these sediments following amplicon sequencing (Chapter 5). On the other hand, *Desulfogranum* were not identified during Chapter 5's amplicon sequencing analysis.

Similarly to *Desulfopila* and *Desulfotalea*, this could suggest low *dsrB* and 16S rRNA primer coverage or that the taxonomic databases need updating.

Hydrogen sulfide is a major metabolite of anaerobic DMS degradation, and a high abundance of *sqr* genes involved in sulfide oxidation was observed (Brito *et al.*, 2009). As mentioned in Chapter 5, *Sulfurimonas*, which likely oxidised the hydrogen sulfide produced by DMS degradation, were found in high relative abundance in the Baltic Sea sediments, explaining the high expression of *sqr* in the metatranscriptomics data (Wang *et al.*, 2021).
Besides hydrogen sulfide, *Sulfurimonas* spp. can also use thiosulfate as an electron donor (Grote *et al.*, 2012; Mammitzsch *et al.*, 2014). However, *psrC*, a gene associated with thiosulfate/polysulfide reduction, was not expressed in our samples (Dietrich and Klimmek, 2002; Liu *et al.*, 2014). Therefore, I hypothesise that *Sulfurimonas* are preferentially oxidising hydrogen sulfide produced by DMS degradation in the Baltic Sea samples.

In conclusion, this study provides the first evidence that DMS is degraded via the activity of TMA and methanol methyltransferases in anoxic sediments and challenges the view that substrate-specific methyltransferases are used for microbial degradation of methylated compounds. Furthermore, various highly expressed SRB were detected in the sediments suggesting the existence of novel DMS-degrading species. Despite this, further investigation is required to understand SRB DMS-degradation in the Baltic Sea.

7 Conclusions and future perspectives

The aim of this PhD project was to understand the potential for anaerobic DMS-degradation in anoxic sediments and to elucidate the diversity and metabolism of DMS-degrading microorganisms underlying this process. I had a set of objectives to address these aims, which were explored in each chapter.

In Chapter 3, my objective was to identify the DMS-degrading microorganisms in anoxic sediments along the sulfate gradient of an estuary. Estuarine sediments are ideal ecosystems to study anaerobic DMS degradation and how sulfate availability affects the fate of its carbon. Using sediment collected along the sulfate gradient of the Medway Estuary (UK), I showed that there was a sulfate-driven niche differentiation of methanogens, with *Methanomethylovorans* dominating the freshwater sediment incubations, *Methanolobus* the brackish ones and *Methanococcoides* the marine ones. However, methane production was not affected despite the differences in the sulfate concentrations and the niche partitioning of methanogens. Specifically, all sites had similar methane yields suggesting sulfate availability did not affect DMS-driven methanogenesis. Interestingly, *Methanococcoides* have not been shown to degrade DMS before suggesting the existence of potentially novel *Methanococcoides* that degrade DMS.

The results from Chapter 3 further suggested that DMS affected the sulfur cycle in the Medway Estuary sediments in two ways. Firstly, DMS was a substrate for SRB growth since certain SRB taxa increased in relative abundance after DMS addition. Secondly, DMS potentially initiated a cryptic sulfur cycle via the accumulation of hydrogen sulfide, which arises during DMS degradation. DMS affecting the sulfur cycle was further supported by the

proliferation of *Sulfurimonas*. This sulfur-oxidising genus most likely oxidised the produced hydrogen sulfide to thiosulfate and sulfate or directly to sulfate.

The second objective of my PhD was to identify the DMS-degrading microorganisms in riverine sediments, which I explored in Chapter 4. Rivers are significant contributors to the global carbon cycle and important methane hotspots. In this chapter, I attempted to quantify the potential for DMS degradation in river sediments with contrasting riverbed grain sizes (sand-dominated and gravel-dominated), hence sediment permeability. The results showed that DMS was an important source of methane in riverine sediments and that sediment permeability was the main factor affecting the DMS-derived methane yield. Sand-dominated rivers exhibited higher methanogenesis than gravel-dominated rivers, potentially due to a lower advective oxygen supply. Regardless of sediment permeability, *Methanomethylovorans* proliferated in all riverine incubations following the addition of DMS. Freshwater sediments have low sulfate concentrations, yet SRB activity can occur in these ecosystems because of cryptic sulfur cycling. Indeed, SRB activity was present in the sediments since SRB taxa *Desulfobulbus* and *Desulfobacca* increased after DMS addition, suggesting novel DMS-degrading SRB exist in these riverine sediments.

In Chapter 5, I set out to explore my third PhD objective and characterised the depth profile of DMS-degrading microorganisms in Baltic Sea sediments. This study gave the first insight into the depth profile of anaerobic DMS-degrading microorganisms across a naturally occurring sulfate concentration gradient. The Baltic Sea is subjected to regular phytoplankton blooms, which release high amounts of DMSP, a DMS precursor. These regular blooms, alongside the Baltic Sea being a brackish ecosystem, make this system ideal for studying DMS degradation. During this study, sediment incubations were established across the natural sulfate depth gradient of the Baltic Sea sediment. Despite the differences in sulfate

concentrations, *Methanolobus* were the dominant DMS-degrading methanogens in all the sediment layers. This was further supported by metagenomics on the sulfate-methane transition zone samples, where methane production and sulfate reduction were observed. Here, *Methanolobus* was the dominant taxon amongst all archaea. Furthermore, phylogenetic analysis of the most abundant *mcrA* genes in the metagenomics datasets, including the *mcrA* genes from the *Methanolobus* metagenome-assembled genomes, suggested that novel *Methanolobus* species were present in these sediments. The results also showed DMS degradation by SRB since certain taxa increased following DMS addition. These SRB may have novel DMS degrading capabilities as they were not shown as DMS-degraders before using cultivation-dependent tools. Sulfate was produced in sediment incubations with very little or no sulfate addition. In these incubations, the hydrogen sulfide accumulation following DMS-degradation appeared to have initiated rapid recycling of sulfate, which is further supported by an increase in the relative abundance of *Sulfurimonas*. Similar to the results in Chapter 3, this highlights the effect of DMS on the sulfur cycle.

The objective of Chapter 6 was to identify the metabolic pathways of the DMS-degrading microorganisms in anoxic sediments, which are not well studied. Previous studies attempting to explore the metabolism of DMS degradation were primarily using cultivation-dependent techniques. In this chapter, through metagenomics and metatranscriptomics, I aimed to elucidate for the first time the genetic and metabolic potential of DMS-degrading microorganisms and their activity in anoxic sediments using cultivation-independent techniques. This chapter's most important outcome was exhibiting DMS degradation via the activity of TMA and methanol methyltransferases for the first time. This contradicts the long-standing view that only substrate-specific methyltransferases are used during the degradation

of methylated compounds, such as DMS. Furthermore, the metatranscriptomics datasets had evidence of highly expressed SRB suggesting the existence of novel DMS-degrading taxa.

Overall, this PhD addressed crucial questions regarding the diversity and metabolism of microorganisms underlying DMS-degradation in anoxic sediments. However, more research is required to fully explore the diversity and metabolism of microorganisms able to carry out this important process. *Methanococcoides* and many unclassified SRB proliferated following DMS addition, suggesting the existence of novel DMS-degrading species. The attempt to culture new DMS-degrading microorganisms or to test already cultured microorganisms for DMS-degrading capabilities is vital for fully understanding the breadth of organisms able to degrade DMS.

The vast majority of microorganisms cannot be cultured due to low abundance, slow growth rate and unknown growth requirements. Therefore, more experiments using cultivation-independent techniques will help answer questions regarding the active DMS degraders in the environment. For example, stable-isotope probing (SIP) coupled with metagenomics can help further explore the active DMS-degrading populations. Lastly, this PhD challenges previous research suggesting that substrate-specific methyltransferases are used during the microbial degradation of methylated compounds. To further understand this outcome, proteomics and transcriptomics experiments are required to fully explore the metabolism behind anaerobic DMS degradation.

In conclusion, this PhD project explored the potential for anaerobic DMS-degradation and the diversity and metabolism of DMS-degrading microorganisms and highlighted the importance of DMS as a methanogenesis substrate. This research also showed that further work is

required to re-evaluate the microbial diversity and pathways of DMS-degradation in anoxic sediments to understand better its impact on the sulfur and carbon cycles in the environment.

References

Agarwala, R., Barrett, T., Beck, J., Benson, D.A., Bollin, C., Bolton, E., *et al.* (2016) Database resources of the National Center for Biotechnology Information. *Nucleic Acids Res* **44**: D7–D19.

Alcolombri, U., Ben-dor, S., Feldmesser, E., Levin, Y., Tawfik, D.S., and Vardi, A. (2015) Identification of the algal dimethyl sulfide–releasing enzyme: A missing link in the marine sulfur cycle. *Science (1979)* **348**: 1466–1469.

van Alstyne, K.L. and Puglisi, M.P. (2007) DMSP in marine macroalgae and macroinvertebrates: Distribution, function, and ecological impacts. *Aquat Sci* **69**: 394–402.

Anantharaman, K., Hausmann, B., Jungbluth, S.P., Kantor, R.S., Lavy, A., Warren, L.A., *et al.* (2018) Expanded diversity of microbial groups that shape the dissimilatory sulfur cycle. *ISME Journal* **12**: 1715–1728.

Ando, H., Kumagai, M., Karashimada, T., and Iida, H. (1957) Diagnostic use of dimethylsulfoxide reduction test within enterobacteriaceae. *Jpn J Microbiol* **1**: 335–338.

Andreae, M.O. (1980) Dimethylsulfoxide in marine and freshwaters. *Limnol Oceanogr* **25**: 1054–1063.

Angel, R., Claus, P., and Conrad, R. (2012) Methanogenic archaea are globally ubiquitous in aerated soils and become active under wet anoxic conditions. *ISME Journal* **6**: 847–862.

Apprill, A., Mcnally, S., Parsons, R., and Weber, L. (2015) Minor revision to V4 region SSU rRNA 806R gene primer greatly increases detection of SAR11 bacterioplankton. *Aquatic Microbial Ecology* **75**: 129–137.

Aufdenkampe, A.K., Mayorga, E., Raymond, P.A., Melack, J.M., Doney, S.C., Alin, S.R., *et al.* (2011) Riverine coupling of biogeochemical cycles between land, oceans, and atmosphere. *Front Ecol Environ* **9**: 53–60.

Bacic, M.K., Newell, S.Y., and Yoch, D.C. (1998) Release of dimethylsulfide from dimethylsulfoniopropionate by plant- associated salt marsh fungi. *Appl Environ Microbiol* **64**: 1484–1489.

Bak, F., Finster, K., and Rothfuß, F. (1992) Formation of dimethylsulfide and methanethiol from methoxylated aromatic compounds and inorganic sulfide by newly isolated anaerobic bacteria. *Arch Microbiol* **157**: 529–534.

Banat, I.M. and Nedwell, D.B. (1984) Inhibition of sulphate reduction in anoxic marine sediment by Group VI anions. *Estuar Coast Shelf Sci* **18**: 361–366.

Barton, L.L. and Fauque, G.D. (2009) Chapter 2 Biochemistry, Physiology and Biotechnology of Sulfate-Reducing Bacteria. In *Advances in Applied Microbiology*. Elsevier Inc., pp. 41–98.

Bastviken, D., Tranvik, L.J., Downing, J.A., Crill, P.M., and Enrich-Prast, A. (2011) Freshwater methane emissions offset the continental carbon sink. *Science (1979)* **331**: 50.

Battin, T.J., Luyssaert, S., Kaplan, L.A., Aufdenkampe, A.K., Richter, A., and Tranvik, L.J. (2009) The boundless carbon cycle. *Nat Geosci* **2**: 598–600.

Bechard, M.J. and Rayburn, W.R. (1979) Volatile organic sulfides from freshwater algae. *J Phycol* **15**: 379–383.

Bentley, R. and Chasteen, T.G. (2004) Environmental VOSCs - Formation and degradation of dimethyl sulfide, methanethiol and related materials. *Chemosphere* **55**: 291–317.

Berg, J.S., Jézéquel, D., Duverger, A., Lamy, D., Laberty-Robert, C., and Miot, J. (2019) Microbial diversity involved in iron and cryptic sulfur cycling in the ferruginous, low-sulfate waters of Lake Pavin. *PLoS One* **14**: 1–21.

Bisanz, J.E. (2018) qiime2R: Importing QIIME2 artifacts and associated data into R sessions.

Bland, C., Ramsey, T.L., Sabree, F., Lowe, M., Brown, K., Kyrpides, N.C., and Hugenholtz, P. (2007) CRISPR Recognition Tool (CRT): A tool for automatic detection of clustered regularly interspaced palindromic repeats. *BMC Bioinformatics* **8**: 1–8.

Blodau, C., Mayer, B., Peiffer, S., and Moore, T.R. (2007) Support for an anaerobic sulfur cycle in two Canadian peatland soils. *J Geophys Res Biogeosci* **112**: 1–10.

Boden, R., Borodina, E., Wood, A.P., Kelly, D.P., Murrell, J.C., and Schäfer, H. (2011) Purification and characterization of dimethylsulfide monooxygenase from Hyphomicrobium sulfonivorans. *J Bacteriol* **193**: 1250–1258.

Bokulich, N.A., Kaehler, B.D., Rideout, J.R., Dillon, M., Bolyen, E., Knight, R., *et al.* (2018) Optimizing taxonomic classification of marker-gene amplicon sequences with QIIME 2's q2-feature-classifier plugin. *Microbiome* **6**: 1–17.

Bolyen, E., Rideout, J.R., Dillon, M.R., Bokulich, N.A., Abnet, C.C., Al-Ghalith, G.A., *et al.* (2019) Reproducible, interactive, scalable and extensible microbiome data science using QIIME 2. *Nat Biotechnol* **37**: 852–857.

de Bont, J.A.M., van Diken, J.P., and Harder, W. (1981) Dimethyl Sulphoxide and Dimethyl Sulphide as a Carbon, Sulphur and Energy Source for Growth of Hjphomicrobium S. *J Gen Microbiol* **1273**: 15–323.

Boone, D.R., Worakit, S., Mathrani, I.M., and Mah, R.A. (1986) Alkaliphilic methanogens from high-pH lake sediments. *Syst Appl Microbiol* **7**: 230–234.

Borges, A. v. and Abril, G. (2011) Carbon Dioxide and Methane Dynamics in Estuaries.

Borodina, E., Kelly, D.P., Rainey, F.A., Ward-Rainey, N.L., and Wood, A.P. (2000) Dimethylsulfone as a growth substrate for novel methylotrophic species of Hyphomicrobium and Arthrobacter. *Arch Microbiol* **173**: 425–437.

Borton, M.A., Daly, R.A., O'Banion, B., Hoyt, D.W., Marcus, D.N., Welch, S., *et al.* (2018) Comparative genomics and physiology of the genus Methanohalophilus, a prevalent methanogen in hydraulically fractured shale. *Environ Microbiol* **20**: 4596–4611.

Bose, A., Pritchett, M.A., and Metcalf, W.W. (2008) Genetic analysis of the methanol- and methylamine-specific methyltransferase 2 genes of Methanosarcina acetivorans C2A. *J Bacteriol* **190**: 4017–4026.

Bowers, R.M., Kyrpides, N.C., Stepanauskas, R., Harmon-Smith, M., Doud, D., Reddy, T.B.K., *et al*. (2017) Minimum information about a single amplified genome (MISAG) and a metagenome-assembled genome (MIMAG) of bacteria and archaea. *Nat Biotechnol* **35**: 725–731.

Boy, M., Kulmala, M., Ruuskanen, T.M., Pihlatie, M., Reissell, A., Aalto, P.P., *et al.* (2005) Sulphuric acid closure and contribution to nucleation mode particle growth. *Atmos Chem Phys* **5**: 863–878.

Brenner, D.J., Krieg, N.R., Garrity, G.M., and Staley, J.T. (2005) Volume 2: The Proteobacteria, Part C: The Alpha-, Beta-, Delta-, and Epsilonproteobacteria, 2nd ed. Garrity, G.M., Bell, J.A., and Lilburn, T. (eds) New York, NY: Springer.

Brettar, I., Labrenz, M., Flavier, S., Bötel, J., Kuosa, H., Christen, R., and Höfle, M.G. (2006) Identification of a Thiomicrospira denitrificans-like epsilonproteobacterium as a catalyst for autotrophic denitrification in the central Baltic Sea. *Appl Environ Microbiol* **72**: 1364–1372.

Brettar, I. and Rheinheimer, G. (1991) Denitrification in the central Baltic: evidence for H2 S-oxidation as motor of denitrification at the oxic-anoxic interface. *Mar Ecol Prog Ser* **77**: 157–169.

Brimblecombe, P. and Shooter, D. (1986) Photo-oxidation of dimethylsulphide in aqueous solution. *Mar Chem* **19**: 343–353.

Brito, J.A., Sousa, F.L., Stelter, M., Bandeiras, T.M., Vonrhein, C., Teixeira, M., *et al.* (2009) Structural and functional insights into sulfide:quinone oxidoreductase. *Biochemistry* **48**: 5613–5622.

Broadbent, A.D. and Jones, G.B. (2004) DMS and DMSP in mucus ropes, coral mucus, surface films and sediment pore waters from coral reefs in the Great Barrier Reef. *Mar Freshw Res* **55**: 849–855.

Broadbent, A.D., Jones, G.B., and Jones, R.J. (2002) DMSP in corals and benthic algae from the Great Barrier Reef. *Estuar Coast Shelf Sci* **55**: 547–555.

Burt, T., Boardman, J., Foster, I., and Howden, N. (2016) More rain, less soil: Long-term changes in rainfall intensity with climate change. *Earth Surf Process Landf* **41**: 563–566.

Bushnell, B. (2014) BBMap: A Fast, Accurate, Splice-Aware Aligner.

Callahan, B.J., McMurdie, P.J., Rosen, M.J., Han, A.W., Johnson, A.J.A., and Holmes, S.P. (2016) DADA2: High-resolution sample inference from Illumina amplicon data. *Nat Methods* **13**: 581–583.

Callbeck, C.M., Lavik, G., Ferdelman, T.G., Fuchs, B., Gruber-Vodicka, H.R., Hach, P.F., *et al.* (2018) Oxygen minimum zone cryptic sulfur cycling sustained by offshore transport of key sulfur oxidizing bacteria. *Nat Commun* **9**: 1–11.

Canfield, D.E., Kristensen, E., and Thamdrup, B. (2005) The Sulfur Cycle. In *Advances in Marine Biology*. pp. 313–381.

Capriotti, K. and Capriotti, J.A. (2012) Dimethyl sulfoxide: History, chemistry, and clinical utility in dermatology. *Journal of Clinical and Aesthetic Dermatology* **5**: 24–26.

Carbonero, F., Oakley, B.B., and Purdy, K.J. (2014) Metabolic flexibility as a major predictor of spatial distribution in microbial communities. *PLoS One* **9**: e85105-.

Carrión, O., Curson, A.R.J., Kumaresan, D., Fu, Y., Lang, A.S., Mercadé, E., and Todd, J.D. (2015) A novel pathway producing dimethylsulphide in bacteria is widespread in soil environments. *Nat Commun* **6**:.

Carrión, O., Pratscher, J., Curson, A.R.J., Williams, B.T., Rostant, W.G., Murrell, J.C., and Todd, J.D. (2017) Methanethiol-dependent dimethylsulfide production in soil environments. *ISME J* **11**: 2379.

Carslaw, K.S., Boucher, O., Spracklen, D. v., Mann, G.W., L. Rae, J.G., Woodward, S., and Kulmala, M. (2010) A review of natural aerosol interactions and feedbacks within the Earth system. *Atmos Chem Phys* **10**: 1701–1737.

Caspi, R., Altman, T., Billington, R., Dreher, K., Foerster, H., Fulcher, C.A., *et al.* (2014) The MetaCyc database of metabolic pathways and enzymes and the BioCyc collection of Pathway/Genome Databases. *Nucleic Acids Res* **42**: 459–471.

Castro H F, Williams N H, and Ogram A (2000) Phylogeny of sulfate-reducing bacteria (1). *FEMS Microbiol Ecol* **31**: 1–9.

Catalan, L., Liang, V., Johnson, A., Jia, C., O'Connor, B., and Walton, C. (2009) Emissions of reduced sulphur compounds from the surface of primary and secondary wastewater clarifiers at a Kraft Mill. *Environ Monit Assess* **156**: 37–49.

Cha, I.-T., Min, U.-G., Kim, S.-J., Yim, K.J., Roh, S.W., and Rhee, S.-K. (2013) Methanomethylovorans uponensis sp. nov., a methylotrophic methanogen isolated from wetland sediment. *Antonie Van Leeuwenhoek* **104**: 1005–1012.

Challenger, F. and Simpson, M.I. (1948) Studies on biological methylation. Part XII. A precursor of the dimethyl sulphide evolved by Polysiphonia fastigiata. Dimethyl-2-carboxyethylsulphonium hydroxide and its salts. *J Chem Soc* **3**: 1591–1597.

Chan, P. and Lowe, T. (2019) tRNAscan-SE: searching for tRNA genes. *Gene Prediction* **1962**: 1–21.

Charlson, R.J., Lovelock, J.E., Andreaei, M.O., and Warren, S.G. (1987) Oceanic phytoplankton, atmospheric sulphur, cloud. *Nature* **330**: 1987.
Chaumeil, P.A., Mussig, A.J., Hugenholtz, P., and Parks, D.H. (2020) GTDB-Tk: A toolkit to classify genomes with the genome taxonomy database. *Bioinformatics* **36**: 1925–1927.
Chen, I.M.A., Chu, K., Palaniappan, K., Ratner, A., Huang, J., Huntemann, M., *et al.* (2021) The IMG/M data management and analysis system v.6.0: New tools and advanced capabilities. *Nucleic Acids Res* **49**: D751–D763.
Chen, M., Zhang, Y.Q., Krumholz, L.R., Zhao, L.Y., Yan, Z.S., Yang, Y.J., *et al.* (2022) Black blooms-induced adaptive responses of sulfate reduction bacteria in a shallow freshwater lake. *Environ Res* **209**: 112732.
Chen, S.C., Huang, H.H., Lai, M.C., Weng, C.Y., Chiu, H.H., Tang, S.L., *et al.* (2018) Methanolobus psychrotolerans sp. nov., a psychrotolerant methanoarchaeon isolated from a saline meromictic lake in siberia. *Int J Syst Evol Microbiol* **68**: 1378–1383.
Chen, Y., Patel, N.A., Crombie, A., Scrivens, J.H., and Murrell, J.C. (2011) Bacterial flavin-containing monooxygenase is trimethylamine monooxygenase. *Proc Natl Acad Sci U S A* **108**: 17791–17796.
Christensen, D. (1984) Determination of substrates oxidized by sulfate reduction in intact cores of marine sediments. *Limnol Oceanogr* **29**: 189–192.
Ciais, P., Sabine, C., Bala, G., Bopp, L., Brovkin, V., Canadell, J., *et al*. (2013) Chapter 6 Carbon and Other Biogeochemical Cycles 6. *Change, IPCC Climate* 465–570.
Clum, A., Huntemann, M., Bushnell, B., Foster, Brian, Foster, Bryce, Roux, S., *et al.* (2021) DOE JGI Metagenome Workflow. *mSystems* **6**: e00804-20.
Cole, J.J. and Caraco, N.F. (2001) Carbon in catchments: Connecting terrestrial carbon losses with aquatic metabolism. *Mar Freshw Res* **52**: 101–110.
Cole, J.J., Prairie, Y.T., Caraco, N.F., McDowell, W.H., Tranvik, L.J., Striegl, R.G., *et al.* (2007) Plumbing the global carbon cycle: Integrating inland waters into the terrestrial carbon budget. *Ecosystems* **10**: 171–184.
Conrad, R. (2020) Importance of hydrogenotrophic, aceticlastic and methylotrophic methanogenesis for methane production in terrestrial, aquatic and other anoxic environments: A mini review. *Pedosphere* **30**: 25–39.
Conrad, R. (2009) The global methane cycle: Recent advances in understanding the microbial processes involved. *Environ Microbiol Rep* **1**: 285–292.
Cosquer, A., Pichereau, V., Pocard, J.A., Minet, J., Cormier, M., and Bernard, T. (1999) Nanomolar levels of dimethylsulfoniopropionate, dimethylsulfonioacetate, and glycine betaine are sufficient to confer osmoprotection to Escherichia coli. *Appl Environ Microbiol* **65**: 3304–3311.
Costa, O.Y.A., de Hollander, M., Kuramae, E.E., and Bodelier, P.L.E. (2022) PhyloFunDB: A Pipeline to Create and Update Functional Gene Taxonomic Databases. *Microorganisms* **10**:.
Crespo, E., Hordijk, C.A., de Graaf, R.M., Samudrala, D., Cristescu, S.M., Harren, F.J.M., and van Dam, N.M. (2012) On-line detection of root-induced volatiles in Brassica nigra plants infested with Delia radicum L. root fly larvae. *Phytochemistry* **84**: 68–77.
Crowe, S.A., Paris, G., Katsev, S., Jones, C.A., Kim, S.T., Zerkle, A.L., *et al.* (2014) Sulfate was a trace constituent of Archean seawater. *Science (1979)* **346**: 735–739.
Curson, A.R.J., Liu, J., Bermejo Martínez, A., Green, R.T., Chan, Y., Carrión, O., *et al.* (2017) Dimethylsulfoniopropionate biosynthesis in marine bacteria and identification of the key gene in this process. *Nat Microbiol* **2**:.
Curson, A.R.J., Todd, J.D., Sullivan, M.J., and Johnston, A.W.B. (2011) Catabolism of dimethylsulphoniopropionate: Microorganisms, enzymes and genes. *Nat Rev Microbiol* **9**: 849–859.

Dacey, J.W., King, G.M., and Wakeham, S.G. (1987) Factors controlling emission of dimethylsulphide from salt marshes. *Nature* **330**: 643–645.
Dacey, J.W.H., King, G.M., and Lobel, P.S. (1994) Herbivory by reef fishes and the production of dimethylsulfide and acrylic acid. *Mar Ecol Prog Ser* **112**: 67–74.
Dacey, J.W.H. and Wakeham, S.G. (1984) Oceanic Dimethylsulfide : Production During Zooplankton Grazing on Phytoplankton. *Science (1979)* **233**: 29–32.
Dahl, C., Koch, H.G., Keuken, O., and Trüper, H.G. (1990) Purification and characterization of ATP sulfurylase from the extremely thermophilic archaebacterial sulfate-reducer, Archaeoglobus fulgidus. *FEMS Microbiol Lett* **67**: 27–32.
Dahl, C. and Truper, H.G. (2001) Sulfite reductase and APS reductase from Archaeoglobus fulgidus. *Methods Enzymol* **331**: 427–441.
DeSantis, T.Z., Hugenholtz, P., Larsen, N., Rojas, M., Brodie, E.L., Keller, K., *et al.* (2006) Greengenes, a chimera-checked 16S rRNA gene database and workbench compatible with ARB. *Appl Environ Microbiol* **72**: 5069–5072.
Dietrich, W. and Klimmek, O. (2002) The function of methyl-menaquinone-6 and polysulfide reductase membrane anchor (PsrC) in polysulfide respiration of Wolinella succinogenes. *Eur J Biochem* **269**: 1086–1095.
Ding, Y.H.R., Zhang, S.P., Tomb, J.F., and Ferry, J.G. (2002) Genomic and proteomic analyses reveal multiple homologs of genes encoding enzymes of the methanol:coenzyme M methyltransferase system that are differentially expressed in methanol- and acetate-grown Methanosarcina thermophila. *FEMS Microbiol Lett* **215**: 127–132.
Distefano, V. and Borgstedt, H.H. (1964) Reduction of Dimethylsulfoxide to Dimethylsulfide in the Cat. *Science (1979)* **144**: 1137–1138.
Donnelly, C., Greuell, W., Andersson, J., Gerten, D., Pisacane, G., Roudier, P., and Ludwig, F. (2017) Impacts of climate change on European hydrology at 1.5, 2 and 3 degrees mean global warming above preindustrial level. *Clim Change* **143**: 13–26.
Dürr, H.H., Laruelle, G.G., van Kempen, C.M., Slomp, C.P., Meybeck, M., and Middelkoop, H. (2011) Worldwide typology of nearshore coastal systems: Defining the estuarine filter of river inputs to the oceans. *Estuaries and Coasts* **34**: 441–458.
Elberson, M.A. and Sowers, K.R. (1997) Isolation of an Aceticlastic Strain of Methanosarcina siciliae from Marine Canyon Sediments and Emendation of the Species Description for Methanosarcina siciliae. *Int J Syst Bacteriol* **47**: 1258–1261.
Esaki, N. and Soda, K. (1987) L-Methionine y-Lyase from Pseudomonas putida and Aeromonas. *Methods Enzymol* **143**: 459–465.
Eyice, Ö., Myronova, N., Pol, A., Carrión, O., Todd, J.D., Smith, T.J., *et al.* (2018) Bacterial SBP56 identified as a Cu-dependent methanethiol oxidase widely distributed in the biosphere. *ISME Journal* **12**: 145–160.
Eyice, Ö., Namura, M., Chen, Y., Mead, A., Samavedam, S., and Schäfer, H. (2015) SIP metagenomics identifies uncultivated Methylophilaceae as dimethylsulphide degrading bacteria in soil and lake sediment. *ISME Journal* **9**: 2336–2348.
Fike, D.A., Bradley, A.S., and Rose, C. v. (2015) Rethinking the Ancient Sulfur Cycle. *Annu Rev Earth Planet Sci* **43**: 593–622.
Finn, R.D., Coggill, P., Eberhardt, R.Y., Eddy, S.R., Mistry, J., Mitchell, A.L., *et al.* (2016) The Pfam protein families database: Towards a more sustainable future. *Nucleic Acids Res* **44**: D279–D285.
Finster, K., King, G.M., and Bak, F. (1990) Formation Of Methylmercaptan And Dimethylsulfide From Methoxylated Aromatic-Compounds In Anoxic Marine And Fresh-Water Sediments. *FEMS Microbiol Ecol* **74**: 295–301.

Finster, K., Tanimoto, Y., and Bak, F. (1992) Fermentation of methanethiol and dimethylsulfide by a newly isolated methanogenic bacterium. *Arch Microbiol* **157**: 425–430.
Fiore, A.M., Naik, V., and Leibensperger, E.M. (2015) Air quality and climate connections. *J Air Waste Manage Assoc* **65**: 645–685.
Fish, J.A., Chai, B., Wang, Q., Sun, Y., Brown, C.T., Tiedje, J.M., and Cole, J.R. (2013) FunGene: The functional gene pipeline and repository. *Front Microbiol* **4**: 1–14.
Franzmann, P.D., Deprez, P.P., Burton, H.R., and van den Hoff, J. (1987) Limnology of organic lake, Antarctica, a meromictic lake that contains high concentrations of dimethyl sulfide. *Australian journal of marine and freshwater research* **38**: 409–417.
Fu, H. and Metcalf, W.W. (2015) Genetic basis for metabolism of methylated sulfur compounds in Methanosarcina species. *J Bacteriol* **197**: 1515–1524.
Fuchsman, C.A., Murray, J.W., and Staley, J.T. (2012) Stimulation of autotrophic denitrification by intrusions of the Bosporus Plume into the anoxic Black Sea. *Front Microbiol* **3**: 1–14.
Fuse, H., Takimura, O., Murakami, K., Yamaoka, Y., and Omori, T. (2000) Utilization of dimethyl sulfide as a sulfur source with the aid of light by Marinobacterium sp. Strain DMS-S1. *Appl Environ Microbiol* **66**: 5527–5532.
Galagan, J.E., Nusbaum, C., Roy, A., Endrizzi, M.G., Macdonald, P., Fitzhugh, W., *et al.* (2002) The genome of M. acetivorans reveals extensive metabolic and physiological diversity. *Genome Res* **12**: 532–542.
Galperin, M.Y., Makarova, K.S., Wolf, Y.I., and Koonin, E. v. (2015) Expanded Microbial genome coverage and improved protein family annotation in the COG database. *Nucleic Acids Res* **43**: D261–D269.
Ginzburg, B., Chalifa, I., Gun, J., Dor, I., Hadas, O., and Lev, O. (1998) DMS formation by dimethylsulfoniopropionate route in freshwater. *Environ Sci Technol* **32**: 2130–2136.
Gittel, A., Seidel, M., Kuever, J., Galushko, A.S., Cypionka, H., and Könneke, M. (2010) Desulfopila inferna sp. nov., a sulfate-reducing bacterium isolated from the subsurface of a tidal sand-flat. *Int J Syst Evol Microbiol* **60**: 1626–1630.
Glud, R.N. (2008) Oxygen dynamics of marine sediments. *Marine Biology Research* **4**: 243–289.
Gonzalez, J.M., Mayer, F., Moran, M.A., Hodson, R.E., and Whitman, W.B. (1997) Sagittula stellata gen. nov., sp. nov., a Lignin-Transforming Bacterium from a Coastal Environment. *Int J Syst Bacteriol* **47**: 773–780.
Gough, J., Karplus, K., Hughey, R., and Chothia, C. (2001) Assignment of homology to genome sequences using a library of hidden Markov models that represent all proteins of known structure. *J Mol Biol* **313**: 903–919.
Gould, W.D. and Kanagawa, T. (1992) Purification and properties of methyl mercaptan oxidase from Thiobacillus thioparus TK-m. *J Gen Microbiol* **138**: 217–221.
Grote, J., Jost, G., Labrenz, M., Herndl, G.J., and Jürgens, K. (2008) Epsilonproteobacteria represent the major portion of chemoautotrophic bacteria in sulfidic waters of pelagic redoxclines of the Baltic and Black seas. *Appl Environ Microbiol* **74**: 7546–7551.
Grote, J., Schott, T., Bruckner, C.G., Glöckner, F.O., Jost, G., Teeling, H., *et al.* (2012) Genome and physiology of a model Epsilonproteobacterium responsible for sulfide detoxification in marine oxygen depletion zones. *Proc Natl Acad Sci U S A* **109**: 506–510.
Haft, D.H., Selengut, J.D., Richter, R.A., Harkins, D., Basu, M.K., and Beck, E. (2013) TIGRFAMs and genome properties in 2013. *Nucleic Acids Res* **41**: 387–395.

Hagy, J.D., Boynton, W.R., Keefe, C.W., and Wood, K. v. (2004) Hypoxia in Chesapeake Bay, 1950-2001: Long-term change in relation to nutrient loading and river flow. *Estuaries* **27**: 634–658.

Hammer, Ø., Harper, D.A.T., and Ryan, P.D. (2001) PAST: Paleontological statistics software package for education and data analysis. *Palaentologia Electronica* **4**: 1–9.

Han, Y. and Perner, M. (2015) The globally widespread genus Sulfurimonas: Versatile energy metabolisms and adaptations to redox clines. *Front Microbiol* **6**: 1–17.

Hanlon, S.P., Holt, R.A., Moore, G.R., and McEwan, A.G. (1994) Isolation and characterization of a strain of Rhodobacter sulfidophilus: A bacterium which grows autotrophically with dimethylsulphide as electron donor. *Microbiology (N Y)* **140**: 1953–1958.

Hannaford, J. (2015) Climate-driven changes in UK river flows: A review of the evidence. *Prog Phys Geogr* **39**: 29–48.

Hao, B., Gong, W., Ferguson, T.K., James, C.M., Krzycki, J.A., and Chan, M.K. (2002) A new UAG-encoded residue in the structure of a methanogen methyltransferase. *Science (1979)* **296**: 1462–1466.

Hatton, A.D., Malin, G., Turner, S.M., and Liss, P.S. (1996) DMSO - A significant compound in the biogeochemical cycle of DMS. *Biological and Environmental Chemistry of Dmsp and Related Sulfonium Compounds* 405–412.

Hawkins, L.N. and Russell, L.M. (2010) Polysaccharides, Proteins, and Phytoplankton Fragments: Four Chemically Distinct Types of Marine Primary Organic Aerosol Classified by Single Particle Spectromicroscopy. *Advances in Meteorology* **2010**: 1–14.

Heitmann, T., Goldhammer, T., Beer, J., and Blodau, C. (2007) Electron transfer of dissolved organic matter and its potential significance for anaerobic respiration in a northern bog. *Glob Chang Biol* **13**: 1771–1785.

Henkel, J. v., Dellwig, O., Pollehne, F., Herlemann, D.P.R., Leipe, T., and Schulz-Vogt, H.N. (2019) A bacterial isolate from the Black Sea oxidizes sulfide with manganese(IV) oxide. *PNAS* **116**: 12153–12155.

Hill, C.R., Shafaei, A., Balmer, L., Lewis, J.R., Hodgson, J.M., Millar, A.H., and Blekkenhorst, L.C. (2022) Sulfur compounds: From plants to humans and their role in chronic disease prevention. *Crit Rev Food Sci Nutr* **0**: 1–23.

Hjerne, O., Hajdu, S., Larsson, U., Downing, A., and Winder, M. (2019) Climate driven changes in timing, composition and size of the Baltic Sea phytoplankton spring bloom. *Front Mar Sci* **6**: 1–15.

Hoang, D.T., Chernomor, O., von Haeseler, A., Minh, B.Q., and Vinh, L.S. (2018) UFBoot2: Improving the Ultrafast Bootstrap Approximation. Molecular biology and evolution. *Mol Biol Evol* **35**: 518–522.

Holmkvist, L., Ferdelman, T.G., and Jørgensen, B.B. (2011) A cryptic sulfur cycle driven by iron in the methane zone of marine sediment (Aarhus Bay, Denmark). *Geochim Cosmochim Acta* **75**: 3581–3599.

Horinouchi, M., Kasuga, K., Nojiri, H., Yamane, H., and Omori, T. (1997) Cloning and characterization of genes encoding an enzyme which oxidizes dimethyl sulfide in Acinetobacter sp. strain 20B. *FEMS Microbiol Lett* **155**: 99–105.

Horinouchi, M., Yoshida, T., Nojiri, H., Yamane, H., and Omori, T. (1999) Polypeptide requirements of multicomponent monooxygenase DsoABCDEF for dimethylsulfide oxidizing activity. *Biosci Biotechnol Biochem* **63**: 1765–1771.

Hu, M., Liu, L., Ma, Q., Zhu, T., Tian, X., and Dai, M. (2005) Spatial-temporal distribution of dimethylsulfide in the subtropical Pearl River Estuary and adjacent waters. *Cont Shelf Res* **25**: 1996–2007.

Huettel, M. and Gust, G. (1992) Impact of bioroughness on interfacial solute exchange in permeable sediments. *Mar Ecol Prog Ser* **89**: 253–267.
Hyatt, D., Chen, G.-L., LoCascio, P.F., Land, M.L., Larimer, F.W., and Hauser, LorenJ. (2010) Prodigal: prokaryotic gene recognition and translation initiation site identification. *BMC Bioinformatics* **11**: 1–11.
Ishimoto, M., Koyama, J., and Nagai, Y. (1954) Biochemical studies on sulfate-reducing bacteria. *The Journal of Biochemistry* **41**: 763–770.
Itoh, T., Suzuki, K., and Nakase, T. (1998) New Genus of Rod-Shaped , Extremely Thermophilic Crenarchaeote. *Int J Syst Bacteriol* **48**: 879–887.
Itoh, T., Suzuki, K., Sanchez, P.C., and Nakase, T. (1999) Caldivirga maquilingensis gen. nov., sp. nov., a new genus of rod-shaped crenarchaeote isolated from a hot spring in the Philippines. *Int J Syst Bacteriol* **49**: 1157–1163.
Jackson, G. and Stuckey, J. (2007) Effects of dimethylsulfoniopropionate (DMSP) produced by the cordgrass Spartina alterniflora on its epiphytic algal community. *Aquat Sci* **69**: 419–426.
James, C.M., Ferguson, T.K., Leykam, J.F., and Krzycki, J.A. (2001) The Amber Codon in the Gene Encoding the Monomethylamine Methyltransferase Isolated from Methanosarcina barkeri Is Translated as a Sense Codon. *Journal of Biological Chemistry* **276**: 34252–34258.
Jameson, E., Stephenson, J., Jones, H., Millard, A., Kaster, A.K., Purdy, K.J., *et al.* (2019) Deltaproteobacteria (Pelobacter) and Methanococcoides are responsible for choline-dependent methanogenesis in a coastal saltmarsh sediment. *ISME Journal* **13**: 277–289.
Janssen, F., Huettel, M., and Witte, U. (2005) Pore-water advection and solute fluxes in permeable marine sediments (II): Benthic respiration at three sandy sites with different permeabilities (German Bight, North Sea). *Limnol Oceanogr* **50**: 779–792.
Jensen, M.M., Kuypers, M.M.M., Lavik, G., and Thamdrup, B. (2008) Rates and regulation of anaerobic ammonium oxidation and denitrification in the Black Sea. *Limnol Oceanogr* **53**: 23–36.
Jiang, B., Parshina, S.N., van Doesburg, W., Lomans, B.P., and Stams, A.J.M. (2005) Methanomethylovorans thermophila sp. nov., a thermophilic, methylotrophic methanogen from an anaerobic reactor fed with methanol. *Int J Syst Evol Microbiol* **55**: 2465–2470.
Johnston, A.W.B., Todd, J.D., Sun, L., Nikolaidou-Katsaridou, M.N., Curson, A.R.J., and Rogers, R. (2008) Molecular diversity of bacterial production of the climate-changing gas, dimethyl sulphide, a molecule that impinges on local and global symbioses. *J Exp Bot* **59**: 1059–1067.
Jones, J.B. and Mulholland, P.J. (1998) Influence of drainage basin topography and elevation on carbon dioxide and methane supersaturation of stream water. *Biogeochemistry* **40**: 57–72.
Jonkers, H.M., van der Maarel, M.J.E.C., van Gemerden, H., and Hansen, T.A. (1996) Dimethylsulfoxide reduction by marine sulfate-reducing bacteria. *FEMS Microbiol Lett* **136**: 283–287.
Jorgensen, B.B. (1990) The Sulfur Cycle of Freshwater Sediments : Role of Thiosulfate. *Limnol Oceanogr* **35**: 1329–1342.
Kadam, P.C., Ranade, D.R., Mandelco, L., and Boone, D.R. (1994) Isolation and Characterization of Methanolobus bornbayensis sp. nov., a Methylotrophic Methanogen That Requires High Concentrations of Divalent Cations. *Int J Syst Bacteriol* **44**: 603–607.
Kadota, H. and Ishida, Y. (1972) Production of volatile sulfur compounds by microorganisms. *Annu Rev Microbiol* 127–138.

Kalinová, B., Podskalská, H., Růžička, J., and Hoskovec, M. (2009) Irresistible bouquet of death-how are burying beetles (Coleoptera: Silphidae: Nicrophorus) attracted by carcasses. *Naturwissenschaften* **96**: 889–899.
Kallistova, A.Y., Merkel, A.Y., Tarnovetskii, I.Y., and Pimenov, N. v. (2017) Methane formation and oxidation by prokaryotes. *Microbiology (Russian Federation)* **86**: 671–691.
Kalvari, I., Argasinska, J., Quinones-Olvera, N., Nawrocki, E.P., Rivas, E., Eddy, S.R., *et al.* (2018) Rfam 13.0: Shifting to a genome-centric resource for non-coding RNA families. *Nucleic Acids Res* **46**: D335–D342.
Kalyaanamoorthy, S., Minh, B.Q., Wong, T.K.F., von Haeseler, A., and Jermiin, L.S. (2017) ModelFinder: Fast model selection for accurate phylogenetic estimates. *Nat Methods* **14**: 587–589.
Kamann, P.J., Ritzi, R.W., Dominic, D.F., and Conrad, C.M. (2007) Porosity and permeability in sediment mixtures. *Ground Water* **45**: 429–438.
Kanehisa, M., Furumichi, M., Sato, Y., Kawashima, M., and Ishiguro-Watanabe, M. (2022) KEGG for taxonomy-based analysis of pathways and genomes. *Nucleic Acids Res* 1–6.
Kang, D.D., Froula, J., Egan, R., and Wang, Z. (2015) MetaBAT, an efficient tool for accurately reconstructing single genomes from complex microbial communities. *PeerJ* **2015**: 1–15.
Keenan, T.W. and Lindsay, R.C. (1968) Evidence for a Dimethyl Sulfide Precursor in Milk. *J Dairy Sci* **51**: 112–114.
Kiełbasa, S.M., Wan, R., Sato, K., Horton, P., and Frith, M.C. (2011) Adaptive seeds tame genomic sequence comparison. *Genome Res* **21**: 487–493.
Kiene, R.P. (1988) Dimethyl sulfide metabolism in salt marsh sediments. *FEMS Microbiol Lett* **53**: 71–78.
Kiene, R.P. and Bates, T.S. (1990) Biological removal of dimethyl sulphide from sea water. *Nature* **345**: 702–705.
Kiene, R.P. and Capone, D.G. (1988) Microbial transformations of methylated sulfur compounds in anoxic salt marsh sediments. *Microb Ecol* **15**: 275–291.
Kiene, R.P. and Hines, M.E. (1995) Microbial Formation of Dimethyl Sulfide in Anoxic Sphagnum Peat. *Appl Environ Microbiol* **61**: 2720–2726.
Kiene, R.P. and Linn, L.J. (2000) Distribution and turnover of dissolved DMSP and its relationship with bacterial production and dimethylsulfide in the Gulf of Mexico. *Limnol Oceanogr* **45**: 849–861.
Kiene, R.P., Linn, L.J., González, J., Moran, M.A., and Bruton, J.A. (1999) Dimethylsulfoniopropionate and methanethiol are important precursors of methionine and protein-sulfur in marine bacterioplankton. *Appl Environ Microbiol* **65**: 4549–4558.
Kiene, R.P., Oremland, R.S., Catena, A., Miller, L.G., and Capone, D.G. (1986) Metabolism of reduced methylated sulfur compounds in anaerobic sediments and by a pure culture of an estuarine methanogen. *Appl Environ Microbiol* **52**: 1037–1045.
Kiene, R.P. and Visscher, P.T. (1987) Production and Fate of Methylated Sulfur Compounds from Methionine and Dimethylsulfoniopropionate in Anoxic Salt Marsh Sediments †. *Appl Environ Microbiol* **53**: 2426–2434.
King, G.M. (1984) Utilization of hydrogen, acetate, and “noncompetitive”; substrates by methanogenic bacteria in marine sediments.
King, G.M., Klug, M.J., and Lovley, D.R. (1983) Metabolism of Acetate, Methanol, and Methylated Amines in Intertidal Sediments of Lowes Cove, Maine. *Appl Environ Microbiol* **45**: 1848–1853.
King, T., Butcher, S., and Zalewski, L. (2017) Apocrita - High Performance Computing Cluster For Queen Mary University Of London. 3–4.

Kirst, G.O. (1990) Salinity Tolerance of Eukaryotic Marine Algae. *Annu Rev Plant Physiol Plant Mol Biol* **41**: 21–53.
Klatt, J.M. and Polerecky, L. (2015) Assessment of the stoichiometry and efficiency of CO2 fixation coupled to reduced sulfur oxidation. *Front Microbiol* **6**:.
Knoblauch, C., Sahm, K., and Jørgensen, B.B. (1999) Psychrophilic sulfate-reducing bacteria from permanently cold Arctic marine sediments: description of Desulfofrigus oceanense gen. nov., sp. nov., Desulfofrigus fragile sp. nov., Desulfofaba gelida gen. nov., sp. *Int J Syst Bacteriol* **49**: 1631–1643.
Kondo, R., Purdy, K.J., de Queiroz Silva, S., and Nedwell, D.B. (2007) Spatial Dynamics of Sulphate-reducing Bacterial Compositions in Sediment along a Salinity Gradient in a UK Estuary. *Microbes Environ* **22**: 11–19.
Kremer, J., Burchfield, S., Frazier, C., and Krzycki, J. (1994) Differential in vitro methylation and synthesis of the 480-kilodalton corrinoid protein in Methanosarcina barkeri grown on different substrates. *J Bacteriol* **176**: 253–255.
Krzycki, J.A. (2005) The direct genetic encoding of pyrrolysine. *Curr Opin Microbiol* **8**: 706–712.
Ksionzek, K.B., Lechtenfeld, O.J., McCallister, S.L., Schmitt-Kopplin, P., Geuer, J.K., Geibert, W., and Koch, B.P. (2016) Dissolved organic sulfur in the ocean: Biogeochemistry of a petagram inventory". *Science (1979)* **354**: 456–459.
Kulmala, M. (2003) How Particles Nucleate and Grow. *Science (1979)* **302**: 1000–1001.
Kurth, J.M., Op den Camp, H.J.M., and Welte, C.U. (2020) Several ways one goal—methanogenesis from unconventional substrates. *Appl Microbiol Biotechnol* **104**: 6839–6854.
Labrenz, M., Grote, J., Mammitzsch, K., Boschker, H.T.S., Laue, M., Jost, G., *et al.* (2013) Sulfurimonas gotlandica sp. nov., a chemoautotrophic and psychrotolerant epsilonproteobacterium isolated from a pelagic redoxcline, and an emended description of the genus Sulfurimonas. *Int J Syst Evol Microbiol* **63**: 4141–4148.
Lahme, S., Callbeck, C.M., Eland, L.E., Wipat, A., Enning, D., Head, I.M., and Hubert, C.R.J. (2020) Comparison of sulfide-oxidizing Sulfurimonas strains reveals a new mode of thiosulfate formation in subsurface environments. *Environ Microbiol* **22**: 1784–1800.
Lana, A., Bell, T.G., Simó, R., Vallina, S.M., Ballabrera-Poy, J., Kettle, A.J., *et al.* (2011) An updated climatology of surface dimethlysulfide concentrations and emission fluxes in the global ocean. *Global Biogeochem Cycles* **25**: 1–17.
Lansdown, K., Heppell, C.M., Dossena, M., Ullah, S., Heathwaite, A.L., Binley, A., *et al.* (2014) Fine-scale in situ measurement of riverbed nitrate production and consumption in an armored permeable riverbed. *Environ Sci Technol* **48**: 4425–4434.
Lansdown, K., McKew, B.A., Whitby, C., Heppell, C.M., Dumbrell, A.J., Binley, A., *et al.* (2016) Importance and controls of anaerobic ammonium oxidation influenced by riverbed geology. *Nat Geosci* **9**: 357–360.
Lazar, C.S., Parkes, R.J., Cragg, B.A., L'Haridon, S., and Toffin, L. (2011) Methanogenic diversity and activity in hypersaline sediments of the centre of the Napoli mud volcano, Eastern Mediterranean Sea. *Environ Microbiol* **13**: 2078–2091.
Lehmann, A., Myrberg, K., Post, P., Chubarenko, I., Dailidiene, I., Hinrichsen, H.H., *et al.* (2022) Salinity dynamics of the Baltic Sea. *Earth System Dynamics* **13**: 373–392.
Letunic, I. and Bork, P. (2018) 20 years of the SMART protein domain annotation resource. *Nucleic Acids Res* **46**: D493–D496.
Letunic, I. and Bork, P. (2021) Interactive tree of life (iTOL) v5: An online tool for phylogenetic tree display and annotation. *Nucleic Acids Res* **49**: W293–W296.

Lever, M.A., Rouxel, O., Alt, J.C., Shimizu, N., Ono, S., Coggon, R.M., *et al.* (2013) Evidence for microbial carbon and sulfur cycling in deeply buried ridge flank basalt. *Science (1979)* **339**: 1305–1308.
Lever, M.A. and Teske, A.P. (2015) Diversity of methane-cycling archaea in hydrothermal sediment investigated by general and group-specific PCR primers. *Appl Environ Microbiol* **81**: 1426–1441.
Lewis, M., Cheney, C.S., and O Dochartaigh, B.E. (2006) Guide to Permeability Indices. *British Geological Survey Open Report* 1–29.
L'Haridon, S., Chalopin, M., Colombo, D., and Toffin, L. (2014) Methanococcoides vulcani sp. nov., a marine methylotrophic methanogen that uses betaine, choline and N,N-dimethylethanolamine for methanogenesis, isolated from a mud volcano, and emended description of the genus Methanococcoides. *Int J Syst Evol Microbiol* **64**: 1978–1983.
Li, D., Liu, C.M., Luo, R., Sadakane, K., and Lam, T.W. (2015) MEGAHIT: An ultra-fast single-node solution for large and complex metagenomics assembly via succinct de Bruijn graph. *Bioinformatics* **31**: 1674–1676.
Liang, L., Sun, Y., Dong, Y., Ahmad, T., Chen, Y., Wang, J., and Wang, F. (2022) Methanococcoides orientis sp. nov., a methylotrophic methanogen isolated from sediment of the East China Sea. *Int J Syst Evol Microbiol* **72**: 005384.
Lidbury, I., Kröber, E., Zhang, Z., Zhu, Y., Murrell, J.C., Chen, Y., and Schäfer, H. (2016) A mechanism for bacterial transformation of dimethylsulfide to dimethylsulfoxide: a missing link in the marine organic sulfur cycle. *Environ Microbiol* **18**: 2754–2766.
Lie, T.J., Godchaux, W., and Leadbetter, E.R. (1999) Sulfonates as terminal electron acceptors for growth of sulfite-reducing bacteria (Desulfitobacterium spp.) and sulfate-reducing bacteria: Effects of inhibitors of sulfidogenesis. *Appl Environ Microbiol* **65**: 4611–4617.
Liss, P., Malin, G., Turner, S., and Holligan, P. (1994) Dimethyl sulphide and Phaeocystis: A review. *Journal of Marine Systems* **5**: 41–53.
Liu, C., Cui, Y., Li, X., and Yao, M. (2021) Microeco: An R package for data mining in microbial community ecology. *FEMS Microbiol Ecol* **97**: 1–9.
Liu, C., Li, X., Mansoldo, F.R.P., An, J., Kou, Y., Zhang, X., *et al.* (2022) Microbial habitat specificity largely affects microbial co-occurrence patterns and functional profiles in wetland soils. *Geoderma* **418**: 115866.
Liu, H., Xin, Y., and Xun, L. (2014) Distribution, diversity, and activities of sulfur dioxygenases in heterotrophic bacteria. *Appl Environ Microbiol* **80**: 1799–1806.
Liu, Y., Boone, D.R., and Choy, C. (1990) Methanohalophilus oregonense sp. nov. a Methylotrophic Methanogen from an Alkaline, Saline Aquifer. *Int J Syst Bacteriol* **40**: 111–116.
Liu, Y. and Whitman, W.B. (2008) Metabolic, phylogenetic, and ecological diversity of the methanogenic archaea. *Ann N Y Acad Sci* **1125**: 171–189.
Lohse, L., Malschaert, J.F.P., Slomp, C.P., Helder, W., and van Raaphorst, W. (1995) Sediment-water fluxes of inorganic nitrogen compounds along the transport route of organic matter in the North Sea. *Ophelia* **41**: 173–197.
Lomans, Bart P, Camp, H.J.M., Op den Pol, A., and Vogels, G.D. (1999) Role of Methanogens and Other Bacteria in Degradation of Dimethyl Sulfide and Methanethiol in Anoxic Freshwater Sediments. *Appl Environ Microbiol* **65**: 2116–2121.
Lomans, B.P., Luderer, R., Steenbakkers, P., Pol, A., van der Drift, C., Vogels, G.D., and Op Den Camp, H.J.M. (2001) Microbial Populations Involved in Cycling of Dimethyl Sulfide and Methanethiol in Freshwater Sediments. *Appl Environ Microbiol* **67**: 1044–1051.

Lomans, Bart P., Maas, R., Luderer, R., Op Den Camp, H.J.M., Pol, A., van der Drift, C., and Vogels, G.D. (1999) Isolation and characterization of Methanomethylovorans hollandica gen. nov., sp. nov., isolated from freshwater sediment, a methylotrophic methanogen able to grow on dimethyl sulfide and methanethiol. *Appl Environ Microbiol* **65**: 3641–3650.

Lomans, Bart P, Op den Camp, H.J.M., Pol, A., van der Drift, C., and Vogels, G.D. (1999) Role of methanogens and other bacteria in degradation of dimethyl sulfide and methanethiol in anoxic freshwater sediments. *Appl Environ Microbiol* **65**: 2116–2121.

Lomans, Bart P., Op Den Camp, H.J.M., Pol, A., and Vogels, G.D. (1999) Anaerobic versus aerobic degradation of dimethyl sulfide and methanethiol in anoxic freshwater sediments. *Appl Environ Microbiol* **65**: 438–443.

Lomans, Bart P, Op Den Camp, H.J.M., Pol, A., and Vogels, G.D. (1999) Anaerobic versus aerobic degradation of dimethyl sulfide and methanethiol in anoxic freshwater sediments. *Appl Environ Microbiol* **65**: 438–443.

Lomans, B.P., Pol, A., and Op den Camp, H.J.M. (2002) Microbial cycling of volatile organic sulfur compounds. *Water Science and Technology* **45**: 55–60.

Lomans, B.P., Smolders, A.J.P., Intven, L.M., Pol, A., Op Den Camp, H.J.M., and van der Drift, C. (1997) Formation of dimethyl sulfide and methanethiol in anoxic freshwater sediments. *Appl Environ Microbiol* **63**: 4741–4747.

Lomsadze, A., Gemayel, K., Tang, S., and Borodovsky, M. (2018) Modeling leaderless transcription and atypical genes results in more accurate gene prediction in prokaryotes. *Genome Res* **28**: 1079–1089.

Lu, X., Fan, C., He, W., Deng, J., and Yin, H. (2013) Sulfur-containing amino acid methionine as the precursor of volatile organic sulfur compounds in algea-induced black bloom. *J Environ Sci (China)* **25**: 33–43.

Lustwerk, R.L. and Burdige, D.J. (1995) Elimination of dissolved sulfide interference in the flow injection determination of SCO2, by addition of molybdate. *Limnol Oceanogr* **40**: 1011–1012.

Lyimo, T.J., Pol, A., Harhangi, H.R., Jetten, M.S.M., and Op Den Camp, H.J.M. (2009) Anaerobic oxidation of dimethylsulfide and methanethiol in mangrove sediments is dominated by sulfate-reducing bacteria. *FEMS Microbiol Ecol* **70**: 483–492.

Lyimo, T.J., Pol, A., and Op Den Camp, H.J.M. (2002) Sulfate reduction and methanogenesis in sediments of mtoni mangrove forest, Tanzania. *Ambio* **31**: 614–616.

Lyimo, T.J., Pol, A., Op Den Camp, H.J.M., Harhangi, H.R., and Vogels, G.D. (2000) Methanosarcina semesiae sp. nov., a dimethylsulfide-utilizing methanogen from mangrove sediment. *Int J Syst Evol Microbiol* **50**: 171–178.

Lyu, Z., Shao, N., Akinyemi, T., and Whitman, W.B. (2018) Methanogenesis. *Current Biology* **28**: R719–R736.

van der Maarel, M.J.E.C. and Hansen, T.A. (1997) Dimethylsulfoniopropionate in anoxic intertidal sediments: A precursor of methanogenesis via dimethyl sulfide, methanethiol, and methiolpropionate. *Mar Geol* **137**: 5–12.

Mahapatra, A., Patel, A., Soares, J.A., Larue, R.C., Zhang, J.K., Metcalf, W.W., and Krzycki, J.A. (2006) Characterization of a Methanosarcina acetivorans mutant unable to translate UAG as pyrrolysine. *Mol Microbiol* **59**: 56–66.

Mahapatra, G.P., Raman, S., Nayak, S., Gouda, S., Das, G., and Patra, J.K. (2020) Metagenomics Approaches in Discovery and Development of New Bioactive Compounds from Marine Actinomycetes. *Curr Microbiol* **77**: 645–656.

Malin, G. and Kirst, G.O. (1997) Algal production of dimethyl sulfide and its atmospheric role. *J Phycol* **33**: 889–896.

Malin, G., Wilson, W.H., Bratbak, G., Liss, P.S., and Mann, N.H. (1998) Elevated production of dimethylsulfide resulting from viral infection of cultures of Phaeocystis pouchetii. *Limnol Oceanogr* **43**: 1389–1393.

Maltby, J., Steinle, L., Löscher, C.R., Bange, H.W., Fischer, M.A., Schmidt, M., and Treude, T. (2018) Microbial methanogenesis in the sulfate-reducing zone of sediments in the Eckernförde Bay, SW Baltic Sea. *Biogeosciences* **15**: 137–157.

Mammitzsch, K., Jost, G., and Jürgens, K. (2014) Impact of dissolved inorganic carbon concentrations and pH on growth of the chemolithoautotrophic epsilonproteobacterium Sulfurimonas gotlandica GD1T. *Microbiologyopen* **3**: 80–88.

Mathrani, I.M., Boone, D.R., Mah, R.A., Fox, G.E., and Lau, P.P. (1988) Methanohalophilus zhilinae sp. nov. , an Alkaliphilic, Halophilic, Methylotrophic Methanogen. *Int J Syst Bacteriol* **38**: 139–142.

Matrai, P.A. and Keller, M.D. (1993) Dimethylsulfide in a large-scale coccolithophore bloom in the Gulf of Maine. *Cont Shelf Res* **13**: 831–843.

Mattei, M.R., D'Acunto, B., Esposito, G., Frunzo, L., and Pirozzi, F. (2015) Mathematical modeling of competition and coexistence of sulfate-reducing bacteria, acetogens, and methanogens in multispecies biofilms. *Desalination Water Treat* **55**: 740–748.

McCrindle, S.L., Kappler, U., and McEwan, A.G. (2005) Microbial dimethylsulfoxide and trimethylamine-N-oxide respiration.

McEwan, A.G., Ferguson, S.J., and Jackson, J.B. (1991) Purification and properties of dimethyl sulphoxide reductase from Rhodobacter capsulatus. A periplasmic molybdoenzyme. *Biochemical Journal* **274**: 305–307.

Middelburg, J.J., Nieuwenhuize, J., Iversen, N., Hoegh, N., de Wilde, H., Helder, W., and Seifert, R., Christof, O., 2002 (2002) Methane distribution in European tidal estuaries. *Biogeochemistry* **59**: 95–119.

Milucka, J., Ferdelman, T.G., Polerecky, L., Franzke, D., Wegener, G., Schmid, M., *et al.* (2012) Zero-valent sulphur is a key intermediate in marine methane oxidation. *Nature* **491**: 541–546.

Mistry, J., Finn, R.D., Eddy, S.R., Bateman, A., and Punta, M. (2013) Challenges in homology search: HMMER3 and convergent evolution of coiled-coil regions. *Nucleic Acids Res* **41**:.

Mölder, F., Jablonski, K.P., Letcher, B., Hall, M.B., Tomkins-tinch, C.H., Sochat, V., *et al.* (2021) Sustainable data analysis with Snakemake [version 1 ; peer review : 1 approved , 1 approved with reservations]. *F1000Res* 1–25.

Monks, P.S., Archibald, A.T., Colette, A., Cooper, O., Coyle, M., Derwent, R., *et al*. (2015) Tropospheric ozone and its precursors from the urban to the global scale from air quality to short-lived climate forcer. *Atmos Chem Phys* **15**: 8889–8973.

Mori, K., Kim, H., Kakegawa, T., and Hanada, S. (2003) A novel lineage of sulfate-reducing microorganisms: Thermodesulfobiaceae fam. nov., Thermodesulfobium narugense, gen. nov., sp. nov., a new thermophilic isolate from a hot spring. *Extremophiles* **7**: 283–290.

Munson, M.A., Nedwell, D.B., and Embley, T.M. (1997) Phylogenetic diversity of Archaea in sediment samples from a coastal salt marsh. *Appl Environ Microbiol* **63**: 4729–4733.

Murphy, R.R., Kemp, W.M., and Ball, W.P. (2011) Long-term trends in Chesapeake Bay seasonal hypoxia, stratification, and nutrient loading. *Estuaries and Coasts* **34**: 1293–1309.

Muyzer, G. and Stams, A.J.M. (2008) The ecology and biotechnology of sulphate-reducing bacteria. *Nat Rev Microbiol* **6**: 441–54.

Myhre, G., Shindell, D., Bréon, F.-M., Collins, W., Fuglestvedt, J., Huang, J., *et al.* (2013) Anthropogenic and natural radiative forcing: Positive feedbacks. In *Climate Change 2013: The Physical Science Basis. Contribution of Working Group I to the Fifth*

Assessment Report of the Intergovernmental Panel on Climate Change. Stocker, T.F., Qin, D., Plattner, G.-K., Tignor, M., Allen, S.K., Boschung, J.., *et al.* (eds). Cambridge, United Kingdom and New York, NY, USA: Cambridge University Press, pp. 659–740.
Nakamura, T., Yamada, K.D., Tomii, K., and Katoh, K. (2018) Parallelization of MAFFT for large-scale multiple sequence alignments. *Bioinformatics* **34**: 2490–2492.
Narrowe, A.B., Borton, M.A., Hoyt, D.W., Smith, G.J., Daly, R.A., Angle, J.C., *et al.* (2019) Uncovering the Diversity and Activity of Methylotrophic Methanogens in Freshwater Wetland Soils. *mSystems* **4**:.
Nauhaus, K., Boetius, A., Krüger, M., and Widdel, F. (2002) In vitro demonstration of anaerobic oxidation of methane coupled to sulphate reduction in sediment from a marine gas hydrate area. *Environ Microbiol* **4**: 296–305.
Nawrocki, E.P. and Eddy, S.R. (2013) Infernal 1.1: 100-fold faster RNA homology searches. *Bioinformatics* **29**: 2933–2935.
Nedwell, D.B. and Abram, J.W. (1979) Relative influence of temperature and electron donor and electron acceptor concentrations on bacterial sulfate reduction in saltmarsh sediment. *Microb Ecol* **5**: 67–72.
Nguyen, L.T., Schmidt, H.A., von Haeseler, A., and Minh, B.Q. (2015) IQ-TREE: A fast and effective stochastic algorithm for estimating maximum-likelihood phylogenies. *Mol Biol Evol* **32**: 268–274.
Ni, S. and Boone, D.R. (1991) Isolation and characterization of a dimethlyl sulphide-degrading methanogen, Methanolobus siciliae HI350, from an oil well, characterization of M. siciliae T4/MT, and emendation of M. siciliae. *Int J Syst Evol Microbiol* **41**: 410–416.
Nolan, P., O'Sullivan, J., and McGrath, R. (2017) Impacts of climate change on mid-twenty-first-century rainfall in Ireland: a high-resolution regional climate model ensemble approach. *International Journal of Climatology* **37**: 4347–4363.
Nriagu, J.O. and Holdway, D.A. (1989) Production and release of dimethyl sulfide from the Great Lakes. *Tellus B* **41 B**: 161–169.
Nurk, S., Meleshko, D., Korobeynikov, A., and Pevzner, P.A. (2017) MetaSPAdes: A new versatile metagenomic assembler. *Genome Res* **27**: 824–834.
Oakley, B.B., Carbonero, F., Dowd, S.E., Hawkins, R.J., and Purdy, K.J. (2012) Contrasting patterns of niche partitioning between two anaerobic terminal oxidizers of organic matter. *ISME Journal* **6**: 905–914.
Oakley, B.B., Carbonero, F., van der Gast, C.J., Hawkins, R.J., and Purdy, K.J. (2010) Evolutionary divergence and biogeography of sympatric niche-differentiated bacterial populations. *ISME Journal* **4**: 488–497.
Oremland, R.S. and Boone, D.R. (1994) Methanolobus taylorii sp. nov., a New Methylotrophic, Estuarine Methanogen. *Int J Syst Bacteriol* **44**: 573–575.
Oremland, R.S., Kiene, R.P., Mathrani, I., Whiticar, M.J., and Boone, D.R. (1989) Description of an Estuarine Methylotrophic Methanogen Which Grows on Dimethyl Sulfide. *Appl Environ Microbiol* **55**: 994–1002.
Oremland, R.S. and Taylor, B.F. (1978) Sulfate reduction and methanogenesis in marine sediments. *Geochim Cosmochim Acta* **42**: 209–214.
Orphan, V.J., Hinrichs, K.U., Ussler, W., Paull, C.K., Taylor, L.T., Sylva, S.P., *et al.* (2001) Comparative Analysis of Methane-Oxidizing Archaea and Sulfate-Reducing Bacteria in Anoxic Marine Sediments. *Appl Environ Microbiol* **67**: 1922–1934.
Oude Elferink, S.J.W.H., Akkermans-van Vliet, W.M., Bogte, J.J., and Stams, A.J.M. (1999) Desulfobacca acetoxidans gen. nov., sp. nov., a novel acetate-degrading sulfate reducer isolated from sulfidogenic granular sludge. *Int J Syst Bacteriol* **49**: 345–350.

Pace, M.C., Bailey, D.M., Donnan, D.W., Narayanaswamy, B.E., Smith, H.J., Speirs, D.C., *et al.* (2021) Modelling seabed sediment physical properties and organic matter content in the Firth of Clyde. *Earth Syst Sci Data* **13**: 5847–5866.
Parada, A.E., Needham, D.M., and Fuhrman, J.A. (2016) Every base matters: Assessing small subunit rRNA primers for marine microbiomes with mock communities, time series and global field samples. *Environ Microbiol* **18**: 1403–1414.
Parkes, R.J., Gibson, G.R., Mueller-Harvey, I., Buckingham, W.J., and Herbert, R.A. (1989) Determination of the Substrates for Sulphate-reducing Bacteria within Marine and Esturaine Sediments with Different Rates of Sulphate Reduction. *J Gen Microbiol* **135**: 175–187.
Parks, D.H., Imelfort, M., Skennerton, C.T., Hugenholtz, P., and Tyson, G.W. (2015) CheckM: Assessing the quality of microbial genomes recovered from isolates, single cells, and metagenomes. *Genome Res* **25**: 1043–1055.
Paul, L. and Krzycki, J.A. (1996) Sequence and transcript analysis of a novel Methanosarcina barkeri methyltransferase II homolog and its associated corrinoid protein homologous to methionine synthase. *J Bacteriol* **178**: 6599–6607.
Peck Jr., H.D. (1959) The ATP-dependent reduction of sulfate with hydrogen in extracts of Desulfovibrio desulfuricans. *Proceedings of the National Academy of Sciences* **45**: 701–708.
Pelikan, C., Herbold, C.W., Hausmann, B., Müller, A.L., Pester, M., and Loy, A. (2016) Diversity analysis of sulfite- and sulfate-reducing microorganisms by multiplex dsrA and dsrB amplicon sequencing using new primers and mock community-optimized bioinformatics. *Environ Microbiol* **18**: 2994–3009.
Pester, M., Knorr, K.H., Friedrich, M.W., Wagner, M., and Loy, A. (2012) Sulfate-reducing microorganisms in wetlands - fameless actors in carbon cycling and climate change. *Front Microbiol* **3**: 1–19.
Purdy, K.J., Munson, M.A., Nedwell, D.B., and Embley, T.M. (2002) Comparison of the molecular diversity of the methanogenic community at the brackish and marine ends of a UK estuary. *FEMS Microbiol Ecol* **39**: 17–21.
Qian, L., Yu, X., Zhou, J., Gu, H., Ding, J., Peng, Y., *et al.* (2022) MCycDB: A curated database for comprehensively profiling methane cycling processes of environmental microbiomes. *Mol Ecol Resour* **22**: 1803–1823.
Qian, Z., Tianwei, H., Mackey, H.R., van Loosdrecht, M.C.M., and Guanghao, C. (2019) Recent advances in dissimilatory sulfate reduction: From metabolic study to application. *Water Res* **150**: 162–181.
Quast, C., Pruesse, E., Yilmaz, P., Gerken, J., Schweer, T., Yarza, P., *et al.* (2013) The SILVA ribosomal RNA gene database project: Improved data processing and web-based tools. *Nucleic Acids Res* **41**: 590–596.
Quinn, P.K. and Bates, T.S. (2011) The case against climate regulation via oceanic phytoplankton sulphur emissions. *Nature* **480**: 51–56.
R Core Team (2020) R: A Language and Environment for Statistical Computing.
Raina, J.B., Tapiolas, D.M., Forêt, S., Lutz, A., Abrego, D., Ceh, J., *et al.* (2013) DMSP biosynthesis by an animal and its role in coral thermal stress response. *Nature* **502**: 677–680.
Rappert, S. and Müller, R. (2005) Odor compounds in waste gas emissions from agricultural operations and food industries. *Waste Management* **25**: 887–907.
Reisch, C.R., Moran, M.A., and Whitman, W.B. (2011) Bacterial catabolism of dimethylsulfoniopropionate (DMSP). *Front Microbiol* **2**: 1–12.

Robeson, M.S., O'Rourke, D.R., Kaehler, B.D., Ziemski, M., Dillon, M.R., Foster, J.T., and Bokulich, N.A. (2021) RESCRIPt: Reproducible sequence taxonomy reference database management.
Robinson, M.D. and Oshlack, A. (2010) A scaling normalization method for differential expression analysis of RNA-seq data. *Genome Biol* **11**: 1–9.
Saari, A. and Martikainen, P.J. (2003) Dimethyl sulphoxide (DMSO) and dimethyl sulphide (DMS) as inhibitors of methane oxidation in forest soil. *Soil Biol Biochem* **35**: 383–389.
Sakai, S., Imachi, H., Hanada, S., Ohashi, A., Harada, H., and Kamagata, Y. (2008) Methanocella paludicola gen. nov., sp. nov., a methane-producing archaeon, the first isolate of the lineage "Rice Cluster I", and proposal of the new archaeal order Methanocellales ord. nov. *Int J Syst Evol Microbiol* **58**: 929–936.
Sanders, I.A., Heppell, C.M., Cotton, J.A., Wharton, G., Hildrew, A.G., Flowers, E.J., and Trimmer, M. (2007) Emission of methane from chalk streams has potential implications for agricultural practices. *Freshw Biol* **52**: 1176–1186.
Saunois, M., Stavert, A.R., Poulter, B., Bousquet, P., Canadell, J.G., Jackson, R.B., *et al.* (2020) The Global Methane Budget 2000-2017. *Earth Syst Sci Data* **12**: 1561–1623.
Savage, C., Leavitt, P.R., and Elmgren, R. (2004) Distribution and retention of effluent nitrogen in surface sediments of a coastal bay. *Limnol Oceanogr* **49**: 1503–1511.
Savant, S.A., Reible, D.D., and Thibodeaux, L.J. (1987) Convective transport within stable river sediments. *Water Resour Res* **23**: 1763–1768.
Sayers, E. (2010) A General Introduction to the E-utilities Usage Guidelines and Requirements Minimizing the Number of Requests. 1–9.
Scarlata, C.J. and Ebeler, S.E. (1999) Headspace solid-phase microextraction for the analysis of dimethyl sulfide in beer. *J Agric Food Chem* **47**: 2505–2508.
Schäfer, H. and Eyice, Ö. (2019) Microbial cycling of methanethiol. *Curr Issues Mol Biol* **33**: 173–181.
Schäfer, H., Myronova, N., and Boden, R. (2010) Microbial degradation of dimethylsulphide and related C1-sulphur compounds: Organisms and pathways controlling fluxes of sulphur in the biosphere. *J Exp Bot* **61**: 315–334.
Schloss, P.D., Westcott, S.L., Ryabin, T., Hall, J.R., Hartmann, M., Hollister, E.B., *et al.* (2009) Introducing mothur: Open-source, platform-independent, community-supported software for describing and comparing microbial communities. *Appl Environ Microbiol* **75**: 7537–7541.
Scholten, J.C.M., Murrell, J.C., and Kelly, D.P. (2003) Growth of sulfate-reducing bacteria and methanogenic archaea with methylated sulfur compounds: A commentary on the thermodynamic aspects. *Arch Microbiol* **179**: 135–144.
Schwarz, G., Mendel, R.R., and Ribbe, M.W. (2009) Molybdenum cofactors, enzymes and pathways. *Nature* **460**: 839–847.
Sciare, J., Mihalopoulos, N., and Nguyen, B.C. (2002) Spatial and temporal variability of dissolved sulfur compounds in European estuaries. *Biogeochemistry* **59**: 121–141.
Seelmann, C.S., Willistein, M., Heider, J., and Boll, M. (2020) Tungstoenzymes: Occurrence, catalytic diversity and cofactor synthesis. *Inorganics (Basel)* **8**: 1–23.
Sela-adler, M., Ronen, Z., Herut, B., Antler, G., Vigderovich, H., and Sela-adler, M. (2017) Co-existence of Methanogenesis and Sulfate Reduction with Common Substrates in Sulfate-Rich Estuarine Sediments. *Front Microbiol* **8**: 1–11.
Seymour, J.R., Simó, R., Ahmed, T., and Stocker, R. (2010) Chemoattraction to dimethylsulfoniopropionate throughout the marine microbial food web. *Science (1979)* **329**: 342–345.
Shaw, G.E. (1983) Bio-controlled thermostasis involving the sulfur cycle. *Clim Change* **5**: 297–303.

Shelley, F., Abdullahi, F., Grey, J., and Trimmer, M. (2015) Microbial methane cycling in the bed of a chalk river: Oxidation has the potential to match methanogenesis enhanced by warming. *Freshw Biol* **60**: 150–160.
Shelley, F., Ings, N., Hildrew, A.G., Trimmer, M., and Grey, J. (2017) Bringing methanotrophy in rivers out of the shadows. *Limnol Oceanogr* **62**: 2345–2359.
Shen, L. dong, Ouyang, L., Zhu, Y., and Trimmer, M. (2019) Active pathways of anaerobic methane oxidation across contrasting riverbeds. *ISME Journal* **13**: 752–766.
Shiklomanov, I.A. (1993) World fresh water resources. In *Water in crisis: A guide to the world's fresh water resources*. Gleick, P.H. (ed). Oxford University Press, pp. 13–24.
Sievert, S.M., Kiene, R.P., and Schulz-Vogt, H.N. (2007) The sulfur cycle. *Oceanography* **20**: 117–123.
Sievert, S.M., Scott, K.M., Klotz, M.G., Chain, P.S.G., Hauser, L.J., Hemp, J., *et al.* (2008) Genome of the epsilonproteobacterial chemolithoautotroph Sulfurimonas denitrificans. *Appl Environ Microbiol* **74**: 1145–1156.
Sigleo, A.C. and Frick, W.E. (2007) Seasonal variations in river discharge and nutrient export to a Northeastern Pacific estuary. *Estuar Coast Shelf Sci* **73**: 368–378.
Sillitoe, I., Dawson, N., Lewis, T.E., Das, S., Lees, J.G., Ashford, P., *et al.* (2019) CATH: Expanding the horizons of structure-based functional annotations for genome sequences. *Nucleic Acids Res* **47**: D280–D284.
Simó, R., Vila-Costa, M., Alonso-Sáez, L., Cardelús, C., Guadayol, Ó., Vázquez-Dominguez, E., and Gasol, J.M. (2009) Annual DMSP contribution to S and C fluxes through phytoplankton and bacterioplankton in a NW Mediterranean coastal site. *Aquatic Microbial Ecology* **57**: 43–55.
Sipilä, M., Berndt, T., Petäjä, T., Brus, D., Vanhanen, J., Stratmann, F., *et al.* (2010) The role of sulfuric acid in atmospheric nucleation. *Science (1979)* **327**: 1243–1246.
Smale, B.C., Lasater, N.J., and Hunter, B.T. (1975) Fate and Metabolism of Dimethyl Sulfoxide in Agricultural Crops. *Ann N Y Acad Sci* **243**: 228–236.
Smith, N.A. and Kelly, D.P. (1988) Mechanism of Oxidation of Dimethyl Disulphide by Thiobacillus thioparus Strain E6. *Microbiology (N Y)* **134**: 3031–3039.
Sørensen, J., Christensen, D., and Jørgensen, B.B. (1981) Volatile Fatty Acids and Hydrogen as Substrates for Sulfate-Reducing Bacteria in Anaerobic Marine Sediment. *Appl Environ Microbiol* **42**: 5–11.
Sowers, K.R., Baron, S.F., and Ferry, J.G. (1984) Methanosarcina acetivorans sp. nov., an Acetotrophic Methane- Producing Bacterium Isolated from Marine Sediments KEVIN. *Microbiology (N Y)* **47**: 971–978.
Spencer, K.L. (2002) Spatial variability of metals in the inter-tidal sediments of the Medway Estuary, Kent, UK. *Mar Pollut Bull* **44**: 933–944.
Stanley, E.H., Casson, N.J., Christel, S.T., Crawford, J.T., Loken, L.C., and Oliver, S.K. (2016) The ecology of methane in streams and rivers: Patterns, controls, and global significance. *Ecol Monogr* **86**: 146–171.
Stefels, J., Steinke, M., Turner, S., Malin, G., and Belviso, S. (2007) Environmental constraints on the production and removal of the climatically active gas dimethylsulphide (DMS) and implications for ecosystem modelling. *Biogeochemistry* **83**: 245–275.
Steinberg, L.M. and Regan, J.M. (2009) mcrA-targeted real-time quantitative PCR method to examine methanogen communities. *Appl Environ Microbiol* **75**: 4435–4442.
Stephens, G.L., Slingo, J.M., Rignot, E., Reager, J.T., Hakuba, M.Z., Durack, P.J., *et al.* (2020) Earth's water reservoirs in a changing climate. *Proceedings of the Royal Society A: Mathematical, Physical and Engineering Sciences* **476**: 1–34.

Strom, S., Wolfe, G., Holmes, J., Stecher, H., Shimeneck, C., Lambert, S., and Moreno, E. (2003) Chemical defense in the microplankton I: Feeding and growth rates of heterotrophic protists on the DMS-producing phytoplankter Emiliania huxleyi. *Limnol Oceanogr* **48**: 217–229.

Sun, H., Zhang, Y., Tan, S., Zheng, Y., Zhou, S., Ma, Q.Y., *et al.* (2020) DMSP-Producing Bacteria Are More Abundant in the Surface Microlayer than Subsurface Seawater of the East China Sea. *Microb Ecol* **80**: 350–365.

Sun, J., Mausz, M.A., Chen, Y., and Giovannoni, S.J. (2019) Microbial trimethylamine metabolism in marine environments. *Environ Microbiol* **21**: 513–520.

Sunda, W.G., Kieber, D., and Kiene, R.P. (2002) An antioxidant function of DMSP and DMS in marine algae oceanic dimethylsulfide (DMS) photolysis. *Nature* **418**: 317–320.

Suylen, G.M.H., Large, P.J., van Dijken, J.P., and Kuenen, J.G. (1987) Methyl Mercaptan Oxidase, a Key Enzyme in the Metabolism of Methylated Sulphur Compounds by Hyphomicrobium EG. *Microbiology (N Y)* **133**: 2989–2997.

Suzuki, D., Ueki, A., Amaishi, A., and Ueki, K. (2007) Desulfopila aestuarii gen. nov., sp. nov., a Gram-negative, rod-like, sulfate-reducing bacterium isolated from an estuarine sediment in Japan. *Int J Syst Evol Microbiol* **57**: 520–526.

Tallant, T.C. and Krzycki, J.A. (1997) Methylthiol:coenzyme M methyltransferase from Methanosarcina barkeri, an enzyme of methanogenesis from dimethylsulfide and methylmercaptopropionate. *J Bacteriol* **179**: 6902–6911.

Tallant, T.C., Paul, L., and Krzycki, J.A. (2001) The MtsA Subunit of the Methylthiol:Coenzyme M Methyltransferase of Methanosarcina barkeri Catalyses Both Half-reactions of Corrinoid-dependent Dimethylsulfide: Coenzyme M Methyl Transfer. *Journal of Biological Chemistry* **276**: 4485–4493.

Talou, T., Gaset, A., Delmas, M., Kulifaj, M., and Montant, C. (1990) Dimethyl sulphide: the secret for black truffle hunting by animals? *Mycol Res* **94**: 277–278.

Tanimoto, Y. and Bak, F. (1994) Anaerobic degradation of methylmercaptan and dimethyl sulfide by newly isolated thermophilic sulfate-reducing bacteria. *Appl Environ Microbiol* **60**: 2450–2455.

Thang, N.M., Brüchert, V., Formolo, M., Wegener, G., Ginters, L., Jørgensen, B.B., and Ferdelman, T.G. (2013) The Impact of Sediment and Carbon Fluxes on the Biogeochemistry of Methane and Sulfur in Littoral Baltic Sea Sediments (Himmerfjärden, Sweden). *Estuaries and Coasts* **36**: 98–115.

Thauer, R.K. (2019) Methyl (Alkyl)-Coenzyme M Reductases: Nickel F-430-Containing Enzymes Involved in Anaerobic Methane Formation and in Anaerobic Oxidation of Methane or of Short Chain Alkanes. *Biochemistry* **58**: 5198–5220.

Thauer, R.K., Kaster, A.K., Seedorf, H., Buckel, W., and Hedderich, R. (2008) Methanogenic archaea: Ecologically relevant differences in energy conservation. *Nat Rev Microbiol* **6**: 579–591.

Thibodeaux, L.J. and Boyle, J.D. (1987) Bedform-generated convective transport in bottom sediment. *Nature* **325**: 341–343.

Thume, K., Gebser, B., Chen, L., Meyer, N., Kieber, D.J., and Pohnert, G. (2018) The metabolite dimethylsulfoxonium propionate extends the marine organosulfur cycle. *Nature* **563**: 412–415.

Tiews, J., Scharrer, E., Harre, N., Flögel, L., and Jöchle, W. (1975) Metabolism and Excretion of Dimethyl Sulfoxide in Cows and Calves After Topical and Parenteral Application. *Ann N Y Acad Sci* **243**: 139–150.

Todd, J.D., Rogers, R., Li, Y.G., Wexler, M., Bond, P.L., Sun, L., *et al.* (2007) Structural and Regulatory Genes Required to Make the Gas Dimethyl Sulfide in Bacteria. *Science (1979)* **315**: 666–669.

Tong, Y., Zhao, Y., Zhen, G., Chi, J., Liu, X., Lu, Y., *et al.* (2015) Nutrient Loads Flowing into Coastal Waters from the Main Rivers of China (2006 – 2012). *Sci Rep* **5**: 1–12.
Trimmer, M., Hildrew, A.G., Jackson, M.C., Pretty, J.L., and Grey, J. (2009) Evidence for the role of methane-derived carbon in a free-flowing, lowland river food web. *Limnol Oceanogr* **54**: 1541–1547.
Trimmer, M., Purdy, K.J., and Nedwell, D.B. (1997) Process measurement and phylogenetic analysis of the sulfate reducing bacterial communities of two contrasting benthic sites in the upper estuary of the Great Ouse, Norfolk, UK. *FEMS Microbiol Ecol* **24**: 333–342.
Tsola, S.L., Zhu, Y., Ghurnee, O., Economou, C.K., Trimmer, M., and Eyice, Ö. (2021) Diversity of dimethylsulfide-degrading methanogens and sulfate-reducing bacteria in anoxic sediments along the Medway Estuary, UK. *Environ Microbiol* **23**: 4434–4449.
Twohy, C.H. and Anderson, J.R. (2008) Droplet nuclei in non-precipitating clouds: Composition and size matter. *Environmental Research Letters* **3**:.
Twomey, S. (1977) The Influence of Pollution on the Shortwave Albedo of Clouds. *J Atmos Sci* **34**: 1149–1152.
Vanwonterghem, I., Evans, P.N., Parks, D.H., Jensen, P.D., Woodcroft, B.J., Hugenholtz, P., and Tyson, G.W. (2016) Methylotrophic methanogenesis discovered in the archaeal phylum Verstraetearchaeota. *Nat Microbiol* **1**: 1–9.
Vigneron, A., Cruaud, P., Alsop, E., de Rezende, J.R., Head, I.M., and Tsesmetzis, N. (2018) Beyond the tip of the iceberg; A new view of the diversity of sulfite- and sulfate-reducing microorganisms. *ISME Journal* **12**: 2096–2099.
Visscher, P.T., Quist, P., and van Gemerden, H. (1991) Methylated sulfur compounds in microbial mats: In situ concentrations and metabolism by a colorless sulfur bacterium. *Appl Environ Microbiol* **57**: 1758–1763.
Vogt, C., Rabenstein, A., Rethmeier, J., and Fischer, U. (1997) Dimethyl sulphoxide reduction with reduced sulphur compounds as electron donors by anoxygenic phototrophic bacteria. *Microbiology (N Y)* **143**: 767–773.
Wagner, M., Roger, A.J., Flax, J.L., Brusseau, G.A., and Stahl, D.A. (1998) Phylogeny of dissimilatory sulfite reductases supports an early origin of sulfate respiration. *J Bacteriol* **180**: 2975–2982.
Wang, Q., Quensen, J.F., Fish, J.A., Lee, T.K., Sun, Y., Tiedje, J.M., and Cole, J.R. (2013) Ecological patterns of nifH genes in four terrestrial climatic zones explored with targeted metagenomics using framebot, a new informatics tool. *mBio* **4**:.
Wang, S., Jiang, L., Hu, Q., Cui, L., Zhu, B., Fu, X., *et al.* (2021) Characterization of Sulfurimonas hydrogeniphila sp. nov., a Novel Bacterium Predominant in Deep-Sea Hydrothermal Vents and Comparative Genomic Analyses of the Genus Sulfurimonas. *Front Microbiol* **12**: 1–20.
Watanabe, T., Cahyani, V.R., Murase, J., Ishibashi, E., Kimura, M., and Asakawa, S. (2009) Methanogenic archaeal communities developed in paddy fields in the Kojima Bay polder, estimated by denaturing gradient gel electrophoresis, real-time PCR and sequencing analyses. *Soil Sci Plant Nutr* **55**: 73–79.
Watts, S.F. (2000) The mass budgets of carbonyl sulfide, dimethyl sulfide, carbon disulfide and hydrogen sulfide. *Atmos Environ* **34**: 761–779.
Webster, G., A.O'Sullivan, L., Meng, Y., Williams, A.S., Sass, A.M., Watkins, A.J., *et al.* (2015) Archaeal community diversity and abundance changes along a natural salinity gradient in estuarine sediments. *FEMS Microbiol Ecol* **91**: 1–11.
"Weekly rainfall and river flow summary – 31 October-06 November 2018" Environmental Agency 2018, version archived 10 November 2018. Retrieved from the UK Government Web Archive: https://webarchive.nationalarchives.gov.uk/ukgwa/20181110235457/https://www.gov.u

k/government/publications/weekly-rainfall-and-river-flow-reports-for-england (accessed 16 December 2022).
"Weekly rainfall and river flow summary – 03 March-09 March 2021" Environmental Agency 2021, version archived 16 March 2021. Retrieved from the UK Government Web Archive: https://webarchive.nationalarchives.gov.uk/ukgwa/20210316210138/https://www.gov.uk/government/publications/weekly-rainfall-and-river-flow-reports-for-england (accessed 16 December 2022).
Wen, X., Yang, S., Horn, F., Winkel, M., Wagner, D., and Liebner, S. (2017) Global biogeographic analysis of methanogenic archaea identifies community-shaping environmental factors of natural environments. *Front Microbiol* **8**: 1–13.
Wentworth, C.K. (1922) A Scale of Grade and Class Terms for Clastic Sediments. *J Geol* **30**: 377–392.
White, R.H. (1982) Analysis of dimethyl sulfonium compounds in marine algae. *J Mar Res* **40**: 529–536.
Whitehead, P.G., Wilby, R.L., Battarbee, R.W., Kernan, M., and Wade, A.J. (2009) A review of the potential impacts of climate change on surface water quality. *Hydrological Sciences Journal* **54**: 101–123.
Wickham, H. (2016) ggplot2: Elegant Graphics for Data Analysis.
Widdel, F. and Pfennig, N. (1982) Studies on dissimilatory sulfate-reducing bacteria that decompose fatty acids II. Incomplete oxidation of propionate by Desulfobulbus propionicus gen. nov., sp. nov. *Arch Microbiol* **131**: 360–365.
Wiesenburg, D.A. and Guinasso, N.L. (1979) Equilibrium Solubilities of Methane , Carbon Monoxide , and Hydrogen in Water and Sea Water. *J Chem Eng Data* **24**: 356–360.
Wilkins, D., Lu, X.Y., Shen, Z., Chen, J., and Lee, P.K.H. (2015) Pyrosequencing of mcrA and archaeal 16s rRNA genes reveals diversity and substrate preferences of methanogen communities in anaerobic digesters. *Appl Environ Microbiol* **81**: 604–613.
Willke, T. (2014) Methionine production—a critical review. *Appl Microbiol Biotechnol* **98**: 9893–9914.
Wilms, R., Sass, H., Köpke, B., Köster, J., Cypionka, H., and Engelen, B. (2006) Specific bacterial, archaeal, and eukaryotic communities in tidal-flat sediments along a vertical profile of several meters. *Appl Environ Microbiol* **72**: 2756–2764.
Wilson, W.H., Carr, N.G., and Mann, N.H. (1996) The effect of phosphate status on the kinetics of cyanophage infection in the oceanic cyanobacterium Synechococcus sp. WH7803. *J Phycol* **32**: 506–516.
Wolfe, G. v., Sherr, E.B., and Sherr, B.F. (1994) Release and consumption of DMSP from Emiliania huxleyi during grazing by Oxyrrhis marina. *Mar Ecol Prog Ser* **111**: 111–120.
Wolfe, G. v. and Steinke, M. (1996) Grazing-activated production of dimethyl sulfide (DMS) by two clones of Emiliania huxleyi. *Limnol Oceanogr* **41**: 1151–1160.
Wörner, S. and Pester, M. (2019) The active sulfate-reducing microbial community in littoral sediment of oligotrophic lake constance. *Front Microbiol* **10**:.
Wyman, M., Gregory, R.P., and Carr, N.G. (1985) Novel Role for Phycoerythrin in a Marine Cyanobacterium, Synechococcus Strain DC2. *Science (1979)* **230**: 818–820.
Yamamoto, I., Ujiiye, T., Matsuzaki, M., Satoh, T., Wada, N., Tachibana, M., *et al.* (1995) Cloning and Nucleotide Sequence of the Gene Encoding Dimethyl Sulfoxide Reductase from Rhodobacter sphaeroides f. Sp. denitrificans. *Biosci Biotechnol Biochem* **59**: 1850–1855.
Yang, S., Liebner, S., Alawi, M., Ebenhöh, O., and Wagner, D. (2014) Taxonomic database and cut-off value for processing mcrA gene 454 pyrosequencing data by MOTHUR. *J Microbiol Methods* **103**: 3–5.

Yao, W. and Millero, F.J. (1996) Oxidation of hydrogen sulfide by hydrous Fe(III) oxides in seawater. *Mar Chem* **52**: 1–16.
Yin, X., Wu, W., Maeke, M., Richter-Heitmann, T., Kulkarni, A.C., Oni, O.E., *et al.* (2019a) CO 2 conversion to methane and biomass in obligate methylotrophic methanogens in marine sediments. *ISME Journal* 2107–2119.
Yin, X., Wu, W., Maeke, M., Richter-Heitmann, T., Kulkarni, A.C., Oni, O.E., *et al.* (2019b) CO 2 conversion to methane and biomass in obligate methylotrophic methanogens in marine sediments. *ISME Journal*.
Yoch, D.C. (2002) Dimethylsulfoniopropionate: Its sources, role in the marine food web, and biological degradation to dimethylsulfide. *Appl Environ Microbiol* **68**: 5804–5815.
Yoch, D.C., Carraway, R.H., Friedman, R., and Kulkarni, N. (2001) Dimethylsulfide (DMS) production from dimethylsulfoniopropionate by freshwater river sediments: Phylogeny of Gram-positive DMS-producing isolates. *FEMS Microbiol Ecol* **37**: 31–37.
Youngblut, N.D., Wirth, J.S., Henriksen, J.R., Smith, M., Simon, H., Metcalf, W.W., and Whitaker, R.J. (2015) Genomic and phenotypic differentiation among Methanosarcina mazei populations from Columbia River sediment. *ISME Journal* **9**: 2191–2205.
Zeug, S.C. and Winemiller, K.O. (2008) Evidence Supporting the Importance of Terrestrial Carbon in a Large-River Food Web. *Ecology* **89**: 1733–1743.
Zeyer, J., Eicher, P., Wakeham, S.G., and Schwarzenbach, R.P. (1987) Oxidation of dimethyl sulfide to dimethyl sulfoxide by phototrophic purple bacteria. *Appl Environ Microbiol* **53**: 2026–32.
Zhang, L., Kuniyoshi, I., Hirai, M., and Shoda, M. (1991) Oxidation of dimethyl sulfide by Pseudomonas acidovorans DMR-11 isolated from peat biofilter. *Biotechnol Lett* **13**: 223–228.
Zhang, M., Zhang, T., Shao, M.F., and Fang, H.H.P. (2009) Autotrophic denitrification in nitrate-induced marine sediment remediation and Sulfurimonas denitrificans-like bacteria. *Chemosphere* **76**: 677–682.
Zhang, X.H., Liu, Ji, Liu, Jingli, Yang, G., Xue, C.X., Curson, A.R.J., and Todd, J.D. (2019) Biogenic production of DMSP and its degradation to DMS—their roles in the global sulfur cycle. *Sci China Life Sci* **62**: 1296–1319.
Zhao, Yingdong, Li, M.C., Konaté, M.M., Chen, L., Das, B., Karlovich, C., *et al.* (2021) TPM, FPKM, or Normalized Counts? A Comparative Study of Quantification Measures for the Analysis of RNA-seq Data from the NCI Patient-Derived Models Repository. *J Transl Med* **19**: 1–15.
Zhao, Yanan, Schlundt, C., Booge, D., and Bange, H.W. (2021) A decade of dimethyl sulfide (DMS), dimethylsulfoniopropionate (DMSP) and dimethyl sulfoxide (DMSO) measurements in the southwestern Baltic Sea. *Biogeosciences* **18**: 2161–2179.
Zheng, Y., Wang, J., Zhou, S., Zhang, Y., Liu, J., Xue, C.X., *et al*. (2020) Bacteria are important dimethylsulfoniopropionate producers in marine aphotic and high-pressure environments. *Nat Commun* **11**:.
Zhuang, G.C., Elling, F.J., Nigro, L.M., Samarkin, V., Joye, S.B., Teske, A., and Hinrichs, K.U. (2016) Multiple evidence for methylotrophic methanogenesis as the dominant methanogenic pathway in hypersaline sediments from the Orca Basin, Gulf of Mexico. *Geochim Cosmochim Acta* **187**: 1–20.
Zhuang, L., Chen, Q., Zhou, S., Yuan, Y., and Yuan, H. (2012) Methanogenesis control using 2-bromoethanesulfonate for enhanced power recovery from sewage sludge in air-cathode microbial fuel cells. *Int J Electrochem Sci* **7**: 6512–6523.
Zinder, S., Anguish, T., and Cardwell, S. (1984) Selective-{Inhibition} by 2-{Bromoethanesulfonate} of {Methanogenesis} from {Acetate} in a {Thermophilic} {Anaerobic} {Digester}. *Appl Environ Microbiol* **47**: 1343–1345.

Zinder, Stephen H. and Brock, T D (1978) Dimethyl Sulfoxide as an Electron Acceptor for Anaerobic Growth. *Arch Microbiol* **116**: 35–40.

Zinder, S. H. and Brock, T.D. (1978) Methane, carbon dioxide, and hydrogen sulfide production from the terminal methiol group of methionine by anaerobic lake sediments. *Appl Environ Microbiol* **35**: 344–352.

Zinder, Stephen H. and Brock, T. D. (1978) Production of methane and carbon dioxode from methane thiol and dimethyl sulphide by anaerobic lake sediments. *Nature* **273**: 226–228.

de Zwart, J.M.M., Nelisse, P.N., and Kuenen, J.G. (1994) Isolation adn characterization of Methylophaga sulfidovorans sp. nov.: an obligately methylotrophic, aerobic, dimethylsulfide oxidizing bacterium from a microbial mat. *FEMS Microbiol Ecol* **20**: 261–270.

Appendix

Appendix Table 1. Theoretical hydrogen sulfide (H_2S) produced following the addition of DMS from methanogenesis and sulfate reduction and theoretical sulfate produced if all H_2S was oxidised. The experimental sulfate values measured at the end of the DMS incubations were lower in all samples than the theoretically expected but still higher than the sulfate originally added to the incubations.

Sample	Theoretical H_2S production (µmol/g)	Theoretical sulfate production (µmol/g)	Initial sulfate (µmol/g)	Experimental sulfate (µmol/g)
H2D1	21	21	40	8
H2D2	42	42	40	4
H2D3	31	31	24	15
H2D4	37	37	8	15
H2D5	32	32	0.4	17
H2D6	29	29	0.4	11
H2D7	20	20	0	4
H3D1	53	53	40	9
H3D2	58	58	40	4
H3D3	50	50	24	15
H3D4	17	17	8	11
H3D5	32	32	0.4	13
H3D6	31	31	0.4	13
H3D7	43	43	0	11
H5D1	26	26	40	2
H5D2	58	58	40	10
H5D3	34	34	24	8
H5D4	19	19	8	10
H5D5	20	20	0.4	13
H5D6	17	17	0.4	7
H5D7	32	32	0	14

Appendix Table 2. Genes involved in acetoclastic methanogenesis. The gene codes are accession IDs belonging to the KEGG database, besides EG11448 which is an EcoCyc accession number (Keseler *et al.*, 2011; Kanehisa *et al.*, 2022).

Gene	Metabolic Pathway	Full Name	Gene Code
ackA	Acetate	Acetate_kinase	K00925
acs	Acetate	Acetyl-CoA synthetase	EG11448
cdhA	Acetate	Anaerobic carbon-monoxide dehydrogenase	K00192
cdhB	Acetate	Anaerobic carbon-monoxide dehydrogenase	K00195
cdhC	Acetate	Acetyl-CoA decarbonylase/synthase	K00193
cdhD	Acetate	Acetyl-CoA decarbonylase/synthase	K00194
cdhE	Acetate	Acetyl-CoA decarbonylase/synthase	K00197
pta	Acetate	Phosphate acetyltransferase	K00625

Appendix Table 3. Genes involved in hydrogenotrophic methanogenesis. The gene codes are accession IDs belonging to the KEGG database (Kanehisa *et al.*, 2022).

Gene	Metabolic Pathway	Full Name	Gene Code
fmdA	Carbon dioxide/Hydrogen	Formylmethanofuran dehydrogenase	K00200
fmdB	Carbon dioxide/Hydrogen	formylmethanofuran dehydrogenase	K00201
fmdC	Carbon dioxide/Hydrogen	formylmethanofuran dehydrogenase	K00202
fmdD	Carbon dioxide/Hydrogen	formylmethanofuran dehydrogenase	K00203
fmdE	Carbon dioxide/Hydrogen	formylmethanofuran dehydrogenase	K11261
fmdF	Carbon dioxide/Hydrogen	4Fe-4S ferredoxin	K00205
ftr	Carbon dioxide/Hydrogen	Formylmethanofuran--tetrahydromethanopterin N-formyltransferase	K00672
hmd	Carbon dioxide/Hydrogen	5,10-methenyltetrahydromethanopterin hydrogenase	K13942
mch	Carbon dioxide/Hydrogen	Methenyltetrahydromethanopterin cyclohydrolase	K01499
mer	Carbon dioxide/Hydrogen	5,10-methylenetetrahydromethanopterin reductase	K00320
mtrA	Carbon dioxide/Hydrogen	Tetrahydromethanopterin S-methyltransferase subunit A	K00577
mtrB	Carbon dioxide/Hydrogen	Tetrahydromethanopterin S-methyltransferase subunit B	K00578
mtrC	Carbon dioxide/Hydrogen	Tetrahydromethanopterin S-methyltransferase subunit C	K00579
mtrD	Carbon dioxide/Hydrogen	Tetrahydromethanopterin S-methyltransferase subunit D	K00580
mtrE	Carbon dioxide/Hydrogen	Tetrahydromethanopterin S-methyltransferase subunit E	K00581
mtrF	Carbon dioxide/Hydrogen	Tetrahydromethanopterin S-methyltransferase subunit F	K00582
mtrG	Carbon dioxide/Hydrogen	Tetrahydromethanopterin S-methyltransferase subunit G	K00583
mtrH	Carbon dioxide/Hydrogen	Tetrahydromethanopterin S-methyltransferase subunit H	K00584

Appendix Table 4. Genes involved in methylotrophic methanogenesis. The gene codes are accession IDs belonging to the KEGG database, besides MA0859, MA4384 and MA4558 which are NBCI locus tags (Agarwala *et al.*, 2016; Kanehisa *et al.*, 2022).

Gene	Metabolic Pathway	Full Name	Gene Code
mtmC	Methylamine	Monomethylamine corrinoid protein	K16177
mtbA	Dimethylamine	[methyl-Co(III) methylamine-specific corrinoid protein]:CoM methyltransferase	K14082
mtbB	Dimethylamine	Dimethylamine---corrinoid protein Co-methyltransferase	K16178
mtbC	Dimethylamine	Dimethylamine corrinoid protein	K16179
mttB	Trimethylamine	Trimethylamine---corrinoid protein Co-methyltransferase	K14083
mttC	Trimethylamine	Trimethylamine corrinoid protein	K14084
mtsA	DMS, MeSH, methylpropanoate	Methylthiol:CoM methyltransferase	K16954
mtsB	DMS, MeSH, methylpropanoate	Methylated-thiol--corrinoid protein	K16955
mtsD	DMS, MeSH, methylpropanoate	Methyltransferase cognate corrinoid protein [Methanosarcina acetivorans C2A]	MA0859
mtsF	DMS, MeSH, methylpropanoate	Cobalamin-dependent protein [Methanosarcina acetivorans C2A]	MA4384
mtsH	DMS, MeSH, methylpropanoate	Cobalamin-dependent protein [Methanosarcina acetivorans C2A]	MA4558
mtaA	Methanol	[methyl-Co(III) methanol/glycine betaine-specific corrinoid protein]:CoM methyltransferase	K14080
mtaB	Methanol	Methanol---5-hydroxybenzimidazolylcobamide Co-methyltransferase	K04480
mtaC	Methanol	Methanol corrinoid protein	K14081

Appendix Table 5. Methanogenesis genes common in all pathways. The gene codes are accession IDs belonging to the KEGG database (Kanehisa *et al.*, 2022). CoM: Coenzyme M; CoB: Coenzyme B.

Gene	Metabolic Pathway	Full Name	Gene Code
mcrA	CoM reduction to methane	Methyl-CoM reductase alpha subunit	K00399
mcrB	CoM reduction to methane	Methyl-CoM reductase beta subunit	K00401
mcrC	CoM reduction to methane	Methyl-CoM reductase subunit C	K03421
mcrD	CoM reduction to methane	Methyl-CoM reductase subunit D	K03422
mcrG	CoM reduction to methane	Methyl-CoM reductase subunit gamma	K00402
cooF	CoB/CoM regeneration	Anaerobic carbon-monoxide dehydrogenase iron sulfur subunit	K00196
cooS	CoB/CoM regeneration	Anaerobic carbon-monoxide dehydrogenase catalytic subunit	K00198
fdhA	CoB/CoM regeneration	Glutathione-independent formaldehyde dehydrogenase	K00148
fdhB	CoB/CoM regeneration	Formate dehydrogenase (coenzyme F420) beta subunit	K00125
fpoA	CoB/CoM regeneration	F420H2 dehydrogenase subunit A	K22158
fpoB	CoB/CoM regeneration	F420H2 dehydrogenase subunit B	K22159
fpoC	CoB/CoM regeneration	F420H2 dehydrogenase subunit C	K22160
fpoD	CoB/CoM regeneration	F420H2 dehydrogenase subunit D	K22161
fpoF	CoB/CoM regeneration	F420H2 dehydrogenase subunit F	K22162
fpoH	CoB/CoM regeneration	F420H2 dehydrogenase subunit H	K22163
fpoI	CoB/CoM regeneration	F420H2 dehydrogenase subunit I	K22164
fpoJ	CoB/CoM regeneration	F420H2 dehydrogenase subunit J	K22165
fpoK	CoB/CoM regeneration	F420H2 dehydrogenase subunit K	K22166
fpoL	CoB/CoM regeneration	F420H2 dehydrogenase subunit L	K22167
fpoM	CoB/CoM regeneration	F420H2 dehydrogenase subunit M	K22168
fpoN	CoB/CoM regeneration	F420H2 dehydrogenase subunit N	K22169
fpoO	CoB/CoM regeneration	F420H2 dehydrogenase subunit O	K22170
frhA	CoB/CoM regeneration	Coenzyme F420 hydrogenase subunit alpha	K00440
frhB	CoB/CoM regeneration	Coenzyme F420 hydrogenase subunit beta	K00441
frhD	CoB/CoM regeneration	Coenzyme F420 hydrogenase subunit delta	K00442
frhG	CoB/CoM regeneration	Coenzyme F420 hydrogenase subunit gamma	K00443
hdrA	CoB/CoM regeneration	Heterodisulfide reductase	K03388
hdrB	CoB/CoM regeneration	Heterodisulfide reductase	K03389
hdrC	CoB/CoM regeneration	Heterodisulfide reductase	K03390
hdrD	CoB/CoM regeneration	Heterodisulfide reductase	K08264
hdrE	CoB/CoM regeneration	Heterodisulfide reductase	K08265
mvdA	CoB/CoM regeneration	F420-non-reducing hydrogenase large subunit	K14126
mvdD	CoB/CoM regeneration	F420-non-reducing hydrogenase iron-sulfur subunit	K14127
mvdG	CoB/CoM regeneration	F420-non-reducing hydrogenase small subunit	K14128
vhoA	CoB/CoM regeneration	Methanophenazine hydrogenase, large subunit	K14068
vhoC	CoB/CoM regeneration	Methanophenazine hydrogenase, cytochrome b subunit	K14069
vhoG	CoB/CoM regeneration	Methanophenazine hydrogenase	K14070

Appendix Table 6. Genes involved in sulfur cycling. The gene codes are accession IDs belonging to the KEGG database besides G-43975 which is an MetaCyc accession number (Caspi *et al.*, 2014; Kanehisa *et al.*, 2022).

Gene	Metabolic Pathway	Full Name	Gene Code
doxA	Thiosulfate oxidation	Thiosulfate dehydrogenase (quinone) small subunit	K16936
doxD	Thiosulfate oxidation	Thiosulfate dehydrogenase (quinone) large subunit	K16937
soxA	Thiosulfate oxidation	L-cysteine S-thiosulfotransferase	K17222
soxB	Thiosulfate oxidation	S-sulfosulfanyl-L-cysteine sulfohydrolase	K17224
soxC	Thiosulfate oxidation	Sulfane dehydrogenase subunit	K17225
soxX	Thiosulfate oxidation	L-cysteine S-thiosulfotransferase	K17223
soxY	Thiosulfate oxidation	Sulfur-oxidizing protein	K17226
soxZ	Thiosulfate oxidation	Sulfur-oxidizing protein	K17227
psrA	Polysulfide reduction	Thiosulfate reductase / polysulfide reductase chain A	K08352
psrB	Polysulfide reduction	Polysulfide reductase chain B	K16293
psrC	Polysulfide reduction	Polysulfide reductase chain C	K16294
fccB	Sulfide oxidation	Sulfide dehydrogenase [flavocytochrome c] flavoprotein chain	K17229
sqr	Sulfide oxidation	Sulfide:quinone oxidoreductase	K17218
sorB	Sulfite oxidation	Sulfite dehydrogenase (cytochrome) subunit B	K00386
soeA	Sulfite oxidation	Sulfite dehydrogenase (quinone) subunit	K21307
soeB	Sulfite oxidation	Sulfite dehydrogenase (quinone)	K21308
soeC	Sulfite oxidation	Sulfite dehydrogenase (quinone)	K21309
sdo	Sulfur oxidation	Sulfur dioxygenase α subunit	G-43975
cysI	Sulfite reduction	Sulfite reductase (NADPH) hemoprotein beta-component	K00381
cysJ	Sulfite reduction	Sulfite reductase (NADPH) flavoprotein alpha-component	K00380
sir	Sulfite reduction	Sulfite reductase (ferredoxin)	K00392
sor	Sulfur reduction	Sulfur oxygenase/reductase	K16952
sreA	Sulfur reduction	Sulfur reductase molybdopterin subunit	K17219
sreB	Sulfur reduction	Sulfur reductase FeS subunit	K17220
sreC	Sulfur reduction	Sulfur reductase membrane anchor	K17221
sat	Dissimilatory sulfate reduction	Sulfate adenylyltransferase	K00958
aprA	Dissimilatory sulfate reduction	Adenylylsulfate reductase, subunit A	K00394
aprB	Dissimilatory sulfate reduction	Adenylylsulfate reductase, subunit B	K00395
dsrA	Dissimilatory sulfate reduction	Dissimilatory sulfite reductase alpha subunit	K11180
dsrB	Dissimilatory sulfate reduction	Dissimilatory sulfite reductase beta subunit	K11181

Agarwala, R., Barrett, T., Beck, J., Benson, D.A., Bollin, C., Bolton, E., *et al.* (2016) Database resources of the National Center for Biotechnology Information. *Nucleic Acids Res* **44**: D7–D19.

Caspi, R., Altman, T., Billington, R., Dreher, K., Foerster, H., Fulcher, C.A., *et al.* (2014) The MetaCyc database of metabolic pathways and enzymes and the BioCyc collection of Pathway/Genome Databases. *Nucleic Acids Res* **42**: 459–471.

Kanehisa, M., Furumichi, M., Sato, Y., Kawashima, M., and Ishiguro-Watanabe, M. (2022) KEGG for taxonomy-based analysis of pathways and genomes. *Nucleic Acids Res* 1–6.

Keseler, I.M., Collado-Vides, J., Santos-Zavaleta, A., Peralta-Gil, M., Gama-Castro, S., Muniz-Rascado, L., *et al.* (2011) EcoCyc: A comprehensive database of Escherichia coli biology. *Nucleic Acids Res* **39**: 583–590.